March 2019

NASCENT DNA PROTEOMICS ANALYSIS UNCOVERS DNA REPLICATION DYNAMICS IN THE HUMAN PATHOGEN TRYPANOSOMA BRUCEI

Maria Rocha Granados
University of Massachusetts Amherst

NASCENT DNA PROTEOMICS ANALYSIS UNCOVERS DNA REPLICATION DYNAMICS IN THE HUMAN PATHOGEN *TRYPANOSOMA BRUCEI*

A Dissertation Presented

by

MARIA C. ROCHA GRANADOS

Submitted to the Graduate School of the
University of Massachusetts Amherst in partial fulfilment
of the requirements for the degree of

DOCTOR OF PHILOSOPHY

February 2019

Department of Microbiology

NASCENT DNA PROTEOMICS ANALYSIS UNCOVERS DNA REPLICATION DYNAMICS IN THE HUMAN PATHOGEN *TRYPANOSOMA BRUCEI*

A Dissertation Presented

by

MARIA C. ROCHA GRANADOS

Approved as to style and content by:

_____
Michele M. Klingbeil, Chair

_____
Yasu S. Morita, Member

_____
M. Sloan Siegrist, Member

_____
Arthur Günzl, Member

_____
James Holden, Department Head
Department of Microbiology

DEDICATION

To God, my faithful companion. To my beautiful Church. To my parents for their advices. To my brother and sisters for their encouragement.

ACKNOWLEDGMENTS

"For the Lord gives wisdom;

From His mouth come knowledge and understanding"

Proverbs 2:6

First, I would like to thank God since He has fulfilled His promises and the desires of my heart. His guidance has been and will always be the most important aspect of my life. I would like to acknowledge my mentor, Dr. Michele Klingbeil, for giving the opportunity to perform research in her lab and to show me how strong I can be. I thank my committee members, Dr. Yasu Morita, Dr. Sloan Siegrist and Dr. Arthur Günzl, for all their support, advice and help in many matters during my Ph.D. Also, I would like to thank all the members of the Klingbeil lab. They all contributed to this project, special thanks to Yahaira Bermudez and Jonathan Miller. I would like to acknowledge the Faculty and the staff of the Microbiology Department for accepting me in the program and for resolving all my questions.

I want to thank my family. My parents for their example and love. Their work and sacrifice allowed me to receive all my education. I want to thank my sisters and my brother for hearing me and making me laugh in the moments that I needed the most. I am blessed for not only having a lovely family in Colombia, but also to have a family here in this country. My church has become my family, and every member has become a true friend.

Finally, I would like to thank my amazing friends. Sylvia Rivera and Garvin Dodard. We really enjoyed doing science together.

ABSTRACT

NASCENT DNA PROTEOMICS ANALYSIS UNCOVERS DNA REPLICATION DYNAMICS IN THE HUMAN PATHOGEN *TRYPANOSOMA BRUCEI*

FEBRUARY 2019

MARIA C. ROCHA GRANADOS, M.Sc., UNIVERSIDAD DE LOS ANDES

Ph.D., UNIVERSITY OF MASSACHUSETTS AMHERST

Director: Professor Michele M. Klingbeil

DNA is the substrate of many cellular processes including DNA replication, transcription and chromatin remodeling. Therefore, these processes are coordinated to maintain genome integrity and ensure accurate duplication of genetic and epigenetic information. Genome-wide studies have provided evidence of the relationship between transcription and DNA replication timing. In mouse embryonic cells, 85% of origins of replication (ORIs) are associated with transcriptional units. In human cells, 75% of activated origins overlapped with transcribed areas of the genome. A global analysis of DNA replication initiation in *T. brucei* showed that TbORC1 (subunit of the origin recognition complex, ORC) binding sites are located at the boundaries of transcription units. Further studies also showed that *T. brucei* has fewer origins of replication than model eukaryotes, a highly divergent ORC complex, and an apparent lack of several replication factor homologs. Although recent studies in *T. brucei* indicate functional links among DNA replication, transcription, and antigenic variation, the underlying mechanisms remain unknown. In this study, we adapted an unbiased technology for the identification of replication fork proteins called iPOND (**i**solation of **p**roteins ***o***n **n**ascent **D**NA) to *T. brucei*,

its first application to a parasite system. The iPOND approach relies on labeling newly replicated DNA with the thymidine analog EdU (5-ethynyl-2′-deoxyuridine), which contains an alkyne functional group that enables the cycloaddition of a biotin azide. This click chemistry reaction yields a stable covalent linkage, facilitating streptavidin capture of cross-linked biotinylated DNA-protein complexes. First, we described how we adapted the iPOND protocol in *T. brucei* procyclic cells in order to generate a suitable sample for mass spectrometry analysis (Chapter 2). Then, we analyzed the iPOND samples and performed label-free quantification to determine which proteins are enriched in an active replication fork in *T. brucei* (Chapter 3). We identified a total of 410 proteins, including key DNA replication factors and proteins associated with transcription, chromatin organization, DNA repair and mRNA splicing. Around 25% of the proteins identified were of unknown function that might have the potential to be essential trypanosome-specific replication proteins. Additionally, we characterized two proteins from our iPOND-derived protein list (Chapter 3). These are a protein annotated as a Replication Factor C subunit (Tb927.10.7990), and a protein of unknown function (Tb927.3.5370). Both revealed nuclear localization throughout the cell cycle. Tb927.10.7990 proved to be essential since its silencing caused a growth defect in procyclic cells and impaired DNA replication. However, Tb927.3.5370 appeared to be a dispensable gene. Our data suggest that DNA replication, transcription, chromatin organization and pre-mRNA splicing events all occur on or near nascent DNA. We propose nucleosomes are assembled close to the replication fork followed by RNA pol II recruitment, transcription, and co-transcriptional RNA splicing. Further studies are needed to determine how these processes are linked and co-regulated, and how rapidly they are initiated during DNA replication.

TABLE OF CONTENTS

Page

LIST OF TABLES

Table Page

LIST OF FIGURES

Figure Page

CHAPTER 1

KINETOPLASTID-RELATED DISEASES, TRYPANOSOMA BIOLOGY AND DNA REPLICATION

1.1 The kinetoplastids and Neglected Tropical Diseases

The family Trypanosomatidae belongs to the class Kinetoplastea and represents a diverse and important group of protozoan organisms. In this family, parasites can exhibit two lifestyles. They can be dixenous (two hosts, one invertebrate and one vertebrate) or monoxenous (single host, either invertebrate or vertebrate) parasites [1]. Genera *Trypanosoma* and *Leishmania* are classified as dixenous parasites of clinical and veterinary importance causing economic burden primarily on tropical and subtropical countries. These include the human pathogenic species *Trypanosoma brucei* causing Human African Trypanosomiasis (HAT) in sub-Saharan Africa, *Trypanosoma cruzi* causing Chagas Disease in South America and approximately 20 species of *Leishmania* causing cutaneous and visceral leishmaniasis in a worldwide distribution [2]. These are considered as neglected tropical diseases (NTDs) since these parasitic infections are dominant in tropical and sub-tropical developing countries with high levels of poverty. For example, 73% of the population located in sub-Saharan Africa lives on less than $2 USD per day. NTDs not only have an impact on health, but also contribute to an economic and social burden causing discrimination, impairment on cognitive development, physical disabilities and loss of social status. Therefore, individuals affected by these diseases cannot carry a productive life, affecting their communities and their economic development [3].

1.2 Human African Trypanosomiasis

In the case of HAT or Sleeping Sickness, 70 million people live in an at-risk area in the sub-Saharan Africa. HAT contributes to approximately 1% of the deaths attributed to NTDs, ranking at the fifth position. In 2016, the Global Health Observatory reported 2,184 new cases of HAT. This number has been remarkable reduced compared to the 10,388 cases reported in 2008. This reduction is part of the efforts of the WHO to overcome the global impact of the NTDs, where HAT is one of the diseases targeted for full elimination by 2030 [4,5].

Many strategies have been implemented to reduce the number of annual cases. These strategies have been focused on screening, treating the patients, surveillance, diagnosis and vector control. The sleeping sickness control program is based on patient self-report to local health centers and active case-finding where teams of health workers seek out patients living in at risk areas. Diagnosis includes blood testing for serological confirmation of antigens in response to the parasite and lumbar puncture to check the cerebrospinal fluid. Recently, loop-mediated isothermal amplification (LAMP) technique has been implemented for a diagnostic purpose. For vector control, the use of insecticide-impregnated screens called “tiny targets” that attracts the flies and kills them has been employed [4].

Two subspecies of *T. brucei* are pathogenic to humans: *T. brucei gambiense* and *T. brucei rhodesiense*. These parasites are transmitted by the bite of infected tsetse flies (vector) to humans. *T. brucei gambiense* causes the chronic and long latency form of the disease in central and west Africa. This subspecies represents 95% of all reported HAT cases. In Gambian African HAT, humans are the main reservoir and transmission agent

within the life cycle of the parasite. *T. brucei rhodesiense* is the acute and more virulent form of the disease in east and southern Africa. The Rhodesian African sleeping sickness is rare, patient deaths often occur within a few months [6,7]. Both forms of HAT can be fatal if left untreated. HAT has two clear clinical stages: The hemolymphatic stage (stage I) and the meningoencephalitic stage (stage II). The hemolymphatic stage is characterized by intermittent fever lasting 1 day to 1 week, separated by intervals of days or months. This fever pattern is a result of the successive cyclical waves of trypanosome parasitemia. Also, the patient can present headache, pruritus and lymphadenopathy. The second stage occurs when trypanosomes cross the blood-brain barrier and invade the central nervous system (CNS). This leads to the development of neuropsychiatric disorders such as disturbance on the patient´s sleep pattern. The sleep disorder consists of daytime somnolence and a sudden overwhelming urge to sleep, and nocturnal insomnia. Other signals include confusion and trouble with motor and mental coordination, personality changes, hallucinations and paranoid delusions together with encephalitis. After observation of these symptoms, the patient falls into a coma stage and dies if left untreated [6,8,9].

Current treatment is based on 5 available drugs: melarsoprol, pentamidine, suramin, eflornithine and nifurtimox. For stage I, pentamidine is the first line treatment for *T. brucei gambiense* and is an alternative treatment for *T. brucei rhodesiense*. It has 95%-98% efficiency and is administrated intramuscularly once daily for 7 days. Suramin is another effective drug to treat stage I of *T. brucei gambiense* and *T. brucei rhodesiense* disease. Compared to pentamidine, suramin is more complicated to administer since it has to be by slow intravenous infusion. Melarsoprol is an arsenic compound and is effective at the stage II of the disease. However, it has high levels of toxicity and there is documentation

indicating anti-parasitic resistance. Currently, the first line to treat the second stage of *T. brucei gambiense* disease is nifurtimox-eflornithine combination therapy (NECT). Compared to Melarsoprol, NECT has higher cure rates, lower fatality rates and less severe secondary effects. NECT consists of nifurtimox delivered orally and eflornithine delivered intravenously. Yet, NECT has a high cost and is complicated to administrate. There have been efforts to develop new medicines to combat HAT. Two new drugs, benzoxaborole SCYX-7158 and fexinidazole are in clinical trials. These two molecules can be administered orally and intend to treat both disease stages [9–11]. Fexinadozole is a nitroimidazole that in clinical phase I trials proved good tolerance in oral doses of 100 to 3600 mg and it was able to effectively cure both acute and chronic disease in mice at doses of 100 mg/kg of body weight/day for 4 days and 200 mg/kg/day for 5 days, respectively. Fexinadozole is in clinical phase III assessing the therapy success under real life conditions [10,12]. Oxaborole SCYX-7158 is a small boron-containing molecule that when administered to 128 healthy humans in phase I clinical trial, they tolerated dose of 960 mg. SCYX-7158 displayed potent activity against *T. brucei rhodesiense* and *T. brucei gambiense*. Infected mice that were administered with oral doses (5 mg/kg/day) of SCYX-7158 daily for 4 days showed 100% cure rate. Based on these observations, SCYX-7158 started its phase II trial in the Democratic Republic of Congo in 2016 [10,13].

Despite the promising results of these two drugs, the quest for new satisfactory and effective therapies continues. Part of the strategies for such quest is to understand the parasite genome and use the proteomic data available to identify attractive targets for the sleeping sickness. The identification of these potential novel targets can contribute to eliminating sleeping sickness as a public health problem in the future.

1.3 *Trypanosoma* cell cycle.

T. brucei follows a typical eukaryotic cell cycle, encompassing G_1, S, G_2 and M phases [14]. However, there are some differences between *T. brucei* and animal cell division. Cytokinesis in *T. brucei* does not involve a contractile actomyosin ring at the cleavage furrow but instead the cleavage plane moves longitudinally through the cell between two defined points [15,16]. In *T. brucei*, the nucleus divides via intranuclear spindle. In many animal cells, the main microtubule organizing center (MCOC) is the centrosomes. However, in *T. brucei* centriole functions as basal body that nucleates the parasite flagellum through the entire cell cycle. Basal bodies never locate at the spindle poles or connect to the intranuclear spindle [16]. Nevertheless, basal body duplication is the first cellular marker at G1 phase followed by the beginning of the synthesis of a new flagellum [17]. *T. brucei* has a number of single copy organelles that have to be duplicated and segregated accurately. This parasite has two DNA containing organelles, the kinetoplast (mitochondrial DNA, located in the single mitochondrion of the parasite) and the nucleus [18]. Kinetoplast DNA (kDNA) replication occurs before nuclear DNA replication. Kinetoplast elongation/division takes place during the S phase of nuclear DNA. Correct segregation and positioning of daughter kinetoplast rely on basal body movement, since the proximal end of the basal body is linked to the kinetoplast via the filaments of the tripartite attachment complex (TAC) [19]. After nuclear S phase, cells enter to M phase and chromosome segregation occurs, followed by complete nuclear division. After this, cleavage furrow ingression occurs between the two flagella resulting in two daughter cells at the end of the cell cycle [18]. Normal course of cell cycle stages in *T. brucei* can be tracked and visualized by staining the DNA content of the kinetoplast (K) and nucleus (N)

with DAPI (4,6-diamidino-2-phenylindole) staining. The normal configurations are 1N1K, 1N K_{div} (elongated V-shaped kinetoplast, indicating kinetoplast replication), 1N2K and 2N2K (Fig 1.1). Most of the 1N1K cells are in G_1 phase, 1N1K_{div} are in S phase, 1N2K are in S-G_2 phase and 2N2K cells are post-mitotic. In asynchronous population of PCF parasites, most of the cells are in G_1 phase (approximately 80%), cells at S phase represent around 20% of the population and G_2 phase cells are near to 2% of the population [20–22].

Cell cycle regulation in Trypanosomes shares some features with other eukaryotes but the parasite has also evolved unusual checkpoint control mechanisms to regulate its cell cycle, including a number of trypanosome specific cell cycle regulators. Cell cycle phases are regulated by CDC2-related kinases (CRKS) and their partner cyclins [14]. For example, CRK1, CRK2, cyclin CYC2 regulate the transition between G_1/S phase [23,24]. CRK1 interacts with four cyclins (CYC2, CYC4, CYC5 and CYC7), whereas CRK2 only interacts with CYC2 [25].Transition of G_2 to M phase in *T. brucei* is regulated by CRK3 and cyclin CYC6 [26]. Checkpoints for mitosis to cytokinesis transition are absent in this parasite [27]. One of the proteins involved in spindle assembly and chromosome segregation is the Aurora B homolog in trypanosomes TbAUK1, which forms a unique chromosomal passenger complex (CPC) with two trypanosome specific proteins TbCPC1 and TbCPC2 [28]. TbAUK1 also has a role in cytokinesis together with a Polo-like kinase TbPLK1. TbAUK1 regulates cytokinesis initiation, furrow ingression and abscission [29,30]. TbPLK1 promotes cytokinesis initiation when it is concentrated at the anterior tip of the new flagellar attachment zone (FAZ) in the late cell cycle stages [30].

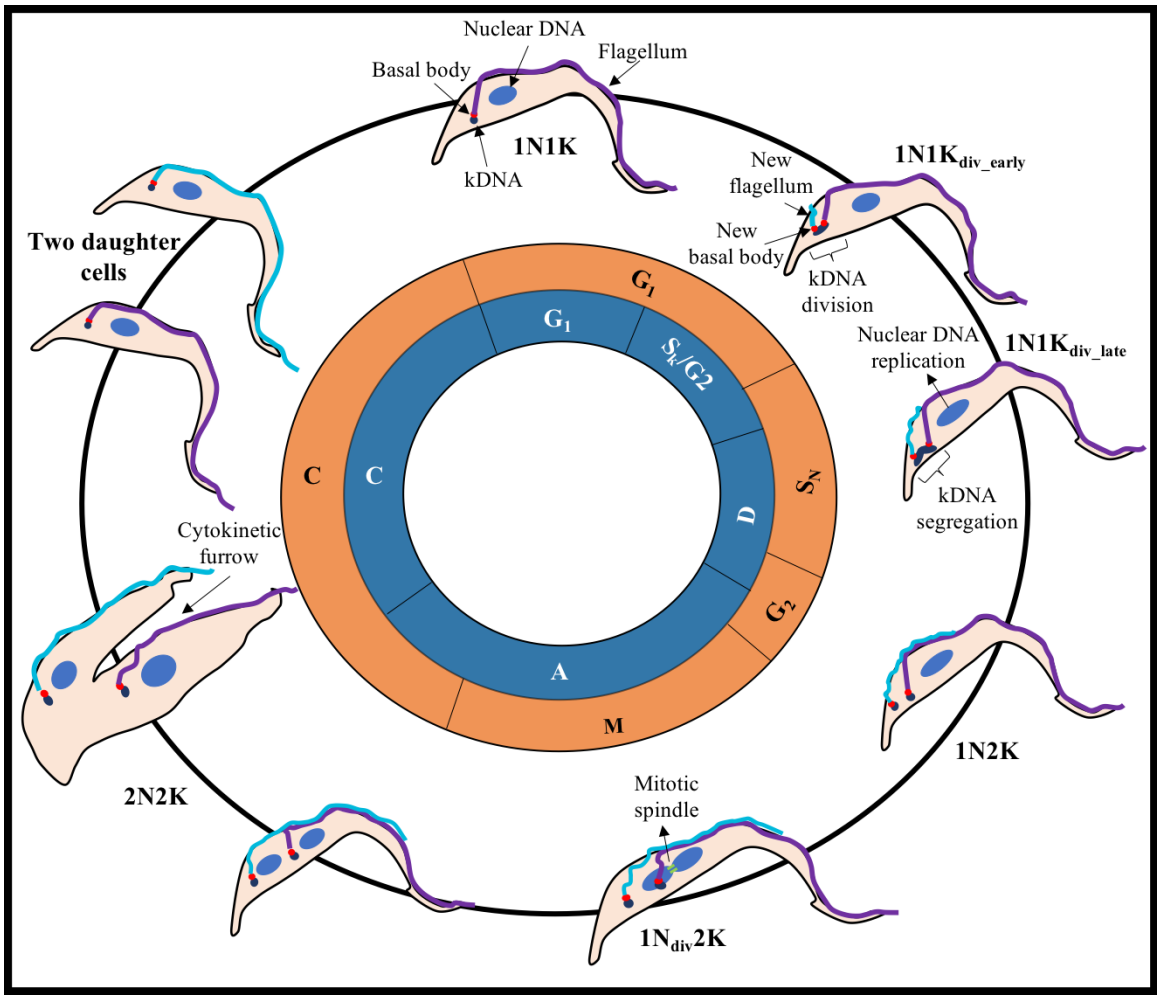

Figure 1.1 - Cell Cycle stages in *T. brucei*. Diagram illustrating the major morphological events of the cell cycle of procyclic *T. brucei*. The cell cycle has two components: kinetoplast division (blue circle) and nuclear division (orange circle). Cells at G_1 phase are in the 1N1K stage. The first event is duplication of the basal body followed by kinetoplast replication (S_k) prior nuclear S phase (S_N). These are 1N1K$_{div}$ cells. The nucleus remains in S phase upon segregation of the kinetoplast (D, division) rising to 1N2K cells. As cell cycle progresses, the basal bodies continue to move apart (A), and cells enter to M phase (mitosis) and chromosome segregation occurs (1N$_{div}$2K). Nuclear division is complete generating 2N2K cells and cleavage furrow ingression occurs between the two flagella to initiate cytokinesis (C). At the end of the cell cycle, there are two daughter cells having one nucleus, one kinetoplast and one flagellum.

1.4 *Trypanosoma* cell biology

Trypanosoma brucei alternates between an insect host and mammalian host during its life cycle, displaying key metabolic adaptations that are reflected by morphological changes. These cellular forms optimize parasite survival and ensure transmission to the next host [9,31]. Metabolic and morphological changes include fine-tuning of energy metabolism, organelle reorganization, and biochemical and structural remodeling [32]. These adaptations are based on major changes in gene expression. There are two life stages. The procyclic form (PCF) and the bloodstream form (BSF). PCF resides in the insect vector (tsetse fly) and BSF resides in the mammalian host. Transcriptome studies have shown that between 6%-30% of *T. brucei* genes are differentially expressed between its different life stages [33–35], and by ribosome profiling studies, approximately 35% of the coding sequences are significantly regulated at the protein level between the two life forms [36]. The entire life cycle of *T. brucei* is represented by extracellular stages. Within the fly´s midgut, the parasite transforms into PCF and proliferates. At this part of the life cycle in the fly, the parasite needs to leave the midgut and find its way to colonize the salivary glands. During this process, the trypanosomes go through an asymmetric division producing short epimastigotes that colonize the salivary glands. Finally, epimastigotes are attached to the epithelium while they differentiate to pre-metacyclics. Once they arrest on G_1, they can be released as metacyclic trypomastigotes (infective form) and be ready to be transmitted to the next mammalian host [37,38]. Within the mammalian host, the parasite transforms into BSF trypomastigotes. They have two stages, the long slender form (proliferative form) that doubles every 7 hours by binary fission and the short stumpy form (division-arrested forms). Differentiation from long slender forms to short stumpy forms

relies on quorum sensing mechanisms and it is an irreversible process [31,39] (Fig 1.2). The BSF parasites overcome the host innate and adaptive immune system by periodically changing their variant surface glycoprotein (VSG) coat. This process is called antigenic variation. This cycle of antigenic variation impedes the immune system to clear the infection since a proportion of the parasites have switched towards the expression of a different VSG that is no longer recognized by antibodies raised against previous VSG antigens. In this manner, the parasite prolongs the infection and optimizes the potential for its transmission [40,41]. Recent investigations have shown that in addition to the blood and brain-blood barrier as the two major niches of *T. brucei* in the mammalian host, adipose tissue [42], skin [43,44] and male testis [45,46] are also reservoirs for this parasite.

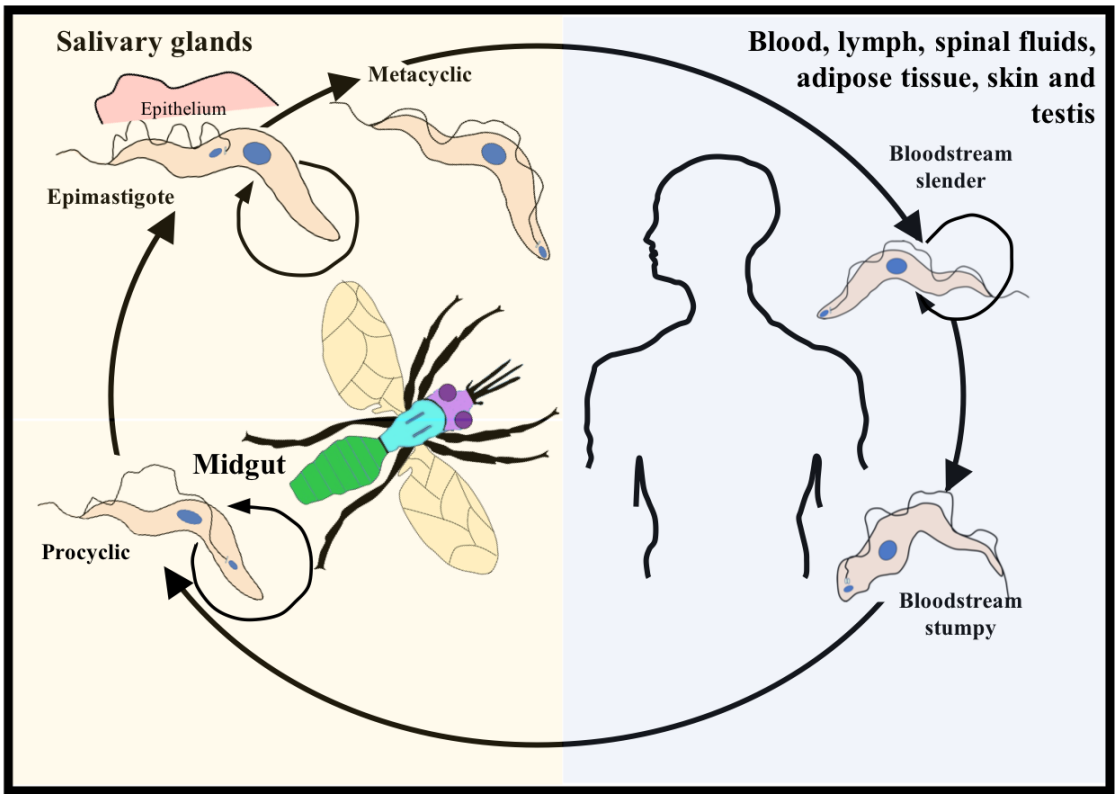

Figure 1.2 - Life Cycle of *T. brucei*. Diagram illustrating the cellular forms of *T. brucei* life cycle. These forms have different morphology. Briefly, the tsetse injects infective metacyclic trypomastigotes into the mammalian host, and the parasite differentiate into proliferative slender BSF (indicated with the arrow) in the blood. In these cells, the kDNA is located at the posterior end of the cell. As the population increases, the slender BSF differentiates into stumpy BSF. This form does not undergo cells division and pre-adapts for transmission to tsetse flies. Once this form is uptake in a tsetse blood meal, it transforms into procyclic cells that proliferates in the fly midgut. After they establish in the midgut, the parasites migrate to the salivary glands where they attach as epimastigotes forms. They proliferate by being attached with the flagellum to the epithelium. In epimastigotes, the kDNA is located in the anterior to the nucleus. Epimastigotes generates non-proliferative metacyclic which are preparing for transmission into a new mammalian host.

1.5 Unusual genomic organization in *T. brucei* and transcription

T. brucei has a genome size of 26 Mbp and comprises eleven diploid megabase-size chromosomes (0.9-6 Mbp), around 100 minichromosomes (30-150 kbp) and approximately 5 intermediate size chromosomes (200-900 kbp). The *T. brucei* genome encodes approximately 10,000 genes [47]. The three types of chromosomes have telomeric repeats. The megabase chromosomes have different segments or regions. It has a core region containing the housekeeping genes, which are transcribed by RNA polymerase II (RNA pol II) [48], and a telomeric region that flanks the core region and harbors arrays of VSG genes and pseudogenes [49]. Minichromosomes and intermediate chromosomes also contain VSG genes [50]. VSG genes are transcribed by RNA polymerase I and this occurs in a molecularly and functionally distinct nuclear compartment observed in the BSF of the parasite called the expression site body (ESB) [51]. In *T. brucei*, there is a transcriptional control mechanism where only one VSG gene is expressed at a given time. This monoallelic expression is based on the activation of only one of the ∼15 bloodstream expression sites (BES) present in *T. brucei* [52].

One of the striking features in *T. brucei* is how they organized their genome. The majority of the encoding genes are organized in directional gene clusters (DGC) also known as polycistronic transcription units (PTUs) [53–55]. The regions between DGCs located in opposite strands are known as strand switch regions (SSRs), and they can be divergent, convergent or have a head to tail orientation (HT) [55,56]. RNA polymerase II (RNA pol II) transcribes these DGC, although no RNA pol II promoter has been defined in *T. brucei* with exception for the spliced-leader (SL) RNA promoter [48]. These polycistronic mRNAs are then processed from the precursor to yield monocystronic

mRNAs through trans-splicing of a capped 5´terminal SL that is fused to the 5´UTR of the pre-mRNA, coupled with polyadenylation of the 3´UTR. These events produce a mature mRNA [57,58].

1.6 Eukaryotic and *T. brucei* DNA replication

DNA replication initiation is a multistep reaction that has to be accurately regulated to promote replication fork assembly and to control origin replication firing [59]. This process can be defined in two main steps. First, is the replication origin licensing where the pre-replication complex (pre-RC) recognizes and binds to the origin. Second is activation of DNA synthesis known as origin firing [60]. DNA replication in eukaryotes is characterized for having multiple origins that are often defined by local DNA structure and chromatin environment than by a sequence conservation [61,62]. An exception of the latter is budding yeast, where DNA segments called autonomous replication sequencing (ARS) serve as ORC recruitment [63]. Only a subset of licensed origins is activated in a cell. Selection of origin activation varies from cell to cell, even in the same cell population. This indicates that origin usage in eukaryotes is flexible [60,64,65]. Origin licensing occurs at G_1 phase, where the origin recognition complex (ORC), CDC6 and Cdt1 load the two MCM2-7 (minichromosome maintenance complex) helicase onto DNA [66–68]. ORC is composed of six subunits ORC1-6. ORC has ATPase activity and its binding to origin DNA requires ATP. ORC1-5 appear to be present in all eukaryotes and conserve the AAA+ folds, including the winged helix domain and the Walker A and Walker B motifs, that allow the ring-shaped structure to encircle DNA double helix. ORC6 has no structural similarity to the other subunits and is poorly conserved between yeast and other eukaryotic species.

In metazoans, ORC1, ORC4 and ORC5 contain functional ATP binding sites [66,69,70]. CDC6 also has an AAA+ domain and homology to ORC1. Once ORC is assembled on chromatin CDC6 binds to ORC. At this point, the ORC/CDC6 complex contains four ATP binding proteins (CDC6, ORC1, ORC4 and ORC5) allowing the recruitment and docking of Cdt1 and MCM2-7 complex onto origins. Cdt1 facilitates the recruitment of the MCM complex by inducing conformational changes within the MCM complex that relieve the autoinhibitory activity of MCM6 subunit [66]. The MCM complex is the core of the replicative DNA helicase and is an heterohexameric complex of 6 subunits MCM 2-7 that form a ring. MCM has two distinct modules. A C-terminal AAA++ domain that provides the ATPase activity for the helicase, and a N-terminal domain required for double hexamer attachment [71,72]. Origin activation requires activation of the MCM helicase complex. At the G1/S phase transition, kinases (DDK) and cyclin-dependent kinases (CDK) phosphorylate several replication factors including MCM10, CDC45, GINS complex (Sls5, Psf1, Psf2 and Psf3 subunits) and polymerase ε promoting their loading on origins. In addition, DDK and CDK phosphorylate several amino acids in the MCM complex that lead to helicase activation and DNA unwinding. At this point, the active helicase consists of CDC45, MCM and GINS, known as the CMG complex. CMG helicase activation recruits components of the replisome such as replication protein A (RPA), proliferating cell nuclear antigen (PCNA), replication factor C (RFC) and other DNA polymerases. This results in two functional replication forks that move in opposite directions from the activated origin [68,73].

Components of the replisome play roles in unwinding the DNA (helicases), processivity (sliding rings clamps and their loaders), DNA protection (single stranded

DNA [ssDNA] binding proteins) and DNA synthesis (primases and polymerases) [74]. PCNA is a homotrimeric sliding clamp that encircles duplex DNA and it binds directly to DNA polymerases, acting as a mobile tether that holds DNA polymerases for processive DNA synthesis [75]. Loading of PCNA onto DNA is performed in an ATP-dependent manner by the clamp loader replication factor C (RFC). RFC is a heteropentameric AAA+ protein complex consisting in subunits RFC1, RFC2, RFC3, RFC4 and RFC5 [76]. One of the major ssDNA binding proteins is replication protein A (RPA), which is a heterotrimeric enzyme. RPA has domains for protein-protein interaction and ssDNA binding [77]. This protein prevents formation of secondary structures and protects the DNA from nuclease degradation by coating exposed ssDNA [78].

DNA replication is a semiconservative process where DNA synthesis occurs in the 5´to 3´direction. The leading strand synthesis proceeds continuously while the lagging strand synthesis occurs in a discontinuous manner [79]. To initiate DNA synthesis, a primase generates a short RNA primer. DNA polymerase alpha (Pol α) is a four-subunit enzyme having two primase subunits that synthesize a 7-12 ribonucleotide oligomer. The 3´end of the oligomer is handed over intramolecularly to the Pol α active site so the RNA primer can be extended using dNTPs to form a strand of approximately 30 nucleotides in length [76,80,81]. In addition to Pol α, there are other two DNA polymerases, Pol δ and Pol ε, that participate on DNA synthesis. Pol α, Pol δ and Pol ε are members of the B family of DNA polymerases [68]. Pol ε synthesizes the leading strand while Pol δ synthesizes the lagging. In the lagging strand, there are discontinues stretches of DNA replication products known as Okakazi fragments, which are processed by FEN-1 endonuclease and DNA ligase. Pol δ extends primers on the lagging strand until encounters

and collides with the 5´end of the preceding Okazaki fragments. Pol δ continues replicating and displaces the RNA primer forming a short 5´end flap. This flap is a substrate for FEN-1 endonuclease which removes the RNA primer and then, the nick is filled by a DNA ligase [82] (Fig 1.3).

As mentioned above, the current view is that Pol ε is involved in leading strand synthesis and Pol δ in the lagging strand synthesis. However, there still uncertainty in these assignments and further studies are needed to clarify their functions in each strand [83]. Pol ε and Pol δ possess a 3´to 5´proofreading exonuclease activity, making them accurate DNA polymerases that can incorporate 2,000 bases/min with less than one single base error per million nucleotides polymerized [84]. Pol ε forms a complex with the CMG helicase complex, associating it with the leading strand, since CMG only encircles the leading strand. Compared to Pol δ, Pol ε does not perform efficient strand displacement synthesis, which is essential for Okazaki fragment maturation on the lagging strand [68]. For this reason, Pol δ is considered to be the major DNA polymerase involved in lagging strand synthesis. There have been observations where Pol ε catalytic subunit is not essential, and Pol α and Pol δ are sufficient to replicate the Simian Virus 40 genome [85]. A recent study proposed that Pol δ replicates both leading and lagging strand and Pol ε plays a role as a proofreading exonuclease removing the Pol δ generated errors from the leading strand [86]. All these studies keep the discussion of polymerase assignment open. Therefore, more studies are needed to propose or confirm any current model (Fig 1.3).

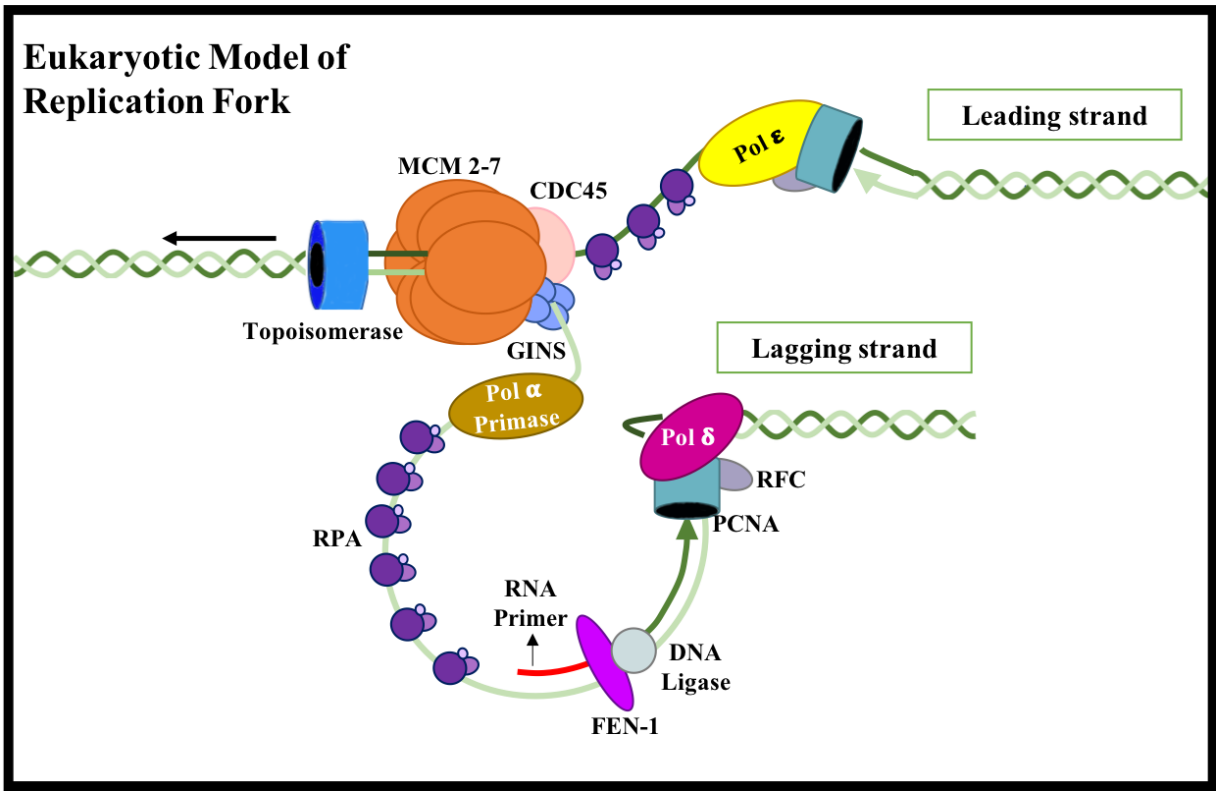

Figure 1.3 - Replication fork progression in model eukaryotes. DNA replication elongation begins with the activation of the MCM2-7 complex during the G1/S transition upon its phosphorylation. This phosphorylation event results in the formation of the CMG complex, which consists of CDC45, MCM2-7 and GINS, and the recruitment of MCM10 and DNA pol ε. Once the CMG complex is assembled and activated, it unwinds DNA to initiate DNA synthesis. Helicase activation recruits other DNA replication factors including RFC, PCNA, RPA and other DNA polymerases. At this point, there are two functional replication forks that move in opposite directions. DNA polymerases start to synthesize DNA from a RNA primer made by the DNA Pol α/ primase complex. This primer is extended by DNA pol δ (lagging strand) and DNA pol ε (leading strand). During DNA synthesis, DNA polymerase processivity is assured by DNA clamps such as PCNA, which is loaded by the clam loader RFC behind the replication fork. FEN-1 endonuclease and DNA ligases process Okazaki fragments in the lagging strand. Adapted from [96]

In *Trypanosoma brucei,* DNA replication has divergent features compared to other eukaryotes. Studies of DNA replication initiation in *T. brucei* have shown that this parasite has a divergent architecture of the ORC complex, where some subunits are not present and a single protein presents homology to both ORC1 and CDC6 (ORC1/CDC6) [87]. Orthologues of *T. brucei* ORC subunits ORC2, ORC3, ORC4, ORC5, and ORC6 could not be identified by sequence homology [88]. The TbORC4 subunit was identified by co-immunoprecipitation of TbORC1/CDC6. TbORC4 appears to be a highly divergent orthologue since it lacks critical and conserved residues involved in nucleotide and Mg++ binding, showing that TbORC4 has a weaker Walker A and B motifs, which are present in the AAA+ superfamily of ATPases [89]. Another factor named TbORC1b was identified and conserves ATPase motifs and interacts with TbORC1/CDC6. However, TbORC1b has failed in displaying ATPase activity [90]. Other factors that were found to interact with TbORC1/CDC6 are the trypanosome-specific factors Tb3120 and Tb7980, which are essential for parasite survival since their depletion caused failure to complete nuclear DNA replication and loss of nuclear DNA. There is weak evidence of an ATPase domain in Tb3120, and for Tb7980 this domain is completely absent [89]. In total, trypanosome expresses at least five ORC proteins (TbORC1/CDC6, TbORC1b, TbORC4, Tb3120 and Tb7980), but there is still no evidence that these proteins form a complex and if there is a sixth ORC like proteins that has not been identified [15].

Components of the MCM helicase complex are conserved in *T. brucei* together with CDC45 and members of the GINS complex. *T. brucei* CMG complex possesses *in vitro* helicase activity and interacts via MCM3 with TbORC1/CDC6 and TbORC1B *in vitro* and *in vivo*. Regulation of some of these components is also different in *T. brucei* when

compared to other eukaryotes. In *T. brucei,* the six subunits of the MCM complex display nuclear localization throughout the cell cycle from G_1 to telophase [90], which differs from the regulation that these subunits have in yeast, where they are exported out of the nucleus after DNA replication [91]. Furthermore, *T. brucei* CDC45 displays cell cycle localization where it resides in the nucleus during G_1 to G_2 phase, and then is excluded from the nucleus upon mitosis [90], while in human cells CDC45 is regulated by protein degradation [92]. Nevertheless, other factors involved in the assembly of the pre-RC complex such as Cdt1 or in the assembly of the CMG complex such as Sld2, Sld3 and DDK were not identified in *T. brucei* genome [47]

Despite these initial studies, the complete replisome of *T. brucei* has not been fully identified or characterized (Fig 1.4). Only one component of DNA replication elongation, PCNA, has been characterized in detailed. *T. brucei* PCNA depletion in BSF parasites resulted in reduction of cell proliferation, defects on DNA replication, cell cycle arrest at S phase and accumulation of parasites at G_2/M phases [93]. Recently, a study showed that TbPCNA is phosphorylated on serine and threonine residues [94], which differs to what is observed in human PCNA which is phosphorylated only in tyrosine residues [95].

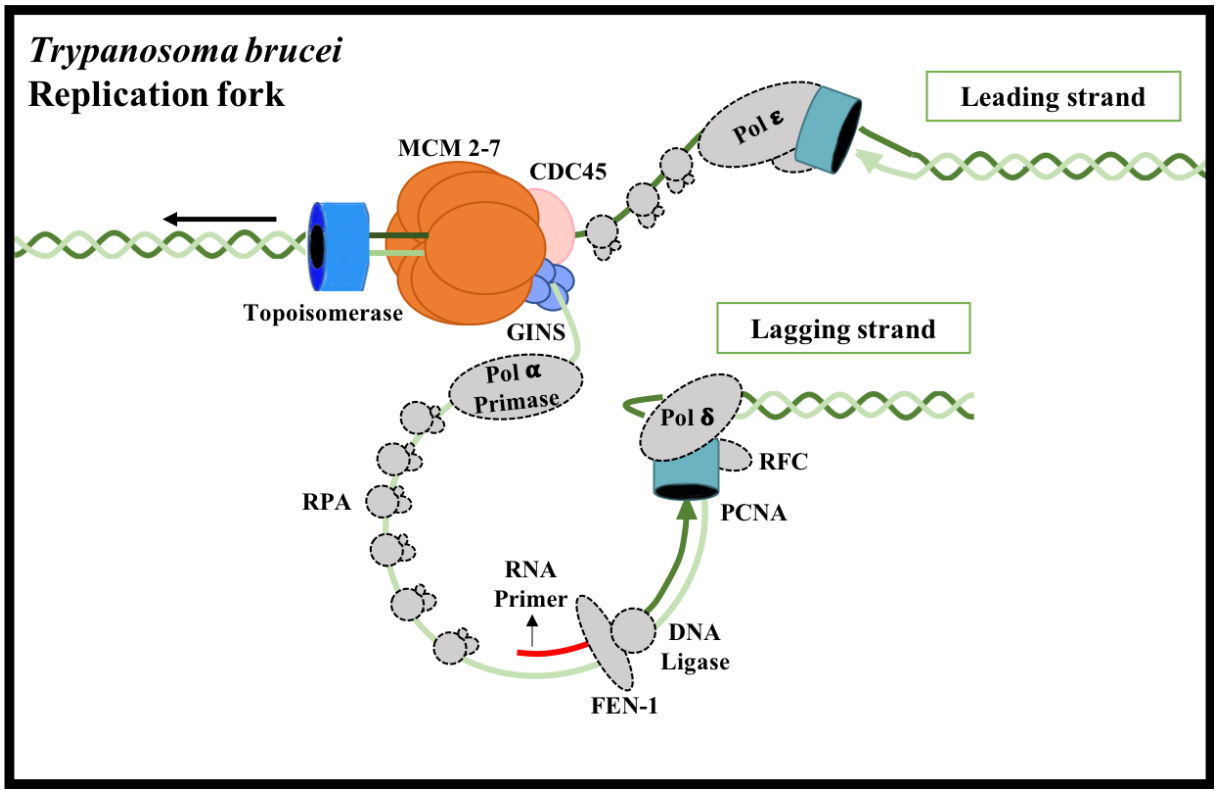

Figure 1.4 Replication fork progression model in *T. brucei*. Components of the replisome have been identified by sequence homology in *T. brucei*. Colored proteins have been characterized. Gray proteins have not been functional characterized in *T. brucei*. Adapted from [96]

1.7 Crosstalk between replication and other cellular processes.

The nucleus is the home of the genetic information of the cell. Genomic DNA is efficiently packed into chromatin but still must be accessible for DNA transactions processes such as DNA replication, DNA repair and transcription [97]. This accessibility is regulated during the cell cycle by having different nuclear compartments. This suggests that genomes function in the context of nuclear architecture, where the nucleus is spatiotemporally and functionally compartmentalized. These compartments can be distinguished by presenting morphological and/or functional differences compared to their surroundings [98]. For example, there are compartments where chromatin is highly condensed and closed for access (heterochromatin) and compartments that are less condensed and open (euchromatin) for different DNA-templated processes [99]. In terms of functionality, replication and transcription foci can be observed within the nucleus. Replication foci are sites where duplication of the chromosomal DNA is occurring and active replicons are located. These replication foci are very dynamic by presenting different distribution patterns within the nucleus at different time-lapse of S phase. In mammalian cells, at early S phase, multiple small foci are distributed in the nucleoplasm. At mid S phase, the pattern changes and the foci are concentrated around the nucleolus. At late S-phase, the foci are reduced by number but their size increases [100]. Transcription is also compartmentalized in the nucleus, where there are transcription foci for RNA polymerase I in the nucleolus [101] and there are transcription foci for RNA polymerase II, which has a heterogeneous distribution throughout the nucleoplasm [102]. There is an interphase between DNA replication and transcription, where active genes are replicated at early S phase, which means that origins of replication that fire at early S phase are located near to

active genes and could be clustered around transcription sites [100].

Genome-wide studies have provided evidence of the relationship between transcription and DNA replication timing. In mouse embryonic cells, 85% of the origins are associated with transcriptional units, and the origins density mapped in the mouse genome strongly correlated with the promoter density. Another interesting finding in this study is that the origins with higher firing efficiency are the ones located at CpG islands promoter sites [103]. Another study in human cells, origins were identified and characterized, and they showed that 75% of the activated origins overlapped with transcribed areas of the genome. This study suggested that colocalization of DNA replication and transcription initiation sites might provide a co-linearity progression of DNA replication forks and transcription complexes to prevent head on collisions and potential collapse [104].

Another two examples can be found in the kinetoplastids organisms *L. major* and *T. brucei.* In a recent study in *Leishmania major*, origins were mapped preferentially at genomic locations where RNA pol II is expected to slow or stall, this means at transcription termination sites (TTS). RNA pol II also localizes at sites where base J is found [105]. Base J is a thymine that is hydroxylated and glucosylated [106], and replaces 1% of thymine in the genome. It is predominantly present in telomeric repeats but, in the case of *Leishmania*, base J is also located at chromosome-internal RNA pol II termination sites [107]. SNS (small leading nascent strand) maxima occur immediately adjacent to the base J location and just downstream of the TTS. This study concludes that the spatial and temporal program of DNA replication in *L. major* can be explained in the context of RNA pol II kinetics [105].

A global analysis of DNA replication initiation in *T. brucei* showed that transcription and DNA replication initiation are very coordinated in terms of position and function. By mapping TbORC1 binding sites by ChIP, it was found that ORC1 localizes where the DGCs diverge, converge or at the junction between head-to-tail units. When performing RNAi of TbORC1, there was an increase in the mRNA levels of genes positioned at DGC boundaries, regions where TbORC1 is localized. Also, this protein was localized at the subtelomeric regions where the VSG genes are positioned [108]. Additionally, a recent study in *T. brucei* BSF parasites used marker frequency analysis with next generation sequencing (MFAseq) in combination with qPCR to measure how early is the replication of the active transcribed VSG gene. As a result, the active BES was the single mapped telomeric site that replicate at early S phase. This suggests that transcription of the active BES in the BSF of the parasite allows the site to become accessible for replication [109].

During DNA replication, the cell must maintain and transmit the proper chromatin organization and structure. Chromatin is disrupted ahead of the replication fork and then must be restored behind the fork on the two new daughter strands. Nucleosome assembly is the first step to maintain the chromatin structure and includes nucleosome remodeling, incorporation of histone variants and restoration of marks on DNA and histones [110]. Using simian virus 40 minichromosomes, it was observed that nucleosomes can be assembled at 250 bp distance from the replication fork [111]. Chromatin factors play a role in DNA replication. As an example, studies have shown that two histones chaperones, FACT and Asf1, are implicated in eukaryotic DNA replication fork progression *in vivo*. FACT has a physical association with CMG and Pol α [62]. Asf1 interacts with MCM via

Histone 3 and Histone 4, and depletion of Asf1 inhibits replisome progression during S phase in human cells [112]. In yeast, chromosome remodelers INO80 or ISW1A, and acetyltransferases Gcn5 and Esa1 stimulate DNA synthesis in the leading strand [62]. A recent study also in yeast showed that chromatin promotes origin dependence and nucleosome assembly during DNA replication regulates Okazaki fragment length by limiting Pol δ progression [113]. Based on these observations chromatin factors modulate replication rates *in vivo* by facilitating DNA replication factors functions at replication forks [62].

1.8 Goal of this study

This study aims to identify the proteins that are associated with an active unperturbed replication fork in *T. brucei*, and contribute to the understanding of the relationship between DNA replication with other cellular processes in this parasite using an unbiased technique called isolation of proteins on nascent DNA (iPOND). The DNA replication repertoire in this parasite has not been completely elucidated. Therefore, the following dissertation research was conducted to solve the following questions:

1) What is the complete repertoire of DNA replication proteins in *T. brucei*?

2) Are any kinetoplastid-specific proteins associated with nuclear DNA replication and its regulation?

3) Are other cellular processes coordinated with the DNA replication fork in *T. brucei*?

1.9 Significance and Contribution of this study.

By applying and optimizing the iPOND technology for the first time in a parasitic system, this study was able to identify the players that are present at active replication fork in *T. brucei.* This study was able to obtained a global view of the cellular processes that are participating in proximity to the replication fork, and provided a list of proteins that can represent trypanosome-specific factors that can be used in the future as therapeutic target to treat kinetoplastid related diseases such as Sleeping Sickness, Chagas disease and Leishmaniasis

1.10 Dissertation Overview

Following this introduction, Chapter 2 is focused on the optimization of the iPOND technology in *T. brucei* using procyclic cells. This chapter highlights several aspects of *T. brucei* biology that were important to consider in order to successfully apply this technique in this parasite, and addresses why iPOND was the best method available to identify the proteins involved in nascent DNA. Additionally, includes the modifications and the evaluation of each step of the iPOND protocol. Chapter 3 covers the mass spectrometry (MS) analysis and the identification of the proteins that were enriched in an active unperturbed replication fork. Provides a GO term analysis and a discussion of the cellular processes that were enriched in an active fork. Includes data of the initial characterization of two proteins identified by MS.

1.11 Bibliography

1. Votýpka J, d'Avila-Levy CM, Grellier P, Maslov DA, Lukeš J, Yurchenko V. New Approaches to Systematics of Trypanosomatidae: Criteria for Taxonomic (Re)description. Trends Parasitol. 2015;31: 460–469. doi:10.1016/j.pt.2015.06.015
2. Kaufer A, Ellis J, Stark D, Barratt J. The evolution of trypanosomatid taxonomy. Parasites and Vectors. Parasites & Vectors; 2017;10: 1–17. doi:10.1186/s13071-017-2204-7
3. Mitra AK, Mawson AR. Neglected Tropical Diseases: Epidemiology and Global Burden. Trop Med Infect Dis. 2017;2: 36. doi:10.3390/tropicalmed2030036
4. Sutherland CS, Stone CM, Steinmann P, Tanner M, Tediosi F. Seeing beyond 2020: an economic evaluation of contemporary and emerging strategies for elimination of Trypanosoma brucei gambiense. Lancet Glob Heal. The Author(s). Published by Elsevier Ltd. This is an Open Access article under the CC BY license; 2017;5: e69–e79. doi:10.1016/S2214-109X(16)30237-6
5. WHO. Report of the first WHO stakeholders meeting on rhodesiense human African trypanosomiasis elimination. 2015; 1–106.
6. Ponte-sucre A. An Overview of Trypanosoma brucei Infections : An Intense Host – Parasite Interaction. 2016;7: 1–12. doi:10.3389/fmicb.2016.02126
7. Aksoy S, Buscher P, Lehane M, Solano P, Abbeele J Van Den. Human African trypanosomiasis control : Achievements and challenges. PLoS Negl Trop Dis. 2017; 1–6.
8. Mogk S, Boßelmann CM, Mudogo CN, Stein J, Wolburg H, Duszenko M. African trypanosomes and brain infection – the unsolved question. 2017;1679: 1675–1687. doi:10.1111/brv.12301
9. Büscher P, Cecchi G, Jamonneau V, Priotto G. Human African trypanosomiasis. 2017;390: 2397–2409. doi:10.1016/S0140-6736(17)31510-6
10. Berninger M, Schmidt I, Ponte-Sucre A, Holzgrabe U. Novel lead compounds in pre-clinical development against African sleeping sickness. Med Chem Commun. 2017;8: 1872–1890. doi:10.1039/C7MD00280G
11. Girdhar S, Girdhar A, Lather V, Pandita D. Novel Therapeutic Targets for Human African Trypanosomiasis. Curr Treat Options Infect Dis. 2017;9: 200–209. doi:10.1007/s40506-017-0120-1
12. Kaiser M, Bray MA, Cal M, Trunz BB, Torreele E, Brun R. Antitrypanosomal activity of fexinidazole, a new oral nitroimidazole drug candidate for treatment of sleeping sickness. Antimicrob Agents Chemother. 2011;55: 5602–5608. doi:10.1128/AAC.00246-11
13. Jacobs RT, Nare B, Wring SA, Orr MD, Chen D, Sligar JM, et al. Scyx-7158, an orally-active benzoxaborole for the treatment of stage 2 human african trypanosomiasis. PLoS Negl Trop Dis. 2011;5. doi:10.1371/journal.pntd.0001151
14. Pasternack DA, Sharma AI, Olson CL, Epting CL, Engman DM. Sphingosine kinase regulates microtubule dynamics and organelle positioning necessary for proper G1/s cell cycle transition in trypanosoma brucei. MBio. 2015;6: 1–11. doi:10.1128/mBio.01291-15
15. Li Z. Regulation of the cell division cycle in Trypanosoma brucei. Eukaryot Cell.

2012;11: 1180–1190. doi:10.1128/EC.00145-12
16. Farr H, Gull K. Cytokinesis in trypanosomes. Cytoskeleton. 2012;69: 931–941. doi:10.1002/cm.21074
17. Wheeler RJ, Scheumann N, Wickstead B, Gull K, Vaughan S. Cytokinesis in trypanosoma brucei differs between bloodstream and tsetse trypomastigote forms: Implications for microtubule-based morphogenesis and mutant analysis. Mol Microbiol. 2013;90: 1339–1355. doi:10.1111/mmi.12436
18. Akiyoshi B, Gull K. Evolutionary cell biology of chromosome segregation: insights from trypanosomes. Open Biol. 2013;3: 130023–130023. doi:10.1098/rsob.130023
19. Gluenz E, Povelones ML, Englund PT, Gull K. The kinetoplast duplication cycle in Trypanosoma brucei is orchestrated by cytoskeleton-mediated cell morphogenesis. Mol Cell Biol. 2011;31: 1012–21. doi:10.1128/MCB.01176-10
20. Woodward R, Gull K. Timing of nuclear and kinetoplast DNA replication and early morphological events in the cell cycle of Trypanosoma brucei. J Cell Sci. 1990;95: 49–57.
21. Siegel TN, Hekstra DR, Cross GAM. Analysis of the Trypanosoma brucei cell cycle by quantitative DAPI imaging. Mol Biochem Parasitol. 2008;160: 171–174. doi:10.1016/j.molbiopara.2008.04.004
22. McKean PG. Coordination of cell cycle and cytokinesis in Trypanosoma brucei. Curr Opin Microbiol. 2003;6: 600–607. doi:10.1016/j.mib.2003.10.010
23. Tu X, Wang CC. Pairwise knockdowns of cdc2-related kinases (CRKs) in Trypanosoma brucei identified the CRKs for G1/S and G2/M transitions and demonstrated distinctive cytokinetic regulations between two developmental stages of the organism. Eukaryot Cell. 2005;4: 755–764. doi:10.1128/EC.4.4.755-764.2005
24. Li Z, Wang CC. A PHO80-like cyclin and a B-type cyclin control the cell cycle of the procyclic form of Trypanosoma brucei. J Biol Chem. 2003;278: 20652–20658. doi:10.1074/jbc.M301635200
25. Gourguechon S, Savich JM, Wang CC. The Multiple Roles of cyclin E1 in Controlling Cell Cycle Progression and Cellular Morphology of Trypanosoma brucei. J Mol Biol. 2007;368: 939–950. doi:10.1016/j.jmb.2007.02.050
26. Tu X, Wang CC. The Involvement of Two cdc2-related Kinases (CRKs) in Trypanosoma brucei Cell Cycle Regulation and the Distinctive Stage-specific Phenotypes Caused by CRK3 Depletion. J Biol Chem. 2004;279: 20519–20528. doi:10.1074/jbc.M312862200
27. Li Z, Wang CC. Changing roles of aurora-B kinase in two life cycle stages of Trypanosoma brucei. Eukaryot Cell. 2006;5: 1026–1035. doi:10.1128/EC.00129-06
28. Li Z, Lee JH, Chu F, Burlingame AL, G??nzl A, Wang CC. Identification of a novel chromosomal passenger complex and its unique localization during cytokinesis in Trypanosoma brucei. PLoS One. 2008;3. doi:10.1371/journal.pone.0002354
29. Tu X, Kumar P, Li Z, Wang CC. An aurora kinase homologue is involved in regulating both mitosis and cytokinesis in Trypanosoma brucei. J Biol Chem. 2006;281: 9677–9687. doi:10.1074/jbc.M511504200

30. Umeyama T, Wang CC. Polo-like kinase is expressed in S/G2/M phase and associated with the flagellum attachment zone in both procyclic and bloodstream forms of Trypanosoma brucei. Eukaryot Cell. 2008;7: 1582–1590. doi:10.1128/EC.00150-08
31. Silvester E, McWilliam K, Matthews K. The Cytological Events and Molecular Control of Life Cycle Development of Trypanosoma brucei in the Mammalian Bloodstream. Pathogens. 2017;6: 29. doi:10.3390/pathogens6030029
32. Stijlemans B, Caljon G, Van Den Abbeele J, Van Ginderachter JA, Magez S, De Trez C. Immune evasion strategies of Trypanosoma brucei within the mammalian host: Progression to pathogenicity. Front Immunol. 2016;7. doi:10.3389/fimmu.2016.00233
33. Siegel TN, Hekstra DR, Wang X, Dewell S, Cross GAM. Genome-wide analysis of mRNA abundance in two life-cycle stages of Trypanosoma brucei and identification of splicing and polyadenylation sites. Nucleic Acids Res. 2010;38: 4946–4957. doi:10.1093/nar/gkq237
34. Veitch N, Johnson PCD, Trivedi U, Terry S, Wildridge D, MacLeod A. Digital gene expression analysis of two life cycle stages of the human-infective parasite , Trypanosoma clusters of co-regulated genes . 2010; 1–14. doi:10.1186/1471-2164-11-124
35. Nilsson D, Gunasekera K, Mani J, Osteras M, Farinelli L, Baerlocher L, et al. Spliced leader trapping reveals widespread alternative splicing patterns in the highly dynamic transcriptome of Trypanosoma brucei. PLoS Pathog. 2010;6: 21–22. doi:10.1371/journal.ppat.1001037
36. Jensen BC, Ramasamy G, Vasconcelos EJR, Ingolia NT, Myler PJ, Parsons M. Extensive stage-regulation of translation revealed by ribosome profiling of trypanosoma brucei. BMC Genomics. 2014;15: 1–21. doi:10.1186/1471-2164-15-911
37. Ooi C-P, Bastin P. More than meets the eye: understanding Trypanosoma brucei morphology in the tsetse. Front Cell Infect Microbiol. 2013;3: 1–12. doi:10.3389/fcimb.2013.00071
38. Savage AF, Kolev NG, Franklin JB, Vigneron A, Aksoy S, Tschudi C. Transcriptome profiling of Trypanosoma brucei development in the tsetse fly vector Glossina morsitans. PLoS One. 2016;11: 1–20. doi:10.1371/journal.pone.0168877
39. Smith TK, Bringaud F, Nolan DP, Figueiredo LM. Metabolic reprogramming during the Trypanosoma brucei life cycle. F1000Research. 2017;6: 683. doi:10.12688/f1000research.10342.1
40. Matthews KR, McCulloch R, Morrison LJ. The within-host dynamics of African trypanosome infections. Philos Trans R Soc B Biol Sci. 2015;370: 20140288. doi:10.1098/rstb.2014.0288
41. MacGregor P, Szöo'R B, Savill NJ, Matthews KR. Trypanosomal immune evasion, chronicity and transmission: An elegant balancing act. Nat Rev Microbiol. 2012;10: 431–438. doi:10.1038/nrmicro2779
42. Trindade S, Rijo-Ferreira F, Carvalho T, Pinto-Neves D, Guegan F, Aresta-Branco F, et al. Trypanosoma brucei Parasites Occupy and Functionally Adapt to the Adipose Tissue in Mice. Cell Host Microbe. 2016;19: 837–848.

doi:10.1016/j.chom.2016.05.002
43. Caljon G, Van Reet N, De Trez C, Vermeersch M, Pérez-Morga D, Van Den Abbeele J. The Dermis as a Delivery Site of Trypanosoma brucei for Tsetse Flies. PLoS Pathog. 2016;12: 1–22. doi:10.1371/journal.ppat.1005744
44. Capewell P, Cren-Travaillï¿½ C, Marchesi F, Johnston P, Clucas C, Benson RA, et al. The skin is a significant but overlooked anatomical reservoir for vector-borne African trypanosomes. Elife. 2016;5: 1–17. doi:10.7554/eLife.17716
45. Carvalho T, Trindade S, Pimenta S, Santos AB, Rijo-Ferreira F, Figueiredo LM. Trypanosoma brucei triggers a marked immune response in male reproductive organs. PLoS Negl Trop Dis. 2018;12: e0006690. doi:10.1371/journal.pntd.0006690
46. Claes F, Vodnala SK, Van Reet N, Boucher N, Lunden-Miguel H, Baltz T, et al. Bioluminescent imaging of Trypanosoma brucei shows preferential testis dissemination which may hamper drug efficacy in sleeping sickness. PLoS Negl Trop Dis. 2009;3: 1–10. doi:10.1371/journal.pntd.0000486
47. Berriman M, Ghedin E, Hertz-Fowler C, Blandin G, Renauld H, Bartholomeu DC, et al. The genome of the African trypanosome Trypanosoma brucei. Science. 2005;309: 416–422. doi:10.1126/science.1112642
48. Schimanski B, Nguyen TN, Gunzl A. Characterization of a Multisubunit Transcription Factor Complex Essential for Spliced-Leader RNA Gene Transcription in Trypanosoma brucei. Mol Cell Biol. 2005;25: 7303–7313. doi:10.1128/MCB.25.16.7303
49. Cross GAM, Kim HS, Wickstead B. Capturing the variant surface glycoprotein repertoire (the VSGnome) of Trypanosoma brucei Lister 427. Mol Biochem Parasitol. Elsevier B.V.; 2014;195: 59–73. doi:10.1016/j.molbiopara.2014.06.004
50. Horn D. Antigenic variation in African trypanosomes. Mol Biochem Parasitol. Elsevier B.V.; 2014;195: 123–129. doi:10.1016/j.molbiopara.2014.05.001
51. Navarro M, Gull K. A poll transcriptional body associated with VSG mono-allelic expression in Trypanosoma brucei. Nature. 2001;414: 759–763. doi:10.1038/414759a
52. Glover L, Hutchinson S, Alsford S, Mcculloch R, Field MC, Horn D. Antigenic variation in African trypanosomes: The importance of chromosomal and nuclear context in VSG expression control. Cell Microbiol. 2013;15: 1984–1993. doi:10.1111/cmi.12215
53. Imboden MA, Laird PW, Affolter M, Seebeck T. Transcription of the intergenic regions of the tubulin gene cluster of Trypanosoma brucei: Evidence for a polyclstronic transcription unit in a eukaryote. Nucleic Acids Res. 1987;15: 7357–7368. doi:10.1093/nar/15.18.7357
54. Muhich ML, Boothroyd JC. Polycistronic transcripts in trypanosomes and their accumulation during heat shock: evidence for a precursor role in mRNA synthesis. Mol Cell Biol. 1988;8: 3837–46. doi:10.1128/MCB.8.9.3837.Updated
55. Daniels J-P, Gull K, Wickstead B. Cell Biology of the Trypanosome Genome. Microbiol Mol Biol Rev. 2010;74: 552–569. doi:10.1128/MMBR.00024-10
56. Siegel TN, Gunasekera K, Cross GAM, Ochsenreiter T. Gene expression in Trypanosoma brucei: Lessons from high-throughput RNA sequencing. Trends Parasitol. Elsevier Ltd; 2011;27: 434–441. doi:10.1016/j.pt.2011.05.006

57. Milhausen M, Nelson RG, Sather S, Selkirk M, Agabian N. Identification of a small RNA containing the trypanosome spliced leader: A donor of shared 5′sequences of trypanosomatid mRNAs? Cell. 1984;38: 721–729. doi:10.1016/0092-8674(84)90267-8
58. Liang X, Haritan A, Uliel S. trans and cis Splicing in Trypanosomatids : Mechanism , Factors , and Regulation MINIREVIEWS trans and cis Splicing in Trypanosomatids : Mechanism , Factors , and Regulation. Eukaryot Cell. 2003;2: 830–840. doi:10.1128/EC.2.5.830
59. Riera A, Barbon M, Noguchi Y, Reuter LM, Schneider S, Speck C. From structure to mechanism—understanding initiation of DNA replication. Genes Dev. 2017;31: 1073–1088. doi:10.1101/gad.298232.117
60. Fragkos M, Ganier O, Coulombe P, Méchali M. DNA replication origin activation in space and time. Nat Rev Mol Cell Biol. Nature Publishing Group; 2015;16: 360–374. doi:10.1038/nrm4002
61. Costa A, Hood I V., Berger JM. Mechanisms for Initiating Cellular DNA Replication. Annu Rev Biochem. 2013;82: 25–54. doi:10.1146/annurev-biochem-052610-094414
62. Kurat CF, Yeeles JTP, Patel H, Early A, Diffley JFX. Chromatin Controls DNA Replication Origin Selection, Lagging-Strand Synthesis, and Replication Fork Rates. Mol Cell. Elsevier Inc.; 2017;65: 117–130. doi:10.1016/j.molcel.2016.11.016
63. Stinchcomb DT, Struhl K, Davis RW. Isolation and characterisation of a yeast chromosomal replicator. Nature. 1979;282: 39–43. doi:10.1038/282039a0
64. Cayrou C, Coulombe P, Vigneron A, Stanojcic S, Ganier O, Peiffer I, et al. Genome-scale analysis of metazoan replication origins reveals their organization in specific but flexible sites defined by conserved features. Genome Res. 2011;21: 1438–1449. doi:10.1101/gr.121830.111
65. Kanter DM, Bruck I, Kaplan DL. Mcm subunits can assemble into two different active unwinding complexes. J Biol Chem. 2008;283: 31172–31182. doi:10.1074/jbc.M804686200
66. Yardimci H, Walter JC. Prereplication-complex formation: A molecular double take? Nat Struct Mol Biol. Nature Publishing Group; 2014;21: 20–25. doi:10.1038/nsmb.2738
67. Masai H, Matsumoto S, You Z, Yoshizawa-Sugata N, Oda M. Eukaryotic Chromosome DNA Replication: Where, When, and How? Annu Rev Biochem. 2010;79: 89–130. doi:10.1146/annurev.biochem.052308.103205
68. Burgers PMJ, Kunkel TA. Eukaryotic DNA Replication Fork. Annu Rev Biochem. 2017;86: 417–438. doi:10.1146/annurev-biochem-061516-044709
69. Duncker BP, Chesnokov IN, McConkey BJ. The origin recognition complex protein family. Genome Biol. 2009;10: 214. doi:10.1186/gb-2009-10-3-214
70. Li, Huilin; Stillman B. The Eukaryotic Replisome: a Guide to Protein Structure and Function. 2012;62: 37–58. doi:10.1007/978-94-007-4572-8
71. Martinez MP, Wacker AL, Bruck I, Kaplan DL. Eukaryotic replicative helicase subunit interaction with DNA and its role in DNA replication. Genes (Basel). 2017;8. doi:10.3390/genes8040117
72. Pellegrini L, Costa A. New Insights into the Mechanism of DNA Duplication by

the Eukaryotic Replisome. Trends Biochem Sci. Elsevier Ltd; 2016;41: 859–871. doi:10.1016/j.tibs.2016.07.011
73. Fragkos M, Ganier O, Coulombe P, Méchali M. DNA replication origin activation in space and time. Nat Rev Mol Cell Biol. Nature Publishing Group; 2015;16: 360–74. doi:10.1038/nrm4002
74. Dewar JM, Walter JC. Mechanisms of DNA replication. Nat Rev Mol Cell Biol. Nature Publishing Group; 2013;18: 403–19. doi:10.5772/52656
75. Georgescu R, Langston L, O'Donnell M. A proposal: Evolution of PCNA's role as a marker of newly replicated DNA. DNA Repair (Amst). Elsevier B.V.; 2015;29: 4–15. doi:10.1016/j.dnarep.2015.01.015
76. Ulrich HD. New insights into replication clamp unloading. J Mol Biol. Elsevier Ltd; 2013;425: 4727–4732. doi:10.1016/j.jmb.2013.05.003
77. Liu T, Huang J. Replication protein A and more: Single-stranded DNA-binding proteins in eukaryotic cells. Acta Biochim Biophys Sin (Shanghai). 2016;48: 665–670. doi:10.1093/abbs/gmw041
78. Chen R, Wold MS. Replication protein A: Single-stranded DNA's first responder: Dynamic DNA-interactions allow replication protein A to direct single-strand DNA intermediates into different pathways for synthesis or repair Prospects & Overviews R. Chen and M. S. Wold. BioEssays. 2014;36: 1156–1161. doi:10.1002/bies.201400107
79. Leman AR, Noguchi E. The replication fork: Understanding the eukaryotic replication machinery and the challenges to genome duplication. Genes. 2013. doi:10.3390/genes4010001
80. Coloma J, Johnson RE, Prakash L, Prakash S, Aggarwal AK. Human DNA polymerase α in binary complex with a DNA:DNA template-primer. Sci Rep. Nature Publishing Group; 2016;6: 1–10. doi:10.1038/srep23784
81. Perera RL, Torella R, Klinge S, Kilkenny ML, Maman JD, Pellegrini L. Mechanism for priming DNA synthesis by yeast DNA Polymerase α. Elife. 2013;2013: 1–22. doi:10.7554/eLife.00482
82. Stodola JL, Burgers PM. Mechanism of DNA replication in eukaryotes. In: Masai H, Foiani M, editors. DNA Replication Advances in Experimental Medicine and Biology. Springer, Singapore; 2017. pp. 117–133.
83. Yao N, O'Donnell M. Bacterial and Eukaryotic Replisome Machines. JSM Biochem Mol Biol. 2016;3: 1–15. doi:10.1038/nbt.3121.ChIP-nexus
84. Kunkel TA, Burgers PMJ. Arranging eukaryotic nuclear DNA polymerases for replication: Specific interactions with accessory proteins arrange Pols α, δ, and ϵ in the replisome for leading-strand and lagging-strand DNA replication. BioEssays. 2017;39: 1–6. doi:10.1002/bies.201700070
85. Stillman B. Reconsidering DNA Polymerases at the Replication Fork in Eukaryotes. Mol Cell. Elsevier Inc.; 2015;59: 139–141. doi:10.1016/j.molcel.2015.07.004
86. Johnson RE, Klassen R, Prakash L, Prakash S. A Major Role of DNA Polymerase delta in Replication of Both the Leading and Lagging DNA Strands. Mol Cell. Elsevier Inc.; 2015;59: 163–175. doi:10.1016/j.molcel.2015.05.038
87. De Melo Godoy PD, Nogueira-Junior LA, Paes LS, Cornejo A, Martins RM, Silber AM, et al. Trypanosome prereplication machinery contains a single

functional Orc1/Cdc6 protein, which is typical of archaea. Eukaryot Cell. 2009;8: 1592–1603. doi:10.1128/EC.00161-09
88. Tiengwe C, Marques CA, McCulloch R. Nuclear DNA replication initiation in kinetoplastid parasites: New insights into an ancient process. Trends Parasitol. Elsevier Ltd; 2014;30: 27–36. doi:10.1016/j.pt.2013.10.009
89. Tiengwe C, Marcello L, Farr H, Gadelha C, Burchmore R, Barry JD, et al. Identification of ORC1/CDC6-interacting factors in trypanosoma brucei reveals critical features of origin recognition complex architecture. PLoS One. 2012;7: 22–24. doi:10.1371/journal.pone.0032674
90. Dang HQ, Li Z. The Cdc45 Mcm2-7 GINS protein complex in trypanosomes regulates DNA replication and interacts with two Orc1-like proteins in the origin recognition complex. J Biol Chem. 2011;286: 32424–32435. doi:10.1074/jbc.M111.240143
91. Nguyen VQ, Co C, Irie K, Li JJ. Clb/Cdc28 kinases promote nuclear export of the replication initiator proteins Mcm2-7. Curr Biol. 2000;10: 195–205. doi:10.1016/S0960-9822(00)00337-7
92. Pollok S, Grosse F. Cdc45 degradation during differentiation and apoptosis. Biochem Biophys Res Commun. 2007;362: 910–915. doi:10.1016/j.bbrc.2007.08.069
93. Valenciano AL, Ramsey AC, Mackey ZB. Deviating the level of proliferating cell nuclear antigen in trypanosoma brucei elicits distinct mechanisms for inhibiting proliferation and cell cycle progression. Cell Cycle. 2015;14: 674–688. doi:10.4161/15384101.2014.987611
94. Valenciano AL, Knudsen GM, Mackey ZB. Extracellular-signal regulated kinase 8 of Trypanosoma brucei uniquely phosphorylates its proliferating cell nuclear antigen homolog and reveals exploitable properties. Cell Cycle. Taylor & Francis; 2016;15: 2827–2841. doi:10.1080/15384101.2016.1222340
95. Wang S-C, Nakajima Y, Yu Y-L, Xia W, Chen C-T, Yang C-C, et al. Tyrosine phosphorylation controls PCNA function through protein stability. Nat Cell Biol. 2006;8: 1359–1368. doi:10.1038/ncb1501
96. da Silva MS, Pavani RS, Damasceno JD, Marques CA, McCulloch R, Tosi LRO, et al. Nuclear DNA Replication in Trypanosomatids: There Are No Easy Methods for Solving Difficult Problems. Trends Parasitol. Elsevier Ltd; 2017;33: 858–874. doi:10.1016/j.pt.2017.08.002
97. Schneider R, Grosschedl R. Dynamics and interplay of nuclear architecture , genome organization , and gene expression. 2007; 3027–3043. doi:10.1101/gad.1604607.The
98. Misteli T. Concepts in nuclear architecture. BioEssays. 2005;27: 477–487. doi:10.1002/bies.20226
99. Yu S, Yang F, Shen WH. Genome maintenance in the context of 4D chromatin condensation. Cell Mol Life Sci. Springer International Publishing; 2016;73: 3137–3150. doi:10.1007/s00018-016-2221-2
100. Chakalova L, Debrand E, Mitchell JA, Osborne CS, Fraser P. Replication and transcription: Shaping the landscape of the genome. Nat Rev Genet. 2005;6: 669–677. doi:10.1038/nrg1673
101. Jackson DA, Hassan AB, Errington RJ, Cook PR. Visualization of focal sites of

transcription within human nuclei. EMBO J. 1993;12: 1059–65.
102. Iborra FJ, Pombo A, Jackson D a, Cook PR. Active RNA polymerases are localized within discrete transcription "factories'' in human nuclei." J Cell Sci. 1996;109; Pt 6: 1427–1436.
103. Sequeira-Mendes J, Díaz-Uriarte R, Apedaile A, Huntley D, Brockdorff N, Gómez M. Transcription initiation activity sets replication origin efficiency in mammalian cells. PLoS Genet. 2009;5. doi:10.1371/journal.pgen.1000446
104. Langley AR, Gräff S, Smith JC, Krude T. Genome-wide identification and characterisation of human DNA replication origins by initiation site sequencing (ini-seq). Nucleic Acids Res. 2016;44: 10230–10247. doi:10.1093/nar/gkw760
105. Lombraña R, Alvarez A, Fernandez-Justel JM, Almeida R, Poza-Carrion C, Gomes F, et al. Transcriptionally Driven DNA Replication Program of the Human Parasite Leishmania major. Cell Rep. 2016;16: 1774–1786. doi:10.1016/j.celrep.2016.07.007
106. Gommers-ampt JH, Teixeira AJR, Van De Werken G, Van Dijk WJ, Borst P. The identification of hydroxymethyluracil in DNA of Trypanosoma brucei. Nucleic Acids Res. 1993;21: 2039–2043. doi:10.1093/nar/21.9.2039
107. Van Luenen HGAM, Farris C, Jan S, Genest PA, Tripathi P, Velds A, et al. Glucosylated hydroxymethyluracil, DNA base J, prevents transcriptional readthrough in Leishmania. Cell. 2012;150: 909–921. doi:10.1016/j.cell.2012.07.030
108. Tiengwe C, Marcello L, Farr H, Dickens N, Kelly S, Swiderski M, et al. Genome-wide analysis reveals extensive functional interaction between DNA replication initiation and transcription in the genome of trypanosoma brucei. Cell Rep. Elsevier; 2012;2: 185–197. doi:10.1016/j.celrep.2012.06.007
109. Devlin R, Marques CA, Paape D, Prorocic M, Zurita-Leal AC, Campbell SJ, et al. Mapping replication dynamics in Trypanosoma brucei reveals a link with telomere transcription and antigenic variation. Elife. 2016;5: 1–30. doi:10.7554/eLife.12765
110. Alabert C, Groth A. Chromatin replication and epigenome maintenance. Nat Rev Mol Cell Biol. Nature Publishing Group; 2012;13: 153–167. doi:10.1038/nrm3288
111. Sogo, J.M; Stahl, H;Koller, Th;Knippers R. Structure of Replicating Simian Virus 40 Minichromosomes The Replication Fork, Core Histone Segregation and Terminal Structures. J mo. 1986; 189–204.
112. Groth A, Corpet A, Cook AJL, Roche D, Bartek J, Lukas J, et al. Regulation of Replication Fork Supply and Demand. Science (80-). 2007;318: 1928–1932.
113. Devbhandari S, Jiang J, Kumar C, Whitehouse I, Remus D. Chromatin Constrains the Initiation and Elongation of DNA Replication. Mol Cell. Elsevier Inc.; 2017;65: 131–141. doi:10.1016/j.molcel.2016.10.035

CHAPTER 2

OPTIMIZATION OF *TRYPANOSOMA BRUCEI* iPOND

2.1 Introduction

2.1.1 Current techniques and improvements to study DNA replication

Research on DNA replication dynamics is progressively growing due to the development of new technologies that are solving many questions about the complexity of DNA replication. These techniques include microscopy methods that allow the quantitative assessment of genome wide replication speed and relative positioning of replicating DNA. Examples of these are single molecule DNA fiber analysis, genome combing, super resolution microscopy and digital image analysis [1–3]. Other advances include techniques that address DNA-protein interactions [4] and proteomics tools that facilitate the identification, purification and quantification of machineries that are at the replication fork [5].

Genomic, proteomic and imaging technologies, such as Repli-seq [6], Chromatin interaction analysis by paired-end tag sequencing (ChIA-PET) [7] and 3D DNA FISH [8], are coming together in the 4D nucleome network project with the purpose to map the structure and dynamics of the genomes in space and time. With the combination of these techniques, the scientific community will achieve a deeper understanding of how the nucleus is organized and define the functional role that several structural features of chromosome organization impact key cellular processes such as DNA replication and transcription [9].

2.1.2 Microscopy analysis of DNA replication

DNA fiber analysis has contributed to the understanding of fork dynamics at single molecule resolution by investigating the pattern of replication origin firing and replication fork velocities [10]. In DNA fiber analysis, ongoing replication events are followed by labelling newly synthesized DNA in a sequential manner using two consecutive thymidine analogs such as 5-iodo-2´-deoxyuridine (IdU) and 5-chloro-2´-deoxyuridine (CldU) [11]. These analogs are visualized by immunostaining to allow genome wide DNA replication tracking of individual DNA molecules, and to monitor changes in replication fork progression, fork symmetry and origin firing [12]. Studies combining DNA fiber analysis with electron microscopy (EM) have led the visualization of a higher number of replication intermediates and monitor their remodeling under stress condition. Using these two tools it was recently shown that human DNA2 (DNA replication helicase/nuclease 2) which is involved in Okazaki processing, is required for stalled fork processing and restart by degrading nascent strands at stalled forks in order to resume DNA synthesis [13]. Another observation was that DNA2 participates in processing reversed replication forks. Replication fork reversal is a protective mechanism where fork progression is reversed when forks encounter DNA lesions and restart DNA synthesis [14]. This study showed that upon DNA2 depletion there was an increment of the frequency of fork reversal events [13]. This study was an example that combining two powerful techniques such as DNA fiber analysis and EM, can highly contribute to the understanding of DNA replication profiles not only under normal conditions but also under stress.

Technical developments and improvements in optical microscopy have allowed the visualization of replication sites in live or fixed cells with a higher spatial resolution [3].

Structured Illumination Microscopy (SIM) is one of the super resolution microscopy techniques that have been extremely useful to study chromatin structure. A 100 nm resolution is achieved using a 3D-SIM microscope allowing the visualization of nuclear compartments and function [15]. The landscape of the nucleus was studied using 3D-SIM and different compartments were identified such as the interchromatin compartment (IC), chromatin domains (CD) and the perichromatin region (PR). The PR is a 100-200 nm thick layer of decondensed chromatin. The distribution of replicating DNA, nascent RNA, RNA polymerase II and the active chromatin mark H3K4me3 was highly enriched at the PR [16].

2.1.3 Tools to study DNA-protein interaction

There are classic techniques that have been used to study DNA-protein interactions. These include *in vitro* techniques such as DNase I footprinting assay, electrophoretic mobility shift assay (EMSA) and yeast one hybrid system (YIH) [17,18]. DNase I footprinting has been used to identify the replication origins in microbial genomes including *Escherichia coli* [19], *Caulobacter crescentus* [20] and the archaeon *Sulfolobus solfataricus* [21]. EMSA is a useful technique to analyze the dynamic subunit composition of protein complexes bound to nucleic acid under different conditions [18]. For example, a recent study using EMSA showed that RPA plays a role in nucleosome assembly during DNA replication since this protein interacts with Histone 3 and Histone 4 in the formation of histone-DNA complexes [22]. The YIH has been used to identify essential proteins, such as ORC6, that interacts *in vivo* with yeast origin of replication [23]. There are also i*n vivo* techniques that have been developed to characterize DNA-protein interactions. An example of these techniques is Chromatin immunoprecipitation (ChIP) and all its variants. One of

the widely used variants is ChIP sequencing (ChIP-seq) since provides a higher resolution, requires less starting material and has a low cost compared to ChIP-chip techniques, where ChIP is combined with microarray technology. ChIP-seq, was used for genome-wide mapping of human ORC1 DNA binding sites and DNA replication origins. It was found that ORC1 binding sites were associated with transcription start sites (TSS) and transcription levels at the ORC1 sites correlated with replication timing [24].

Other approach to study DNA-protein interactions is by manipulating *Xenopus laevis* eggs [4]. Soluble egg extracts are used as a model system for DNA replication studies since they reconstitute the essential nuclear changes of the eukaryotic cells *in vitro* as they occur *in vivo* [25]. *Xenopus* eggs are arrested in metaphase of meiosis II, resembling the mitotic phase in somatic cells. These extracts can be induced to enter to interphase. When exogenous DNA is added to egg extracts at interphase it is first organized into chromatin and then incorporated into fully functional synthetic nuclei. These nuclei can undergo rounds of DNA replication allowing the study of this essential cellular process [4,25–27]. *Xenopus* eggs extracts were recently used to show that nucleosomes are not required for the condensation of mitotic chromosome. This study indicated the formation of chromatid-like structures that were assembled in almost complete absence of nucleosomes and that condensins could bind to the DNA of these structures in a nucleosome-independent manner [28].

2.1.4 Proteomic techniques in DNA replication studies

Proteomic techniques that aim to identify the proteins at the replication forks have been developed. These can be separated into two main approaches. The first approach

identifies and purifies interacting partners of a known replisome protein that acts as a bait. However, this approach is unable to directly distinguish machineries involved in active forks and cannot purify the complete machinery present at the replication fork and its vicinity unless using multiple protein baits. In the second approach, DNA is the bait and these techniques are able to monitor spatiotemporally the protein dynamics at the replication fork by purifying proteins associated with newly synthesized DNA and the ones associated with the bulk of chromatin in pulse chase experiments [5,29,30]. Examples of the second approach include a technology called nascent chromatin capture (NCC) and isolation of proteins on nascent DNA (iPOND). NCC allows to profile the chromatin dynamics during replication by labeling with biotin-dUTP nascent DNA and performing affinity purification coupled with quantitative proteomics. In NCC, biotin-dUTP cannot be incorporated into intact cells. Therefore, cells have to be permeabilized by exposing them to a short hypotonic shift that will not affect S phase progression or trigger a DNA damage response [5,31]. Using NCC, a recent study determined that in nascent chromatin new histones were exclusively unmethylated at H4K20. This indicates that H4K20me0 is a signature of post-replicative chromatin [32]. In iPOND newly replicated DNA is labeled with the thymidine analog 5-ethynyl-2′-deoxyuridine (EdU) [33]. One of the advantages of EdU labeling is that it does not require sample fixation or DNA denaturation [33]. EdU contains an alkyne functional group that enables the cycloaddition of a biotin azide. This click chemistry reaction [34] yields a stable covalent linkage, facilitating streptavidin capture of cross-linked biotinylated DNA-protein complexes [29] (see below).

2.1.5 Isolation of Proteins on nascent DNA (iPOND)

The iPOND technology was developed with the aim to provide site-specific analysis of replisomes by the identification of proteins associated with replication forks and to determine how these factors are coordinated at the replication site to maintain genome integrity [35]. This technology has been used to track protein recruitment to active and damaged forks, and to monitor chromatin deposition and maturation [36–39]. Different methods have been used to assess cell proliferation, including detection of replicating cells by immunolabeling methods that use thymidine analogs such as 5-bromo-2′-deoxyuridine (BrdU) [40]. However, BrdU detection requires harsh treatment methods to give access to anti-BrdU antibody to nucleosides in genomic DNA. These treatments include DNA denaturation and hydrolysis with HCl and DNase [41]. The iPOND technology uses EdU as the thymidine analog to label newly synthesized DNA. EdU has several advantages compared to BrdU. It is a molecule small enough to diffuse freely through DNA and the cells are not subjected to harsh denaturation conditions for its detection. EdU has a terminal alkyne group that allows its detection when performing a copper catalyzed cycloaddition (click chemistry reaction) with a biotin azide. This click chemistry reaction does not require a denaturation step and therefore, the material is preserved during the process [33,42].

The iPOND procedure has the following key steps: EdU-labeling of nascent DNA, formaldehyde cross-linking of DNA-protein complexes, click chemistry, cell lysis, DNA sonication, streptavidin capture, protein elution and Mass Spectrometry (MS) analysis. The first step in the iPOND procedure is incubating cells with EdU for a short period time (between 2-10 min) followed by formaldehyde cross-linking to stop DNA replication and cross-link DNA-protein complexes and protein-protein complexes. Next, cells are

permeabilized and click chemistry reaction is performed to yield a stable covalent linkage between EdU and the biotin azide. The cells are then lysed under denaturation conditions followed by a sonication step that generates solubilized DNA-protein. In the streptavidin capture step, only those DNA-protein complexes in which DNA is biotin-labeled will be purified, and after proteins are eluted from DNA and separated from each other by SDS and heat treatment, the samples can be analyzed by MS or immunoblotting [5,29]. There are two different negative controls that can be used in iPOND. One negative control is to not expose the cells to EdU but instead are treated with only the carrier, DMSO. In the other negative control cells are exposed to EdU but the click chemistry reaction cocktail lacks biotin-azide. The iPOND procedure can also be applied to distinguish the proteins associated with active replisomes from the ones that are part of the bulk of chromatin by performing an EdU pulse-thymidine chase experiment. In this manner, iPOND can monitor changes in chromatin located at various distances from the replication fork [29,35,36].

The application of iPOND has identified 290 proteins that are enriched in nascent DNA at active, stalled and collapsed replication forks in human cells [35]. Around 84% of the identified proteins did not have a known role in DNA replication or damage response [35]. This technology was also applied in mouse embryonic stem cells and showed that there is a marked enrichment of protein complexes involved in chromatin remodeling and modification at the replication fork such as the nucleosomal remodeling and deacetylase (NuRD) complex [37]. Recently, iPOND was adapted in vaccinia virus, the prototype poxvirus, to identify proteins involved in viral DNA replication [43]. In addition to known viral replication proteins, viral DNA-dependent RNA polymerase and transcription initiation and elongation factors were identified on nascent DNA. This suggested that there

is temporal coupling of DNA replication and transcription at active replication forks in poxviruses [43].

These data highlight the potential of iPOND as a tool to elucidate the complete functional replisome by the identification of unknown factors that are present at active replication forks and chromatin maturation. *T. brucei* proteins are extremely divergent in sequence and it is very likely that many replication proteins remain to be identified. To study DNA replication dynamics in the human pathogen *Trypanosoma brucei*, we have optimized the iPOND technique for the first time in a parasitic system using an ORC1PTP single expresser cell line. Here we describe the aspects of *T. brucei* biology that were needed to be considered for making accurate modifications to the original iPOND protocol. We include the evidence that the key steps of the iPOND procedure were optimized in order to purify DNA replication factors from the parasite such that the final elution was suitable for a meaningful MS analysis.

2.2 Materials and methods

2.2.1 ORC1PTP Single expresser cell line (Generated by Anthula Vandoros)

The PTP coding sequence [44] was inserted into the endogenous ORC1 allele by transfecting the parasites with the pORC1-PTP-NEO plasmid. This construct was generated by amplifying the C-terminal end of ORC1 using primers containing ApaI and EagI restrictions sites. The final construct was sent for sequencing. The procyclic *T. brucei* Lister 427 strain was transfected with SalI-linearized pORC1-PTP-NEO plasmid by electroporation. Initial selection of a stable population was done in SDM-79 media containing 50 μg/ml of G418. After performing limited dilution as described previously

[45], a clonal cell line, PIG5, was selected by verifying PTP expression by western blot and chromosomal integration via PCR and Southern blot. TbORC1$^{PTP/WT}$ PIG5 was transfected using the pKOORC1^{Hyg} plasmid (gift from Dr. Bibo Li Lab) digested with ApaI and NotI. Selection of a stable population was done using SDM-79 media supplemented with 50 μg/ml of G418 and 50 μg/ml of Hygromycin. Limited dilution was performed again and final clonal cell line (TbORC1$^{PTP/KO}$ P2C2) was verified by western blot for PTP expression. Chromosomal integration of the PTP tag allele and KO allele was checked by Southern blot. TbORC1$^{PTP/KO}$ P2C2 cell line (TbORC1PTP) was functional by having a double time similar to wild-type cells of approximately 10 hours.

2.2.2 *T. brucei* iPOND EdU pulse and Negative controls

A total of 3 x10^{10} cells were labeled with 150 μM EdU (Santa Cruz) for 10 min. Cells were pelleted at 3000 *x g* for 7 min, the supernatant was discarded and the cell pellet was resuspended to a cell density of approximately 7.5 x 10^8 cells/mL in SDM 079 medium containing 1.1% formaldehyde and incubated for 20 min at room temperature (RT) to cross-link DNA-protein complexes. The reaction was quenched by adding 2M glycine to a final concentration of 0.125 M and incubated for 5 min at RT. Fixed samples were washed three times with cold 1X PBS for 7 min each at 1250 *x g*, and frozen at -80°C. Cell pellets were thawed on ice for 30 min followed by homogenization in 0.25% Triton-X 100 (permeabilization buffer), using a douncer until no cell clumps were visible. Solubilized sample was incubated for 30 min at RT with a cell density of 1 x 10^9 cells/mL at 112 rpm. After 2 washes, one in 0.5% BSA 1X PBS, the other one in 1X PBS, the click chemistry cocktail (0.2M biotin-azide, 50 mM sodium ascorbate and 10 mM of $CuSO_4$) was prepared

and used to resuspend the cells using a vortex. Cells were incubated in the click chemistry cocktail for 2 hours at RT and using a rotator. Cells were then washed once with 0.5% BSA 1X PBS buffer and a second time with 1X PBS buffer. For cell lysis, the suspension was homogenized 30 times with a douncer and treated with 0.1% NP40 in SME buffer (0.25M sucrose, 10mM MOPS pH 7.2, 2mM EDTA, 1mM PMSF, and 1µg/ml leupeptin and one tablet of cOmplete EDTA-free Protease Inhibitor Cocktail (Roche)) for 1 hour on ice with shaking. This was followed by nitrogen cavitation at 2250 psi (equilibration time of 20 min using SME buffer with 0.1% SDS). If necessary, this step was repeated until 85% -99% lysis (via microscopy) was achieved using psi to 1500 and 10 min of equilibration time. Differential centrifugation was applied to enrich nuclear fraction at 1250 x g for 10 min. Nuclear fraction was washed once with SME buffer with no additives and a second time with PBS. Nuclear fraction or pellet was then resuspended and homogenize in sonication buffer (0.7% wt/vol SDS in 50 mM Tris pH 8.0, 1 µg/ml leupeptin and one tablet of cOmplete EDTA-free Protease Inhibitor Cocktail (Roche)). This nuclear suspension was sonicated 5X (10 min 30s $^{ON/OFF}$) using the Bioruptor UCD-200 (Diagenode). To remove debris, the sonicated sample was centrifuged at 16000 *x g* for 10 min. Streptavidin agarose beads were equilibrated by washing twice the beads (250 µl beads slurry) with Sonication buffer and one time with 1XPBS containing protease inhibitor. Beads were resuspended in 1:1 volume of PBS until added to the sonicated suspension (input). To capture the biotinylated DNA-protein complexes, the input was applied to the beads and incubated O/N at 4°C using a rotator. Streptavidin-agarose beads with captured DNA-protein were pelleted or 3 min at 3500 rpm RT and washed first with streptavidin wash buffer (2% wt/vol SDS in 50 mM Tris-HCl, pH 7.4, 150 mM NaCl) followed with a 1M NaCl wash and

finally by repeating two washes with streptavidin wash buffer. Each washing step included 5 min of rotation and a centrifugation step of 1 min at 1800 *x g* at RT. Tubes were changed between washes. Proteins were eluted by heating the beads at 95°C for 25 min in 2X SDS Laemmli buffer supplemented with 5% BME. Protein samples were used for MS and western blot analysis. Two negative controls were used to discriminate background, one is DMSO control where the cells were not exposed with EdU, and the second negative control is the No Click Chemistry control where the click chemistry cocktail lacks biotin-azide. Three biological replicates were done for each condition

2.2.3 *T. brucei* iPOND Pulse-Chase experiments (Performed by Dr. Michele Klingbeil and Yahaira Bermudez)

A total of 3 x 10^{10} cells was pulsed with 150 μM EdU for 10 min and immediately centrifuged at 3000 x g for 7 min at RT. All media left that contained EdU was siphon off using an aspirator. Cells were resuspended in new media containing 150μM Thymidine and incubated for 10 min. the remaining steps such as formaldehyde cross-linking, permeabilization, click chemistry, cell lysis, sonication, streptavidin capture and protein elution were performed as described above.

2.2.4 Cross-Link Reversal and DNA fragmentation analysis

To reverse the cross-links, the input fraction from each iPOND condition were treated with a final concentration of 0.2M of NaCl and incubated O/N at 64°C. DNA samples were treated with RNase for 30 min at 37°C followed by Proteinase K (Ambion) treatment for 2 hours at 45°C. DNA was concentrated by performing a Phenol/Chloroform

extraction followed by Ethanol precipitation. DNA was quantified using a nanodrop 800 (Thermo Scientific). To visualize the DNA fragments, a 100 ng of DNA was loaded in a 1.5% Agarose gel and ran for 2 hours at 75 V.

2.2.5 Dot blot Click Chemistry efficiency test

Serially diluted biotinylated tubulin primers ranging from 0.25 pmol to 16 pmol served as the standard. Input fractions from each iPOND condition were quantified by nanodrop. Biotinylated oligo DNA and input fraction DNA (2 µg per replicate) were treated with 1 M NaOH, heated at 55°C (30 min) followed by addition of 2 M of ammonium acetate. Subsequently, samples and biotinylated standards are ready to be spotted onto a nylon membrane (GE healthcare science). Biotinylated standards were spotted in triplicate and the sonicated samples were spotted in duplicate. Membrane was air dried and UV cross-linked for 7 min using a UV Stratalinker 1800 (Stratagene). Membrane was immediately placed in blocking solution (20% non-fat milk) for 2 hours at 37˚C. Membrane was then rinsed three times in 0.1% PBST and incubated with Avidin-HRP (1:3000, Life Technologies) for 30 min at 37 ˚C followed by 3 washes in 0.1 % PBST for 15 min. ImageQuant LAS 4000 mini (GE healthcare science) was used for detection and data were quantified using ImageJ.

2.2.6 EdU and PTP Immunofluorescence

TbORC1PTP cell line was labeled with 150μM of EdU for 10 min. Cells were harvested for 5 min at 1,000 × g, washed with 1XPBS and adhered to poly-L-Lysine-coated slides. Cells were then fixed in 3% PFA for 5 min and washed three times (5 min each) in

1XPBS containing 0.1 M glycine (pH 7.4) followed by permeabilization with 0.1% Triton for 5 min and washed three times in 1XPBS. Click chemistry was performed the Picolyl Azide Toolkit (Life Technologies) manufacture´s recommendations. The click chemistry reaction was incubated for 1 hour at RT followed by three washes of 5 min in 1XPBS. DNA was stained with 3 μg/ml 4′-6′-diamidino-2-phenylindole (DAPI), and slides were washed 3 times in PBS prior to mounting in Vectashield (Vector Laboratories).

2.2.7 Western blot

For Histone 3 (H3) and for mono-, di- and trimethylated H3 at lysine 76 (H3K76) detection, samples were run on a SDS-PAGE and transfer O/N at 85 mAmp. Blocking was done in 3% non-fat milk in 1XPBS for two hours for H3 and for the H3K76me1, H3K76me2 and H3K76me3 blocking solution was 3% of BSA in 1XPSB. The membrane was probe against Histone 3, H3K76me1, H3K76me2 and H3K76me3 using the respective polyclonal antibodies that were kindly provided by Christian Janzen. For H3 the rabbit antiserum was diluted 1:50000 in 0.3% blocking solution, for H3K76me1 1:300, H3K76me2 1:1500 and H3K76me3 1:3000. Membrane was incubated for 2 hours. After three washes with 1X TBS with 0.1% tween 20, the blot was incubated with HRP anti-rabbit secondary antibody (1:5000) for 1 hour in 0.3% blocking solution. Blot was washed three times with 1X TBS with 0.1% tween 20.

ORC1PTP tagged protein was detected using Peroxidase-Anti-Peroxidase (PAP) (1:2000) for PTP detection. For Hsp70 detection the blot was probed against *Crithidia fasciculata* specific Hsp70 antibody (1:10000) followed by secondary chicken anti-rabbit

antibody (1:2000). Detection was observed by ImageQuant LAS 4000 mini (GE healthcare science).

2.3. Results

2.3.1 Biological aspects of *T. brucei* for iPOND optimization

To purify proteins that associate with nascent DNA in *T. brucei*, we adapted the original iPOND method developed in the laboratory of Dr. David Cortez (Vanderbilt University) [36]. A major limitation of iPOND is the large amount of starting material needed to recover enough protein for proteomic analysis. Therefore, several aspects of trypanosome biology were considered when calculating the amount of starting material needed for efficient purification. These biological aspects included *T. brucei* genome size 26 Mbp [46], the time of S phase (90 min) [47], the percentage of cells that are in S phase in an unsynchronized population (20%-30%) [48], and the DNA replication rate which is 3.7 kb/min in *T. brucei* procyclic form (PFC) (Table 2.1). Using this information, we modified several steps of the iPOND original procedure [35] including the total number of cells labeled with EdU, EdU concentration, biotin azide concentration, lysis conditions, sonication conditions for DNA fragmentation and streptavidin capture conditions (Fig. 2.1). All these modifications were with the purpose to label approximately 28 μg of DNA in a 10 min pulse. This amount of EdU-labeled DNA was achieved in iPOND procedures performed in a mammalian system using a total of 1.6×10^9 cells. In *T. brucei* iPOND, 3×10^{10} of TbORC1PTP PCF cells were needed to obtained that amount (Table 2.1). Additionally, compared to the mammalian system where 10 μM of EdU was used to label DNA, *T. brucei* PCF required 150 μM of EdU to its incorporation in a 10 min pulse (Fig.

2.2A). *T. brucei* required 15 times more of EdU because it lacks high affinity transporters for thymidine [49]. The high EdU concentration in our study is in accordance with other *T. brucei* labeling studies in which 100-300 μM EdU was applied for 1 hr to uniformly label the nucleus for studies on PCNA [50,51]. Our conditions to label DNA in a 10 min pulse we were able to observe discrete spots that likely represent DNA replication foci (Fig. 2.2A). No modifications were needed for the cross-linking step.

Due the increment on EdU concentration and to yield an efficient click chemistry reaction in *T. brucei*, we modified the final concentration of biotin azide (200 μM) in the reaction cocktail 20 times more compared to the original protocol developed in mammals (10 μM), and in this way we are saturating the system so all the EdU molecules available will be bound to a biotin-azide. This modified amount of biotin azide was used also in iPOND procedures performed in mouse embryonic cells [37]. Cell lysis conditions were also modified. Because *T. brucei* possess a sub-pellicular corset of microtubules [52], the parasites were too rigid to lyse after cross-linking with formaldehyde, therefore nitrogen cavitation was used together with detergent treatment to open the cells (Fig 2.1). Under these conditions, 85%-95% of the cells were lysed. The whole cell extract (WCE) was centrifuged and the pellet (P_1) fraction was observed under the microscope to confirm nuclear integrity and enrichment (Fig 2.2B). At this step, the pellet was ready for sonication. All these modifications based on *T. brucei* biology were essential to make iPOND a suitable tool to study DNA replication in parasites.

Table 2.1 Comparison of DNA replication parameters between mammalian cells and *T. brucei* for iPOND optimization

Parameter	Mammalian cells (293T) [a]	*Trypanosoma brucei* (procyclic form)
Genome size	3000 Mb[b]	26 Mb
% of cells in S phase	50%[c]	20%-30%[d]
Replication time	480 min[e]	90 min
Replication rate	1.5 kb/min[f]	3.7 kb/min
~Kbp labeled in 10 min	15	37
Estimate firing forks	2138[g]	78[h]
Kbp labeled/fork	32070	2886
Number of cells	1.6×10^9	3×10^{10}
Cells in S phase	8×10^8	7.5×10^9
Total labeled kbp	2.56×10^{13}	2.16×10^{13}
Total µg labeled DNA	**28.1 µg**	**23.7 µg**
Total µg of DNA	5399.1	854.6
% DNA labeled	0.52%	2.77%

[a] Human embryonic kidney cells [29]
[b] [53]
[c] [54]
[d] [48]
[e] [55]
[f] [56]
[g] [57]

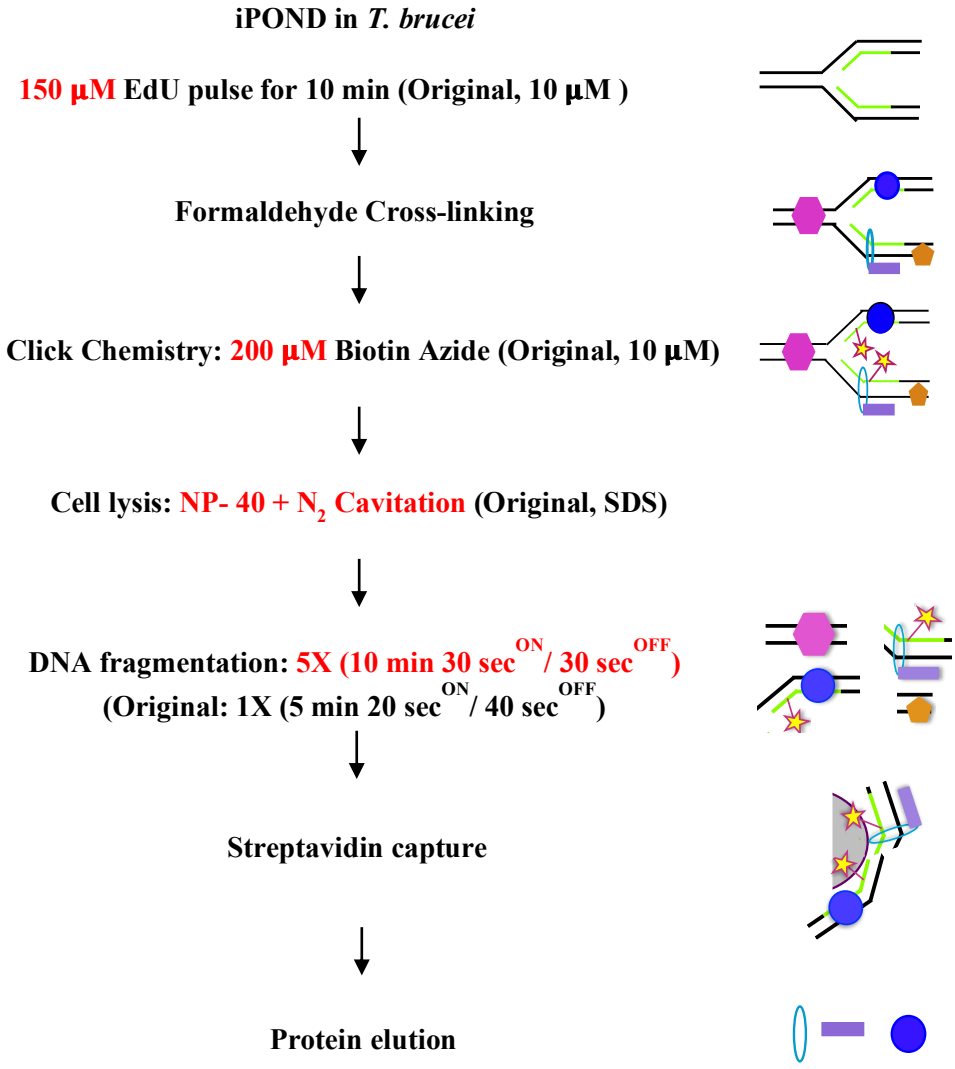

Figure 2.1 - Schematic overview of modified iPOND procedure for *T. brucei*

In red the modifications that were implemented in several steps of the iPOND procedure compared to the original method performed in mammalian cells. The iPOND procedure consist in labeling nascent DNA *in vivo* using EdU (green), cross-linking DNA protein complexes with formaldehyde, a click chemistry reaction that covantly links EdU-labeled DNA with biotin azide (stars), lysing the cells and fragmenting DNA by sonication, capturing DNA-protein complexes by streptavidin affinity and protein elution by heat and detergent treatment.

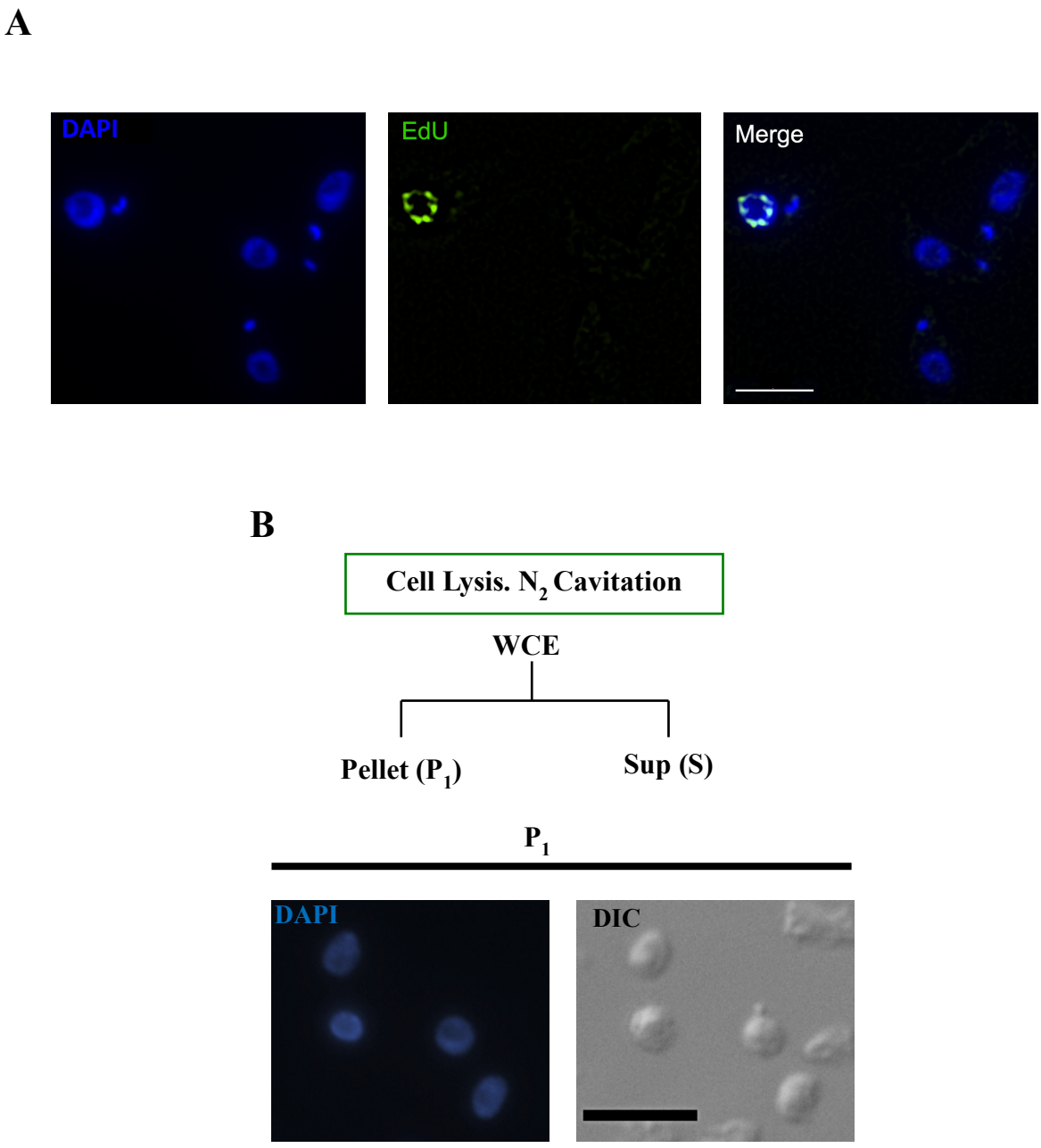

Figure 2.2 - EdU incorporation on nascent DNA and Nuclear enrichment

A) Cells were EdU-labeled with 150 μM Edu (for 10 min**)**. DNA is stained with DAPI. Size bar is 5 **µ**m B) *Upper panel***.** Schematic representation of the cell lysis and differential centrifugation**.** *Lower panel.* Microscopy showing enrichment of nuclear fraction in the pellet. Integrity of the nucleus is maintained after cell lysis. Size bar is 6 **µ**m

2.3.2. Verification and Validation of *T. brucei* iPOND procedure

To validate our iPOND procedure with its modification, we performed iPOND in four different conditions, two negative controls and two experimental conditions. The two negative controls are called DMSO (D) and No Click (C-). The D negative control consists of cells that were not EdU labeled and only were exposed with the carrier, DMSO, but the click chemistry cocktail had biotin azide. The C- control consists of cells that were EdU labeled but the click chemistry reaction did not have the biotin azide. One experimental condition is exposing the cells for a 10 min EdU pulse (E), while the other condition is a 10 min EdU pulse followed by a 60 min thymidine chase, (ThD chase, T). All these conditions were tested by dot blotting for click chemistry efficiency, DNA fragmentation, western blotting for detection of markers and MS analysis (see chapter 3)

The iPOND technology relies on click chemistry, which is a copper-catalyzed reaction that allows the cycloaddition of an alkyne functional group (present in EdU) to an azide (conjugated in biotin) yielding a stable covalent bond. To evaluate if our modification in the click chemistry reaction cocktail allowed detection of biotinylated DNA in our samples we performed dot blotting with a standard curve of biotinylated tubulin oligomers and with the sonicated or input fraction from the different four iPOND conditions (Fig 2.3A). The standard curve consisted of biotinylated tubulin primers ranging from 0.25 pmol to 16 pmol that were used to the estimate amount of biotinylated DNA following click chemistry. To test the four conditions, approximately 2 μg of reversed cross-linked DNA from the input fraction from each condition (D, C-, E and T) were spotted on a membrane and probed against biotinylation (Fig 2.3B, Left panel; Fig 2.3C). Both negative controls have no detection. Detection of biotinylated DNA was observed in the EdU pulse sample

and using the standard curve, the detection signal corresponded to 1.76 pmoles (~0.12µg of DNA) of biotinylated DNA from the 2 µg of DNA that were spotted (Fig. 2.3B, Right panel). For the standard curve, we did not consider the 16 pmol intensity since it was oversaturated. Biotinylated DNA was also present in our EdU pulse-Thymidine chase experiment (T) (Fig. 2.3C).

Prior to the sonication step, we probed the pellet (P_1) and supernatant (S) fraction (Fig. 2.3A) against our nuclear marker Occ1PTP and mitochondrial marker Hsp70. ORC1PTP was only detected in the pellet fraction were the nucleus is enriched (Fig 2.4A). The pellet fraction was sonicated and yielded DNA fragments between 50-200 bp (Fig 2.4B), facilitating the capture of DNA-protein complexes by streptavidin beads.

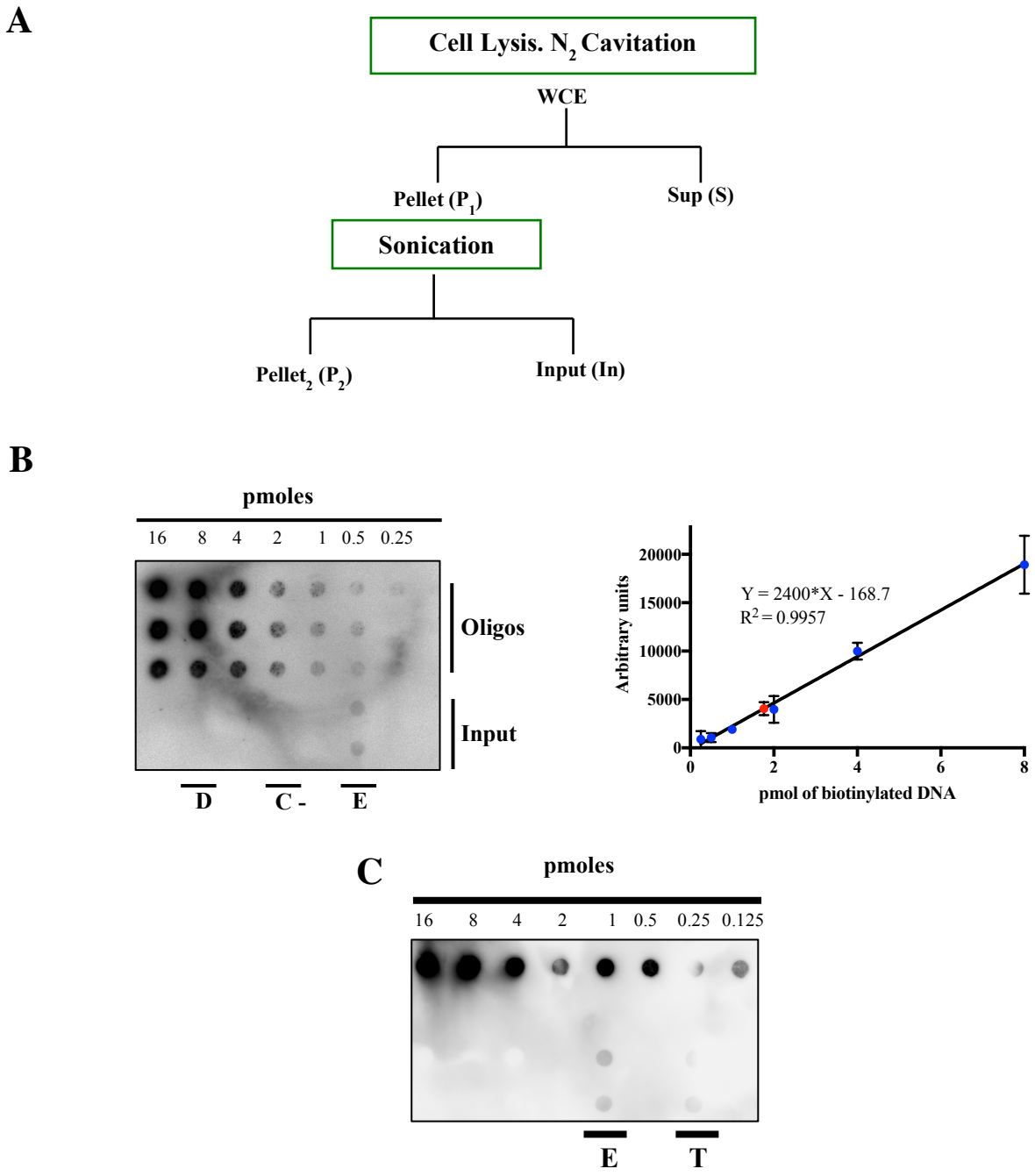

Figure 2.3 - Biotin detection after Click Chemistry reaction

A) Schematic representation of the different fractions used to track iPOND optimization. B) Quantification of biotinylated DNA in four iPOND conditions. *Left panel*, Dot blot to measure biotin incorporation in sonicated samples (input) from negative controls (DMSO; D and Click-; C-), ThD chase (T), and EdU (E) pulse samples. *Right panel*. Standards (blue circles) and EdU sample (red square) were plotted. An estimate of 1.67 pmoles of biotinylated DNA is obtained in the E sample. C) Detection of biotinylated DNA from EdU pulse (E) and ThD chase sample (T). Standard curve was included.

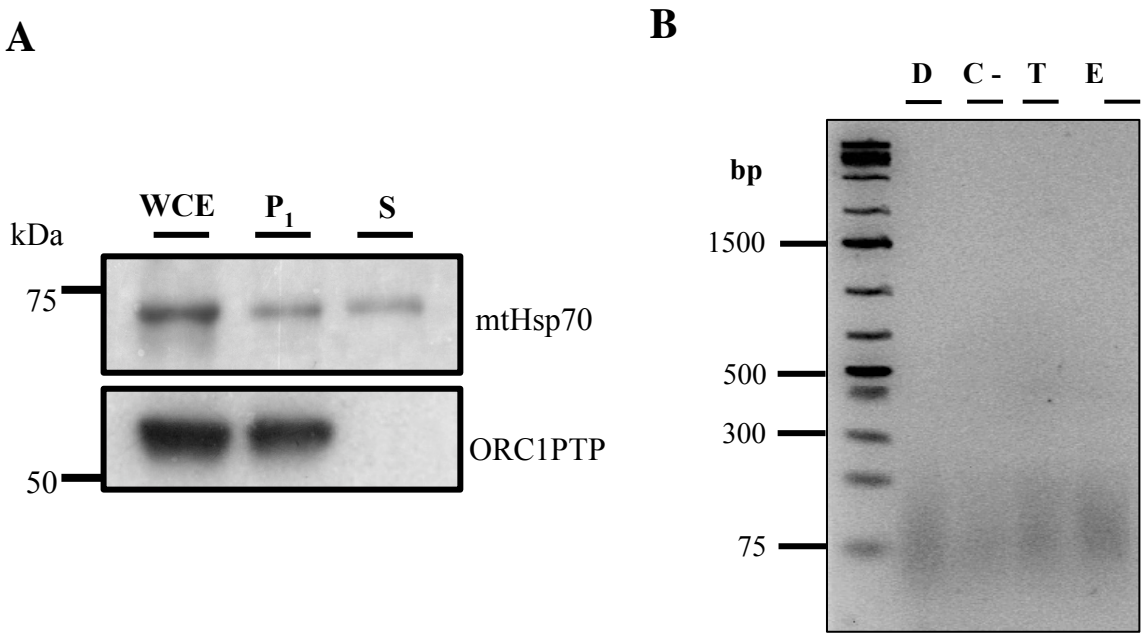

Figure 2.4 - Nuclear marker enrichment in pellet fraction and DNA fragmentation analysis

A) Differential centrifugation separated the nuclear fraction (P_1) from mitochondria and cell debris (S). Enrichment of nucleus was determined by western blot probing against ORC1PTP and mitochondrial Hsp70. B) A total 5 cycles of sonication yielded DNA fragments between 50 bp to 200 bp, 100 bp fragments are enriched in all iPOND conditions. DMSO (D), Click- (C-), ThD chase (T), and EdU pulse (E)

2.3.3 Final eluate analysis.

To differentiate between proteins associated with nascent DNA, such as DNA polymerase α and the bulk of chromatin, such as modified histones, we compared iPOND from a 10 min EdU pulse with iPOND from a 10 min EdU pulse followed by a 60 min ThD chase. The short pulse should restrict DNA labeling to the vicinity of the replication fork, while during the ThD chase labeled DNA should have moved away from the fork and undergone chromatin deposition and remodeling. Histone deposition (without modification) is coupled with DNA replication, although the precise timing of deposition is still debated [58,59].

Final eluates from our negative controls (D and C-), EdU pulse (E) and ThD chase (T) (Fig 2.5A) were analyzed by western blot prior to MS analysis by detection of *T. brucei* histone 3 (H3) and for 1, 2 and 3 methylated groups in H3 at lysine 76 (H3K76me1, H3K76me2 and H3K76me3, respectively) (Fig 2.5B). There is a subtle detection H3 in the EdU sample while its signal increases in the ThD chase sample (Fig 2.5B and C). Methylated H3 are mainly detected in the chase sample (Fig 2.5B and C). For some EdU samples minor amounts of H3K76me1 can be detected (Fig 2.5B), however methylated H3 was rarely detected in the EdU samples (Fig 2.5C). Band intensity quantification was done using ImageJ [60]. All pixel intensity values were background subtracted and normalized based on cell equivalents loaded. Percentage of recovery is calculated using the average signal intensity detected in both Western blots. Quantification of band intensities revealed a 1.5% recovery of total H3 signal in the EdU elution compared to its input signal (Table 2.2). In contrast, 13% of the H3 signal is recovered in the chase elution compared to the input (Table 2.2). Additionally, the H3K76 methylation variants are enriched in the chase

sample with an average of 8.5% recovery (Table 2.2). H3K76me3 is undetectable in the EdU pulse sample even when increased cell equivalents were loaded and longer exposures analyzed (Fig 2.5C). The average percentage of recovery for H3K76me1 in the EdU sample was of 0.14% (Table 2.2). In previous studies, immunofluorescence localization of H3K76me1 and H5K76me2 indicated that these modified histones are not detected in S phase cells showing a different pattern when compared to PCNA, a DNA replication marker [61]. Additionally, H3K76me2 is detected mainly during mitosis and cytokinesis suggesting that this histone modification is a mitosis marker in *T. brucei*. H3K76me3 mark is present at all cell cycle stages [62]. This observation agrees with our results in regards to mono- and di-methylated H3K76, where the H3K76me1 detection was minor and variable between EdU pulse samples (Fig 2.5B and C). Even though that H3K76me3 was detected in all stages of the cell cycle, its deposition may not occur in newly synthesized DNA, and therefore we could not detect it in our EdU pulse (E) elution sample (Fig 2.5B). In another study, it was observed that acetylation of Histone 4 lysine 4 (H4K4) is cell cycle regulated. In cells at S phase, unmodified H4K4 is strongly enriched [63], supporting the observation that deposition of unmodified histones is occurring in newly synthesized DNA, and that histone modification such as methylation or acetylation occurs later in the cell cycle of *T. brucei.* Based on these results, it appeared that the differences between the EdU and ThD chase iPOND samples likely represent early replicating conditions for the short pulse and matured chromatin for the chase conditions and, therefore, were suitable for proteomic analyses (see Chapter 3)

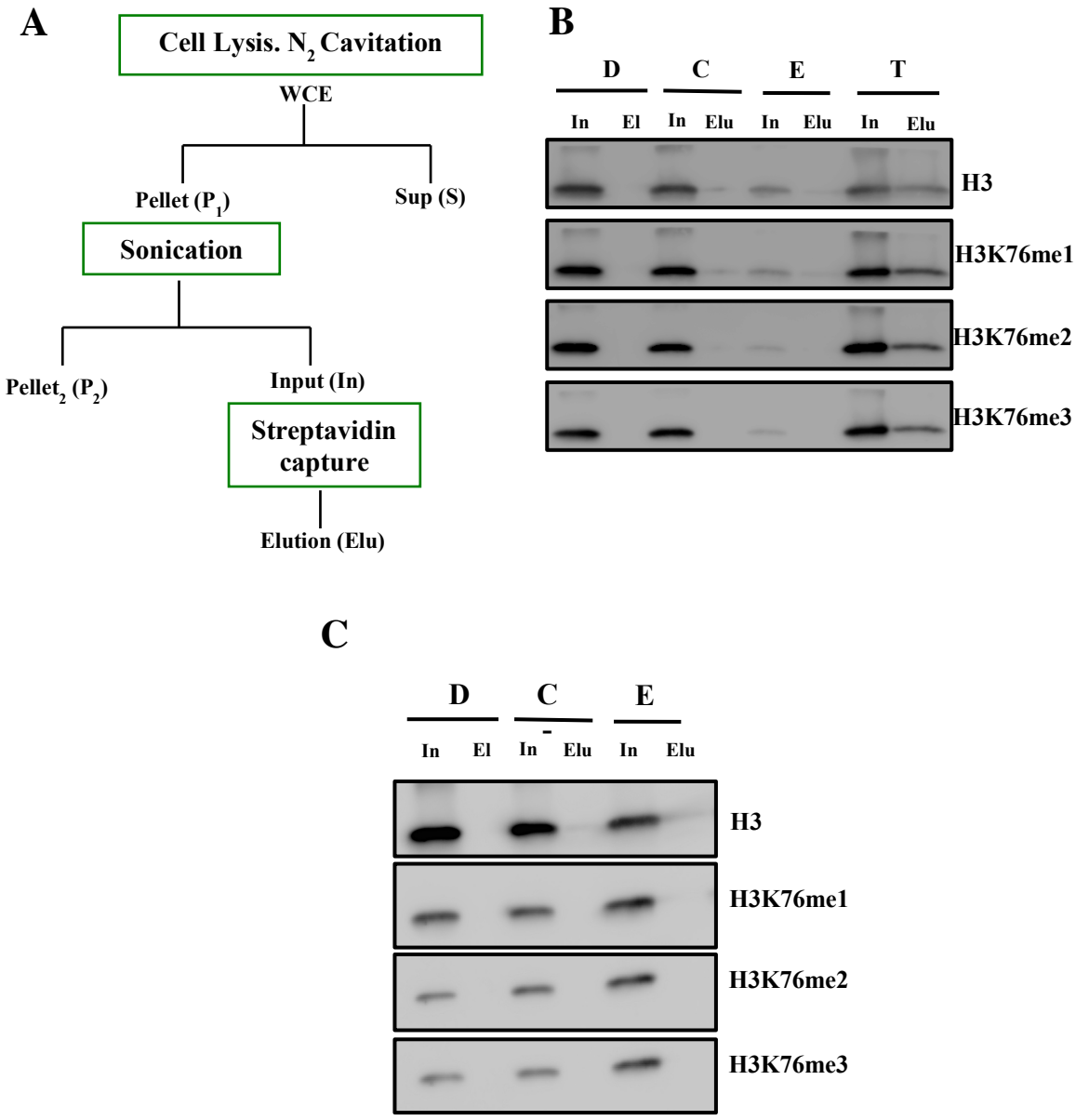

Figure 2.5 - Detection of H3 and modified H3 in final elutions

A) Schematic representation of the fractions used to probe against DNA-binding protein markers. B) and C) Detection of Histone 3 (H3) and methylated H3 in four iPOND conditions. H3 was used as a DNA-bound protein marker. The input (In) and the final elution (Elu) were probed against H3 and one, two and three methylation groups present H3 Lysine 76 (H3K76met) in the four iPOND conditions.

Table 2.2. Quantification of H3 and H3K76me signal in ThD chase and EdU pulse samples

ThD chase Blot				
Fraction	**Input**	**Elution**	**Normalized Elution**	**% of Recovery**
H3	23327.9	13972.2	3037.4	13.0
H3K76me1	20570.5	10560.0	2295.7	11.2
H3K76me2	20910.6	6737.3	1464.6	7.0
H3K76me3	19765.2	6809.1	1480.2	7.5
EdU pulse Blot				
Fraction	**Input**	**Elution**	**Normalized Elution**	**% of Recovery**
H3	21809.8	2415.4	322.1	1.5
H3K76me1	23503.2	238.5	31.8	0.14
H3K76me2	17049.5	0.0	0.0	0.0
H3K76me3	16886.1	0.0	0.0	0.0

2.4 Discussion

Sequencing of the *T. brucei* genome in 2005 [46] initiated the search for proteins homologs involved in DNA replication in this human pathogen. The result of this quest was that some of the key components of eukaryotic DNA replication are highly divergent when compared to their eukaryotic homologs while others appear to be absent. For example, the architecture of the origin of recognition complex in *T. brucei* lacks 4 subunits and instead, appears to include trypanosome specific factors [64,65]. These differences opened the possibility that DNA replication in kinetoplastids can be used as a therapeutic target to treat kinetoplastid related diseases such as Human African Trypanosomiasis, Chagas diseases and Leishmaniasis [66]. Therefore, several studies have focused on gene by gene investigations to understand the mechanism of DNA replication in these parasites. To date, the ORC complex [64,65,67], the MCM complex and the GINS complex [68] have been characterized in *T. brucei* as factors involved in DNA replication initiation. These investigations have shown these factors are also regulated differently in kinetoplastids compared to what is observed in other model eukaryotes. For example, Cdc45 which plays a crucial role in DNA replication initiation by loading the replicative DNA polymerase α and DNA polymerase ε to the onto replication origins [69,70], is regulated differently in trypanosomes by displaying dynamic localization throughout the cell cycle [68] instead of being degraded by ubiquitination as occurs in human cells [71].

Recently, genome wide studies determined that replication origins and ORC1 binding sites localize at the boundaries of the polycistronic transcription units in *T. brucei* [72]. This suggested a functional overlap between replication and transcription in this parasite. Another study using single molecule analysis of DNA replication in *T. brucei*

provided information related to the replication rate in the two proliferative forms of the parasite, the procyclic form (3,7 kbp/min) and the blood stream form (4.4 kbp/min) (PCF and BSF, respectively) [73]. In *Leishmania*, two different studies investigated DNA replication using MFAseq and DNA combing. Both studies highlighted that this parasite has few origins compared to other eukaryotes and suggested that origin firing may proceed mainly in a stochastic manner [74–76]. Even though that these techniques and investigations have contributed greatly to the understating of DNA replication in trypanosomes, the repertoire of the trypanosome replication machinery has not been analyzed comprehensively, and questions in regards to the functional coordination and interplay between replication and transcription remain open.

For this reason, we considered that iPOND could contribute to the identification of factors that are at the replication fork and in its vicinity. Here we provided data that this technique was successfully optimized for *T. brucei* with great potential to not only solve questions of DNA replication but also elucidate DNA repair and restart, and the process chromatin maturation in this parasite. The resolution of iPOND relies mostly in the length of the EdU pulse and the rate of DNA synthesis. These two parameters define the total amount of EdU-labeled DNA. In *T. brucei* iPOND, 3 x 10^{10} cells were needed to label almost the same amount of DNA that was obtained in mammalian iPOND. With this number of cells, we were expecting to labeled approximately 28 µg of DNA. Based on our results from the dot blot analysis, we could estimate how much DNA was biotinylated in 3 x 10^{10} cells. Our calculation indicates that approximately 1.8 µg of DNA was biotinylated. This represents around 6% of the expected 30 µg of labeled DNA. Despite this low percentage of biotinylated DNA, we were able to purify DNA-binding proteins

such as H3 in our EdU pulse and ThD chase sample. This protein was not detected in our negative controls. Based on our western blot results, we concluded that our samples were ready for MS analysis to identify proteins associated with the replication fork.

To validate our iPOND procedure, we used histone 3 and its methylated status as markers of DNA replication, and to monitor DNA associated proteins that are at a greater distance from the replication fork. Histones and their post-translational modification were used in previous iPOND studies together with other markers such as PCNA, CAF1 and RPA [35–37]. For example, using iPOND was observed that maturation of new chromatin requires the addition and removal of histone post-translational modifications. In this study methylation of H4K20 progressively increased as the newly synthesized DNA moves away from the active replication fork, while acetylation H4K5 detection decreased [35]. In embryonic cells, this pattern is also observed, where a deacetylation and methylation are makers of chromatin maturation [37]. Our results also indicated that methylation of H3 is not present at nascent DNA since it was not detected in the 10 min EdU pulse, but instead, it is associated with recently synthesized DNA that is in a greater distance from the replication fork, as it is observed in our ThD chase experiment.

Some modifications may further improve iPOND in trypanosomes. For example, instead of using streptavidin agarose beads, superparamagnetic beads can be used. An iPOND procedure applied in embryonic cells compared streptavidin-agarose beads with streptavidin-superparamagnetic beads, and the latter reduced non-specific interactions and increased the percentage of recovery of PCNA [37]. Therefore, superparamagnetic beads could also enhance the percentage of recovery in *T. brucei* iPOND. Improving the uptake of EdU in the parasite could also reduce the time of EdU labeling which determines the

length of DNA labeled. If we could reduce the EdU pulse to 5 min, 18.5 kbp will be labeled which is similar to what was labeled in mammalians cells (15 kbp) in a 10 min pulse. To achieve this, the parasites could be engineered such they express high affinity transporters for thymidine analogues, which will accelerate EdU uptake and its phosphorylation before incorporation into DNA. Another strategy to improve iPOND is to synchronize the cells in S phase for the EdU pulse. A recent study has applied centrifugal-counter flow elutriation to synchronize *T. brucei* PCF and BSF parasites. Parasites at the G1 cell cycle state were isolated and without impacting the viability and proliferation [77]. By applying this technique, we would be able to label a complete population that is in S phase and purify a larger amount of proteins associated with DNA replication.

Even though that we could assume that the DNA replication machinery between PCF and BSF is not that different, it would be interesting to applied iPOND in BSF parasites to define the role that this cellular process has in VSG antigenic variation by directing locus-specific recombination (52,53).

In conclusion, there is a lot of potential of the iPOND technique in the parasitology field to help solve questions about the different mechanisms that kinetoplastids have to replicate their DNA. Coupling iPOND with MS analysis can identify new players and provide a global view of the choreography of the factors present at the replication fork. Essential kinetoplastid-specific factors could represent a pocketful of candidates to treat diseases associated with *T. brucei* and other kinetoplastids.

2.5 Bibliography

1. Reinhart M, Cardoso MC. A journey through the microscopic ages of DNA replication. Protoplasma. 2017;254: 1151–1162. doi:10.1007/s00709-016-1058-8
2. Técher H, Koundrioukoff S, Azar D, Wilhelm T, Carignon S, Brison O, et al. Replication dynamics: Biases and robustness of DNA fiber analysis. J Mol Biol. 2013;425: 4845–4855. doi:10.1016/j.jmb.2013.03.040
3. Stratmann SA, van Oijen AM. DNA replication at the single-molecule level. Chem Soc Rev. 2014;43: 1201. doi:10.1039/c3cs60391a
4. Carneiro DG, Clarke T, Davies CC, Bailey D. Identifying novel protein interactions: Proteomic methods, optimisation approaches and data analysis pipelines. Methods. 2016;95: 46–54. doi:10.1016/j.ymeth.2015.08.022
5. Cortez D. Proteomic Analyses of the Eukaryotic Replication Machinery. 1st ed. Methods in Enzymology. 2017. doi:10.1016/bs.mie.2017.03.002
6. Marchal C, Sasaki T, Vera D, Wilson K, Sima J, Rivera-Mulia JC, et al. Genome-wide analysis of replication timing by next-generation sequencing with E/L Repli-seq. Nat Protoc. 2018;13: 819–839. doi:10.1038/nprot.2017.148
7. Tang Z, Luo OJ, Li X, Zheng M, Zhu JJ, Szalaj P, et al. CTCF-Mediated Human 3D Genome Architecture Reveals Chromatin Topology for Transcription. Cell. 2015;163: 1611–1627. doi:10.1016/j.cell.2015.11.024
8. Ragoczy T, Bender MA, Telling A, Byron R, Groudine M. The locus control region is required for association of the murine B-globin locus with engaged transcription factories during erythroid maturation. Genes Dev. 2006;20: 1447–1457. doi:10.1101/gad.1419506
9. Dekker J, Belmont AS, Guttman M, Leshyk VO, Lis JT, Lomvardas S, et al. The 4D nucleome project. Nature. 2017;549: 219–226. doi:10.1038/nature23884
10. Kaykov A, Taillefumier T, Bensimon A, Nurse P. Molecular Combing of Single DNA Molecules on the 10 Megabase Scale. Sci Rep. 2016;6: 80–84. doi:10.1038/srep19636
11. Vindigni A, Lopes M. Combining electron microscopy with single molecule DNA fiber approaches to study DNA replication dynamics. Biophys Chem. 2017;225: 3–9. doi:10.1016/j.bpc.2016.11.014
12. Quinet A, Carvajal-Maldonado D, Lemacon D, Vindigni A. DNA Fiber Analysis: Mind the Gap! 1st ed. Methods in Enzymology. 2017. doi:10.1016/bs.mie.2017.03.019
13. Thangavel S, Berti M, Levikova M, Pinto C, Gomathinayagam S, Vujanovic M, et al. DNA2 drives processing and restart of reversed replication forks in human cells. J. Cell. Biol. 2015;208:545-562. doi:10.1083/jcb.201406100
14. Quinet A, Lemaçon D, Vindigni A. Replication Fork Reversal: Players and Guardians. Mol Cell. 2017;68: 830–833. doi:10.1016/j.molcel.2017.11.022
15. Lakadamyali M, Cosma MP. Advanced microscopy methods for visualizing chromatin structure. FEBS Lett. 2015;589: 3023–3030. doi:10.1016/j.febslet.2015.04.012
16. Markaki Y, Gunkel M, Schermelleh L. Functional Nuclear Organization of Transcription and DNA Replication : A Topographical Marriage between

Chromatin Domains and the Interchromatin Compartment Functional Nuclear Organization of Transcription and DNA Replication A Topographical Marriage betw. 2011;LXXV. doi:10.1101/sqb.2010.75.042
17. Dey B, Thukral S, Krishnan S, Chakrobarty M, Gupta S, Manghani C, et al. DNA-protein interactions: Methods for detection and analysis. Mol Cell Biochem. 2012;365: 279–299. doi:10.1007/s11010-012-1269-z
18. Cai YH, Huang H. Advances in the study of protein-DNA interaction. Amino Acids. 2012;43: 1141–1146. doi:10.1007/s00726-012-1377-9
19. Fuller RS, Funnell BE, Kornberg A. The dnaA protein complex with the E. coli chromosomal replication origin (oriC) and other DNA sites. Cell. 1984;38: 889–900. doi:10.1016/0092-8674(84)90284-8
20. Taylor JA, Ouimet MC, Wargachuk R, Marczynski GT. The Caulobacter crescentus chromosome replication origin evolved two classes of weak DnaA binding sites. Mol Microbiol. 2011;82: 312–326. doi:10.1111/j.1365-2958.2011.07785.x
21. Robinson NP, Dionne I, Lundgren M, Marsh VL, Bernander R, Bell SD. Identification of Two Origins of Replication in the Single Chromosome of the Archaeon Sulfolobus solfataricus. Cell. 2004;116: 25–38. doi:10.1016/S0092-8674(03)01034-1
22. Liu S, Xu Z, Leng H, Zheng P, Yang J, Chen K, et al. RPA binds histone H3-H4 and functions in DNA replication-coupled nucleosome assembly. Science. 2017;355: 415–420. doi:10.1126/science.aah4712
23. Li JJ, Herskowitz I. Isolation of ORC6, a component of the yeast origin recognition complex by a one-hybrid system. Science.1993;262: 1870–1874. doi:10.1126/science.8266075
24. Dellino GI, Cittaro D, Piccioni R, Luzi L, Banfi S, Segalla S, et al. Genome-wide mapping of human DNA-replication origins: Levels of transcription at ORC1 sites regulate origin selection and replication timing. Genome Res. 2013;23: 1–11. doi:10.1101/gr.142331.112
25. Gillespie PJ, Gambus A, Blow JJ. Preparation and use of Xenopus egg extracts to study DNA replication and chromatin associated proteins. Methods. 2012;57: 203–213. doi:10.1016/j.ymeth.2012.03.029
26. Powers M, Evans EK, Yang J, Kornbluth S. Preparation and use of interphase Xenopus egg extracts. Curr Protoc Cell Biol. 2001;Chapter 11: Unit 11.10. doi:10.1002/0471143030.cb1110s09
27. Ma L, Aslanian A, Sun H, Jin M, Shi Y, Yates JR, et al. Identification of Small Ubiquitin-like Modifier Substrates with Diverse Functions Using the *Xenopus* Egg Extract System. Mol Cell Proteomics. 2014;13: 1659–1675. doi:10.1074/mcp.M113.035626
28. Shintomi, Keishi; Inoue, Fukashi; Watanabe, Hiroshi; Ohsumi, Keita; Ohsugi, Miho; Hirano T. Mitotic chromosome assembly despite nucleosome depeltion in Xenopous egg extracts. Science. 2017;356: 1284–1287.
29. Sirbu BM, Couch FB, Cortez D. Monitoring the spatiotemporal dynamics of proteins at replication forks and in assembled chromatin using isolation of proteins on nascent DNA. Nat Protoc. 2012;7: 594–605. doi:10.1038/nprot.2012.010
30. Wiest NE, Tomkinson AE. Optimization of Native and Formaldehyde iPOND

Techniques for Use in Suspension Cells [Internet]. 1st ed. Methods in Enzymology. 2017. doi:10.1016/bs.mie.2017.03.001
31. Alabert C, Bukowski-Wills JC, Lee SB, Kustatscher G, Nakamura K, De Lima Alves F, et al. Nascent chromatin capture proteomics determines chromatin dynamics during DNA replication and identifies unknown fork components. Nat Cell Biol. 2014;16: 281–291. doi:10.1038/ncb2918
32. Saredi G, Huang H, Hammond CM, Alabert C, Bekker-Jensen S, Forne I, et al. H4K20me0 marks post-replicative chromatin and recruits the TONSL–MMS22L DNA repair complex. Nature. 2016;534: 714–718. doi:10.1038/nature18312
33. Salic A, Mitchison TJ. A chemical method for fast and sensitive detection of DNA synthesis in vivo. Proc Natl Acad Sci U S A. 2008;105: 2415–2420. doi:10.1073/pnas.0712168105
34. Kolb HC, Finn MG, Sharpless KB. Click Chemistry: Diverse Chemical Function from a Few Good Reactions. Angew Chem Inte Ed. 2001;40: 2004–2021. doi:10.1002/1521-3773(20010601)40:11<2004::AID-ANIE2004>3.0.CO;2-5
35. Sirbu BM, Couch FB, Feigerle JT, Bhaskara S, Hiebert SW, Cortez D. Analysis of protein dynamics at active , stalled , and collapsed replication forks. Genes Dev. 2011;25: 1320–1327. doi:10.1101/gad.2053211.
36. Sirbu BM, McDonald WH, Dungrawala H, Badu-Nkansah A, Kavanaugh GM, Chen Y, et al. Identification of proteins at active, stalled, and collapsed replication forks using isolation of proteins on nascent DNA (iPOND) coupled with mass spectrometry. J Biol Chem. 2013;288: 31458–31467. doi:10.1074/jbc.M113.511337
37. Aranda S, Rutishauser D, Ernfors P. Identification of a large protein network involved in epigenetic transmission in replicating DNA of embryonic stem cells. Nucleic Acids Res. 2014;42: 6972–6986. doi:10.1093/nar/gku374
38. Chaudhuri AR, Callen E, Ding X, Gogola E, Duarte AA, Lee JE, et al. Replication fork stability confers chemoresistance in BRCA-deficient cells. Nature. 2016;535: 382–387. doi:10.1038/nature18325
39. Dembowski JA, DeLuca NA. Selective Recruitment of Nuclear Factors to Productively Replicating Herpes Simplex Virus Genomes. PLoS Pathog. 2015;11: 1–35. doi:10.1371/journal.ppat.1004939
40. Gratzner HG. Monoclonal Antibody to 5-Bromo- and 5-Iododeoxyuridine : A New Reagent for Detection of DNA Replication Placental Mononuclear Phagocytes as a Source of Interleukin-1. Science. 1982;218: 474–475. doi:10.1126/science.7123245
41. Mead TJ, Lefebvre V. Proliferation Assays (BrdU and EdU) on Skeletal tissue sections. In: Hilton M, editor. Skeletal Development and Repair Methods in Molecular Biology. 2014. pp. 233–243. doi:10.1007/978-1-62703-989-5
42. Mead TJ, Lefebvre V. Skeletal Development and Repair. 2014;1130: 1–10. doi:10.1007/978-1-62703-989-5
43. Senkevich TG, Katsafanas GC, Weisberg A, Olano LR, Moss B. Identification of vaccinia virus replisome and transcriptome proteins by isolation of proteins on nascent DNA coupled with mass spectrometry. J Virol. 2017;91: 1–20. doi:10.1128/JVI.01015-17
44. Schimanski B, Nguyen TN, Gu A. Highly Efficient Tandem Affinity Purification

of Trypanosome Protein Complexes Based on a Novel Epitope Combination. Eukaryot Cell. 2005;4: 1942–1950. doi:10.1128/EC.4.11.1942
45. Chandler J, Vandoros A V., Mozeleski B, Klingbeil MM. Stem-loop silencing reveals that a third mitochondrial DNA polymerase, POLID, is required for kinetoplast DNA replication in trypanosomes. Eukaryot Cell. 2008;7: 2141–2146. doi:10.1128/EC.00199-08
46. Berriman M, Ghedin E, Hertz-Fowler C, Blandin G, Renauld H, Bartholomeu DC, et al. The genome of the African trypanosome Trypanosoma brucei. Science. 2005;309: 416–422. doi:10.1126/science.1112642
47. Woodward R, Gull K. Timing of nuclear and kinetoplast DNA replication and early morphological events in the cell cycle of Trypanosoma brucei. J Cell Sci. 1990;95: 49–57.
48. Siegel TN, Hekstra DR, Cross GAM. Analysis of the Trypanosoma brucei cell cycle by quantitative DAPI imaging. Mol Biochem Parasitol. 2008;160: 171–174. doi:10.1016/j.molbiopara.2008.04.004
49. Ranjbarian F, Vodnala M, Vodnala SM, Rofougaran R, Thelander L, Hofer A. Trypanosoma brucei thymidine kinase is tandem protein consisting of two homologous parts, which together enable efficient substrate binding. J Biol Chem. 2012;287: 17628–17636. doi:10.1074/jbc.M112.340059
50. Kaufmann D, Gassen A, Maiser A, Leonhardt H, Janzen CJ. Regulation and spatial organization of PCNA in Trypanosoma brucei. Biochem Biophys Res Commun. 2012;419: 698–702. doi:10.1016/j.bbrc.2012.02.082
51. Valenciano AL, Ramsey AC, Mackey ZB. Deviating the level of proliferating cell nuclear antigen in trypanosoma brucei elicits distinct mechanisms for inhibiting proliferation and cell cycle progression. Cell Cycle. 2015;14: 674–688. doi:10.4161/15384101.2014.987611
52. Sherwin T, Gull K. Visualization of detyrosination along single microtubules reveals novel mechanisms of assembly during cytoskeletal duplication in trypanosomes. Cell. 1989;57: 211–221. doi:10.1016/0092-8674(89)90959-8
53. Venter JC, Adams MD, Myers EW, Li PW, Mural RJ, Sutton GG, et al. The sequence of the human genome. Science. 2009;291: 1304–1351. doi:10.1126/science.1058040
54. Burgess A, Lorca T, Castro A. Quantitative Live Imaging of Endogenous DNA Replication in Mammalian Cells. PLoS One. 2012;7. doi:10.1371/journal.pone.0045726
55. Conti C, Sacca B, Herrick J, Lalou C, Pommier Y, Bensimon A. Replication Fork Velocities at Adjacent Replication Origins Are Coordinately Modified during DNA Replication in Human Cells. Int J Biol Sci. 2007;6: 569–583. doi:10.1091/mbc.E06
56. Jackson DA, Pombo A. Replicon Clusters Are Stable Units of Chromosome Structure Evidence That Nuclear Organization Contributes to the Efficient Activation and Propagation of S Phase in Human Cells. 1998;140: 1285–1295.
57. DePamphillls M, Bell SD. Genome duplication. Concepts, mechanisms, evolution, and disease. New York: Garland Science; 2011.
58. Yadav T, Whitehouse I. Replication-Coupled Nucleosome Assembly and Positioning by ATP-Dependent Chromatin-Remodeling Enzymes. Cell Rep.

2016;15: 715–723. doi:10.1016/j.celrep.2016.03.059
59. Prado F, Maya D. Regulation of replication fork advance and stability by nucleosome assembly. Genes. 2017;8. doi:10.3390/genes8020049
60. Eliceiri K, Schneider CA, Rasband WS, Eliceiri KW. NIH Image to ImageJ : 25 years of image analysis HISTORICAL commentary NIH Image to ImageJ : 25 years of image analysis. Nat Methods. 2012;9: 671–675. doi:10.1038/nmeth.2089
61. Gassen A, Brechtefeld D, Schandry N, Arteaga-Salas JM, Israel L, Imhof A, et al. DOT1A-dependent H3K76 methylation is required for replication regulation in Trypanosoma brucei. Nucleic Acids Res. 2012;40: 10302–10311. doi:10.1093/nar/gks801
62. Janzen CJ, Hake SB, Lowell JE, Cross GAM. Selective Di- or Trimethylation of Histone H3 Lysine 76 by Two DOT1 Homologs Is Important for Cell Cycle Regulation in Trypanosoma brucei. Mol Cell. 2006;23: 497–507. doi:10.1016/j.molcel.2006.06.027
63. Siegel TN, Kawahara T, DeGrasse JA, Janzen CJ, Horn D, Cross GAM. Acetylation of histone H4K4 is cell cycle regulated and mediated by HAT3 in Trypanosoma brucei. Mol Microbiol. 2008;67: 762–771. doi:10.1111/j.1365-2958.2007.06079.x
64. De Melo Godoy PD, Nogueira-Junior LA, Paes LS, Cornejo A, Martins RM, Silber AM, et al. Trypanosome prereplication machinery contains a single functional Orc1/Cdc6 protein, which is typical of archaea. Eukaryot Cell. 2009;8: 1592–1603. doi:10.1128/EC.00161-09
65. Tiengwe C, Marcello L, Farr H, Gadelha C, Burchmore R, Barry JD, et al. Identification of ORC1/CDC6-interacting factors in trypanosoma brucei reveals critical features of origin recognition complex architecture. PLoS One. 2012;7: 22–24. doi:10.1371/journal.pone.0032674
66. Calderano SG, Godoy PD de M, da Cunha JPC, Elias MC. Trypanosome Prereplication Machinery: A Potential New Target for an Old Problem. Enzyme Res. 2011;2011: 1–8. doi:10.4061/2011/518258
67. Benmerzouga I, Concepción-Acevedo J, Kim HS, Vandoros A V., Cross GAM, Klingbeil MM, et al. Trypanosoma brucei Orc1 is essential for nuclear DNA replication and affects both VSG silencing and VSG switching. Mol Microbiol. 2013;87: 196–210. doi:10.1111/mmi.12093
68. Dang HQ, Li Z. The Cdc45 Mcm2-7 GINS protein complex in trypanosomes regulates DNA replication and interacts with two Orc1-like proteins in the origin recognition complex. J Biol Chem. 2011;286: 32424–32435. doi:10.1074/jbc.M111.240143
69. Kubota Y, Takase Y, Komori Y, Hashimoto Y, Arata T, Kamimura Y. A novel ring-like complex of Xenopus proteins essential for the initiation of DNA replication A novel ring-like complex of Xenopus proteins essential for the initiation of DNA replication. Genes Dev. 2003;17: 1141–1152. doi:10.1101/gad.1070003
70. Langston LD, Zhang D, Yurieva O, Georgescu RE, Finkelstein J, Yao NY, et al. CMG helicase and DNA polymerase form a functional 15-subunit holoenzyme for eukaryotic leading-strand DNA replication. Proc Natl Acad Sci. 2014;111: 15390–15395. doi:10.1073/pnas.1418334111

71. Pollok S, Grosse F. Cdc45 degradation during differentiation and apoptosis. Biochem Biophys Res Commun. 2007;362: 910–915. doi:10.1016/j.bbrc.2007.08.069
72. Tiengwe C, Marcello L, Farr H, Dickens N, Kelly S, Swiderski M, et al. Genome-wide analysis reveals extensive functional interaction between DNA replication initiation and transcription in the genome of trypanosoma brucei. Cell Rep. 2012;2: 185–197. doi:10.1016/j.celrep.2012.06.007
73. Calderano SG, Drosopoulos WC, Quaresma MM, Marques CA, Kosiyatrakul S, McCulloch R, et al. Single molecule analysis of Trypanosoma brucei DNA replication dynamics. Nucleic Acids Res. 2015;43: 2655–2665. doi:10.1093/nar/gku1389
74. Marques CA, Dickens NJ, Paape D, Campbell SJ, McCulloch R. Genome-wide mapping reveals single-origin chromosome replication in Leishmania, a eukaryotic microbe. Genome Biol. Genome Biology; 2015;16: 230. doi:10.1186/s13059-015-0788-9
75. Rocha-Granados MC, Klingbeil MM. Leishmania DNA Replication Timing: A Stochastic Event? Trends Parasitol. 2016;32: 755–757. doi:10.1016/j.pt.2016.05.011
76. Stanojcic S, Sollelis L, Kuk N, Crobu L, Balard Y, Schwob E, et al. Single-molecule analysis of DNA replication reveals novel features in the divergent eukaryotes Leishmania and Trypanosoma brucei versus mammalian cells. Sci Rep. 2016;6: 23142. doi:10.1038/srep23142
77. Benz C, Dondelinger F, McKean PG, Urbaniak MD. Cell cycle synchronisation of Trypanosoma brucei by centrifugal counter-flow elutriation reveals the timing of nuclear and kinetoplast DNA replication. Sci Rep. 2017;7: 1–10. doi:10.1038/s41598-017-17779-z

CHAPTER 3

iPOND-LABEL-FREE MS ANALYSIS AND INITIAL CANDIDATE STUDIES

3.1 Introduction

3.1.1 iPOND combined with MS analysis

The iPOND methodology has been combined with different types of MS analysis to identify the replication fork proteome. It can be divided in two main groups: One is using label-free quantification [1], and the other is using chemical labeling methods such as iTRAQ (isobaric tags for relative and absolute quantification) [2,3] or SILAC (Stable isotope labeling with amino acids in cell culture) [4]. Label-free quantification compares datasets that are generated independently and utilizes the number of peptide spectra for a given proteins or measures the intensity of the precursor ion peak to assign an abundance value to a protein within the data set. Since the datasets are generated independently, there might be variability between replicates of each experiment. In label-free quantification, the EdU pulse and chase samples are collected independently and compared after sample processing [1]. Two studies have used spectral counts for quantification and estimated pulse:chase ratios to distinguish between proteins present at nascent DNA and proteins that are part of bulk chromatin in human cells. One study was able to identify 84 proteins that are enriched at the replication fork in human cells. The highest GO terms associated with this set of proteins was DNA metabolism [5]. In the other study, key components of the replication fork such as RFC, PCNA, DNA polymerases and components of the MCM helicase complex displayed high fold enrichments when over the chase sample, indicating that these components were specifically associated with nascent DNA; they identified 100

proteins [6]. A third study used label-free quantification utilizing the peak of the precursor ion intensity to measure protein abundance. After performing 6 replicates and comparing the pulse:chase ratio, this study was able to identify the bona fide replisome components in addition to proteins that have been directly or indirectly associated with replication such as the mismatch repair (MMR) protein MSH2. MMR proteins like MSH6 and MSH3 have a direct interaction with PCNA, and therefore are required at the replication site. Furthermore, this study revealed that proteins involved in SUMOylation were concentrated in replisomes [7]. One disadvantage of label-fee quantification is that it can generate high false-positive and false negative discovery rates. However, this method can provide a starting candidate list of new replication machinery proteins.

In order to reduce the number of false positive hits in label-free quantification, researchers have used chemical labeling methods for MS analysis in iPOND procedures. Combining iPOND with SILAC quantification in human cells provided a list of 218 proteins that are at associated with nascent DNA. Among core replication proteins, fold enrichment of the MCM2-7 subunits displayed a low variability with less of a 10% difference between replicates. This means that the variability observed in label-free quantification is greatly reduced by applying labeling methods. Also, using iPOND-SILAC, a new subunit (ZNF644) of the G9a/GLP methyltransferase complex was identified. ZNF644 travels just behind the replication fork to modify newly deposited histones [8]. A second example is using iPOND-iTRAQ [9]. This study used human cells to determine how the SUMO-rich (Small Ubiquitin-like Modifier) and ubiquitin-poor environment is maintained at sites of DNA replication. In this study, the role and the abundance of ubiquitin specific protease (USP) around replisomes was determined using

iTRAQ quantification to evaluate their presence in nascent and mature chromatin. Different USPs were enriched in the replisome fraction including USP7 which was found to be essential for DNA replication. This protein has interaction with subunits of the MCM complex and when it was specifically inhibit chemically, there was a loss on EdU incorporation in human cells [9].

Based on these studies, coupling MS analysis with iPOND is a potential tool to study DNA replication by defining the replication fork proteome. Label-free MS quantification provides a starting list of proteins and a global view of what might be occurring at the replication fork. These proteins can be further characterized and studied in the context DNA replication. Incorporating SILAC or iTRAQ quantification, improves the analysis by reducing variability between the replicates and increasing the confidence of identified proteins being part of active replication forks or part of the bulk chromatin. In sum, the iPOND-MS approach is likely to increase our knowledge on regulation and coordination of DNA and chromatin replication and to provide an opportunity to better understand how the DNA and chromatin machineries respond to replication challenges.

3.1.2 DNA and Chromatin Replication

Eukaryotic genomes are packed into chromatin, where duplex DNA is wrapped around a histone octamer and associated with other proteins [10,11]. Accurate transmission of genomic information during cell proliferation and maintaining the epigenetic marks from one generation to the next are fundamental process in a living cell [12–14]. Chromatin is critical to efficient execution of DNA-related processes such as DNA replication, transcription, repair and recombination [15].

DNA replication and inheritance of genomic histone and its modification state to daughter cells are two processes that are linked together. A recent study in yeast showed that chromatin plays a key role in origin selection by preventing non-specific loading of the MCM helicase complex. Also, histone chaperones and histone acetylation stimulate replication by increasing the replication rate *in vitro* [11]. In addition, there is a dynamic mechanism in which histone deposition is coordinated with fork progression to maintain genome stability. During DNA duplication, a parental nucleosome is disassembled ahead of the replication fork and two new nucleosomes must assemble on the daughter strands using new and recycled histones. It was shown in human cells that histone chaperone Asf1 forms a complex with MCM helicase through histone H3 and histone H4, and when cells are depleted of Asf1, DNA unwinding is blocked at replication sites [16]. A final example of the relationship between DNA replication and chromatin was reported in a recent study in which replication protein A (RPA) bound to free H3 and H4 and promoted DNA-H3-H4 complexes. RPA can target histone deposition to replication fork and promote nucleosome assembly on nascent chromatin [17]. Therefore, it is expected chromatin proteins in addition to replication proteins to be present at the replication fork.

3.1.3 DNA replication and Transcription.

DNA replication and transcription are fundamental cellular processes. DNA replication and transcription machineries compete for the same DNA template causing collisions. The coordination of these two machineries is extremely important to maintain genome stability since collisions can alter fork progression, generate replication stress and interfere with the gene transcription program [18]. The cells have acquired different

strategies to avoid those collisions or fix any DNA damage upon collision. A study aimed to understand the role of RNA polymerase II (RNA pol II) in maintaining genome stability by generating different mutants of RNA polymerase II in yeast. Mutants that retained RNA pol II at chromatin impaired fork progression and increased the number of recombination events, they displayed high levels of DNA damage sensitivity and a strong dependence on double-strand break repair pathway for viability. In these mutants, accumulation of Rrm3, a factor required for the progression of replication forks when obstacles are present in the DNA, occurred in ORFs and in origin of replication sites. Also, in these mutants Rrm3 enrichment correlates with gene expression levels. This supports the idea that replication obstacles occur preferentially at highly transcribed genes. Therefore, the data suggested that RNA pol II can facilitate fork progression and avoid transcription-replication collisions by contributing to its own release from the replication site [19].

The link between replication and transcription can also be observed in different genome-wide studies that focused on understanding DNA replication timing and extent of transcription. For example, in *Drosophila melanogaster* this relationship was tested by comparing at a genomic scale gene expression status with replication timing of each individual gene. The result of that analysis indicated that early replication in S phase coincided with a higher likelihood of gene activity [20]. Other examples were found in mouse embryonic cells in which origins density correlated with promoter density [21], and a similarly in human cells, where activated origins overlapped with transcribed areas of the genome [22]. This study suggested that colocalization of DNA replication and transcription initiation sites might provide co-linearity to the progression of DNA replication forks and transcription complexes to prevent head on collisions and potential collapse of the

replication and transcription machineries. Based on these examples, transcription machinery can be expected in near distance of the replication fork.

Here we have analyzed our iPOND samples using label-free quantification MS analysis. We generated a starting list of protein candidates that might be present in an unperturbed replication fork in *T. brucei.* We analyzed our two negative controls, DMSO (D) and No Click (C-), together with EdU pulse (E) and a ThD chase (T) samples, to distinguish proteins that are likely associated with nascent DNA form the ones participating in chromatin maturation. We set filtering criteria to remove false positive hits and performed a bioinformatic analysis to identify the GO terms associated with our data set. We found that other cellular processes are present in coordination with DNA replication in *T. brucei*, including transcription and nucleosome assembly. We also characterized a protein annotated as a Replication Factor C subunit (Tb927.10.7990), and a protein of unknown function (Tb927.3.5370). Both proteins retain nuclear localization throughout the cell cycle. While Tb927.3.5370 appeared to be a dispensable gene, Tb927.10.7990 proved to be essential since its silencing caused a growth defect in procyclic cells and impaired DNA replication.

3.2 Material and methods

3.2.1 MS sample preparation and Analysis

Final elutions from iPOND procedures, including negative controls DMSO (D) and No Click (C-), and EdU pulse and thymidine (ThD) chase, were denaturated in SDS-PAGE and sent for MS analysis to Keck Biotechnology Center of Yale University. Three replicates were analyzed for the EdU pulse condition, two replicates for both negative

controls, and one replicate for the ThD chase. At the Keck Biotechnology Center, gel slices were chopped into small pieces and washed three times with 1 ml of 50% acetonitrile/50 mM NH_4HCO_3 for 15 minutes. After a final wash with 50% acetonitrile/12.5 mM NH_4HCO_3, the gel pieces were dried by speed vacuum. Each sample was resuspended in 25 mM NH_4HCO_3 containing 2.5 ng/µl digestion grade trypsin (Promega) using enough volume to cover the gel pieces and incubated at 37ºC for 14 hours. After digestion, peptides were extracted from the gels with two volumes of 80% acetonitrile, 0.1% formic acid for 15 minutes, then dried by speed vacuum. Peptides were dissolved in 30 µl of MS loading buffer (2% acetonitrile, 0.2% trifluoroacetic acid), with 5 µl injected for mass spec analysis.

LC-MS/MS acquisition was performed on a Thermo Scientific Q Exactive Plus coupled to a Waters nanoAcquity UPLC system. The binary solvent system consisted of 100% water, 0.1% formic acid (Buffer A) and 100% acetonitrile, 0.1% formic acid (Buffer B). Trapping was done at 5 µl/min, 97% Buffer A for 3 min using a Waters Symmetry® C18 180 µm x 20 mm trap column. Peptide separation was carried out on a ACQUITY UPLC PST (BEH) C18 nanoACQUITY Column (1.7 µm, 75 µm x 250 mm) at 37 ºC and a flow rate of 300 nl/min using the following gradient: 3% buffer B at initial conditions; 5% B at 1 minute; 30% B at 140 minutes; 50% B at 155 minutes; 90% B at 160-170; and back to initial conditions at 171 minutes. MS scans were acquired in profile mode over the 300-1,500 m/z range using 1 microscan, 70K resolution, AGC (automated gain control) target of 3E6 ions counts, and a full max ion time of 45 ms. MS/MS were acquired in centroid mode using 1 microscan, 17.5K resolution, AGC target of 1E5, full max IT of 100 ms, 1.7 m/z isolation window, normalized collision energy of 28. Up to 20 MS/MS were

collected per MS scan on species with an intensity threshold of 1E4, charge states 2-6, peptide match preferred, and dynamic exclusion set to 20 seconds.

For database searching, tandem mass spectra were extracted by Proteome Discoverer version 2.1.1.21 (ThermoFisher). Charge state deconvolution and deisotoping were not performed. Data were searched in-house using the Mascot algorithm (version 2.6.0) (Matrix Science, London, UK). Mascot was set up to search a *Trypanosoma brucei* database (version 27, containing Lister strain 427 and TREU927, downloaded from http://tritrypdb.org/tritrypdb/). Search parameters used were trypsin digestion (strict) with up to 2 missed cleavages, peptide mass tolerance of 10 ppm, MS/MS fragment tolerance of 0.02 Da, and variable modifications of methionine oxidation, propionamide adduct to cysteine, and deamidation of asparagine and glutamine.

Scaffold (version Scaffold_4.8.2, Proteome Software Inc.) was used to validate MS/MS based peptide and protein identifications. Peptide identifications were accepted if they could be established at greater than 95.0% probability by the Scaffold Local FDR algorithm. Protein identifications were accepted if they could be established at greater than 99.0% probability and contained at least 2 identified peptides. Protein probabilities were assigned by the Protein Prophet algorithm [23]. Proteins that contained similar peptides and could not be differentiated based on MS/MS analysis alone were grouped to satisfy the principles of parsimony. Proteins sharing significant peptide evidence were grouped into clusters.

3.2.2 iBAQ Analysis

Protein abundance was estimated using the iBAQ (Intensity-based absolute quantification) value of each protein hit in the four different samples in the Scaffold program. The iBAQ value is based on the sum of all identified peptides intensities matching to a specific protein divided by the number of theoretically peptides observable, yielding an accurate proxy of protein level [24]. In order to maximize the likelihood of identifying replication-relevant proteins, the mass spectrometric data was analyzed as follows: we only considered those proteins which were identified in at least two of the three biological replicates in the EdU pulse condition. For these proteins, we calculated the fold change (FC) of the EdU sampled over the two negative controls, DMSO (FC EdU/DMSO) and No Click Chemistry (FC EdU/C-), using the iBAQ value as a reference. To determine if a protein is enriched has to filled the following criteria: 1) the protein had a total FC EdU/ C- equal or higher than 10, 2) had a total FC EdU/DMSO ratio equal or higher than 1.5, and 3) displayed nuclear localization in a recent nuclear proteome analysis [25]. However, the latter analysis did not comprise all known nuclear proteins. Therefore, we considered to be nuclear when they exhibited nuclear localization in the trypanosome genome wide localization resource [26], or have a predicted gene ontology (GO) term associated with DNA replication, nucleic acid binding or nuclear localization.

To include proteins in our list that were identified in our nascent DNA analysis but absent in either negative control, e.g. obtained an infinite value (INF) for fold change, we set the fold change value from INF to the highest fold change value obtained in a particular experiment. To estimate a total score in order to rank the protein list the fold change (FC) EdU/No click and the FC EdU/DMSO were standardized to a 0-100 scale in each MS

replicate. The average from each FC was calculated and the total score was determined by adding average FC EdU/No click by average FC EdU/DMSO. Also, the FC EdU/ThD ratio was calculated but was not considered in the final score since it has only one replicate, but was used to make initial observations of the proteins that might be associated with nascent DNA.

3.2.3 Bioinformatic Analysis

UniProt IDs of the proteins identified were acquired using the TriTrypDB database accession numbers [27] (http://www.tritrypdb.org/). However, each protein did not have a UniProt ID. GO term analysis and enrichment was performed using PANTHER classification system [28]. The UniProt IDs list was mapped against the *Trypanosoma brucei* reference list in PANTHER version 13.0 (released version 20171205) with the following selections: analysis type, overrepresentation test; annotation database, PANTHER GO-slim Biological process; and test type, Fisher´s Exact test with False discover rate (FDR) < 0.05. The results were sorted by hierarchically order to observe the enriched functional classes. Analysis of protein interaction networks was performed using STRING database [29]. Only interactions from curated databases and text-mining information were considered (confidence interaction score >0.65). The network was visualized using Cytoscape version 3.6.0 [30].

Protein sequences from selected candidates were analyzed using the NCBI conserved domain database search (CDD) [31] to identify possible functional domains present in proteins of unknown function. Sequences were aligned using Clustal Omega with default parameters [32]. Motif search for Tb5370 was performed using the Eukaryotic

Linear Motif (ELM) resource for Functional Sites in Proteins [33] with a cutoff for motif probability of 100.

3.2.4 Nuclear Localization Criteria

Proteins were classified according to the following nuclear localization criteria. 1) Represents proteins that were isolated in the nuclear proteome study [25] and displayed nuclear localization in the TrypTag project [26]; 2) comprises proteins that were isolated in the nuclear proteome but were not analyzed in the TrypTag project; 3) denotes proteins with nuclear localization by TrypTag only; 4) comprises proteins that were not identified in the nuclear proteome or localized in the nucleus by TrypTag but have a predicted GO term associated with DNA or nuclear localization; and 5) proteins that were tagged in the TrypTag project but did not display nuclear localization however, have a predicted GO term associated with nucleus or DNA.

3.2.5 PTP endogenous tagging for candidates (Construct for Tb7990 was generated by Yahaira Bermudez)

For selected iPOND candidates Tb427.03.5370 (Tb5370) and Tb427.10.7990 (Tb7990), the C-terminal coding sequence was PCR amplified from *T. brucei* 427 genomic DNA using the primers listed in supplemental Table 1. Forward primers contained ApaI restriction site and reverse primers contained EagI restriction site. The PCR-amplified product for Tb5370 (699 bp) was ligated into ApaI and NotI restriction sites of pC-PTP-NEO and for Tb7990 the PCR-amplified product (498 bp) was ligated into ApaI and NotI restriction sites of pCPTP-PURO [34] to generate the respective iPOND candidate PTP-

vector. All final constructs were sequenced. For transfection, pTb5370-PTP-NEO was linearized using AvaI and pTb7990-PURO with XcmI. Procyclic *T. brucei* strain Lister 427 were transfected with the corresponding linearized plasmid using the Amaxa nucleofector 2b (Lonza) [35]. Stable population was first selected using 50 μg/ml of G418 and 1 μg/ml of puromycin, followed by limited dilution as previously described [36] to obtain a clonal cell line. Verification of chromosomal integration was done by PCR and PTP expression was confirmed by western blot.

3.2.6 RNAi Constructs (performed by Yahaira Bermudez)

The pSTL (stem-loop) vector for RNAi interference of each iPOND candidate was constructed as previously described using the pLEW 100 and pJM326 plasmids [37]. Briefly, for Tb5370 a 542 bp and for Tb7990 a 417 bp fragment from the coding sequence was PCR amplified from *T. brucei* 427 genomic DNA using the corresponding primers listed in the supplemental Table 1. These primers had the proper restriction enzyme linkers to generate the two fragments for the following cloning steps. The final construct has two copies of each candidate fragment in opposite direction and separated by an unrelated stuffer region. Final pSTL vector was linearized with EcoRV and transfected into *T. brucei* 29-13 cells using Amaxa nucleofector 2b (Lonza) [35]. A stable population was first selected using 2.5 μg/ml of phleomycin followed by limited dilution as previously described [36] to obtain a clonal cell line.

3.2.7 EdU and PTP Immunofluorescence (Performed by Dr. Klingbeil and Yahaira Bermudez)

EdU incorporation for a 10 min pulse was confirmed using the Picolyl azide Toolkit (Life Technologies). Cells were labeled with 150 μM EdU for 10 min, immediately harvested, washed with ice-cold PBS and adhered to poly-L-lysine coated slides (5 min). Cells were then fixed in 3% PFA (5 min, RT), washed in PBS containing 0.1 M glycine (pH7.4) three times (5 min, RT), and permeabilized with 0.1% Triton X-100 in PBS (5 min, RT). After three additional washes with PBS (5 min, RT), Click chemistry was performed using the Click-iT Plus Alexa Fluor Picolyl Azide Toolkit (Life Technologies) according to manufacturer's directions. Following click incubation for 1 hour at RT, cells were washed three times (5 min, PBS) and processed for immunofluorescence. Cells were incubated with anti-protein A antibody (Sigma) diluted 1:20,000 in PBS/1% BSA for 60 min, washed three times in PBS/0.1% Tween 20, and incubated with Alexa Fluor 594 goat anti-rabbit antibody diluted 1:250 in PBS/1% BSA for 60 min. DNA was stained with 3 μg/ml 4′-6′-diamidino-2-phenylindole (DAPI), and slides were washed 3 times in PBS prior to mounting in Vectashield (Vector Laboratories). Parasites were visualized and images captured either with a Nikon Eclipse E600 microscope with a cooled CCD Spot-digital camera (Diagnostic Instruments) using a 100X Plan Fluo 1.3 (oil) objective or with a Nikon N-SIM E superresolution microscope equipped with an RCA-Flash 4.0 sCOS camera (Hamamatsu Photonics) and a CFI SR Apochromate TIRF 100X (NA1.49) objective. Z-stacks (6 μm, 240 nm thickness) were acquired using the NIS-Elements Ar software. Image slices were reconstructed using default software parameters and 3D deconvolution using the automatic method in NSIM modality was applied. Images'

brightness and contrast were adjusted using Adobe Photoshop CS4 for presentation in figures.

3.2.8 EdU labeling Quantification (Performed by Dr. Klingbeil and Maria Rocha Granados) and Tb7990 microscopy analysis

Cells were incubated with 150 μM EdU for 30 min, immediately harvested and processed as described above for EdU immunofluorescence. Cells were then incubated with rat monoclonal antibody YL1/2 (Abcam) (60 min, 1:500 in PBS + 1% BSA) for basal body staining, washed three times in PBS + 0.1% Tween 20 and then incubated with Alexa Fluor 594 goat anti-rat and stained with DAPI.

For EdU fluorescence intensity quantification, only EdU positive cells were captured using the Nikon E600/Spot digital camera system. Non-saturating exposure times were used and non-adjusted images were analyzed using CellProfiler 3.0.0 [38] to measure EdU pixel intensity. Images were segmented with a DAPI signal to generate masks matching cell nuclei from which the mean EdU signal was calculated. A minimum of 220 EdU positive (EdU+) cells were analyzed from each time point. Data were represented using Prism 7 (GraphPad).

3.2.9 Conserved domain Analysis and Protein alignment

Protein sequence from selected candidates were analyzed using the NCBI conserved domain database search (CDD) [31] to look for domains present in our candidates. Eukaryotic Linear Motif (ELM) resource for Functional Sites in Proteins [33] was used to search motif in Tb5370. Both alignments were done using Clustal Omega

server [32]. For protein alignment for Tb5370, the following sequences were aligned: *T. brucei* (Tb, Tb927.03.5370), *Trypanosoma cruzi* (Tc, TcCLB.508409.180), *Leishmania braziliensis* (Lb, LbrM.29.0530), *Crithidia fasciculata* (Cf, CFAC1_100024000), *Leptomonas seymouri (*Ls, Lsey_0584_0010), *Bodo saltans* (Bs, CUG89542.1), *Phytomonas sp.* (CCW59550). Motifs were identified using ELM.

For Tb7990 alignment analysis, the following sequences were used: *Trypanosoma brucei* Tb7990 (Tb, Tb927.10.7990), *Leishmania major* (Lm, LmjF.36.6710), *Trypanosoma cruzi* (Tc, TcCLB.506247.270), *Chrithidia fasciculata* (Cf, CFAC1_280077100), *Homo sapiens* (Hs, AAV38474), *Saccharomyces cerevisiae* (Sc, NP_009644) and *Xenopus tropicalis* (XP_002934079)

3.3 Results

Our goal was to apply a stringent analysis to identify the proteins at the replication fork and its vicinity with few false positives. For that purpose, our filtering criteria was based on the following: Proteins should i) be identified in at least two of the EdU pulse replicates, ii) have a FC EdU/C- equal or above 10 and a FC EdU/DMSO equal or above 1.5, iii) should have been identified in the nuclear proteome analysis and/or displayed nuclear localization in the TrypTag project and/or a GO term associated with DNA. Based on these criteria, we identified and enriched a total of 410 proteins, where 99 are proteins of unknown function that currently are annotated as hypothetical proteins (Supplemental Table 1). Standard contaminants of proteomic analyses in trypanosomes such as ribosomal proteins, chaperones and retrotransposon-encoded proteins were eliminated [39]. Gene Ontology (GO) enrichment analysis using the tool PANTHER (37) revealed 23 GO terms

with >3-fold enrichment and a P-value of <0.001 (Fig 3.1, Table 3.1). The most abundant types of proteins were those involved in chromatin organization (fold enrichment, 10.7), transcription (9.91), DNA replication (7.43) and pre-mRNA splicing (7.03). To gain additional insight into the proteins enriched on trypanosome nascent DNA, we examined their potential relationships using the STRING database (38). After manually classifying proteins according to the best-known function, the analysis revealed a network of 9 clusters with abundant interactions between DNA replication and the categories DNA repair and nucleic acid metabolism. However, there were also abundant links between DNA replication and transcription clusters (Fig 3.2).

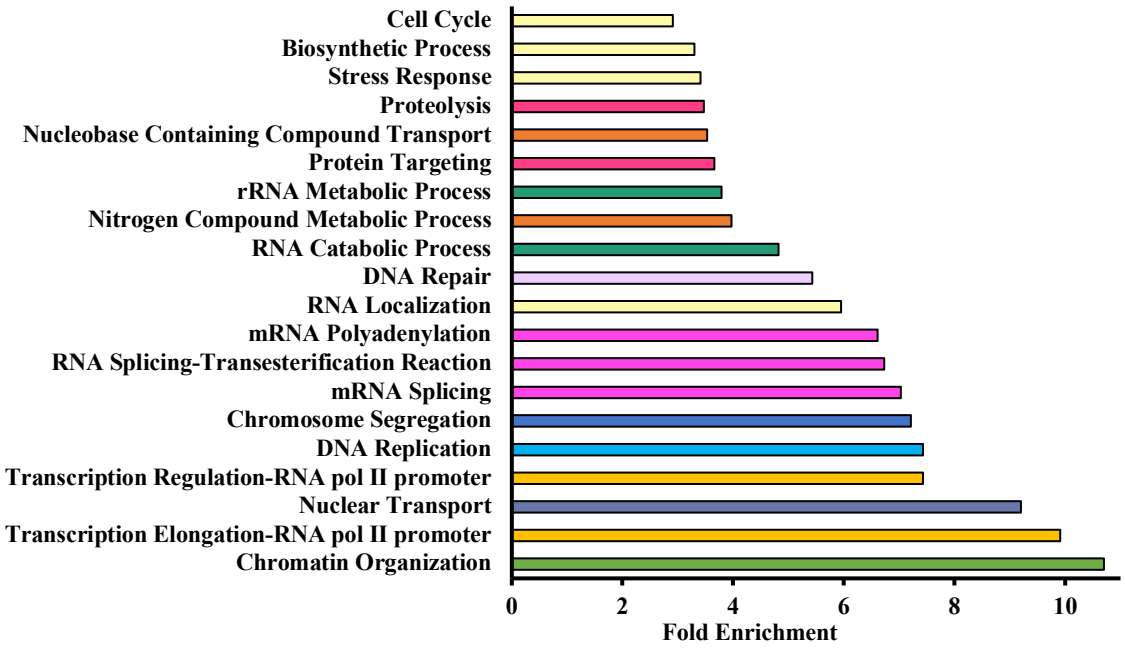

Figure 3.1 – GO analysis of *T. brucei* replication fork proteomics

Gene ontology (GO) analysis of the biological processes of the proteins identified in an unperturbed DNA replication fork. Graph represents the fold enrichment of each GO term in a hierarchy order.

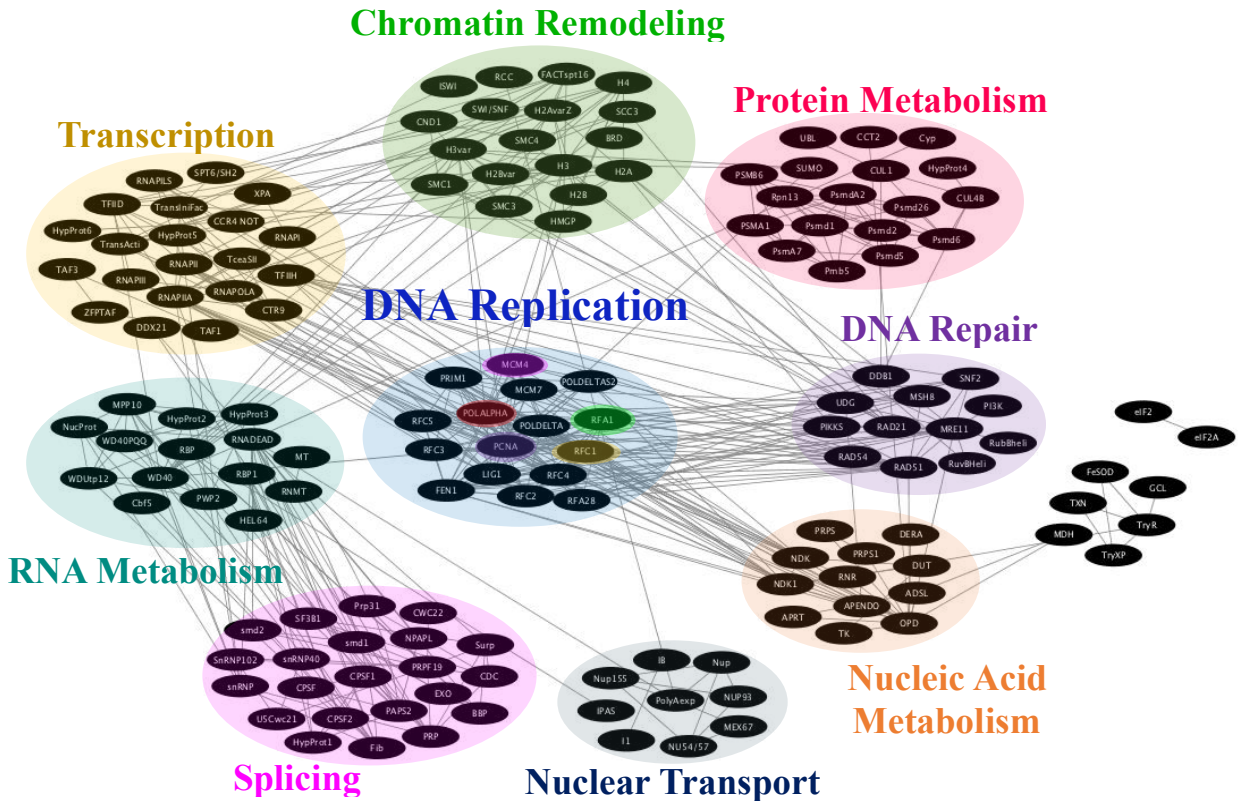

Figure 3.2 - STRING analysis of *T. brucei* replication fork proteomics

The protein–protein interaction network analysis of an active replication fork in *T. brucei* defined by STRING. The topology is organized according to functional classification. Nodes that are highlighted in the figure. DNA polymerase alpha, red; replication factor C, orange; replication factor 1 A, green; MCM4, purple; and PCNA, pink.

Table 3.1. Fold Enrichment and P value of enriched GO terms identified in *T. brucei* iPOND

GO slim PANTHER TERM	Fold enrichment	P value
Chromatin Organization	10.70	2.91×10^{-12}
Transcription Elongation-RNA pol II promoter	9.91	3.66×10^{-4}
Nuclear Transport	9.20	1.49×10^{-8}
Transcription Regulation-RNA pol II promoter	7.43	4.18×10^{-7}
DNA Replication	7.43	1.40×10^{-9}
Chromosome Segregation	7.21	4.28×10^{-5}
mRNA Splicing	7.03	2.21×10^{-7}
RNA Splicing-Transesterification Reaction	6.73	9.67×10^{-7}
mRNA Polyadenylation	6.61	5.06×10^{-3}
RNA Localization	5.95	3.65×10^{-4}
DNA Repair	5.43	8.10×10^{-8}
RNA Catabolic Process	4.82	2.49×10^{-3}
Nitrogen Compound Metabolic Process	3.97	2.91×10^{-34}
rRNA Metabolic Process	3.79	1.61×10^{-4}
Protein Targeting	3.66	1.32×10^{-3}
Nucleobase Containing Compound Transport	3.53	5.42×10^{-3}
Proteolysis	3.47	1.12×10^{-4}
Stress Response	3.41	2.49×10^{-5}
Biosynthetic Process	3.30	3.13×10^{-13}
Cell Cycle	2.91	3.98×10^{-5}

3.3.1 DNA replication proteins identified in *T. brucei* iPOND

As expected, we were able to identify proteins that have roles in DNA replication (Table 3.2) with a GO fold enrichment of 7.43 (P value 1.40 x 10^{-9}) (Fig 3.1, Table 3.1). We have identified proteins involved in DNA unwinding, DNA synthesis, processivity, DNA protection and Okazaki fragment processing. These include components of the heterohexameric MCM complex (MCM4 and MCM7), DNA polymerases α (Pol α) and δ (Pol δ), PCNA and replication factor C subunits, replication factor A subunits and FEN-1 endonuclease, respectively. These DNA replication factors were part of the DNA replication cluster in the STRING analysis (Fig 3.2). In the STRING analysis, interactions are derived from multiple sources including curated databases that include known experimental interactions and text mining that incorporates statistical links between proteins [29]. In the DNA replication cluster, PCNA was a key node to other DNA replication proteins but also to other clusters (Fig. 3.2, purple node). Its interactions with a subunit of the replication factor complex (RFC1; Fig 3.2, yellow node), and from RPA (RFA1; Fig 3.2, green node), as well as interactions with MCM4 (Fig 3.2, pink node) and DNA polymerase α (Pol α; Fig. 3.2B, red node) were expected. RFC1 is part of the clamp loader involved in PCNA loading, and RFA1 is part of the single-stranded DNA-binding protein complex RPA [40]. *T. brucei* RFC1 and RFA1 were enriched in our data set having ranking positions of 238 and 321 respectively, while PCNA ranked 311 (Table 3.2). *T. brucei* PCNA shows nuclear localization during the G1/S transition and S phase. Regulation of its proper levels is critical for DNA replication and proliferation and is uniquely regulated by the kinase TbERK8 [41–43]. Pol α and MCM4 ranked much higher

at the 9 and 13 position. The *T. brucei* MCM complex has been characterized and the single MCM4 subunit was able to unwind circular DNA *in vitro* as well as the complex [44]

Some of these factors did not display a high score, but this could be explained because they are at a low copy number at the replication fork. Nonetheless, after applying our stringency criteria, these proteins were still considered enriched. Some known DNA replication proteins did not pass the filtering criteria including DNA polymerase epsilon catalytic subunit, MCM2, Replication Factor A (51kDa subunit) and topoisomerase II.

Comparing the enriched *T. brucei* iPOND DNA replication proteins with two other studies that used label free quantification [5,45], several homologs of known *T. brucei* DNA replication were identified in those studies. Additionally, we were able to identify expected DNA replication factors that those studies did not detect such as MCM and primase subunits (Table 3.2). These observations give confidence to our data and our analysis.

To test if the DNA replication proteins identified are enriched on nascent DNA, we calculated the FC EdU/ThD chase for these proteins. The FC EdU/ThD chase was calculated for the three EdU pulse replicates with the single ThD chase sample, these three values were added and averaged to obtain a final FC. From this initial analysis, RFC4 and MCM4 were only detected in the EdU and absent in the ThD chase sample (INF value). The remaining DNA replication proteins identified have an average FC ranging from 0.6 to 4.7, where PCNA becomes a highly enriched (FC of 4.7) compared to the ThD chase sample (Table 3.3). This was expected since PCNA interacts with nascent DNA as it is shown in other studies [45,46] where this protein is highly enriched in the short EdU pulse, but its detection decreased in the ThD chase.

Table 3.2. *T. brucei* DNA replication proteins identified by iPOND.

Tb927 Protein ID	Product Description	Mol. Weight [kDa]	Ranking Position	Total Score	Identified by Cortez lab[a]	Identified by Ernforns lab[b]
Tb927.8.4880	DNA polymerase alpha catalytic subunit	152	9	134.02	no	yes
Tb927.11.12250	DNA replication licensing factor MCM4	93	13	132.20	no	yes
Tb927.10.7990	ATPase, putative, replication factor 3	39	15	114.68	no	yes
Tb927.3.830	flap endonuclease-1 (FEN-1), putative	44	71	77.62	no	yes
Tb927.11.16140	DNA replication licensing factor MCM7	81	93	73.57	no	yes
Tb927.3.1130	DNA polymerase delta subunit 2, putative	62	134	70.40	no	yes
Tb927.11.9550	replication factor C, subunit 4, putative	38	149	69.20	yes	yes
Tb927.9.12300	replication factor C, subunit 3, putative	40	180	51.86	no	yes
Tb927.2.1800	DNA polymerase delta catalytic subunit, putative	117	189	48.39	yes	yes
Tb927.6.3890	replication factor C, subunit 2, putative	39	216	42.93	yes	yes
Tb927.7.2310	DNA primase small subunit, putative	48	219	42.80	no	no
Tb927.11.5650	replication factor C, subunit 1, putative	65	238	41.01	yes	yes
Tb927.4.1330	DNA topoisomerase IB, large subunit	79	283	37.39	yes	no
Tb927.9.5190	proliferative cell nuclear antigen (PCNA), putative	32	311	28.61	yes	yes
Tb927.6.4780	DNA ligase I, putative	83	319	18.60	yes	yes
Tb927.11.9130	Replication factor A protein 1	52	321	17.37	yes	no
Tb927.5.1700	replication Factor A 28 kDa subunit, putative	28	388	7.89	no	no

Table 3.3. Enrichment of DNA Replication Proteins in EdU vs. Thymidine Chase

Tb927 Protein ID	Product Description	Average FC EdU/ThD
Tb927.11.12250	DNA replication licensing factor MCM4	INF
Tb927.11.9550	replication factor C, subunit 4, putative	INF
Tb927.9.5190	proliferative cell nuclear antigen (PCNA), putative	4.7
Tb927.9.12300	replication factor C, subunit 3, putative	3.5
Tb927.5.1700	replication Factor A 28 kDa subunit, putative	3.4
Tb927.11.5650	replication factor C, subunit 1, putative	2.8
Tb927.3.830	flap endonuclease-1 (FEN-1), putative	2.4
Tb927.8.4880	DNA polymerase alpha catalytic subunit	2.3
Tb927.7.2310	DNA primase small subunit, putative	1.9
Tb927.10.7990	ATPase, putative, replication factor C	1.8
Tb927.11.16140	DNA replication licensing factor MCM7	1.5
Tb927.11.9130	Replication factor A protein 1	1.5
Tb927.6.3890	replication factor C, subunit 2, putative	1.3
Tb927.4.1330	DNA topoisomerase IB, large subunit	1.2
Tb927.6.4780	DNA ligase I, putative	1.2
Tb927.2.1800	DNA polymerase delta catalytic subunit, putative	0.8
Tb927.3.1130	DNA polymerase delta subunit 2, putative	0.6

3.3.2 Chromatin and Transcription proteins identified in *T. brucei* iPOND

GO terms associated with chromatin proteins (remodeling, organization, assembly and epigenetic changes) were the highest enriched biological processes identified in our data set, with chromatin organization displaying the highest fold enrichment (10.70; P-value of 2.91 x 10^{-12}) (Fig 3.1, Table 3.1). This is expected since nucleosomes assemble immediately behind the DNA replication fork with the first deposited nucleosome detected at a distance of only ~250 bp from the replication fork [47], and even though nucleosomes are disrupted ahead the replication fork and histones are disassociated from DNA, they remain in near proximity during fork passage for their inheritance during DNA replication [48,49]. Additionally, we estimated that in a 10 min EdU pulse we have labeled 37 kbp of *T. brucei* DNA. This number of EdU-labeled kbp increases the likelihood of identifying chromatin-associated proteins on nascent DNA. In our data set, nucleosome components were enriched such as histone H3, 4 (H4), 2A(H2A), 2B (H2B), 2A variant Z (H2AZ), 2B variant (H2BV) and 3 variant (H3V) were detected (Table 3.4). Histone chaperones such as FACT, contribute to rapid nucleosome assembly at the replication fork, and chromatin remodeling enzymes such as Isw1 help load and position nucleosomes during DNA replication [50]. Accordingly, there are representatives from at least 3 chromatin remodeling complexes present in the data set, namely both FACT subunits (rank 212, 375), two INO80 RuvB-like proteins (rank 338, 397), and 3 of the 4 ISWI complex proteins (rank 96, 255, 324). In addition, several other putative nucleosome assembly proteins were detected (Table 3.4 and Sup Table 1). Interestingly, when comparing average FC EdU/ThD chase, several of the chromatin associated proteins, especially the FACT components, were

enriched on nascent DNA further supporting the notion that nucleosome assembly occurs in proximity to the replication fork (Table 3.4).

In model organisms such as *Drosophila melanogaster,* early replicating domains of the genome associate with transcriptionally active euchromatin, while late replicating domains associate with heterochromatin. Genome-wide studies of replication timing in *Drosophila* showed that early replication sequences are defined by chromosomal regions of active transcription [51]. Additionally, heterochromatin marks such as H3K27me3, H3K9me2 and H3K9me3 are associated with late replication sequences, suggesting a correlation of replication timing with chromatin landscape [52]. Genome-wide analyses mapped *T. brucei* ORC1 binding sites to the boundaries of DGCs revealing an unprecedented level of functional interaction between transcription and DNA replication [53]. Additionally, in the related trypanosomatid *L. major*, genome wide studies indicated that initiation and timing of DNA replication depend on RNA pol II transcription dynamics that are also a driving force for nucleosomal organization [54].

In support of an association between transcription and DNA replication, the transcription GO term had a 9.91-fold enrichment (P-value of 3.66×10^{-4}) (Fig 3.1; Table 3.1), and STRING analysis showed transcription proteins interacting with all clusters except for nuclear transport and protein metabolism (Fig 3.2). Subunits of all three nuclear RNA polymerases were identified, together with other important transcription proteins such as TATA-box binding protein (rank 16), two elongation factors (rank 98, 110), and several basal transcription initiation factors (rank 68, 72, 131, 147, 240) (Table 3.5). These findings are in accordance with enrichment of transcription machinery in iPOND studies conducted in other systems [45,55,56].

Table 3.4 Selected chromatin-associated proteins identified in *T. brucei* iPOND

Tb927 Protein ID	Product Description	Mol. Weight [kDa]	Ranking Position	Total Score	Total FC EdU/ThD
Tb927.11.7350	Histone H2B variant V	16	63	84.12	4.05
Tb927.2.1810	chromatin-remodeling complex ATPase chain isw1	133	96	73.49	7.56
Tb927.7.6360	histone H2A variant Z	19	175	53.42	7.06
Tb927.10.14390	Histone chaperone Rttp106-like, putative	61	212	43.51	9.19
Tb927.10.15180	nucleosome assembly protein, putative	41	222	42.59	2.63
Tb927.7.1060	ISWI complex protein	54	255	39.69	2.32
Tb927.11.13400	Bromodomain, putative	74	268	38.70	7.14
Tb927.9.5730	nucleosome assembly protein-like protein	48	271	38.42	4.46
Tb927.10.15350	histone H3 variant V	16	295	36.35	4.34
Tb927.10.5450	ISWI complex protein	107	324	15.82	4.33
Tb927.7.2820	histone H2A, putative	14	337	13.58	9.23
Tb927.4.1270	ruvB-like DNA helicase, putative	50	338	12.98	6.06
Tb927.5.4220	histone H4, putative	11	358	10.57	INF
Tb927.3.3490	High mobility group protein TDP1	31	368	9.62	6.88
Tb927.3.5620	Facilitates chromatin transcription complex subunit spt16 FACT	113	375	9.00	6.96
Tb927.10.10530	histone H2B, putative	13	382	8.53	INF
Tb927.4.2000	ruvB-like DNA helicase, putative	53	397	6.80	5.1
Tb927.1.2470	histone H3, putative	15	401	6.36	INF

Table 3.5 Selected transcription proteins identified in *T. brucei* iPOND

Tb927 Protein ID	Product Description	Mol. Weight [kDa]	Ranking Position	Total Score
Tb927.4.5320	Component of IIS longevity pathway SMK-1, putative	97	7	134.65
Tb927.10.15950	TATA-box-binding protein	29	16	109.87
Tb927.4.5020	DNA-directed RNA polymerase II subunit RPB1	170	29	104.03
Tb927.11.1390	class I transcription factor A, subunit 1	53	68	78.98
Tb927.1.1700	AATF protein, putative (Apoptosis-antagonizing transcription factor)	55	69	78.31
Tb927.2.5030	transcription initiation protein, putative	80	72	77.59
Tb927.1.1680	Transcription elongation factor 1 domain-containing protein	26	98	73.27
Tb927.4.3490	DNA-directed RNA polymerases II and III subunit RPB6, putative	16	99	73.21
Tb927.8.5090	DNA-directed RNA polymerase I largest subunit	196	104	73.03
Tb927.11.370	repressor activator protein 1	93	105	72.94
Tb927.2.3580	transcription elongation factor s-II, putative	52	110	72.53
Tb927.8.5980	TFIIH basal transcription factor complex helicase subunit, putative	92	131	70.54
Tb927.11.9430	TFIIH basal transcription factor subunit	41	147	69.28
Tb927.1.540	DNA-directed RNA polymerase III, putative	127	217	42.92
Tb927.10.8720	CCR4-NOT transcription complex subunit 10, putative	61	236	41.14
Tb927.11.1410	class I transcription factor A, subunit 3	47	240	40.68
Tb927.10.15370	DNA-directed RNA polymerases I and III subunit RPAC1, putative	37	242	40.47
Tb927.9.5710	general transcription factor IIB	38	245	40.30
Tb927.3.1270	PRP38 family, putative	61	256	39.67
Tb927.4.1310	ZFP family member, putative zin finger transcription factor	47	294	36.37
Tb927.11.630	RNA polymerase I second largest subunit	179	323	16.03
Tb927.4.3810	DNA-directed RNA polymerase II subunit 2, putative	134	336	13.67
Tb927.9.12900	RNA polymerase-associated protein LEO1, putative	65	354	10.92
Tb927.5.4420	nucleolar RNA helicase II, putative	69	380	38.72
Tb927.8.1510	ATP-dependent RNA helicase DBP2B, putative	62	381	8.68

3.3.4 DNA repair proteins identified in *T. brucei* iPOND

DNA repair was another GO term enriched in our data set with a fold enrichment of 5.43 (P-value $8.10 \bullet 10^{-8}$) (Fig 3.1; Table 3.1). Proteins involved in DNA repair such as RAD54 (rank 12) and RAD51 (rank 378) (Table 3.6) were identified. These factors participate in repairing DNA double-strand breaks by homologous recombination and have physical and functional interaction. RAD54 drives branch migration and stimulates RAD51 strand exchange activity [57] whereas RAD51 mediates homology search, strand invasion, and D-loop formation steps [58]. When RAD51 was silenced in *T. brucei*, the parasites were more sensitive to DNA damaging agents and they lost their ability to undergo VSG (variant surface glycoproteins) switching [59]. VSG switching is the process that leads to antigenic variation in the BSF and occurs by homologous recombination, double strand breaks and telomere proteins [60]. We also enriched BRCA2 (rank 50) (Table 3.6), another protein associated with VSG switching in *T. brucei* [61]. BRCA2 interacts with RAD51 and regulates RAD51 nuclear localization and its DNA binding ability in humans [62]. In *T. brucei* was shown that BRCA2 is involved in DNA repair and recombination, and when this gene is depleted the frequency of VSG switching is reduced from 8 to 11 fold relative to WT [61].

The fact that we are enriching proteins related to DNA repair on nascent DNA might indicate that DNA repair is active during new synthesis or shortly after DNA is replicated. Enrichment of DNA recombination proteins in active replication forks might suggest that these events of recombination can occur in newly synthesized DNA in procyclic parasites. It would be interesting to see if these proteins colocalize with newly synthesized DNA in BSF to evaluate if VSG switching occurs during S phase.

Table 3.6 DNA repair and recombination proteins identified in *T. brucei* iPOND

Tb927 Protein ID	Product Description	Mol. Weight [kDa]	Ranking Position	Total Score
Tb927.11.5430	DNA repair and recombination protein RAD54, putative	114	12	133.33
Tb927.11.3550	XPA-interacting protein, putative	32	37	103.01
Tb927.10.6410	DNA mismatch repair protein MSH6, putative	110	47	101.11
Tb927.1.640	BRCA2, nucleoside diphosphate kinase, putative	176	50	100.67
Tb927.9.5240	mismatch repair protein MSH3, putative	102	58	90.62
Tb927.10.13970	uracil-DNA glycosylase, putative	33	111	72.5
Tb927.11.14680	phosphatidylinositol 3-related kinase, putative	321	115	72.09
Tb927.3.5440	SNF2 DNA repair protein, putative	167	145	69.68
Tb927.8.5510	apurinic/apyrimidinic endonuclease, putative	44	167	67.46
Tb927.11.9050	p21-C-terminal region-binding protein, putative	45	202	45.36
Tb927.6.5110	damage-specific DNA binding protein, putative	138	207	44.30
Tb927.2.5810	Holliday-junction resolvase-like of SPT6/SH2 domain containing protein, putative	174	210	43.62
Tb927.2.4390	endo/exonuclease Mre11	82	220	42.77
Tb927.11.9490	CobW/HypB/UreG, nucleotide-binding domain containing protein, putative	38	227	41.90
Tb927.3.4160	XPC-binding domain/UBA/TS-N domain containing protein	36	285	37.38
Tb927.8.3500	mms19 nucleotide excision repair protein homolog	104	297	36.22
Tb927.11.8190	DNA repair protein RAD51	41	378	8.84

3.3.4 RNA Splicing

One GO term that we were surprised to see enriched was mRNA splicing with a fold enrichment 7.03 (P-value of 2.21 x 10^{-7}) (Fig 3.1; Table 3.1). Proteins that are part of the spliceosome such as SmB (rank 42), SmD2 (rank 163) and U5-40K (rank 308) were identified. Also, proteins involved in polyadenylation and capping were identified (Table 3.7). Recently, the link between nucleosome occupancy, RNA pol II levels and splicing elements in *T. brucei* was addressed [63]. This study was found that RNA pol II sites are in close proximity of regions associated with TSS marked by histone variants such as H2A.Z. RNA pol II-initiated transcription at the 5´end of H2A.Z peaks and its enrichment was across 2 kbp. Therefore, the regions upstream of RNA pol II enrichment could mark sites of transcription initiation. These data suggest that the position of nucleosomes at exon boundaries acts as a barrier causing RNA pol II enrichment and transcription pausing which lead to the recruitment of splicing factors and increase trans-splicing efficiency. In our data set, we have enriched H2A.Z (Table 3.4), RNA pol II subunits (Table 3.5) and splicing factors (Table 3.7) suggesting that co-transcriptional splicing events might occur in near proximity of newly replicated DNA.

Table 3.7. Selected RNA Splicing factors identified in *T. brucei* iPOND

Tb927 Protein ID	Product Description	Mol. Weight [kDa]	Ranking Position	Total Score
Tb927.6.4600	pre-mRNA splicing factor ATP-dependent RNA helicase, putative	114	25	104.52
Tb927.11.11850	splicing factor 3B subunit 1, putative	122	41	102.53
Tb927.2.4540	Small nuclear ribonucleoprotein-associated protein B (snRNP-B) (Sm protein B) (SmB), putative	12	42	102.50
Tb927.9.3480	U5Cwc21 small nuclear ribonucleoprotein	16	46	101.50
Tb927.3.2190	Capping enzyme RNA triphosphatase 1	29	82	74.92
Tb927.8.2000	cyclophilin, putative	33	103	73.05
Tb927.4.1340	cleavage and polyadenylation specificity factor subunit, putative	85	106	72.78
Tb927.10.7280	pre-mRNA splicing factor ATP-dependent RNA helicase, putative	121	125	71.12
Tb927.2.5850	small nuclear ribonucleoprotein SmD2	12	163	68.10
Tb927.7.3780	Nuclear poly(A) polymerase 2	74.00	170	62.25
Tb927.10.10700	splicing factor Prp31	40	179	51.90
Tb927.8.900	splicing factor TSR1	37	218	42.91
Tb927.11.10750	pre-mRNA-splicing factor CWC22, putative	67	193	47.21
Tb927.11.6720	mRNA cap guanine-N7 methyltransferase, putative	118	234	41.22
Tb927.11.11150	U5 snRNP-specific 40 kDa protein, putative	35	308	34.40
Tb927.11.2370	mRNA export factor MEX67	56	348	11.29
Tb927.2.5240	pre-mRNA splicing factor 19	54	399	6.65

3.3.5. Initial characterization of Tb427.10.7990 (Tb7990).

Many of the key DNA replication elongation factors in *T. brucei* have not been characterized [64]. Therefore, we decided to study Tb427.10.7990 (Tb7990) (Rank 15) for since is annotated as replication factor C subunit 3 (RFC3). Replication factor C (RFC) is a protein that participates in DNA replication, repair and cell cycle checkpoints [65]. It is composed of five essential subunits and acts as a clamp loader for sliding clamps such as PCNA. Subunit 1 (RFC1) is the largest subunit, while the other 4 (RFC2-5) have similar molecular weight [66]. RFC binds to primed DNA and by using ATP, directs the loading of PCNA onto DNA [65]. Additionally, we used this protein as a positive control to study DNA replication defects. First, we performed a protein alignment using Tb790 sequence with other RFC3 factors from other kinetoplastids and model eukaryotes (Fig 3.3). The ATP-binding Walker A motif, the magnesium ion-binding Walker B motif that is required for ATP hydrolysis [67], and the SRC motif (also called an arginine finger) that senses bound ATP and participates in ATP hydrolysis [68] were identified in Tb7990. We noticed that in our RFC3 alignment there are distinct substitutions in the Walker A and Walker B motifs. Instead of having the consensus GXXXXGKT [69], the analyzed RFC3 sequences have the sequence GXXXXGKK; and for the Walker B region instead of the hhhhDExx consensus [70], Tb7990 and the other kinetoplastids have the hhhhNExx sequence.

We confirmed Tb7990 nuclear localization and its colocalization with newly synthesized DNA using a Tb7990-PTP-tagged cell line. Tb7990-PTP localized as several punctate foci in the nucleus and was excluded from the nucleolus. While there was colocalization with EdU foci, the two patterns did not precisely overlap (Fig 3.4A).

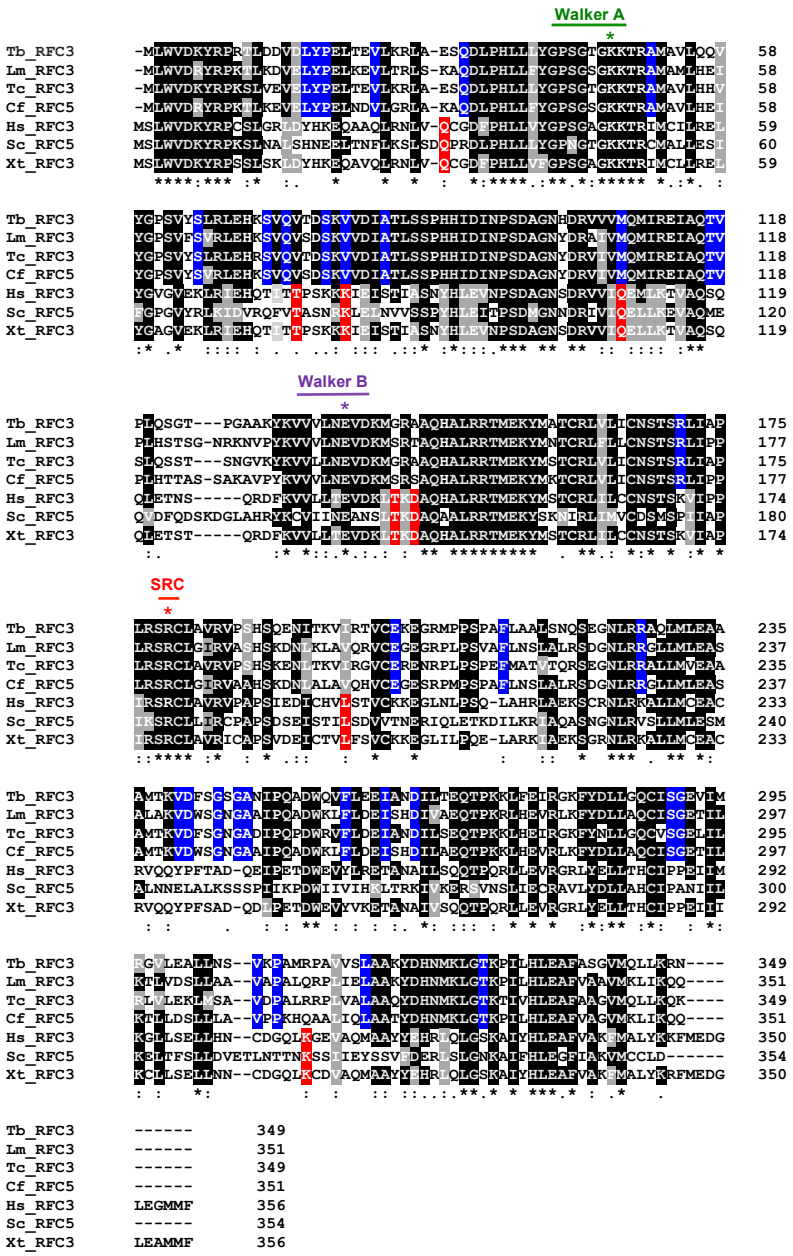

Figure 3.3 - Replication Factor C alignment

Alignment highlights motifs found in RFC subunits and key residues such as the lysine (green asterisk) in the Walker A motif involved in ATP binding, the glutamate (purple asterisk) in the Walker B motif that contributes to the RFC binding to PCNA and DNA, and the arginine finger (red asterisk) present in the SRC (Ser-Arg-Cys) motif that promotes ATP hydrolysis. Positions having more than 50% of identity were highlighted in black. Strongly conserved residues are highlighted in gray. In blue positions that are conserved only in kinetoplastids, and in red residues that are not conserved in kinetoplastids. Stars and colons represent identical or similar positions. Tb (*T. brucei*), Lm (*L. major*), Tc (*T. cruzi*), Cf (*C. fasciculata*), Hs (*H. sapiens*), Sc (*S. cerevisiae)* and Xt (*X. tropicalis*)

RNAi knockdown of Tb7990 yielded a 75% reduction of its mRNA and a loss of fitness starting on D3 (day 3) (Fig 3.4B). We used fluorescence microscopy to observe the effects of Tb7990 depletion in an asynchronous population during the course of RNAi knockdown. To track cell cycle stages, we used DAPI and basal body staining. DAPI staining is used to assign a specific cell cycle stage based on kDNA and nuclear DNA morphology [71]. In *T. brucei*, kDNA duplication occurs before nuclear DNA replication. An elongated kinetoplast is an indicator that the cells are in nuclear S phase [71]. Basal body duplication is one of the earliest markers in *T. brucei* cell cycle and is linked to kDNA replication and segregation [72]. The distance between the two duplicated basal bodies increases as the cell cycle progresses until cytokinesis occurs [73]. Basal bodies can be visualized by using the YL1/2 antibody that detects tyrosinated tubulin. During the course of RNAi knockdown, we observed that on D3 cells at the 1N2K configuration were EdU+ with a high fluorescence intensity (Fig 3.5A). In *T. brucei*, cells in this configuration are in G2 phase or undergoing mitosis [71,74,75] as is observed in uninduced (UN) cells (Fig 3.5A), and no EdU uptake is expected. EdU incorporation and fluorescence intensity were reduced in D5 (day 5), especially in cells at the $1N1K_{div}$ configuration. At this cell cycle stage, cells are in nuclear S phase [71,74,75] and therefore, it is expected to be EdU+. Additionally, at D5 we observed the presence of zoids (cells without nucleus, 0N1K) and abnormal cells (Fig 3.5A and B). Zoids arise from cytokinesis of 1N2K cells that completed kDNA replication and cell division but were unable to perform nuclear division. However, procyclic cells in *T. brucei* can undergo cytokinesis without having completed mitosis [76]. Therefore, to test if the formation of zoids is a result of DNA replication defect, we quantified the EdU fluorescence intensity during the course of Tb7990 silencing (Fig

3.5C). UN cells have an EdU fluorescence intensity ranging from 0.055-0.20. This pattern was similar for D1 (day 1) cells but in D2 (day 2) a reduction in EdU intensity was observed. Surprisingly, at D3 EdU fluorescence intensity increased and had a range from 0.064-0.28. This was statically significant when compared to UN cells. This might indicate that the cells in D3 are continuously duplicating their DNA because there are unable to proceed to next cell cycle stage. From D4 (day 4) to D5, there was a reduction in EdU intensity where D5 displayed the lowest intensities ranging from 0.011-0.18, and were also statically different from UN cells. Tb7990 depletion effects are similar to the ones reported when silencing *T. brucei* DNA replications proteins such as ORC1 [77], MCM subunits (3, 5 and 7) [44] and PCNA [42], where there was zoid accumulation and a reduction of BrdU (5-Bromo-2′-deoxyuridine) uptake, another thymidine analog.

A

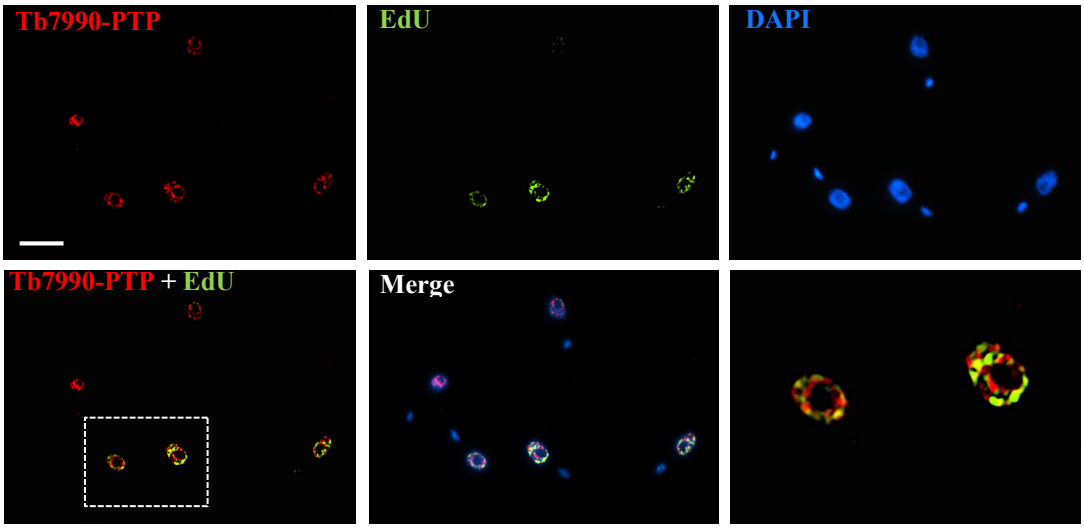

B

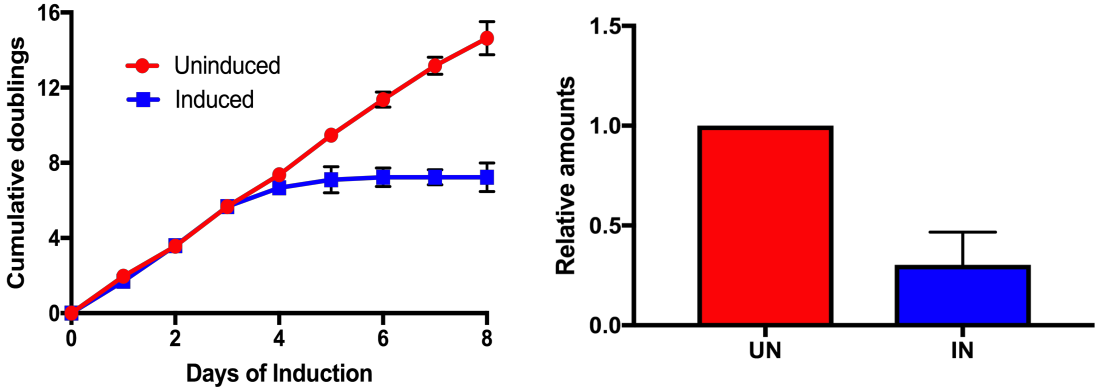

Figure 3.4 - Nuclear localization and RNAi knockdown of Tb7990

Characterization of Tb7990. A) Localization of Tb7990 PTP-tagged protein in asynchronous populations labeled with EdU using SIM microscopy. PTP tag was detected with anti-protein A (red), EdU incorporation (green) and DNA was stained with DAPI (blue). Enlargement correspond to the white dashed boxes. Size bar, 5 µm. B) Tb7990 RNAi knockdown clonal cell line characterization. *Left Panel*. Growth curves in the presence and absence of tetracycline induction. *Right panel*. qRT-PCR analysis of uninduced (red) and induced (blue) cells after 48 hours of growth. Data are normalized using TERT.

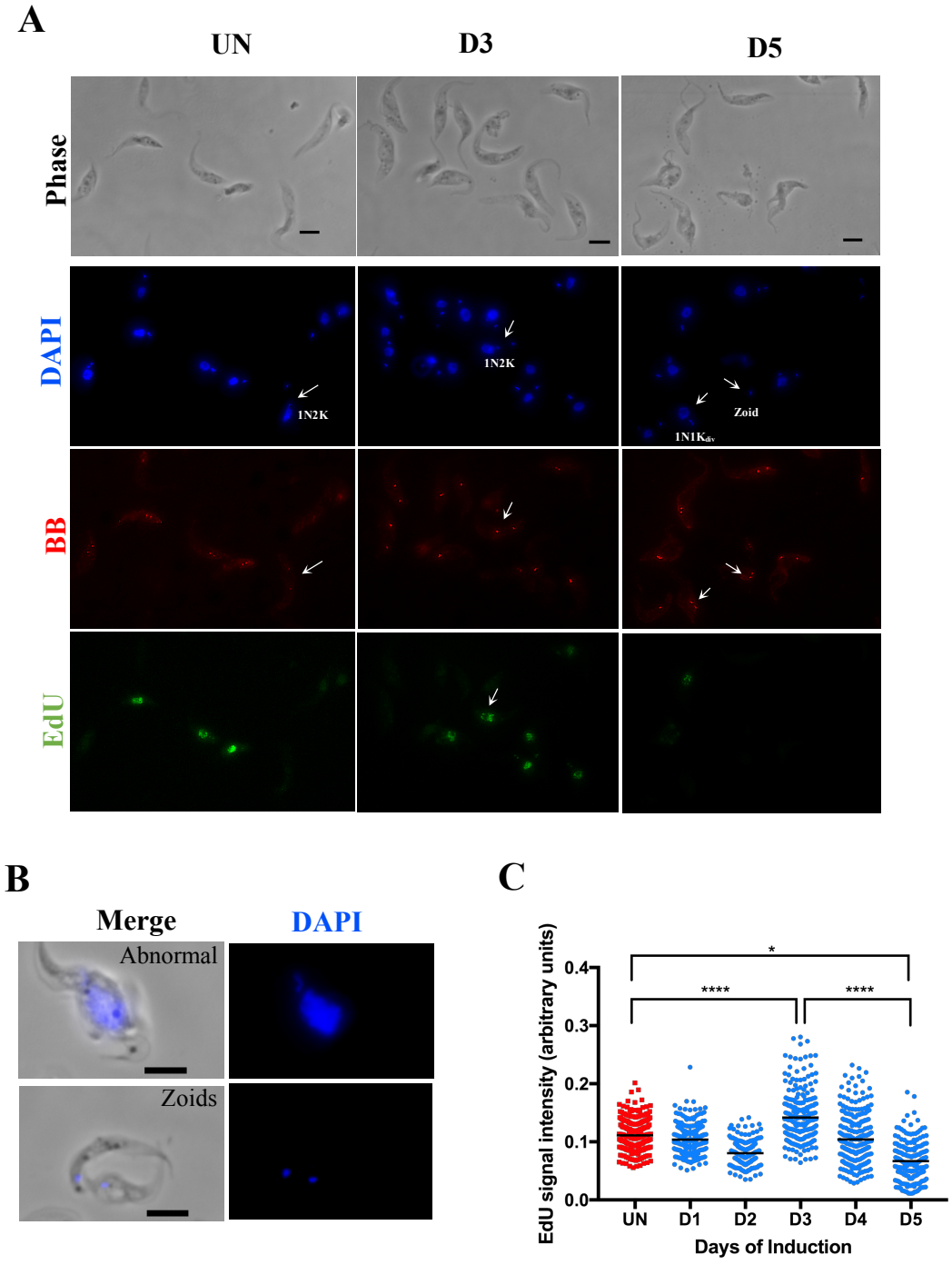

Figure 3.5 – Analysis of RNAi knockdown of Tb7990

Cells were induced for the indicated days and then EdU labeled. A) Microscopy analysis of Tb7990 depletion. DNA is stained with DAPI (blue), basal body detected with YL1/2 antibody (red) and EdU incorporation is detected with Alexa Fluor™ 488 picolyl azide (green). Size bar, 5 µm. B) Examples of zoids and abnormal cells upon Tb7990 silencing. Size bar, 5 µm C) EdU fluorescence quantification analysis. Each dot represents EdU signal intensity per nucleus for each induction day. Statistical analysis unpaired two-tailed t-test ****P < 0.0001, *P <0.02.

3.3.6. Initial characterization of Hypothetical proteins Tb427.03.5370 (Tb5370).

To analyze whether our data set revealed new replication proteins, we picked one protein of unknown function, Tb5370 (rank 123), from our data set for functional characterization. This protein was selected because of its strong expression during S phase [78] and it was related to the Topo2C family (domain cl25574, E-value 5.16 x 10^{-5}) of type II topoisomerases after performing a domain search using the NCBI Conserved Domain tool [31]. DNA topoisomerases manage the topological state of the DNA and they are required in DNA transaction processes in the cell such as replication, transcription and repair. Topoisomerases can be classified in two main types based in their mechanism and sequence similarity. Type I Topoisomerases cleave one strand of DNA while DNA topoisomerases II cleave two strands [79,80]. Type II topoisomerases participates in DNA replication, sister chromatid segregation and chromosome condensation [81,82]. We also observed that Tb5370 depletion can impact negatively parasite fitness mostly in procyclic cells based on RIT-seq (RNA interference target sequencing) data [83]. However, protein alignment of Tb5370 with other type II topoisomerases showed Tb5370 was lacking key residues involved in topoisomerase activity and therefore we decided to analyze the protein sequence by inspecting for motifs in Tb5370 and the corresponding homologs in other trypanosomatids. In this analysis, we identified the FHA (forkheaded associated domain) phosphopeptide ligand motif and the CDK (cyclin dependent kinases) phosphorylation site motif (Fig 3.6). We verified if there are serine or threonine residues within the CDK phosphorylation site motif that are phosphorylated by using the phosphoproteomic data available for *T. brucei* [84]. Three serine residues are phosphorylated in this motif at the 231, 233 and 235 positions (Fig 3.6). CDKs phosphorylate protein substrates that are

associated with regulation of cell cycle transitions [85], such as DNA synthesis and mitosis [86]. In addition, these kinases also phosphorylates proteins involved in DNA damage [87]. Since Tb5370 is predicted to have FHA motifs which are present in proteins involved in DNA repair and transcription [88], and to be phosphorylated by CDKs, we decided to further characterize this gene. We corroborate Tb5370 nuclear localization and colocalization with newly synthesized DNA. Tb5370 was fused at the C-terminus with a PTP tag and detected using anti-protein A antibodies. Nuclear DNA was labeled with DAPI and newly synthesized DNA with EdU in a 10 min pulse. Tb5370 displayed nuclear localization in all cell cycle stages and had a perinuclear distribution similar to what is observed nucleoporins. It did not colocalize with EdU foci. (Fig 3.7A). Contrary to what was observed from the RNAi targeting data, when we silenced the Tb5370 gene for a period of 8 days, we could not detect a growth defect in PCF cells (Fig 3.7B). We confirmed depletion of Tb5370 by qPCR and the knockdown reduced 90% of Tb5370 mRNA.

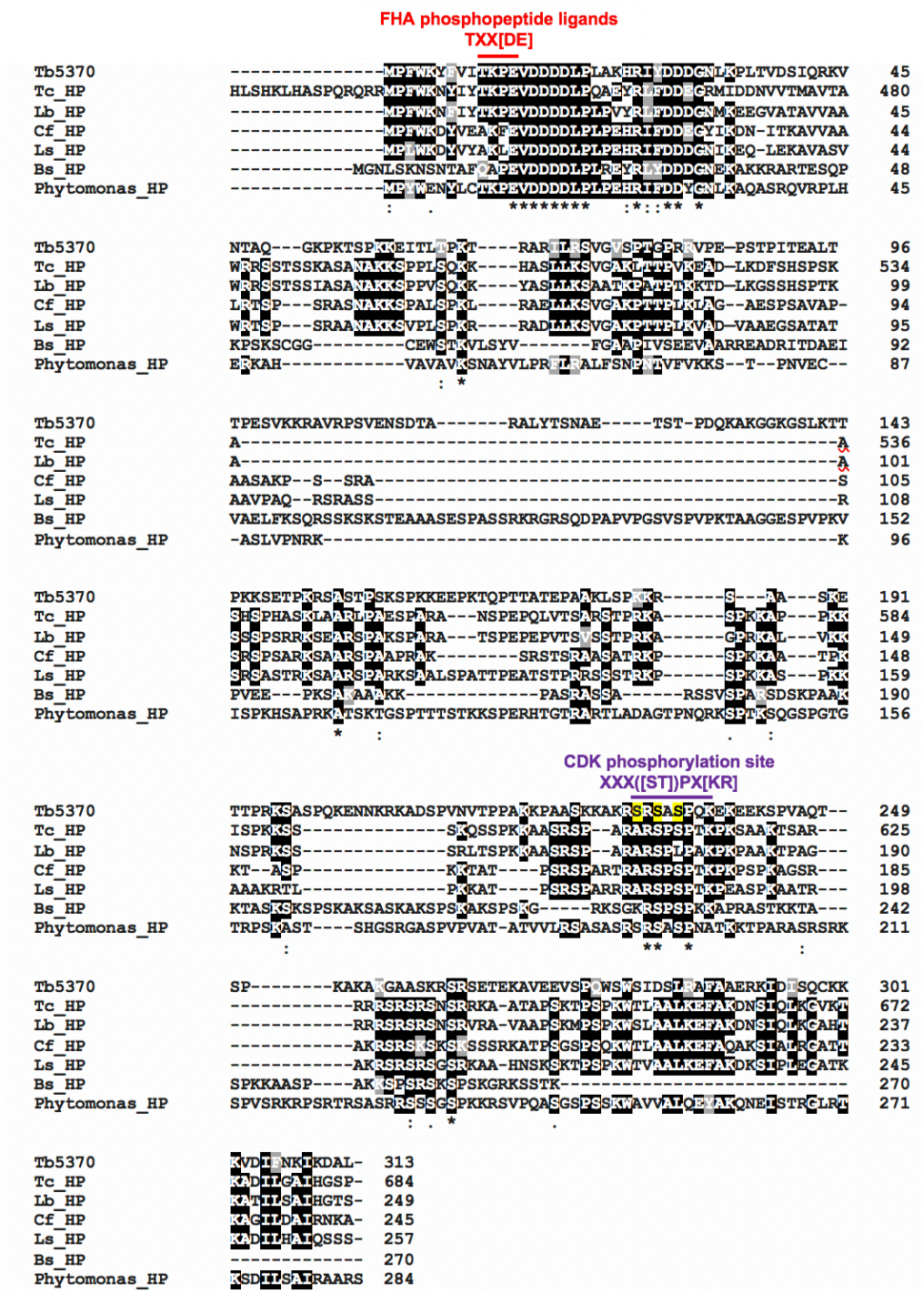

Figure 3.6 - Tb5370 Alignment using selected kinetoplastid sequences

Motifs were identified using ELM where X represents any residue. FHA motif (red); CDK phosphorylation site motif (purple). In yellow, serine residues that are phosphorylated. Positions having more than 50% of identity were highlighted in black. Residues that were strongly conserved are highlighted in gray. Stars and colons represent identical or similar positions. Tc (*T. cruzi*), Lb (*L. braziliensis*), Cf (*C. fasciculata),* Ls (*L. seymouri*), Bd (*B. saltans*) and *Phytomonas sp.*

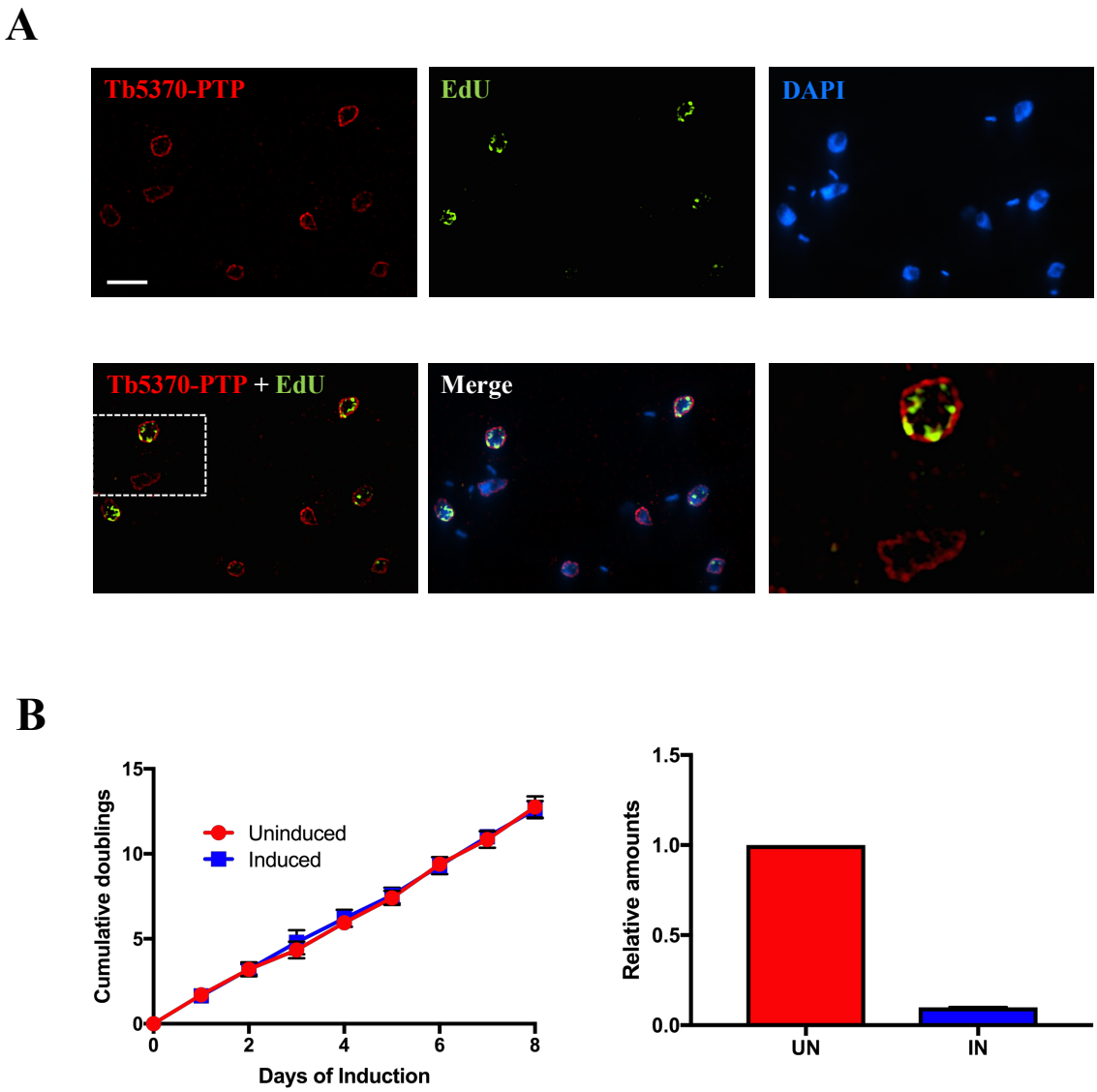

Figure 3.7 - Nuclear localization and RNAi knockdown of Tb5370

Characterization of Tb5370. A) Localization of Tb5370 PTP-tagged protein in asynchronous populations labeled with EdU using SIM microscopy. PTP tag was detected with anti-protein A (red), EdU incorporation (green) and DNA was stained with DAPI (blue). Enlargement corresponds to the white dashed boxes. Size bar, 5 µm. B) Tb5370 RNAi knockdown clonal cell line characterization. *Left Panel*. Growth curves in the presence and absence of tetracycline induction. *Right panel*. qRT-PCR analysis of uninduced (red) and induced (blue) cells after 48 hours of growth. Data are normalized using TERT.

3.4 Discussion

Using iPOND-Label-free MS quantification, we were able to generate a list of proteins that are present in the vicinity of the replication fork. Additionally, we obtained a panoramic view of the cellular processes that in coordination with DNA replication, help to maintain genomic stability in *T. brucei*. Compared to other iPOND-label-free quantification MS, we were able to identify and enriched known key players of DNA replication found in previous iPOND experiments (Table 3.2), including subunits of the MCM complex that were missing in iPOND applied in mammalian cells by the Dr. David Cortez group [5].

The most enriched DNA replication protein was DNA polymerase α catalytic subunit (Fig. 3.2, red node), ranking at the 9th position (Table 3.2). Pol α is recruited to the replication fork after the CMG complex (**C**dc45, **M**CM 2-7 subunits and the **G**INS complex) is activated by MCM 10 and triggers DNA unwinding at the origin of replication [89,90]. To initiate replication, Pol α synthesizes RNA primers and then passes DNA synthesis to Pol δ and DNA polymerase ε (Pol ε), which have a proofreading exonuclease domain in their catalytic subunit compared to Pol α, making them more accurate for DNA synthesis. Physical interactions at the replication fork using eSPAN (enrichment and sequencing of protein-associated nascent DNA) showed that the catalytic subunit of Pol α was enriched together with replication factor C 1 (RFC1) and replication factor A subunit 1 (Rfa1). Rfc1 is part of the RFC complex that acts as a clamp loader involved in PCNA loading, and Rfa1 is part of the single-stranded DNA-binding protein complex RPA [40]. Both, *T. brucei* RFC1 (Fig. 3.2, yellow node) and RFA1 (Fig. 3.2, green node) were identified and enriched in our data set having ranking positions of 238 and 321 respectively

(Table 3.2). The MCM4 subunit (Fig. 3.2, purple node) from the MCM was also enriched ranking at the 13h position. This complex has been characterized in *T. brucei* and it was found that MCM4 alone is able to unwind circular DNA *in vitro* compared to other MCM subunits. It interacts with other MCM subunits (3, 5 and 6) and with Cdc45. However, when inducing RNAi for this subunit, no growth defect was observed. The authors suggested that the parasites have excess of this protein and the knockdown was unable to reveal its function [44]. All these DNA replication proteins are expected to be interacting with nascent DNA and, accordingly, we were able to identify them in our iPOND-derived data set.

The most enriched GO term in our protein list is chromatin organization. Replicated DNA has to be wrapped into nucleosomes, and this can occur at a distance from the replication fork of ~250 bp as shown in simian virus 40 (SV40) minichromosomes, indicating that nucleosomes are assembled immediately following DNA synthesis [47]. Histone chaperones in yeasts such as Rtt106, which was enriched in our data set (rank 212) (Table 3.4), contributes to the rapid nucleosome assembly at replication fork, and chromatin remodeling enzymes such as Isw1 (rank 255) (Table 3.4) help load and position nucleosome during DNA replication [50]. We noticed that histone H3 was not identified in our ThD chase sample by MS. Histone H3 in *T. brucei* can be mono-, di- and trimethylated at lysine 76 (H3K76me1-2-3). H3K76me is involved in antigenic variation, origin licensing, cell cycle progression and differentiation (91). H3K76me1 is undetectable in S phase cells, H3K76me2 is detected mainly during cytokinesis and mitosis and H3K76me3 is not cell cycle regulated [91,92]. This suggests that newly incorporated H3 is unmethylated on nascent DNA during S phase. Histone methylation, as observed in

chapter 2, was detected by western blot in our ThD sample. Therefore, H3 detection was masked by methylation in our MS analysis that did not include detection of posttranslational modifications. Another possible explanation of why chromatin organization was the most enriched GO terms can rely on our experimental design. A longer EdU pulse was required in our iPOND procedure since *T. brucei* lacks high affinity thymidine transporters [93], and longer DNA stretches were EdU labeled (37 kbp) because *T. brucei* has a fast replication rate (3.7 kbp/min) [94] favoring the capture of chromatin-associated proteins.

The second most enriched GO term was transcription (Fig 3.2). Studies on DNA replication observed that early replication regions were associated with transcriptionally active regions of euchromatin, while late replicating regions were associated with inactive regions and gene-poor heterochromatin. Therefore, replication and transcription prefer the same chromatin landscape [52]. TbORC1 localizes to the boundaries of transcription units, and when performing RNAi knockdown of this protein there was an increase on the mRNA levels upstream and downstream of the transcription units [95]. Also, this protein was localized at subtelomeric regions where VSG (variant surface glycoproteins) genes are positioned [53]. Additionally, a recent study in *T. brucei* BSF parasites used marker frequency analysis with next generation sequencing (MFAseq) in combination with qPCR to measure how early the replication of the actively transcribed VSG gene occurs. In *T. brucei*, there is a transcriptional control mechanism where only one VSG gene is expressed at a given time. This monoallelic expression takes place in only one of the ~15 bloodstream expression site (BES) present in *T. brucei*. As a result, the active BES was the single mapped telomeric site that replicated at early S-phase [96]. The active VSG in BSF and

procylin genes, the major cell surface proteins of PCF trypanosomes, are transcribed by RNA polymerase I [97]. Additionally, RNA pol III-transcribed genes, including tRNAs genes, are located at convergent SSRs that are associated with the end DGCs [98,99]. Even thought that a small percentage of TbORC1 binding sites are associated with convergent SSRs, these sites were early replication origins and might overlap with RNA pol III transcribed genes [53]. Accordingly, we enriched subunits from all three nuclear RNA polymerases (Table 3.5) in newly synthesized DNA, which supports the notion that transcription and replication are coordinated in *T. brucei,* too.

We have also enriched proteins associated with mRNA splicing. It has been proposed that increased levels of nucleosome occupancy can slow the rate of RNA polymerase II transcription, allowing the recruitment of splicing factors [100]. We have enriched nucleosome components such as H2A.Z (rank 175) (Table 3.4), transcription proteins such as RNA polymerase II subunit RPB1 (rank 29) (Table 3.5), and components of *T. brucei* spliceosome such as SmB protein (rank 42) (Table 3.7). Since nucleosome are assembled in near proximity to the replication fork and we have enriched RNA polymerase II subunits, there is the possibility that after replication and after a certain distance from the replication fork, splicing can occur co-transcriptionally, and therefore we are identifying all these components.

We selected two proteins identified and enriched in our iPOND-derived protein list. These were a known DNA replication (Tb7990) protein and an uncharacterized protein (Tb5370). Both proteins have nuclear localization as expected (Fig 3.4A and Fig 3.6A). However, only Tb7990, which is annotated as RFC3, was essential for parasite proliferation (Fig 3.4B). There are four different RFC complexes in eukaryotes: RFC1-

RFC, Ctf18-RFC, Elg1-RFC and Rad17-RFC [101]. These three complexes share the four small RFC subunits (RFC2, 3, 4, and 5) but differ in the largest subunit [102,103]. RFC1-RFC is the canonical RFC complex that acts as a processivity factor for DNA polymerases during DNA replication [66]. Ctf18-RFC is involved in chromatid cohesion [104], Elg1-RFC plays role in genome stability [105] and Rad17-RFC is part of DNA damage checkpoints responses [106]. When we tested if Tb7990 colocalize with newly synthesized DNA, we noticed that not all Tb7990 foci overlap with EdU foci (Fig 3.4A). The Tb7990 foci could indicate the participation of this protein in other RFC complexes that are not only involved in DNA replication but for example, in chromatid cohesion. Further characterization of this protein could include the identification of interacting partners by coimmunoprecipitation assays and biochemical assays to test its ATPase activity.

We decided to characterize Tb5370 since initial bioinformatic analysis suggested that this protein could be an unidentified DNA replication factor since domain search analysis identified a Topo type II family domain. However, a more detail analysis did not identify key residues that are present in topoisomerases and instead, lead to the identification of the FHA and CDK phosphorylation site motif (Fig 3.5). When we analyzed Tb5370 cellular localization, we noticed that this protein displayed a perinuclear localization and did not overlap with EdU distribution pattern (Fig 3.6A). This distribution in the nuclear periphery is similar to what is observed in *T. brucei* nucleoporins [107,108]. Nucleoporins are part of nuclear pore complex (NPC) and embedded in the nuclear envelope. These proteins have multiple roles that not only include trafficking of macromolecules but also in transcription regulation, chromosome segregation [109] and DNA replication origin licensing by its association with MCM helicase [110].

Nucleoporins are also of CDK substrates [111]. In *T. brucei*, characterization of nucleoporin NUP-1 showed that this proteins has roles in chromosome organization, gene expression regulation at telomere-proximal regions and VSG expression [107]. Based on this observation, probably Tb5370 interacts with components of NPC. Even though that there was no loss of fitness upon Tb5370 knockdown in PCF cells (Fig 3.6B), it would be interesting to evaluate if Tb5370 is essential in BSF parasites and determine if colocalizes and interacts with nucleoporins. It is worth to mention that our protein list includes the identification of several nucleoproteins, including NUP-65 (rank 31) and NUP-1 (rank 377) (Supplemental Table 1)

Our data suggest that DNA replication, transcription, chromatin organization and pre-mRNA splicing events all occur on or near nascent DNA. These different cellular processes may be coordinated or just occur in the vicinity of each other. Based on our observations, we propose nucleosomes are assembled close to the replication fork followed by RNA pol II recruitment, transcription, and co-transcriptional RNA splicing. Also, regions with epigenetics marks such as H4K10ac and specific histone variant such as H2A.Z are preferred binding sites for proteins associated with these cellular processes suggesting an elegant choreography between these machineries (Fig 3.7). Further studies are needed to determine how these processes are linked and co-regulated, and how rapidly they are initiated during DNA replication. In addition, our data set has provided a list of hypothetical proteins that can be characterized to determine their function in DNA replication and could represent trypanosome specific factors that can potentially be used as drug targets to treat kinetoplastid diseases.

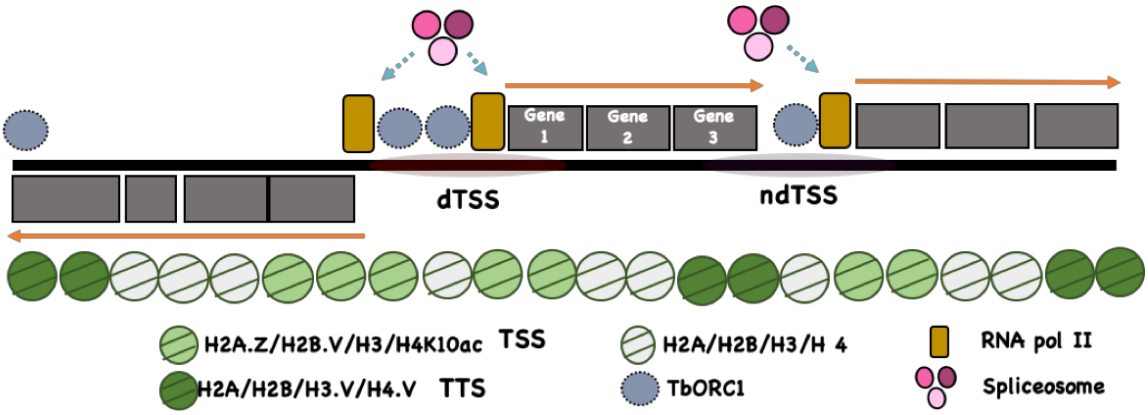

Figure 3.8 – Model of *T. brucei* genome organization

Diagram illustrates transcription start sites in a divergent (dTSS) or not divergent orientation (ndTSS) marked by nucleosomes containing histones variants H2A.Z and H2B.V, and modified histones H4K10ac (light green). Transcription termination sites are marked by nucleosomes containing histone variates H3.V and H4.V (dark green). Orange arrows indicate direction of transcription. Binding sites of RNA pol II (gold rectangle) and ORC1 (blue circle) are shown. Broken blue arrows indicate recruitment of spliceosome components upon RNA pol II enrichment and transcription pausing.

3.5. Bibliography

1. Cortez D. Proteomic Analyses of the Eukaryotic Replication Machinery [Internet]. 1st ed. Methods in Enzymology. 2017. doi:10.1016/bs.mie.2017.03.002
2. Ross PL, Huang YN, Marchese JN, Williamson B, Parker K, Hattan S, et al. Multiplexed Protein Quantitation in *Saccharomyces cerevisiae* Using Amine-reactive Isobaric Tagging Reagents. Mol Cell Proteomics. 2004;3: 1154–1169. doi:10.1074/mcp.M400129-MCP200
3. Wiese S, Reidegeld KA, Meyer HE, Warscheid B. Protein labeling by iTRAQ: A new tool for quantitative mass spectrometry in proteome research. Proteomics. 2007;7: 340–350. doi:10.1002/pmic.200600422
4. Ong S-E, Blagoev B, Kratchmarova I, Kristensen DB, Steen H, Pandey A, et al. Stable Isotope Labeling by Amino Acids in Cell Culture, SILAC, as a Simple and Accurate Approach to Expression Proteomics. Mol Cell Proteomics. 2002;1: 376–386. doi:10.1074/mcp.M200025-MCP200
5. Sirbu BM, McDonald WH, Dungrawala H, Badu-Nkansah A, Kavanaugh GM, Chen Y, et al. Identification of proteins at active, stalled, and collapsed replication forks using isolation of proteins on nascent DNA (iPOND) coupled with mass spectrometry. J Biol Chem. 2013;288: 31458–31467. doi:10.1074/jbc.M113.511337
6. Lossaint G, Larroque M, Ribeyre C, Bec N, Larroque C, Décaillet C, et al. FANCD2 Binds MCM Proteins and Controls Replisome Function upon Activation of S Phase Checkpoint Signaling. Mol Cell. 2013;51: 678–690. doi:10.1016/j.molcel.2013.07.023
7. Lopez-Contreras AJ, Ruppen I, Nieto-Soler M, Murga M, Rodriguez-Acebes S, Remeseiro S, et al. A Proteomic Characterization of Factors Enriched at Nascent DNA Molecules. Cell Rep. 2013;3: 1105–1116. doi:10.1016/j.celrep.2013.03.009
8. Dungrawala H, Rose KL, Bhat KP, Mohni KN, Glick GG, Couch FB, et al. The Replication Checkpoint Prevents Two Types of Fork Collapse without Regulating Replisome Stability. Mol Cell. 2015;59: 998–1010. doi:10.1016/j.molcel.2015.07.030
9. Lecona E, Rodriguez-Acebes S, Specks J, Lopez-Contreras AJ, Ruppen I, Murga M, et al. USP7 is a SUMO deubiquitinase essential for DNA replication. Nat Struct Mol Biol. 2016;23: 270–277. doi:10.1038/nsmb.3185
10. Yu S, Yang F, Shen WH. Genome maintenance in the context of 4D chromatin condensation. Cell Mol Life Sci. 2016; 1–14. doi:10.1007/s00018-016-2221-2
11. Kurat CF, Yeeles JTP, Patel H, Early A, Diffley JFX. Chromatin Controls DNA Replication Origin Selection, Lagging-Strand Synthesis, and Replication Fork Rates. Mol Cell. 2017;65: 117–130. doi:10.1016/j.molcel.2016.11.016
12. Alabert C, Groth A. Chromatin replication and epigenome maintenance. Nat Rev Mol Cell Biol. 2012;13: 153–167. doi:10.1038/nrm3288
13. Budhavarapu VN, Chavez M, Tyler JK. How is epigenetic information maintained through DNA replication? Epigenetics and Chromatin. Epigenetics & Chromatin; 2013;6: 1. doi:10.1186/1756-8935-6-32
14. Gómez-Escoda B, Jenny Wu PY. The organization of genome duplication is a critical determinant of the landscape of genome maintenance. Genome Res.

2018;28: 1179–1192. doi:10.1101/gr.224527.117
15. Yu S, Yang F, Shen WH. Genome maintenance in the context of 4D chromatin condensation. Cell Mol Life Sci. 2016;73: 3137–3150. doi:10.1007/s00018-016-2221-2
16. Groth A, Corpet A, Cook AJL, Roche D, Bartek J, Lukas J, et al. Regulation of Replication Fork Supply and Demand. Science. 2007;318: 1928–1932.
17. Liu S, Xu Z, Leng H, Zheng P, Yang J, Chen K, et al. RPA binds histone H3-H4 and functions in DNA replication-coupled nucleosome assembly. Science. 2017;355: 415–420. doi:10.1126/science.aah4712
18. Brambati A, Colosio A, Zardoni L, Galanti L, Liberi G. Replication and transcription on a collision course: eukaryotic regulation mechanisms and implications for DNA stability. Front Genet. 2015;6: 1–8. doi:10.3389/fgene.2015.00166
19. Felipe-Abrio I, Lafuente-Barquero J, García-Rubio ML, Aguilera A. RNA polymerase II contributes to preventing transcription-mediated replication fork stalls. EMBO J. 2015;34: 236–50. doi:10.15252/embj.201488544
20. Schübeler D, Scalzo D, Kooperberg C, van Steensel B, Delrow J, Groudine M. Genome-wide DNA replication profile for Drosophila melanogaster: a link between transcription and replication timing. Nat Genet. 2002;32: 438–442. doi:10.1038/ng1005
21. Sequeira-Mendes J, Díaz-Uriarte R, Apedaile A, Huntley D, Brockdorff N, Gómez M. Transcription initiation activity sets replication origin efficiency in mammalian cells. PLoS Genet. 2009;5. doi:10.1371/journal.pgen.1000446
22. Langley AR, Gräff S, Smith JC, Krude T. Genome-wide identification and characterisation of human DNA replication origins by initiation site sequencing (ini-seq). Nucleic Acids Res. 2016;44: 10230–10247. doi:10.1093/nar/gkw760
23. Nesvizhskii AI, Keller A. A statistical model for identifying proteins by tandem mass spectrometry. Anal Chem. 2003;75: 4646–4658. doi:10.1021/ac0341261
24. Schwanhüusser B, Busse D, Li N, Dittmar G, Schuchhardt J, Wolf J, et al. Global quantification of mammalian gene expression control. Nature. 2011;473: 337–342. doi:10.1038/nature10098
25. Goos C, Dejung M, Janzen CJ, Butter F, Kramer S. The nuclear proteome of Trypanosoma brucei. PLoS One. 2017;12: e0181884. doi:10.1371/journal.pone.0181884
26. Dean S, Sunter JD, Wheeler RJ. TrypTag.org: A Trypanosome Genome-wide Protein Localisation Resource. Trends Parasitol. 2017;33: 80–82. doi:10.1016/j.pt.2016.10.009
27. Aslett M, Aurrecoechea C, Berriman M, Brestelli J, Brunk BP, Carrington M, et al. TriTrypDB: A functional genomic resource for the Trypanosomatidae. Nucleic Acids Res. 2009;38: 457–462. doi:10.1093/nar/gkp851
28. Mi H, Muruganujan A, Casagrande JT, Thomas PD. Large-scale gene function analysis with the panther classification system. Nat Protoc. 2013;8: 1551–1566. doi:10.1038/nprot.2013.092
29. Szklarczyk D, Franceschini A, Wyder S, Forslund K, Heller D, Huerta-Cepas J, et al. STRING v10: Protein-protein interaction networks, integrated over the tree of life. Nucleic Acids Res. 2015;43: D447–D452. doi:10.1093/nar/gku1003

30. Smoot ME, Ono K, Ruscheinski J, Wang PL, Ideker T. Cytoscape 2.8: New features for data integration and network visualization. Bioinformatics. 2011;27: 431–432. doi:10.1093/bioinformatics/btq675
31. Marchler-Bauer A, Bo Y, Han L, He J, Lanczycki CJ, Lu S, et al. CDD/SPARCLE: Functional classification of proteins via subfamily domain architectures. Nucleic Acids Res. 2017;45: D200–D203. doi:10.1093/nar/gkw1129
32. Sievers F, Wilm A, Dineen D, Gibson TJ, Karplus K, Li W, et al. Fast, scalable generation of high-quality protein multiple sequence alignments using Clustal Omega. Mol Syst Biol. 2011;7. doi:10.1038/msb.2011.75
33. Dinkel H, Roey K Van, Michael S, Kumar M, Uyar B, Altenberg B, et al. ELM 2016 –data update and new functionality of the eukaryotic linear motif resource. 2018;44: 294–300. doi:10.1093/nar/gkv1291
34. Schimanski B, Nguyen TN, Gu A. Highly Efficient Tandem Affinity Purification of Trypanosome Protein Complexes Based on a Novel Epitope Combination. Eukaryot Cell. 2005;4: 1942–1950. doi:10.1128/EC.4.11.1942
35. Sakyiama J, Zimmer SL, Ciganda M, Williams N, Read LK. Ribosome biogenesis requires a highly diverged XRN family 5'->3' exoribonuclease for rRNA processing in Trypanosoma brucei. Rna. 2013;19: 1419–1431. doi:10.1261/rna.038547.113
36. Chandler J, Vandoros A V., Mozeleski B, Klingbeil MM. Stem-loop silencing reveals that a third mitochondrial DNA polymerase, POLID, is required for kinetoplast DNA replication in trypanosomes. Eukaryot Cell. 2008;7: 2141–2146. doi:10.1128/EC.00199-08
37. Wang Z, Morris JC, Drew ME, Englund PT. Inhibition of Trypanosoma brucei gene expression by RNA interference using an integratable vector with opposing T7 promoters. J Biol Chem. 2000;275: 40174–40179. doi:10.1074/jbc.M008405200
38. Carpenter AE, Jones TR, Lamprecht MR, Clarke C, Kang IH, Friman O, et al. CellProfiler: image analysis software for identifying and quantifying cell phenotypes. Genome Biol. 2006;7. doi:10.1186/gb-2006-7-10-r100
39. Srivastava A, Badjatia N, Lee JH, Hao B, Günzl A. An RNA polymerase II-associated TFIIF-like complex is indispensable for SL RNA gene transcription in Trypanosoma brucei. Nucleic Acids Res. 2017;46: 1695–1709. doi:10.1093/nar/gkx1198
40. Yu C, Gan H, Han J, Zhou ZX, Jia S, Chabes A, et al. Strand-Specific Analysis Shows Protein Binding at Replication Forks and PCNA Unloading from Lagging Strands when Forks Stall. Mol Cell. 2014;56: 551–563. doi:10.1016/j.molcel.2014.09.017
41. Kaufmann D, Gassen A, Maiser A, Leonhardt H, Janzen CJ. Regulation and spatial organization of PCNA in Trypanosoma brucei. Biochem Biophys Res Commun. 2012;419: 698–702. doi:10.1016/j.bbrc.2012.02.082
42. Valenciano AL, Ramsey AC, Mackey ZB. Deviating the level of proliferating cell nuclear antigen in trypanosoma brucei elicits distinct mechanisms for inhibiting proliferation and cell cycle progression. Cell Cycle. 2015;14: 674–688. doi:10.4161/15384101.2014.987611
43. Valenciano AL, Knudsen GM, Mackey ZB. Extracellular-signal regulated kinase 8

of Trypanosoma brucei uniquely phosphorylates its proliferating cell nuclear antigen homolog and reveals exploitable properties. Cell Cycle; 2016;15: 2827–2841. doi:10.1080/15384101.2016.1222340
44. Dang HQ, Li Z. The Cdc45 Mcm2-7 GINS protein complex in trypanosomes regulates DNA replication and interacts with two Orc1-like proteins in the origin recognition complex. J Biol Chem. 2011;286: 32424–32435. doi:10.1074/jbc.M111.240143
45. Aranda S, Rutishauser D, Ernfors P. Identification of a large protein network involved in epigenetic transmission in replicating DNA of embryonic stem cells. Nucleic Acids Res. 2014;42: 6972–6986. doi:10.1093/nar/gku374
46. Sirbu BM, Couch FB, Feigerle JT, Bhaskara S, Hiebert SW, Cortez D. Analysis of protein dynamics at active , stalled , and collapsed replication forks. Genes Dev. 2011;25: 1320–1327. doi:10.1101/gad.2053211.
47. Sogo, J.M; Stahl, H;Koller, Th;Knippers R. Structure of Replicating Simian Virus 40 Minichromosomes The Replication Fork, Core Histone Segregation and Terminal Structures. J mo. 1986; 189–204.
48. Madamba EV, Berthet EB, Francis NJ. Inheritance of Histones H3 and H4 during DNA Replication In Vitro. Cell Rep. 2017;21: 1361–1374. doi:10.1016/j.celrep.2017.10.033
49. Reverón-Gómez N, González-Aguilera C, Stewart-Morgan KR, Petryk N, Flury V, Graziano S, et al. Accurate Recycling of Parental Histones Reproduces the Histone Modification Landscape during DNA Replication. Mol Cell. 2018; 1–11. doi:10.1016/j.molcel.2018.08.010
50. Yadav T, Whitehouse I. Replication-Coupled Nucleosome Assembly and Positioning by ATP-Dependent Chromatin-Remodeling Enzymes. Cell Rep. 2016;15: 715–723. doi:10.1016/j.celrep.2016.03.059
51. MacAlpine DM, Macalpine DM, Rodriguez HK, Bell SP, Bell SP. Coordination of replication and transcription along a. Genes Dev. 2004; 3094–3105. doi:10.1101/gad.1246404.ster
52. Lubelsky Y, Prinz J a, Denapoli L, Li Y, Belsky J a, Macalpine DM. DNA replication and transcription programs respond to the same chromatin cues. Genome Research. 2014; 1102–1114. doi:10.1101/gr.160010.113
53. Tiengwe C, Marcello L, Farr H, Dickens N, Kelly S, Swiderski M, et al. Genome-wide analysis reveals extensive functional interaction between DNA replication initiation and transcription in the genome of trypanosoma brucei. Cell Rep. 2012;2: 185–197. doi:10.1016/j.celrep.2012.06.007
54. Lombraña R, Alvarez A, Fernandez-Justel JM, Almeida R, Poza-Carrion C, Gomes F, et al. Transcriptionally Driven DNA Replication Program of the Human Parasite Leishmania major. Cell Rep. 2016;16: 1774–1786. doi:10.1016/j.celrep.2016.07.007
55. Senkevich TG, Katsafanas GC, Weisberg A, Olano LR, Moss B. Identification of vaccinia virus replisome and transcriptome proteins by isolation of proteins on nascent DNA coupled with mass spectrometry. J Virol. 2017;91: 1–20. doi:10.1128/JVI.01015-17
56. Dembowski JA, DeLuca NA. Selective Recruitment of Nuclear Factors to Productively Replicating Herpes Simplex Virus Genomes. PLoS Pathog. 2015;11:

1–35. doi:10.1371/journal.ppat.1004939
57. Mazin A V., Mazina OM, Bugreev D V., Rossi MJ. Rad54, the motor of homologous recombination. DNA Repair. 2010;9: 286–302. doi:10.1016/j.dnarep.2009.12.006
58. Li B. DNA double-strand breaks and telomeres play important roles in Trypanosoma brucei antigenic variation. Eukaryot Cell. 2015;14: 196–205. doi:10.1128/EC.00207-14
59. McCulloch R, Barry JD. A role for RAD51 and homologous recombination in Trypanosoma brucei antigenic variation. Genes Dev. 1999;13: 2875–2888. doi:10.1101/gad.13.21.2875
60. Horn D, McCulloch R. Molecular mechanisms underlying the control of antigenic variation in African trypanosomes. Curr Opin Microbiol. 2010;13: 700–705. doi:10.1016/j.mib.2010.08.009
61. Hartley CL, McCulloch R. Trypanosoma brucei BRCA2 acts in antigenic variation and has undergone a recent expansion in BRC repeat number that is important during homologous recombination. Mol Microbiol. 2008;68: 1237–1251. doi:10.1111/j.1365-2958.2008.06230.x
62. Davies AA, Masson J, Mcilwraith MJ, Stasiak AZ, Stasiak A, Venkitaraman AR, et al. Role of BRCA2 in Control of the RAD51 Recombination and DNA Repair Protein Adelina. Mol Cell. 2001;7: 273–282. doi:10.1016/S1097-2765(01)00175-7
63. Wedel C, Förstner KU, Derr R, Siegel TN. GT-rich promoters can drive RNA pol II transcription and deposition of H2A.Z in African trypanosomes. EMBO J. 2017;36: e201695323. doi:10.15252/embj.201695323
64. da Silva MS, Pavani RS, Damasceno JD, Marques CA, McCulloch R, Tosi LRO, et al. Nuclear DNA Replication in Trypanosomatids: There Are No Easy Methods for Solving Difficult Problems. Trends Parasitol. 2017;33: 858–874. doi:10.1016/j.pt.2017.08.002
65. Venclovas E, Colvin ME, Thelen MP. Molecular modeling-based analysis of interactions in the RFC-dependent clamp-loading process. Protein Science. 2002; 11: 2403–2416. doi:10.1110/ps.0214302.Protein
66. Yao NY, Donnell MO. The RFC Clamp Loader: Structure and Function. Subcell Biochem. 2012; 62: 259–279. doi:10.1007/978-94-007-4572-8
67. Neuwald AF. Evolutionary clues to eukaryotic DNA clamp-loading mechanisms : analysis of the functional constraints imposed on replication factor C AAA + ATPases. Nucleic Acids Res. 2005;33: 3614–3628. doi:10.1093/nar/gki6744
68. Johnson A, Yao NY, Bowman GD, Kuriyan J, Donnell MO. The Replication Factor C Clamp Loader Requires Arginine Finger Sensors to Drive DNA Binding and Proliferating Cell Nuclear Antigen Loading. J Biol Chem. 2006;281: 35531–35543. doi:10.1074/jbc.M606090200
69. Cai J, Yao N, Gibbs E, Finkelstein J, Phillips B, O´Donnell M, et al. ATP hydrolysis catalyzed by human replication factor C requires participation of multiple subunits. Proc Natl Acad Sci. 1998;95: 11607–11612.
70. Chiraniya A, Finkelstein J, Bloom LB. A Novel Function for the Conserved Glutamate Residue in the Walker B Motif of Replication Factor C. Genes. 2013; 134–151. doi:10.3390/genes4020134
71. Siegel TN, Hekstra DR, Cross GAM. Analysis of the Trypanosoma brucei cell

cycle by quantitative DAPI imaging. Mol Biochem Parasitol. 2008;160: 171–174. doi:10.1016/j.molbiopara.2008.04.004
72. Gluenz E, Povelones ML, Englund PT, Gull K. The kinetoplast duplication cycle in Trypanosoma brucei is orchestrated by cytoskeleton-mediated cell morphogenesis. Mol Cell Biol. 2011;31: 1012–21. doi:10.1128/MCB.01176-10
73. Robinson, D.R & Gull K. Basal Body movement as a mechanism for mitochondrial genome segregation in the trypanosome cell cycle. Nature. 1991;352: 731–733. http://www.nature.com/nature/journal/v352/n6337/pdf/352731a0.pdf
74. Sherwin T, Gull K. Visualization of detyrosination along single microtubules reveals novel mechanisms of assembly during cytoskeletal duplication in trypanosomes. Cell. 1989;57: 211–221. doi:10.1016/0092-8674(89)90959-8
75. Benz C, Dondelinger F, McKean PG, Urbaniak MD. Cell cycle synchronisation of Trypanosoma brucei by centrifugal counter-flow elutriation reveals the timing of nuclear and kinetoplast DNA replication. Sci Rep. 2017;7: 1–10. doi:10.1038/s41598-017-17779-z
76. Hammarton TC, Clark J, Douglas F, Boshart M, Mottram JC. Stage-specific differences in cell cycle control in Trypanosoma brucei revealed by RNA interference of a mitotic cyclin. J Biol Chem. 2003;278: 22877–22886. doi:10.1074/jbc.M300813200
77. Benmerzouga I, Concepción-Acevedo J, Kim HS, Vandoros A V., Cross GAM, Klingbeil MM, et al. Trypanosoma brucei Orc1 is essential for nuclear DNA replication and affects both VSG silencing and VSG switching. Mol Microbiol. 2013;87: 196–210. doi:10.1111/mmi.12093
78. Archer SK, Inchaustegui D, Queiroz R, Clayton C. The cell cycle regulated transcriptome of Trypanosoma brucei. PLoS One. 2011;6. doi:10.1371/journal.pone.0018425
79. Vos SM, Tretter EM, Schmidt BH, Berger JM. All tangled up: how cells direct, manage and exploit topoisomerase function. Nat Rev Mol Cell Biol. 2011;12: 827–41. doi:10.1038/nrm3228
80. Champoux JJ. DNA TOPOISOMERASES : Structure,Function ,. Annu Rev Biochem. 2001;70: 369–413.
81. Canela A, Maman Y, Jung S, Wong N, Callen E, Day A, et al. Genome Organization Drives Chromosome Fragility. Cell. 2017; 507–521. doi:10.1016/j.cell.2017.06.034
82. Singh BN, Achary VMM, Panditi V, Sopory SK, Reddy MK. Dynamics of tobacco DNA topoisomerases II in cell cycle regulation: to manage topological constrains during replication, transcription and mitotic chromosome condensation and segregation. Plant Mol Biol. 2017;94: 595–607. doi:10.1007/s11103-017-0626-4
83. Alsford S, Turner DJ, Obado SO, Sanchez-flores A, Glover L, Berriman M, et al. High-throughput phenotyping using parallel sequencing of RNA interference targets in the African trypanosome High-throughput phenotyping using parallel sequencing of RNA interference targets in the African trypanosome. Genome Res. 2011;21: 915–924. doi:10.1101/gr.115089.110
84. Urbaniak MD, Martin DMA, Ferguson MAJ. Global quantitative SILAC

phosphoproteomics reveals differential phosphorylation is widespread between the procyclic and bloodstream form lifecycle stages of Trypanosoma brucei. J Proteome Res. 2013;12: 2233–2244. doi:10.1021/pr400086y
85. Errico A, Deshmukh K, Tanaka Y, Pozniakovsky A, Hunt T. Identification of substrates for cyclin dependent kinases. Adv Enzyme Regul. 2010;50: 375–399. doi:10.1016/j.advenzreg.2009.12.001
86. Chang EJ, Begum R, Chait BT, Gaasterland T. Prediction of Cyclin-Dependent Kinase Phosphorylation Substrates. PLoS One. 2007;2: e656. doi:10.1371/journal.pone.0000656
87. Johnson N, Shapiro GI. Cyclin-dependent kinases (cdks) and the DNA damage response: rationale for cdk inhibitor–chemotherapy combinations as an anticancer strategy for solid tumors. Expert Opin Ther Targets. 2010;14: 1199–1212. doi:10.1111/j.1743-6109.2008.01122.x.Endothelial
88. Durocher D, Jackson SP. The FHA domain. FEBS Lett. 2002;513: 58–66. doi:10.1016/S0014-5793(01)03294-X
89. Lõoke M, Maloney MF, Bell SP. Mcm10 regulates DNA replication elongation by stimulating the CMG replicative helicase. Genes Dev. 2017;31: 291–305. doi:10.1101/gad.291336.116
90. Zhu W, Ukomadu C, Jha S, Senga T, Dhar SK, Wohlschlegel J a, et al. Mcm10 and And-1 / CTF4 recruit DNA polymerase α to chromatin for initiation of DNA replication. Genes Dev. 2007; 2288–2299. doi:10.1101/gad.1585607.Mcm10
91. Gassen A, Brechtefeld D, Schandry N, Arteaga-Salas JM, Israel L, Imhof A, et al. DOT1A-dependent H3K76 methylation is required for replication regulation in Trypanosoma brucei. Nucleic Acids Res. 2012;40: 10302–10311. doi:10.1093/nar/gks801
92. Janzen CJ, Hake SB, Lowell JE, Cross GAM. Selective Di- or Trimethylation of Histone H3 Lysine 76 by Two DOT1 Homologs Is Important for Cell Cycle Regulation in Trypanosoma brucei. Mol Cell. 2006;23: 497–507. doi:10.1016/j.molcel.2006.06.027
93. Ranjbarian F, Vodnala M, Vodnala SM, Rofougaran R, Thelander L, Hofer A. Trypanosoma brucei thymidine kinase is tandem protein consisting of two homologous parts, which together enable efficient substrate binding. J Biol Chem. 2012;287: 17628–17636. doi:10.1074/jbc.M112.340059
94. Calderano SG, Drosopoulos WC, Quaresma MM, Marques CA, Kosiyatrakul S, McCulloch R, et al. Single molecule analysis of Trypanosoma brucei DNA replication dynamics. Nucleic Acids Res. 2015;43: 2655–2665. doi:10.1093/nar/gku1389
95. Tiengwe C, Marcello L, Farr H, Gadelha C, Burchmore R, Barry JD, et al. Identification of ORC1/CDC6-interacting factors in trypanosoma brucei reveals critical features of origin recognition complex architecture. PLoS One. 2012;7: 22–24. doi:10.1371/journal.pone.0032674
96. Devlin R, Marques CA, Paape D, Prorocic M, Zurita-Leal AC, Campbell SJ, et al. Mapping replication dynamics in Trypanosoma brucei reveals a link with telomere transcription and antigenic variation. Elife. 2016;5: 1–30. doi:10.7554/eLife.12765
97. Günzl A, Bruderer T, Laufer G, Tu L, Chung H, Lee P, et al. RNA Polymerase I Transcribes Procyclin Genes and Variant Surface Glycoprotein Gene Expression

Sites in Trypanosoma brucei RNA Polymerase I Transcribes Procyclin Genes and Variant Surface Glycoprotein Gene Expression Sites in Trypanosoma brucei. Eukaryot Cell. 2003;2: 542–551. doi:10.1128/EC.2.3.542
98. Marchetti MA, Tschudi C, Silva E, Ullu E. Physical and transcriptional analysis of the Trypanosoma brucei genome reveals a typical eukaryotic arrangement with close interspersion of RNA polymerase II- and III-transcribed genes. Nucleic Acids Res. 1998;26: 3591–3598. doi:10.1093/nar/26.15.3591
99. Siegel TN, Hekstra DR, Kemp LE, Figueiredo LM, Lowell JE, Fenyo D, et al. Four histone variants mark the boundaries of polycistronic transcription units in Trypanosoma brucei. Genes Dev. 2009;23: 1063–1076.doi:10.1101/gad.1790409.7
100. Naftelberg S, Schor IE, Ast G, Kornblihtt AR. Regulation of Alternative Splicing Through Coupling with Transcription and Chromatin Structure. Annu Rev Biochem. 2015;84: 165–198. doi:10.1146/annurev-biochem-060614-034242
101. Kim J, MacNeill SA. Genome Stability: A New Member of the RFC family. Curr Biol. 2003;13: 873–875. doi:10.1016/j.cub.2003.10.048
102. Shiomi Y, Nishitani H. Control of genome integrity by RFC complexes; conductors of PCNA loading onto and unloading from chromatin during DNA replication. Genes. 2017;8. doi:10.3390/genes8020052
103. Shiomi Y, Hayashi A, Ishii T, Shinmyozu K, Nakayama J -i., Sugasawa K, et al. Two Different Replication Factor C Proteins, Ctf18 and RFC1, Separately Control PCNA-CRL4Cdt2-Mediated Cdt1 Proteolysis during S Phase and following UV Irradiation. Mol Cell Biol. 2012;32: 2279–2288. doi:10.1128/MCB.06506-11
104. Hanna JS, Kroll ES, Lundblad V, Spencer F a. Saccharomyces cerevisiae CTF18 and CTF4 are required for sister chromatid cohesion. Mol Cell Biol. 2001;21: 3144–3158. doi:10.1128/MCB.21.9.3144-3158.2001
105. Aroya S Ben, Kupiec M. The Elg1 replication factor C-like complex: A novel guardian of genome stability. DNA Repair (Amst). 2005;4: 409–417. doi:10.1016/j.dnarep.2004.08.003
106. Zou L, Cortez D, Elledge SJ. Regulation of ATR substrate selection by Rad17-dependent loading of Rad9 complexes onto chromatin. Genes Dev. 2002;16: 198–208. doi:10.1101/gad.950302
107. DuBois KN, Alsford S, Holden JM, Buisson J, Swiderski M, Bart JM, et al. NUP-1 is a large coiled-coil nucleoskeletal protein in trypanosomes with lamin-like functions. PLoS Biol. 2012;10. doi:10.1371/journal.pbio.1001287
108. Obado SO, Brillantes M, Uryu K, Zhang W, Ketaren NE, Chait BT, et al. Interactome Mapping Reveals the Evolutionary History of the Nuclear Pore Complex. PLoS Biol. 2016;14: 1–30. doi:10.1371/journal.pbio.1002365
109. Ibarra A, Hetzer MW. Nuclear pore proteins and the control of genome function. Genes Dev. 2015;29: 337–349. doi:10.1101/gad.256495.114.Cytoplasmic
110. Gillespie PJ, Khoudoli GA, Stewart G, Swedlow JR, Blow JJ. ELYS/MEL-28 Chromatin Association Coordinates Nuclear Pore Complex Assembly and Replication Licensing. Curr Biol. 2007;17: 1657–1662. doi:10.1016/j.cub.2007.08.041
111. Garvey D, H BJ. Cdk phosphorylation of a Nucleoporin controls localization of active genes through the Cell Cylce. Mol Biol Cell. 2010;21: 3421–3432. doi:10.1091/mbc.E10

CHAPTER 4

FUTURE DIRECTIONS AND CONCLUSIONS

We have optimized for the first time the iPOND technology in a parasitic organism. We have provided a starting list of proteins that are present in the vicinity of the replication fork. Future studies can focus on the characterization of these proteins, especially the hypothetical proteins or proteins of uncharacterized function (Table 4.1), to define their role in DNA replication in *T. brucei*. These studies can include the cellular localization of the proteins during the cell cycle by endogenous tagging, knocking down each gene to observe any loss of fitness, growth impairment and defects on DNA replication, co-localization with newly synthesized DNA by EdU labeling, and biochemical characterization by performing enzymatic activity assays and protein-protein interaction experiments with known DNA replication proteins. One interesting protein to study is the hypothetical protein Tb427tmp.244.2780 (Tb2780) (Tb927.9.15070). By looking for conserved domain in this protein, it was predicted to be part of the DNA recombination-mediator protein A or SMF family. DNA processing protein A (DprA) is a DNA binding protein that has an essential role in bacteria natural transformation favoring genetic diversity. DprA, together with RecA, play a key role in protecting incoming or exogenous ssDNA from nucleases, since their depletion completely impaired the internalization of DNA. DprA is able to bind linear and circular ssDNA and favors the loading of RecA on naked ssDNA. This data indicates that DprA is a recombinant-mediator protein [1]. In eukaryotes, Rad51, which is homolog of bacterial RecA, also relies on recombinant mediator factors such as Rad52, to assist its loading during DNA recombination and repair processes [2,3]. The hypothetical protein Tb2780 shows 28% of identity with members of

the DprA. It would be interesting to see the role that this protein has in *T. brucei*, especially in VSG switching that involves homologous recombination in the blood stream form (BSF) of the parasite. Also, would be interesting to do a phylogenetical analysis of this protein and how is related to the bacteria DprA since there are no homologous of this protein in other model eukaryotes.

An additional candidate to study is the hypothetical protein Tb427tmp.160.4710 (Tb4710). Domain search of this protein predicted to be a member of the SMC (structural maintenance of chromosomes) family. Members of this family have roles in chromatin and DNA dynamics by playing important roles in chromosome condensation, sister chromatid cohesion and DNA repair. Eukaryotes have six SMC paralogues. SMC1-SMC3 are involved in sister chromatid cohesion, SMC2-SMC4 are condensins that play roles in compacting and segregating chromosomes, and the SMC5-SMC6 complex tethers DNA ends during DNA repair and other DNA damage responses [4]. In *Trypanosoma brucei*, the SMC cohesin and condensin complex are conserved but the SMC5-SMC6 complex is absent [5]. To study the role of Tb4710, first would be interesting to see if this protein interacts either with *T. brucei* cohesins or condensins. To test this, Tb4710 can have an endogenous PTP tag and perform a co-immunoprecipitation assay and identify the interacting partners by MS analysis. RNAi depletion of Tb4710 could help determine if this protein is essential for karyokinesis and cell cycle progression. To define if Tb4710 has a role in DNA repair, parasites could be exposed to DNA damaged agents and see by immunolocalization if this protein is localized at the sites of DNA repair together with other proteins such as Rad51.

In terms of the DNA replication proteins identified in this study, only the MCM complex and PCNA have been functional characterized in *T. brucei*. For example, would be interesting to characterize *T. brucei* DNA polymerase δ (TbPOLδ) and see how efficient is compared to the other POLδ in other model organisms. Biochemical assays to test the catalytic activity of TbPOLδ can be done in PTP purified protein or by generating a recombinant protein. In this way, polymerase and exonuclease assays can be tested *in vitro* to compare the activity of TbPOLδ versus its homologous in other eukaryotes. DNA polymerase ε was identified in our data set but was unable to pass the stringent enrichment criteria we used to define the proteins at the replication fork. The current model of DNA replication is that polymerase ε replicates the leading strand and polymerase δ is in charge of the lagging strand. This is based on the observation that mutation on DNA polymerase ε lead to the accumulation of mutations in the leading strand, and the analogous observation occurs where mutation on polymerase δ yield mismatches in the lagging strand [6]. However, there are studies that showed that DNA polymerase δ is able to replicate both DNA strands as observed in SV40 replication [7]. Also, DNA polymerase activity of polymerase ε was found to be not essential in yeast studies, whereas the activity of δ is crucial for viability [8]. Two recent studies have shed light into the contribution that polymerase δ can have in leading strand synthesis in yeast DNA replication. The first one suggests that polymerase δ is the key replicase in both leading and lagging strand and polymerase ε proofreads errors made by polymerase delta as it replicates the leading DNA strand [9]. The second study suggests that polymerase δ contributes to the initiation of leading strand synthesis and that in the absence of polymerase ε, polymerase δ can

synthesize both strands but very poorly which leads to genetic instability [10]. It is unknown the distribution of DNA polymerases in *T. brucei*, therefore would be interesting to perform a strand specific analysis to determine the specific binding of DNA replication proteins. One of the techniques that can be used is eSPAN (enrichment and sequencing of protein-associated nascent DNA). This technique is based on chromatin immunoprecipitation of the protein of interest from synchronized early S phase cells. The ChIP DNA is then denatured into ssDNA. The protein-ssDNA complex is marked with BrdU, a thymidine analog, and enriched using anti-BrdU antibodies. The ssDNA is ligated at the 3´end with an adaptor so the strand information of each ssDNA is retained. Each tag is sequenced and mapped to the leading and lagging strand genome reference. If a protein prefers to bind to the leading or the lagging strand, the eSPAN peaks will display a leading or lagging strand pattern [11]. It would be interesting to apply this technique in *T. brucei* to define the distribution of the replisome in both strands and to propose a model of replication in this parasite. This technique could also verify the presence of transcription proteins on nascent DNA and support our iPOND results.

One interesting finding in this project is that many cellular processes are present at the vicinity of the replication fork. By doing high resolution microscopy, such as 3D SIM, the nuclear distribution of these processes can be observed in the context of a cell population that is in S phase. For example, the distribution of a PTP-tagged-RNA polymerase II or PTP-tagged-cyclophilin during DNA replication can be observed using EdU labeling. With high resolution microscopy, the distance of these proteins to the replication foci can be determined, and this way know how close co-transcriptional splicing is occurring from the replication fork. These studies can be done in a synchronized

population using centrifugal counter-flow elutriation [12] and be able to distinguish patterns of these proteins and EdU labeling at early, mid, and late S phase.

We consider that to define which proteins are at the nascent DNA more replicates of the pulse chase experiments are needed, and performed iPOND with chemical labeling MS, such as SILAC or iTRAQ can reduced the variability we have observed in the iPOND-label free quantification and make a more accurate distinction between the proteins that are at nascent DNA and the bulk of chromatin. Another condition that would be interesting to apply is using iPOND to identify the machinery involved in DNA replication re-start and repair by treating the cells with hydroxyurea and by inducing DNA damage with UV exposure.

We have done iPOND in the procyclic form of the parasite. However, it would be interesting to apply this technique in the BSF of the parasite to define how DNA replication is involved in antigenic variation via VSG switching in *T. brucei,* and the machinery involved in this mechanism. Also, would be interesting to see if the fork replisome varies between these two life forms. However, BSF parasite cannot pass a certain cell density (1 x 10^6 cells/mL) and will make iPOND more laborious since larger cultures will be needed. In 2016, there was the development of a new technique called SIRF (*in situ* analysis of protein interactions at DNA replication forks), where few cells are needed. This technique is based on a proximity ligation assay (PLA) that allows the analysis at nascent replication forks on a single-cell level. SIRF also uses EdU labeling and the cycloaddition of a biotin azide via a click chemistry reaction but includes the incubation with a primary antibody against a protein of interest and against biotin, followed by incubation with secondary PLA antibodies containing a DNA-oligomers. If PLA antibodies are in a distance of less of 40

nm, the DNA oligomers are able to anneal forming a nicked circular DNA. Ligation of the nick enables rolling circle amplification. DNA sequence-specific fluorescence DNA probes anneal to the amplified DNA, providing a strong fluorescence signal that allows the detection of protein-nascent DNA interactions [13]. In this way, we could test if the proteins identified in *T. brucei* iPOND using procyclic cells are also interacting with nascent DNA in BSF parasites. Good candidates could be the hypothetical proteins identified in our data set, and DNA recombination proteins such as the Holliday-junction resolvase-like of SPT6/SH2 that could play a role in VSG switching.

Surprisingly, DNA replication in *T. brucei* has not been studied in detail. Therefore, we consider that iPOND opens the door to future investigations on DNA replication in this parasite and other kinetoplastids, with the purpose to find suitable drug targets to treat the diseases associated with kinetoplastid parasites such as Chagas diseases, Leishmaniasis and Human African trypanosomiasis.

4.1 Bibliography

1. Mortier-barrie I, Velten M, Dupaigne P, Mirouze N, Pie O, Mcgovern S, et al. A Key Presynaptic Role in Transformation for a Widespread Bacterial Protein : DprA Conveys Incoming ssDNA to RecA. Cell. 2007; 824–836. doi:10.1016/j.cell.2007.07.038
2. Claverys JP, Martin B, Polard P. The genetic transformation machinery: Composition, localization, and mechanism. FEMS Microbiol Rev. 2009;33: 643–656. doi:10.1111/j.1574-6976.2009.00164.x
3. Yadav T, Carrasco B, Myers AR, George NP, Keck JL, Alonso JC. Genetic recombination in Bacillus subtilis: A division of labor between two single-strand DNA-binding proteins. Nucleic Acids Res. 2012;40: 5546–5559. doi:10.1093/nar/gks173
4. Kim H, Loparo JJ. Multistep assembly of DNA condensation clusters by SMC. Nat Commun. 2016;7: 1–12. doi:10.1038/ncomms10200
5. Gluenz E, Sharma R, Carrington M, Gull K. Functional characterization of cohesin subunit SCC1 in Trypanosoma brucei and dissection of mutant phenotypes in two life cycle stages. Mol Microbiol. 2008;69: 666–680. doi:10.1111/j.1365-2958.2008.06320.x
6. Daigaku Y, Keszthelyi A, Müller CA, Miyabe I, Brooks T, Retkute R, et al. A global profile of replicative polymerase usage. 2015;22. doi:10.1038/nsmb.2962
7. Waga S, Stillman B. Anatomy of a DNA replication fork revealed by reconstitution of SV40 DNA replication in vitro. Nature. 1994;369.
8. Simon M, Giot L, Faye G. The 3 ’ to 5 ’ exonuclease activity located in the DNA polymerase 6 subunit of Saccharomyces cerevisiae is required for accurate replication. EMBO J. 1991;10: 2165–2170. doi:10.1002/j.1460-2075.1991.tb07751.x
9. Johnson RE, Klassen R, Prakash L, Prakash S. A Major Role of DNA Polymerase delta in Replication of Both the Leading and Lagging DNA Strands. Mol Cell. 2015;59: 163–175. doi:10.1016/j.molcel.2015.05.038
10. Garbacz MA, Lujan SA, Burkholder AB, Cox PB, Wu Q, Zhou Z, et al. Evidence that DNA polymerase δ contributes to initiating leading strand DNA replication in Saccharomyces cerevisiae. Nat Commun. S: 1–11. doi:10.1038/s41467-018-03270-4
11. Yu C, Gan H, Han J, Zhou ZX, Jia S, Chabes A, et al. Strand-Specific Analysis Shows Protein Binding at Replication Forks and PCNA Unloading from Lagging Strands when Forks Stall. Mol Cell. 2014;56: 551–563. doi:10.1016/j.molcel.2014.09.017
12. Benz C, Dondelinger F, McKean PG, Urbaniak MD. Cell cycle synchronisation of Trypanosoma brucei by centrifugal counter-flow elutriation reveals the timing of nuclear and kinetoplast DNA replication. Sci Rep. 2017;7: 1–10. doi:10.1038/s41598-017-17779-z
13. Roy S, Luzwick JW, Schlacher K. SIRF : Quantitative in situ analysis of protein interactions at DNA replication forks. J Cell Biol. 2018;JCB: 1–16. doi:10.1083/jcb.201709121

APPENDIX

DYNAMIC LOCALIZATION AND ACETYLATION OF *T. BRUCEI* MITOCHONDRIAL PIF1 HELICASE

I. Introduction

One distinctive feature of kinetoplastids is their mitochondrial DNA known as kinetoplast DNA (kDNA) [1]. In the single mitochondrion of *Trypanosoma brucei*, the kDNA forms a condensed disk-like structure. The kDNA is a network of interlocked DNA rings of two types, minicircles and maxicircles. In *T. brucei*, minicircles are ~1 kb and maxicircles are ~23 kb in size [2]. Maxicircles encode subunits of the respiratory complexes and mitochondrial ribosomal RNA. Maxicircles transcripts undergo the process of RNA editing, where there is the insertion and/or deletion of uridine residues to yield functional open reading frames. These editing events are coordinated by guide RNAs (gRNAs), which are encoded by the minicircles [3]. Within the minicircles, there is a conserved region known as the Universal Minicircle Sequence (UMS), which serves as the initiation site for DNA replication for the leading strand [4]. The replication of the kDNA network is essential for parasite survival in any stage of its life cycle. Due to the complex structure of kDNA, its replication is highly coordinated and involves the participation of multiple proteins with similar activities but different functions. The kDNA replication proteins can be localized in different regions. They can be found within the kDNA disk, at the region between the kDNA disk and the mitochondrial membrane near the flagella basal

body known as the kinetoflagellar zone (KFZ), or at the antipodal site, which are two proteins assemblies located at opposite sites at the periphery of the kinetoplast [5].

Minicircles and maxicircles replicate unidirectionally via theta intermediates. Maxicircles remain catenated and attached to the network while minicircles are released vectorially from the network into the KFZ to be replicated. Minicircle are covalently closed prior replication [6,7]. They are released from the network via the action of a type II topoisomerase[8]. At the KFZ replication is initiated. Proteins involved in replication includes the universal minicircle sequence-binding protein (UMSBP)[9], p38 that binds to the replication origin [10], primase [11], DNA polymerases [12], helicases [13] and a topo IA isomerase [6]. During later stages of kDNA replication, the minicircles that contain gaps and RNA primers migrate to the antipodal sites. These nicked/gaped minicircles undergo Okazaki fragment processing at the antipodal sites by enzymes in charge of primer removal and repair such as the structure-specific endonuclease 1 (SSE1) [14], DNA polymerase β and ligase κβ. These enzymes repair most but not all the gaps [15]. As replication proceeds, the network elongates as a result of the increment of minicircle copy number. The double-sized network splits in two and all the minicircles gaps are repaired by DNA polymerase βPAK and ligase κα [16]. After the kDNA is duplicated, the progeny networks have to segregate into the daughter cells, a process that is mediated by a cytoskeletal structure named the tripartite attachment complex (TAC) [17,18].

Additional features of kDNA replication include replication once per cell cycle in near synchrony with nuclear S phase and multiplicity of DNA polymerases (6), helicases (6) and primases (2) [1]. Structural changes that occurs inside the cell such as basal body duplication and maturation are used as markers to track cell cycle stages and kDNA

replication. Basal body duplication is one of the first cytological events during trypanosome cell cycle and kDNA duplication is linked with basal body dynamics [19]. The proximal end of the basal body is connected to the kinetoplast via the filaments of the TAC. Therefore, basal body movement directs the proper segregation and positioning of the replicated kinetoplast in preparation for cytokinesis [20]. Cells at G1 phase possess a single kinetoplast, a single nucleus (1N1K) and a mature basal body (mBB), which nucleates the flagellar axoneme and an adjacent pro-basal body (pBB). Upon entry into the S phase, the pBB nucleates the assembly of a new flagellum resulting in a new mBB, followed by the assembly of new pBBs next to the two mBBS. One mBB/pBB pair moves to the posterior end of the cells [21]. The kinetoplast shows an elongated shape and the nucleus is still in S phase ($1N1K_{div}$). As cell cycle progresses, segregation of basal bodies separates the two daughter kDNA networks (1N2K). Then, cells enter nuclear M phase and chromosome segregation occurs and finally nuclear division is complete (2K2N) [22].

The replication of kDNA is very dynamic and demands coordination of the factors involved. Using basal body dynamic and observation of kDNA morphology with DAPI staining, the localization and dynamics of the proteins that participate in kDNA can be studied in their cell cycle context. These proteins seem to be localized at the kDNA disk, antipodal sites and KFZ. It has been shown that there is dynamic localization of kDNA proteins as a mode to regulate the replication process. In *T. brucei* it has been shown that DNA polymerase ID (POLID) displays dynamic localization. This polymerase localizes at the antipodal sites during S phase and then switches to a mitochondrial distribution at all the other cell cycle stages [23]. Another reported example is with SSE1 endonuclease,

which has an antipodal site distribution at S phase and is not detectable by immunofluorescence in the other cell cycle stages [24].

A study has identified that *T. brucei* six mitochondrial PIF1-like helicases. The localization of each helicase was determined by overexpression each PIF1-like helicase gene. *T. brucei* PIF1 (TbPIF1) and Pif2 (TbPif2) localized at the mitochondrial matrix; TbPif4, 7 and 8 localize mainly in the kDNA disk; and TbPif5 is at the antipodal sites [13]. However, another study clarified the localization of TbPIF1 stating that this protein localizes at the antipodal sites in 80% of the cells in an asynchronous population, suggesting that this protein probably does not display dynamic localization. They attributed the difference on the localization pattern from the previous study because of the use of an overexpression system that could saturate the normal localization of TbPIF1 provoking its mitochondrial matrix distribution. TbPIF1 was shown to be an ATP-dependent helicase, having a specific activity of 122 mol of hydrolyzed ATP/mol enzyme/min. TbPIF1 could unwind a 36mer oligonucleotide and its unwinding activity was dependent on ATP and Mg^{2+}. When cells were depleted of TbPIF1 via RNAi they stop growing at day 4 after induction. RNAi of TbPIF1 lead to shrinkage and disappearance of kDNA. Southern blot was shown that TbPIF1 depletion cause minicircle loss since day 1 of induction and at day 5 there is no detection of any minicircle. This suggested that TbPIF1 mainly participates in minicircle replication [25].

We embarked on studying in more detail TbPIF1 localization using cell cycle markers such as basal body to confirm whether this protein has dynamic localization. We also questioned if this protein could suffer any post-translation modifications (PTMs) such as acetylation. A study has shown that proteins involved in Okazaki fragment processing

such as human Flap endonuclease 1 (FEN1) and Dna2 endonuclease/helicase (Dna2) are acetylated. Acetylation of FEN1 impacted negatively its endonuclease activity by impairing flap cleavage. However, acetylation of Dna2 stimulated its 5´-3´endonuclease and helicase activity as well as its DNA-dependent ATPase activities. Additionally, acetylated Dna2 displayed a higher affinity for DNA substrates in comparison to the non-acetylated form [26]. Therefore, we hypothesized that in addition to dynamic localization of kDNA replication proteins, PTMs such acetylation can also play a role in regulation and coordination of kDNA replication.

II. Materials and Methods

pPIF1PTP-Neo (Done by Dr. Amy Springer)

TbPIF1 C terminal coding sequence (1492 bp) was PCR amplified from *Trypanosoma brucei* 427 genomic DNA using forward (5´-TAA GAT GGG CCC TTC GTG AAG ATC CGC CTG G-3´) and reverse (5´-TAT CTT CGG CCG TTC CAA CGA CTC ACC AGA GG-3´) primers containing ApaI and EagI restriction sites, respectively. The PCR amplified product was ligated into ApaI and Not1 restriction sites of pC-PTP-Neo [27] to create pPIF1PTP-Neo vector.

PIF1 knockout construct pKOPIF1^{Hyg} (Done by Dr. Amy Springer)

A PIF1 5´UTR fragment was amplified using the forward (5´-CTC GAG CGT ATG CAC GAG TAA AAG GCT-3´) and reverse (5´-AAG CTT CTT AGA CGC ACA AAC AGT AGA TTA ACC-3´) primers containing XhoI and HindIII sites respectively and ligated into pKO^{Hyg} [28]. Subsequently, a PIF1 3´UTR primer was amplified using the

forward (5´-ACT AGT GTT TGT TAC AGT TCT TCC TTA CCC-3´) and reverse (5´-TCT AGA CTA TAT TTC GGA TCC CTG AGG C-3´) primers containing SpeI and XbaI sites respectively and ligated into the vector to obtain the final pKOPIF1^{Hyg} construct.

Trypanosome growth and transfection (Done by Dr. Amy Springer)

Procyclic *T. brucei* Lister 427 WT strain was cultured in SDM-79 media supplemented with 15% heat inactivated serum at 27°C and were co-transfected by nucleofection with linearized AvrII pPIF1PTP-Neo plasmid and XhoI/NotI digested pKOPIF1^{Hyg} plasmid. A stable population was selected with 50 μg/mL G418 and 50 μg/mL hygromycin followed by limiting dilution for selection of a clonal TbPIF1$^{PTP/KO}$ (TbPIF1PTP) cell line.

PIF1PTP immunofluorescence and Basal Body labeling

The TbPIF1PTP cells were harvested for 5 min at 1000 *x g*, washed and resuspended in 1X phosphate buffered saline (PBS). Cells were adhered to poly-L-lysine (1:10) coated slides for 5 min. Cells were fixed with 1.5% paraformaldehyde and washed three times with 1X PBS containing 0.1M glycine and permeabilized with 0.1% Triton X-100 for 5 min. Then, cells were washed with 1X PBS three times for 5 min, followed by incubation with anti-protein A (1:1000) and YL1/2 (1:3000) antibodies for 60 min using 1% BSA in 1X PBS. Cells were washed with 1X PBS containing 0.1% Tween-20 three times for 5 min and incubated with secondary antibody mix containing Alexa Fluor 488 goat-anti rabbit (1:250) and goat-anti rat (1:250) antibodies in 1% BSA in 1X PBS for 60 min. After three washes with 1X PBS containing 0.1% Tween-20, DNA was stained with

3 μg/ml 4´-6´-diamidino-2-phenylindole (DAPI) for 5 min. Slides were washed three times with 1X PBS and mounted in Vectashield.

In Situ TdT labeling

The TbPIF1PTP cells were fixed and permeabilized as described above. Cells were rehydrated in 1X PBS and incubated for 20 min at RT in 25 μl of 1X TdT reaction buffer containing 2mM $CoCl_2$. Cell were then labeled for 60 min at room temperature in 25 μl reaction solution containing (1X TdT reaction buffer; 2.0 mM $CoCl_2$, 10 μM dATP, 5 μM Alexa Fluor 594-dUTP and 40 Units of TdT). The reaction was stopped with three 5-min washes in 2× SSC followed by immunolabeling of PifPTP tagged protein and DAPI staining as described above.

EdU labeling

TbPIF1PTP cells were incubated for 90 min with 350 μM 5-ethynyl-2'-deoxyuridine (EdU) at 27°C. Cells were harvest, fixed and permeabilized as describe above. Cells were incubated in Click-iT reaction cocktail following manufacture´s recommendation (Picolyl Azide Toolkit C10641 LifeTech). Immunolabeling of PIF1PTP tagged protein and DAPI staining was performed as described above.

Cyclohexamide treatment

Transgenic cells expressing PIF1-PTP and Cyc6-HA tagged proteins were incubated with 100 ug/ml of cyclohexamide for 8 hours. Samples were collected every two hours and cell lysates were separated by SDS-PAGE. Tagged proteins were detected by

western blot using Peroxidase-Anti-Peroxidase (PAP) (1:2000) for PTP detection, and for HA detection anti-HA (1:1000) and goat anti-rat (1:2000) antibodies were used. For loading control, the blot was probed against *Crithidia fasciculata* specific Hsp70 antibody (1:10000) followed by secondary chicken anti-rabbit antibody (1:2000).

TSA treatment and immunoprecipitation

Cells expressing PIF1-PTP tagged proteins were incubated with 2μM of Trichostatin A (TSA) for 0, 6, and 24 hours. A total of 5 x 10^8 cells from each time point were collected and lysed using the cold extraction buffer (150 mM KCl, 20 mM Tris-HCl pH 7.5, 3 mM $MgCl_2$, 0.5% NP-40). The suspension was incubated on ice for 30 min with gently shaking. The lysate was pass through a 22 ½ gauge needle 10 times to remove any remaining clumps followed by a centrifugation at high speed for 20 min at 4°C. The soluble fraction was added to a pre-equilibrated IgG beads suspension and incubated at 4°C in a rotating carousel for 2 hours. After separating the unbound fraction, the beads were washed with chilled Wash buffer (150 mM KCl, 20 mM Tris-HCl pH 7.5, 3 mM $MgCl_2$, 0.1% NP-40 and 1mM DTT) five times. For the elution step, Laemmli buffer supplemented with 5% BME was added to the beads and heated for 10 min at 95°C. Each elution was separated by SDS-PAGE. Tagged proteins were detected by western blot using with PAP (1:2000), and acetylation was detected using anti-acetylated lysine (1:2000) and secondary anti-rabbit antibody (1:2000).

III. Results

1. PIF1PTP is not detected in all cell cycles stages

Previously was suggested that TbPIF1 localization is at the antipodal sites in all the cell cycles of *T. brucei* procyclic cells. However, this study did not include a cell cycle marker such as the dynamic of basal body to confirm their observation [25]. Therefore, to investigate in more detail TbPIF1 distribution at the different cell cycle stage, we generated a single expresser cell line by co-transfecting 427 WT procyclic cells with linearized pC-PIF1PTP-Neo and digested pKOPIF1-Hyg vectors. In this cell line, TbPIF1$^{PTP/KO}$, one allele is deleted and the other one is fused to a PTP tag at the 3´end of TbPIF1 (Fig. 1A). As an important note, the confirmation of PTP integration and the successful knockout has not been confirmed by southern blot analysis. There was no growth defect in the clonal cell lines and the clone selected for further study was TbPIF1$^{PTP/KO}$P1H2 (TbPIF1PTP cell line) with a doubling time of 12 hours (data not shown). The expected product of PIF1PTP (132 kDa) was detected by western blot using peroxidase-Anti peroxidase (PAP) antibody. The PTP tag was only detected in the whole cell extract of the TbPIF1PTP clonal cell line with no cross reactivity with the whole cell extract from 427 WT cells (Fig. 1B). Fluorescence microscopy of TbPIF1PTP cell line showed that only a subset of cells has PTP signal and an initial observation indicated that cells where the kDNA is not elongated did not have a PTP signal (Fig. 1C, white arrows). Additionally, two different patterns of PIF1-PTP signal were observed. In the first pattern, PIF1PTP has a kDNA disk distribution while the second pattern PIF1PTP localizes at the antipodal sites (Fig. 1C).

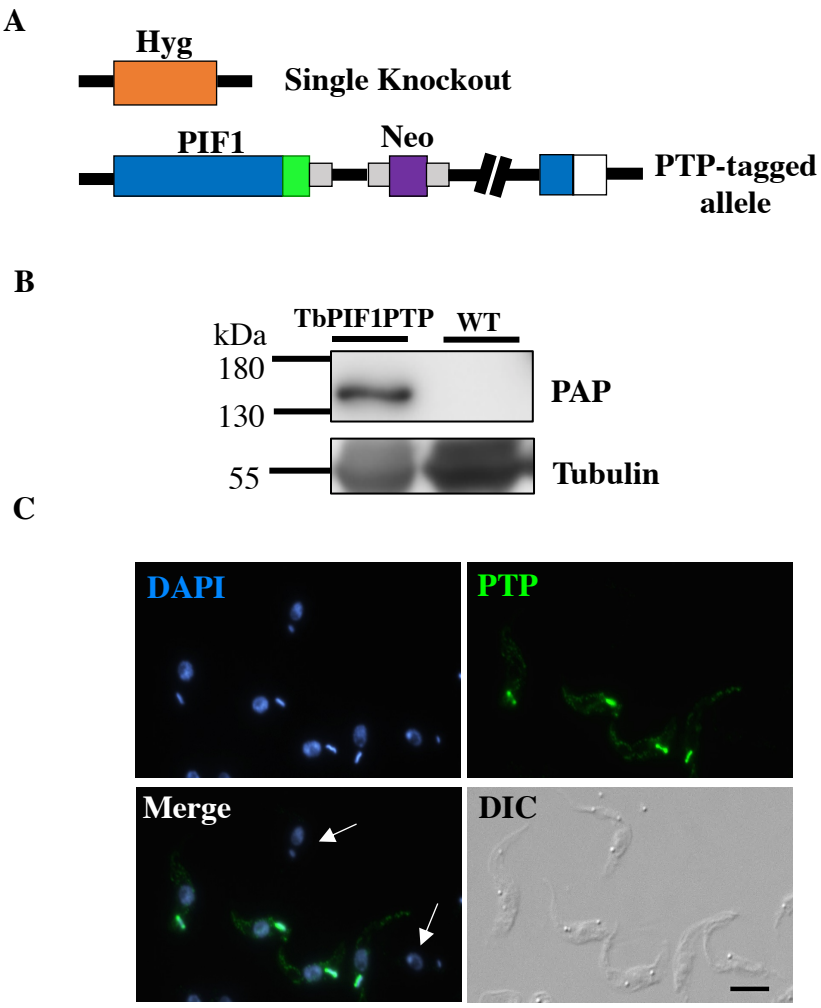

Figure 1 - TbPIF1PTP single expresser cell line and PIF1PTP localization

(A) Diagram depicting PIF1PTP (not to scale) gene locus in the TbPIF1PTP cell line. TbPIF1 gene (blue) was replaced in one allele by a hygromycin resistance gene (Hyg). The second allele was fused to a PTP sequence at the 3´end. Selective marker for PTP integration is neomycin (Neo). (B) Western blot analysis of whole cell extracts of WT and TbPIF1PTP cells. PTP tagged protein is only detected in TbPIF1PTP cells using PAP reagent. Tubulin was used a loading control. (C) Localization of PIF1PTP in an unsynchronized population using anti-protein A. White arrows indicate cells with no PIF1PTP signal. Scale bar 6 μm.

2. PIF1PTP is only detected during kDNA replication and is not regulated by proteolysis

We further investigate the localization pattern of PIF1PTP during *T. brucei* cell cycle using basal body staining and dynamics. A total of 317 cells (n =1) were quantified for detection of PIF1PTP at different cell cycle stages. Detection of PIF1PTP signal is only found after basal body duplication and the signal is no longer detected after kDNA duplication (Fig. 2A and 2B). Approximately 30% of the cells at the $1N1K_{div}$ stage have PIF1PTP positive signal (Fig. 2B) and they displayed two different patterns: kDNA disk and antipodal sites seen as 2 foci. From this subset of cells, we quantified the number of cells with a PIF1PTP signal at the antipodal site (2 foci) and how many have a signal at the kDNA disk. Based on our quantification analysis, almost 80% of the $1N1K_{div}$ cells have a PIF1PTP signal at the antipodal sites by displaying the 2 foci pattern (Fig. 2C), and at later stages of $1N1K_{div}$ (Fig. 2A, $1N1K_{div}$ panel) ~20% of the PIF1PTP signal is detected at the kDNA disk (Fig. 2C). Since PIF1PTP signal is not detected after kDNA synthesis, we tested if this protein is regulated by proteolysis by the mitochondrial protease HslVU. This protease is involved in regulating protein levels of another mitochondrial helicase in *T. brucei*, TbPif2. The protein levels of PIF1PTP were measured every 2 hours during an 8-hour treatment with the protein synthesis inhibitor cycloheximide (CHX). During the CHX treatment, PIF1PTP levels remained unchanged in comparison to our positive control Cyclin 6 (Cyc6) which protein levels were reduced in the course of the treatment. Mitochondrial Hsp70 was used as a loading and negative control. These data demonstrate that PIF1PTP is a stable protein that is not regulated by proteolysis (Fig. 3)

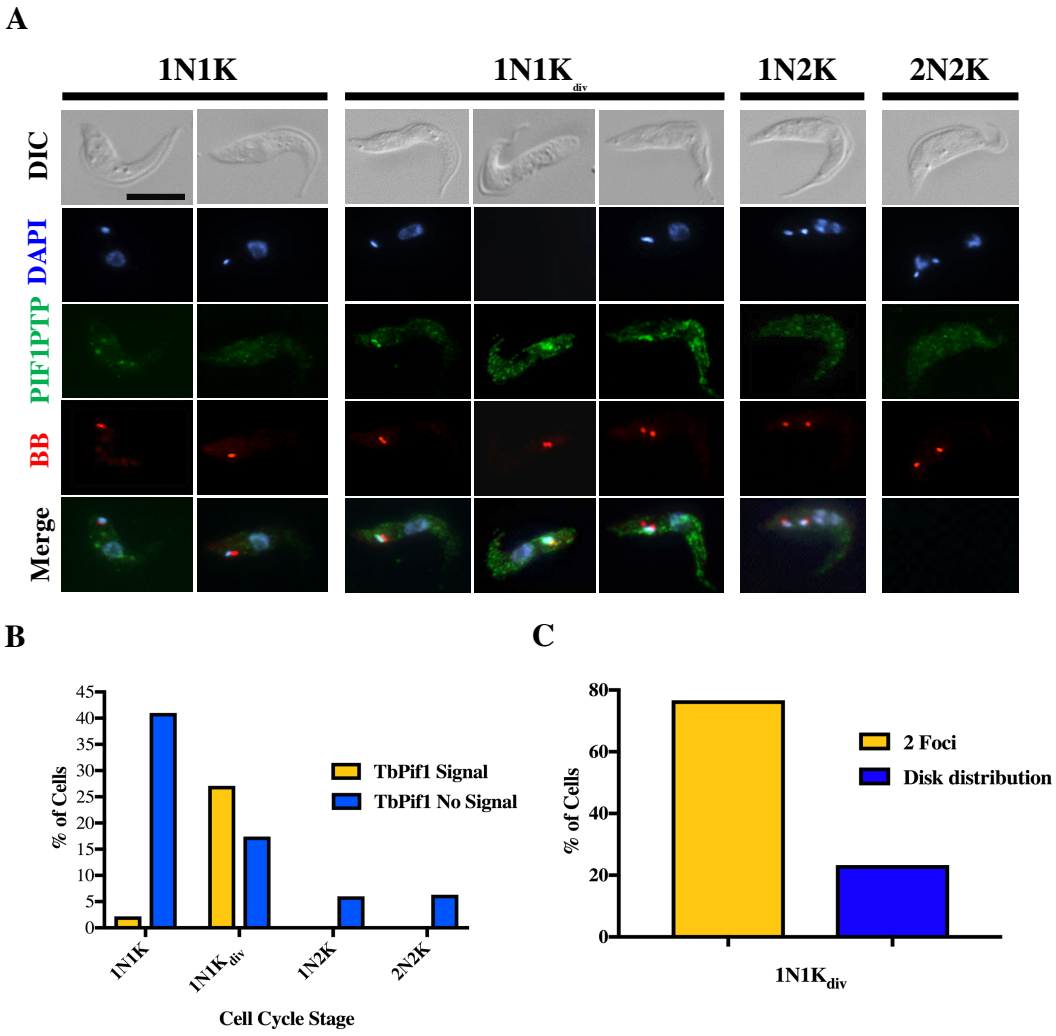

Figure 2 - Localization of PIF1PTP during the cell cycle

(A) Representative cells from unsynchronized population. Double labeling of PIF1PTP (green) and basal body (red) indicated that changes in PIF1-PTP localization are coordinated with the cell cycle. Scale bar 6 µm. (B) A total of 317 cells were quantified for detection of PIF1PTP at different cell cycle stages. Only cells at $1N1K_{div}$ presented signal of PIF1PTP (27% of cell population). (C) The PIF1PTP signal in $1N1K_{div}$ subpopulation (86 cells) could be observed as two foci at early basal body duplication (76.7 %) or as disperse signal in the kDNA disk (23.3%) as the two basal bodies separated from each other.

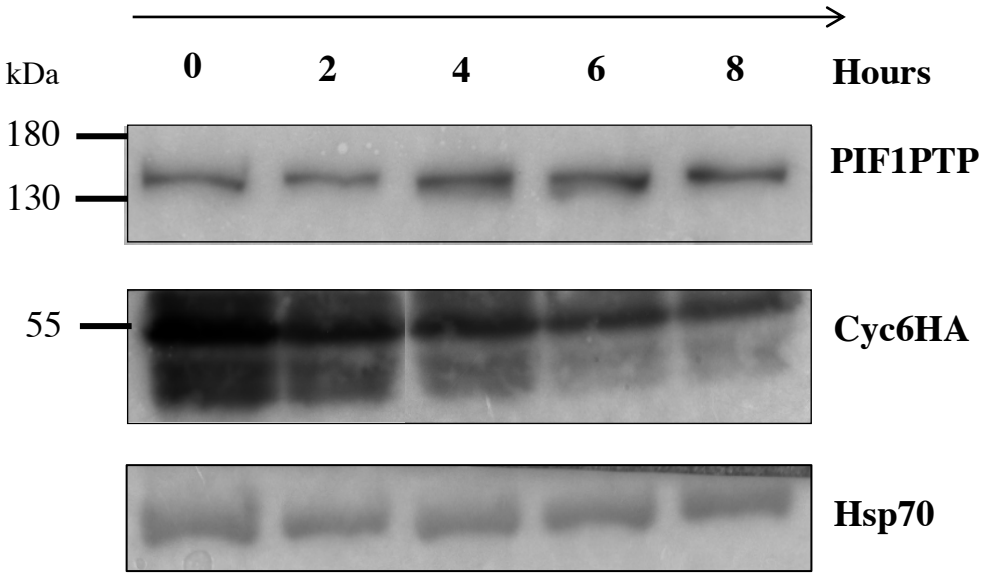

Fig 3 - PIF1PTP protein levels after CHX treatment

Western blot detection of PIF1PTP, Cyc6HA and Hsp70 protein levels after CHX treatment. Cyc6HA was used as a positive control and Hsp70 as a loading control. PIF1PTP protein stability was not affected upon CHX treatment. PIF1PTP is not regulated by proteolysis.

3. TbPIF1-PTP colocalizes with gapped minicircles at the antipodal sites

To confirm that the two foci distribution of PifPTP correspond to an antipodal site localization, we fluorescently labeled replication minicircles with terminal deoxynucleotidyl transferase (TdT) and fluorescein conjugated dUTP. Replicating minicircles containing gaps accumulate at the antipodal sites prior reattachment to the disk during kDNA S phase. TdT labeling has different patterns during *T. brucei* cell cycle. At 1N1K stage, there is no replication of minicircles and maxicircles and they remain covalently close with no gapped or nicked regions. Therefore, these cells are TdT negative (TdT -). There is no PIF1PTP signal in this subset of cells (Fig. 4A). When cells enter to early stages of kDNA S phase ($1N1K_{div}$), multiple gapped minicircles are enriched at the antipodal sites. TdT has a strong positive signal (TdT +; early) in this subset of cells. PIF1PTP signal is similar with TdT showing localization at the antipodal sites (Fig. 4A and 4B). At later stages of kDNA S phase ($1N1K_{div}$), gapped minicircles progeny is attached to the kDNA network and TdT signal is at the kDNA disk (TdT +; late). PIF1PTP signal displayed the same pattern as TdT showing a kDNA network localization (Fig. 4A and 4C). Cells at the 1N2K stage, all the minicircles are repaired and therefore they can no longer be labeled. These cells are TdT negative and PIF1PTP is no longer detected in post replicating networks that were TdT negative (Fig. 4A)

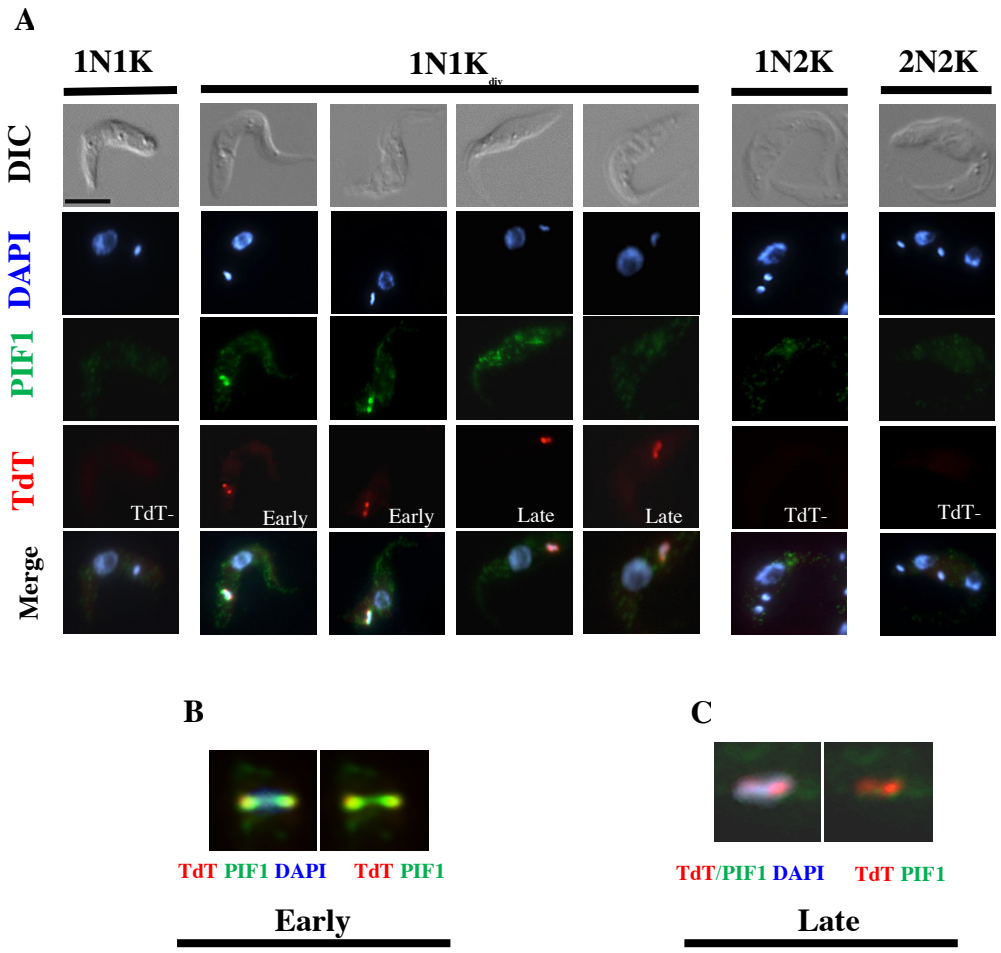

Figure 4 - Localization of PIF1PTP with TdT labeled gapped minicircles

(A) Relative localization of PIF1PTP (green) with TdT labeled replicating minicircles (red) at the antipodal sites at different cell cycle stages in an unsynchronized population. Scale bar 6 μm. (B) PIF1PTP is detected as two foci at the antipodal sites at early stages of TdT labeling. (C) PIF1PTP signal intensity decreases at late stages of TdT labeling presenting a localization near the kDNA disk.

4. TbPIF1-PTP colocalizes with replicating minicircles

Newly replicated DNA can be visualized by labeling the cells with 5-ethynyl-2´-deoxyuridine (EdU), a thymidine analog that allows a click chemistry reaction by having an alkyne group that interacts with a fluorophore azide [29]. When labeling with EdU an unsynchronized population of *T. brucei* procyclic cells, the 1N1K cells does not show any signal of EdU. In 1N1K$_{div}$ EdU signal is at the antipodal sites and in the nucleus. The 1N2K cells showed EdU signal at the nucleus only, and 2N2K cells do not have EdU signal. We investigated if PIF1PTP colocalizes with replicating minicircles by microscopy and did quantification of the signal by analyzing 197 cells (n =1). By fluorescence microscopy, EdU signal at the antipodal sites colocalized with PIF1PTP signal (Fig. 5A). In an unsynchronized population, 34% of the cells showed PIF1PTP signal and were EdU positive (Fig. 5B) corresponding to cells at the 1N1K$_{div}$ stage. At this subset of cells, PIF1PTP signal is mostly found in cells that are EdU positive for kDNA and nuclear incorporation (60.6%) (Fig. 5C). This data suggests that PIF1PTP signal is detected a kDNA and nuclear DNA S phase.

5. PIF1PTP is acetylated

Acetylation is a post-translational modification (PTM) that causes diverse effects on protein levels and metabolism in the cells. Even though that acetylated residues were first identified in histones, many proteins in the cells can be acetylated. One effect of this PTMS is that it can determine the subcellular localization of the proteins. A second effect is modulation of protein-protein interactions and therefore it can increase the affinity between protein partners. A third effect is that acetylation can regulate protein function by

affecting enzymatic activity [30]. Helicases can be modulated by PTMs such as acetylation [31]. An example is the WRN (Werner syndrome gene) helicase, a member of the RecQ family of DNA helicases, that plays a role in recombination, replication, telomere maintenance and base excision repair. WRN helicase is acetylated by the acetyltransferase p300 and this event increments the translocation of WRN from the nucleolus to nucleoplasmic foci after DNA damage [32]. We hypothesized that *T. brucei* PIF1 could be acetylated and that PTM could affect its cellular localization. To test this hypothesis, we probed a WCE fraction from our TbPIF1PTP cell line against acetylated lysine and we also performed immnunoprecipitation (IP) of PIF1PTP and determine detection of acetylation in the purified product. We are able to observe detection of acetylation in the WCE and also after performing the IP (Fig. 6A). To confirm this observation, we treat the TbPIF1PTP cells with a Trichostatin A (TSA), which inhibits deacetylases and therefore protein acetylation should increase over time. We exposed the cells to TSA for 24 hours and recollect samples at the 0, 6 and 24-hour period. Then we performed an IP from these conditions and probe against PIF1PTP acetylation. Acetylation of PifPTP seems to increase over time after exposing the cells with TSA (Fig. 6B). These initial observations indicate the possibility that PIF1PTP is acetylated and this PTM can potentially regulate kDNA replication.

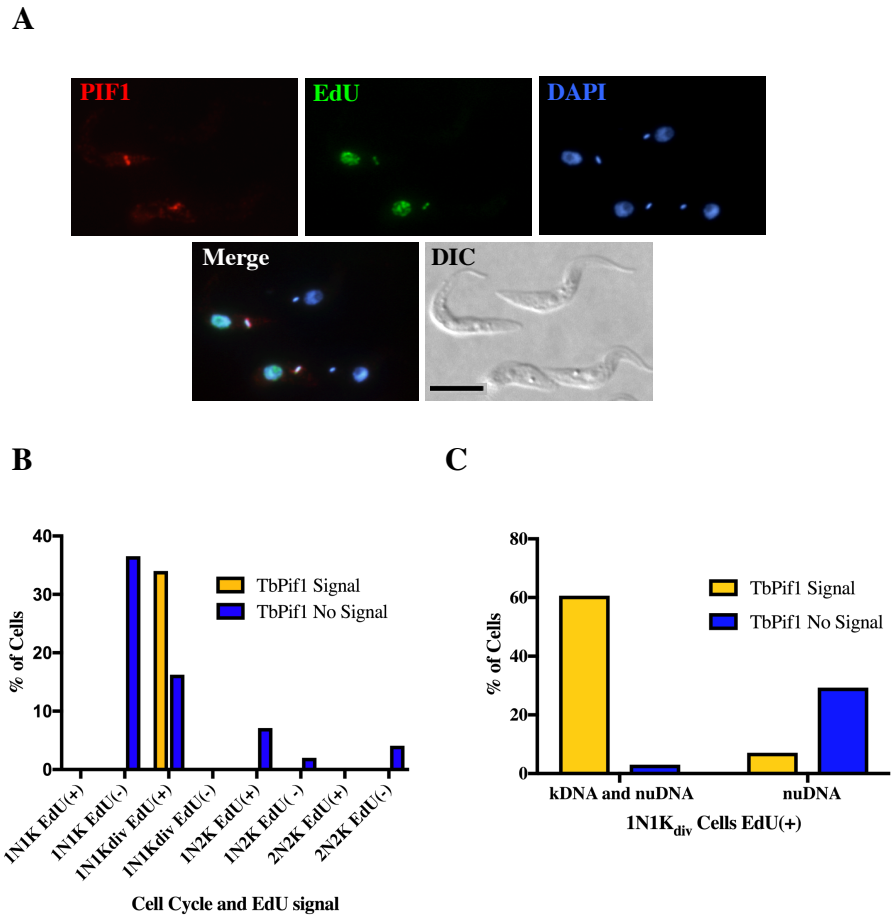

Figure 5 - PIF1PTP localization with EdU labeled DNA.

(A) Localization of PIF1PTP (red) relative to the localization of active DNA synthesis sites using EdU labeling (green) in an unsynchronized population. PIF1PTP colocalizes with active kDNA replication forks. Scale bar 6 μm. (B) A total 197 cells were quantified for PIF1PTP detection relative to DNA synthesis. PIF1 is detected mainly in the EdU positive 1N1K$_{div}$ cell subpopulation (34%). (C) PIF1PTP signal is mostly found at kDNA and nuDNA S-phase (60.6%) in the 1N1K$_{div}$ subpopulation (99 cells).

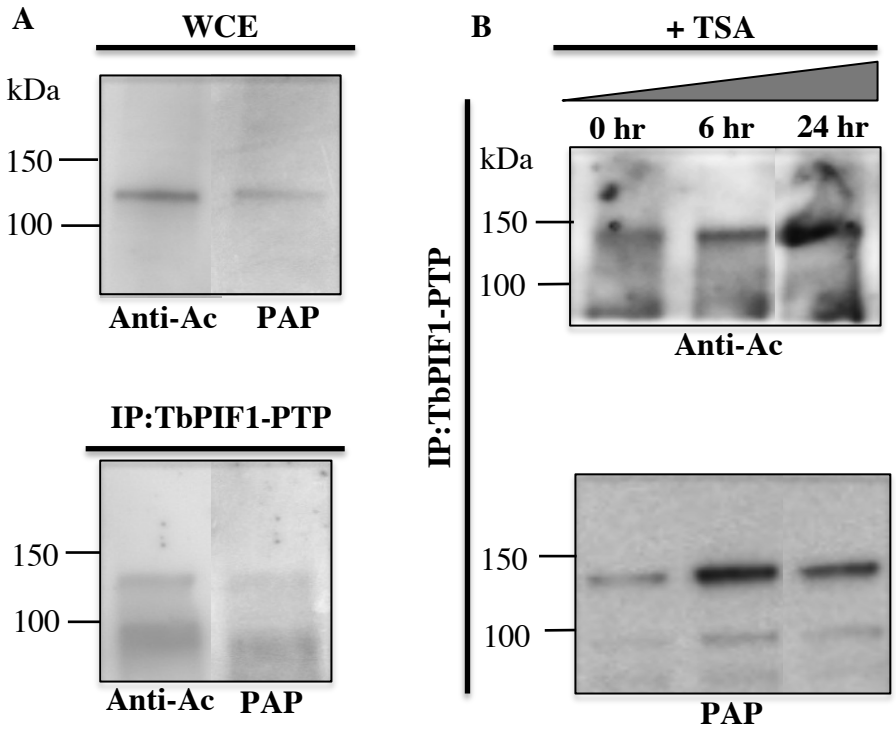

Figure 6 - PIF1PTP acetylation upon TSA treatment

(A) *Upper panel*. Western blot analysis probing against acetylated lysine of whole cell extracts from PIF1PTP cell line showed detection around the PIF1PTP molecular weight (132 kDa). *Lower Panel*. Acetylation of PIF1PTP was also observed after performing an IP using IgG beads. (B) Treatment with TSA increased the PIF1 acetylation. Cell cultures of TbPIF1PTP cell line were treated with TSA for 0, 6 and 24 hours. An IP was performed for each sample followed by probing the membrane against acetylated lysines and PAP.

IV. Discussion

Due the complexity of the kDNA structure, its replication has to be coordinated and monitored by several proteins. This suggests that the factors involved in this process have to communicate and be at the correct location in the precise moment that their function is needed for kDNA replication. Two main locations are assigned for kDNA replication which are the KFZ, where the replication initiates; and the antipodal sites where Okazaki fragment processing occurs. This spatial and temporal separation of events demands an elegant choreography of kDNA replication proteins to ensure proper replication of the kDNA and its segregation. As observed in the mitochondrial DNA polymerase ID (POLID), which its localization is dynamic through the cell cycle by presenting a mitochondrial matrix distribution at all the cell cycles except at kDNA S phase where it displays antipodal site localization [23]; we conducted initial experiments to elucidate the distribution of PIF1PTP throughout the cell cycle of *T. brucei* and the cellular events that can regulate its localization. In comparison to POLID, the changes on localization patterns in PIF1PTP are subtler, by moving from the antipodal sites to the kDNA disk at early and late stages of kDNA S phase, respectively (Fig. 2A). Although is worth to mention that PIF1PTP signal is only detected at the $1N1K_{div}$ cell stage. This phenomenon is also observed in *Crithidia fasciculata* kDNA proteins such as Pol β, where its detection at the antipodal sites is cycle dependent. Pol β is at the antipodal sites during S phase but is no longer detected after network replication. Based on these observations, we conclude that PIF1PTP has also a cell cycle dependent localization that can contribute to the regulation of kDNA replication [33]. As observed in pol β, PIF1PTP is also a stable protein since its levels were not reduced upon CHX treatment (Fig. 3A). Another mode to regulate protein localization

is by PTMs. Our initial experiments suggest that PIF1 can be acetylated (Fig. 6) and this can interfere with its cellular localization. Acetylation might interfere with the microscopy detection of the protein at other cell cycle stages. Acetylation of PIF1 might have also an effect on its interaction with other kDNA proteins as well as with its ATPase and helicase activity. The effects of acetylation in PIF1 enzymatic activity can be tested by performing *in vitro* assays using recombinant PIF1 that is acetylated versus the deacetylated PIF1. In addition, the identification of the lysines that are being acetylated can be done by mass spectrometry analysis. In this way, parasites that are expressing mutated PIF1 lacking the residues for acetylation will allow us to determine the effect that acetylation has on PIF1 localization and its overall impact on kDNA replication role.

A general consensus of the specific role of PIF1 in kDNA replication has not been defined yet. Based on the RNAi data it is clear that PIF1 is involved in minicircle replication since its depletion reduces the amount of minicircles sooner than the amount of maxicircles. It is suggested that this protein has a role in segregation of minicircle progeny together with topoisomerase 2 (Topo2). RNAi of both of these enzymes independently lead to the enrichment of a replication intermediate known as fraction U. Fraction U is a heterogeneous family of multiply interlocked dimeric minicircles and is believed to derive from an intermediate that is upstream of nicked/gapped circles [25]. Our microscopy analysis using TdT (Fig. 4) and EdU (Fig. 5) labeling confirmed the role of PIF1 in minicircle replication. However, it is important to highlight that EdU signal and incorporation in the kDNA is only observed at the antipodal sites and no signal was observed at KFZ where replication starts. This observation indicates that probably the minicircles moves faster to the antipodal sites where active replication forks can still be in

function. It is possible that PIF1 could play a role on both segregation and at the replication fork. Future experiments are needed to define the precise roles of PIF1.

V. Bibliography

1. Jensen RE, Englund PT. Network news: the replication of kinetoplast DNA. Annu Rev Microbiol. 2012;66: 473–91. doi:10.1146/annurev-micro-092611-150057
2. Lukeš J, Hashimi H, Zíková A. Unexplained complexity of the mitochondrial genome and transcriptome in kinetoplastid flagellates. Curr Genet. 2005;48: 277–299. doi:10.1007/s00294-005-0027-0
3. Aphasizhev R, Aphasizheva I. Uridine insertion/deletion editing in trypanosomes: A playground for RNA-guided information transfer. Wiley Interdiscip Rev RNA. 2011;2: 669–685. doi:10.1002/wrna.82
4. Milman N, Motyka SA, Englund PT, Robinson D, Shlomai J. Mitochondrial origin-binding protein UMSBP mediates DNA replication and segregation in trypanosomes. Proc Natl Acad Sci U S A. 2007;104: 19250–19255. doi:10.1073/pnas.0706858104
5. Ferguson ML, Torri AF, Pérez-Morga D, Ward DC, Englund PT. Kinetoplast DNA replication: Mechanistic differences between Trypanosoma brucei and Crithidia fasciculata. J Cell Biol. 1994;126: 631–639. doi:10.1083/jcb.126.3.631
6. Scocca JR, Shapiro TA. A mitochondrial topoisomerase IA essential for late theta structure resolution in African trypanosomes. Mol Microbiol. 2008;67: 820–829. doi:10.1111/j.1365-2958.2007.06087.x
7. Englund PT. Free Minicircles of Kinetoplast DNA in Crithidia fasciculata. J Biol Chem. 1979;254..
8. Lindsay ME, Gluenz E, Gull K, Englund PT. A new function of Trypanosoma brucei mitochondrial topoisomerase II is to maintain kinetoplast DNA network topology. Mol Microbiol. 2008;70: 1465–1476. doi:10.1111/j.1365-2958.2008.06493.x
9. Abu-Elneel K, Robinson DR, Drew ME, Englund PT, Shlomai J. Intramitochondrial localization of universal minicircle sequence-binding protein, a trypanosomatid protein that binds kinetoplast minicircle replication origins. J Cell Biol. 2001;153: 725–733. doi:10.1083/jcb.153.4.725
10. Liu B, Molina H, Kalume D, Pandey A, Griffith JD, Englund PT. Role of p38 in Replication of Trypanosoma brucei Kinetoplast DNA. Mol Cell Biol. 2006;26: 5382–5393. doi:10.1128/MCB.00369-06
11. Li C, Englund PT. A mitochondrial DNA primase from the trypanosomatid Crithidia fasciculata. J Biol Chem. 1997;272: 20787–20792. doi:10.1074/jbc.272.33.20787
12. Klingbeil MM, Motyka SA, Englund PT. Multiple Mitochondrial DNA Polymerases in Trypanosoma brucei. Mol Cell. 2002;10: 175–186.
13. Liu B, Wang J, Yaffe N, Lindsay ME, Zhao Z, Zick A, et al. Trypanosomes have six mitochondrial DNA helicases with one controlling kinetoplast maxicircle

replication. Mol Cell. 2009;35: 490–501. doi:10.1016/j.molcel.2009.07.004
14. Engel ML, Ray DS. A structure-specific DNA endonuclease is enriched in kinetoplasts purified from Crithidia fasciculata. Nucleic Acids Res. 1998;26: 4733–4738. doi:10.1093/nar/26.20.4733
15. Downey N, Hines JC, Sinha KM, Ray DS. Mitochondrial DNA Ligases of Trypanosoma brucei. Eukaryot Cell. 2005;4: 765–774. doi:10.1128/EC.4.4.765-774.2005
16. Saxowsky TT, Choudhary G, Klingbeil MM, Englund PT. Trypanosoma brucei has two distinct mitochondrial DNA polymerase beta enzymes. J Biol Chem. 2003;278: 49095–49101. doi:10.1074/jbc.M308565200
17. Povelones ML. Beyond replication: division and segregation of mitochondrial DNA in kinetoplastids. Mol Biochem Parasitol. 2014;196: 53–60. doi:10.1016/j.molbiopara.2014.03.008
18. Hoffmann A, Käser S, Jakob M, Amodeo S, Peitsch C, Týč J, et al. Molecular model of the mitochondrial genome segregation machinery in *Trypanosoma brucei*. Proc Natl Acad Sci. 2018; 201716582. doi:10.1073/pnas.1716582115
19. Woodward R, Gull K. Timing of nuclear and kinetoplast DNA replication and early morphological events in the cell cycle of Trypanosoma brucei. J Cell Sci. 1990;95: 49–57.
20. Koltzscher M, Neumann C, Kö S, Gerke V. A High-Order Trans-Membrane Structural Linkage Is Responsible for Mitochondrial Genome Positioning and Segregation by Flagellar Basal Bodies in Trypanosomes. Mol Biol Cell. 2003;14: 2372–2384. doi:10.1091/mbc.E02
21. Dang HQ, Zhou Q, Rowlett VW, Hu H, Lee KJ, Margolin W, et al. Proximity Interactions among Basal Body Components in Trypanosoma brucei Identify Novel Regulators of Basal Body Biogenesis and Inheritance. MBio. 2017;8: 1–15. doi:10.1128/mBio.02120-16
22. McKean PG. Coordination of cell cycle and cytokinesis in Trypanosoma brucei. Curr Opin Microbiol. 2003;6: 600–607. doi:10.1016/j.mib.2003.10.010
23. Concepción-Acevedo J, Luo J, Klingbeil MM. Dynamic localization of Trypanosoma brucei mitochondrial DNA polymerase ID. Eukaryot Cell. 2012;11: 844–55. doi:10.1128/EC.05291-11
24. Engel ML, Ray DS. The kinetoplast structure-specific endonuclease I is related to the 5' exo/endonuclease domain of bacterial DNA polymerase I and colocalizes with the kinetoplast topoisomerase II and DNA polymerase beta during replication. Proc Natl Acad Sci U S A. 1999;96: 8455–60. doi:10.1073/PNAS.96.15.8455
25. Liu B, Yildirir G, Wang J, Tolun G, Griffith JD, Englund PT. TbPIF1, a Trypanosoma brucei mitochondrial DNA helicase, is essential for kinetoplast minicircle replication. J Biol Chem. 2010;285: 7056–66. doi:10.1074/jbc.M109.084038
26. Balakrishnan L, Stewart J, Polaczek P, Campbell JL, Bambara RA. Acetylation of Dna2 endonuclease/helicase and flap endonuclease 1 by p300 promotes DNA stability by creating long flap intermediates. J Biol Chem. 2010;285: 4398–4404. doi:10.1074/jbc.M109.086397
27. Schimanski B, Nguyen TN, Gu A. Highly Efficient Tandem Affinity Purification

of Trypanosome Protein Complexes Based on a Novel Epitope Combination. Eukaryot Cell. 2005;4: 1942–1950. doi:10.1128/EC.4.11.1942

28. Lamb JR, Fu V, Wirtz E, Bangs JD. Functional Analysis of the Trypanosomal AAA Protein TbVCP with trans-Dominant ATP Hydrolysis Mutants. J Biol Chem. 2001;276: 21512–21520. doi:10.1074/jbc.M100235200
29. Buck SB, Bradford J, Gee KR, Agnew BJ, Clarke ST, Salic A. Detection of S-phase cell cycle progression using 5-ethynyl-2′-deoxyuridine incorporation with click chemistry, an alternative to using 5-bromo-2′-deoxyuridine antibodies. Biotechniques. 2008;44: 927–929. doi:10.2144/000112812
30. Drazic A, Myklebust LM, Ree R, Arnesen T. The world of protein acetylation. Biochim Biophys Acta - Proteins Proteomics. 2016;1864: 1372–1401. doi:10.1016/j.bbapap.2016.06.007
31. Wu Y. Unwinding and rewinding: Double faces of helicase? J Nucleic Acids. 2012;2012. doi:10.1155/2012/140601
32. Blandert G, Zalle N, Daniely Y, Taplick J, Gray MD, Oren M. DNA damage-induced translocation of the Werner helicase is regulated by acetylation. J Biol Chem. 2002;277: 50934–50940. doi:10.1074/jbc.M210479200
33. Johnson CE, Englund PT. Changes in organization of Crithidia fasciculata kinetoplast DNA replication proteins during the cell cycle. J Cell Biol. 1998;143: 911–9. http://www.pubmedcentral.nih.gov/articlerender.fcgi?artid=2132953&tool=pmcentrez&rendertype=abstract

BIBLIOGRAPHY

1. Abu-Elneel K, Robinson DR, Drew ME, Englund PT, Shlomai J. Intramitochondrial localization of universal minicircle sequence-binding protein, a trypanosomatid protein that binds kinetoplast minicircle replication origins. J Cell Biol. 2001;153: 725–733. doi:10.1083/jcb.153.4.725

2. Akiyoshi B, Gull K. Evolutionary cell biology of chromosome segregation: insights from trypanosomes. Open Biol. 2013;3: 130023–130023. doi:10.1098/rsob.130023

3. Aksoy S, Buscher P, Lehane M, Solano P, Abbeele J Van Den. Human African trypanosomiasis control : Achievements and challenges. PLoS Negl Trop Dis. 2017; 1–6.

4. Alabert C, Bukowski-Wills JC, Lee SB, Kustatscher G, Nakamura K, De Lima Alves F, et al. Nascent chromatin capture proteomics determines chromatin dynamics during DNA replication and identifies unknown fork components. Nat Cell Biol. 2014;16: 281–291. doi:10.1038/ncb2918

5. Alabert C, Groth A. Chromatin replication and epigenome maintenance. Nat Rev Mol Cell Biol. Nature Publishing Group; 2012;13: 153–167. doi:10.1038/nrm3288

6. Alsford S, Turner DJ, Obado SO, Sanchez-flores A, Glover L, Berriman M, et al. High-throughput phenotyping using parallel sequencing of RNA interference targets in the African trypanosome High-throughput phenotyping using parallel sequencing of RNA interference targets in the African trypanosome. Genome Res. 2011;21: 915–924. doi:10.1101/gr.115089.110

7. Aphasizhev R, Aphasizheva I. Uridine insertion/deletion editing in trypanosomes: A playground for RNA-guided information transfer. Wiley Interdiscip Rev RNA. 2011;2: 669–685. doi:10.1002/wrna.82

8. Aranda S, Rutishauser D, Ernfors P. Identification of a large protein network involved in epigenetic transmission in replicating DNA of embryonic stem cells. Nucleic Acids Res. 2014;42: 6972–6986. doi:10.1093/nar/gku374

9. Archer SK, Inchaustegui D, Queiroz R, Clayton C. The cell cycle regulated transcriptome of Trypanosoma brucei. PLoS One. 2011;6. doi:10.1371/journal.pone.0018425

10. Aroya S Ben, Kupiec M. The Elg1 replication factor C-like complex: A novel guardian of genome stability. DNA Repair (Amst). 2005;4: 409–417. doi:10.1016/j.dnarep.2004.08.003

11. Aslett M, Aurrecoechea C, Berriman M, Brestelli J, Brunk BP, Carrington M, et al. TriTrypDB: A functional genomic resource for the Trypanosomatidae. Nucleic Acids Res. 2009;38: 457–462. doi:10.1093/nar/gkp851

12. Balakrishnan L, Stewart J, Polaczek P, Campbell JL, Bambara RA. Acetylation of Dna2 endonuclease/helicase and flap endonuclease 1 by p300 promotes DNA stability by creating long flap intermediates. J Biol Chem. 2010;285: 4398–4404. doi:10.1074/jbc.M109.086397

13. Benmerzouga I, Concepción-Acevedo J, Kim HS, Vandoros A V., Cross GAM, Klingbeil MM, et al. Trypanosoma brucei Orc1 is essential for nuclear DNA replication and affects both VSG silencing and VSG switching. Mol Microbiol. 2013;87: 196–210. doi:10.1111/mmi.12093

14. Benz C, Dondelinger F, McKean PG, Urbaniak MD. Cell cycle synchronisation of Trypanosoma brucei by centrifugal counter-flow elutriation reveals the timing of nuclear and kinetoplast DNA replication. Sci Rep. 2017;7: 1–10. doi:10.1038/s41598-017-17779-z

15. Berninger M, Schmidt I, Ponte-Sucre A, Holzgrabe U. Novel lead compounds in pre-clinical development against African sleeping sickness. Med Chem Commun. 2017;8: 1872–1890. doi:10.1039/C7MD00280G

16. Berriman M, Ghedin E, Hertz-Fowler C, Blandin G, Renauld H, Bartholomeu DC, et al. The genome of the African trypanosome Trypanosoma brucei. Science. 2005;309: 416–422. doi:10.1126/science.1112642

17. Blandert G, Zalle N, Daniely Y, Taplick J, Gray MD, Oren M. DNA damage-induced translocation of the Werner helicase is regulated by acetylation. J Biol Chem. 2002;277: 50934–50940. doi:10.1074/jbc.M210479200

18. Brambati A, Colosio A, Zardoni L, Galanti L, Liberi G. Replication and transcription on a collision course: eukaryotic regulation mechanisms and implications for DNA stability. Front Genet. 2015;6: 1–8. doi:10.3389/fgene.2015.00166

19. Buck SB, Bradford J, Gee KR, Agnew BJ, Clarke ST, Salic A. Detection of S-phase cell cycle progression using 5-ethynyl-2′-deoxyuridine incorporation with click chemistry, an alternative to using 5-bromo-2′-deoxyuridine antibodies. Biotechniques. 2008;44: 927–929. doi:10.2144/000112812

20. Budhavarapu VN, Chavez M, Tyler JK. How is epigenetic information maintained through DNA replication? Epigenetics and Chromatin. Epigenetics & Chromatin; 2013;6: 1. doi:10.1186/1756-8935-6-32

21. Burgers PMJ, Kunkel TA. Eukaryotic DNA Replication Fork. Annu Rev Biochem. 2017;86: 417–438. doi:10.1146/annurev-biochem-061516-044709

22. Burgess A, Lorca T, Castro A. Quantitative Live Imaging of Endogenous DNA Replication in Mammalian Cells. PLoS One. 2012;7. doi:10.1371/journal.pone.0045726

23. Büscher P, Cecchi G, Jamonneau V, Priotto G. Human African trypanosomiasis. 2017;390: 2397–2409. doi:10.1016/S0140-6736(17)31510-6

24. Cai J, Yao N, Gibbs E, Finkelstein J, Phillips B, O´Donnell M, et al. ATP hydrolysis catalyzed by human replication factor C requires participation of multiple subunits. Proc Natl Acad Sci. 1998;95: 11607–11612.

25. Cai YH, Huang H. Advances in the study of protein-DNA interaction. Amino Acids. 2012;43: 1141–1146. doi:10.1007/s00726-012-1377-9

26. Calderano SG, Drosopoulos WC, Quaresma MM, Marques CA, Kosiyatrakul S, McCulloch R, et al. Single molecule analysis of Trypanosoma brucei DNA replication dynamics. Nucleic Acids Res. 2015;43: 2655–2665. doi:10.1093/nar/gku1389

27. Calderano SG, Godoy PD de M, da Cunha JPC, Elias MC. Trypanosome Prereplication Machinery: A Potential New Target for an Old Problem. Enzyme Res. 2011;2011: 1–8. doi:10.4061/2011/518258

28. Caljon G, Van Reet N, De Trez C, Vermeersch M, Pérez-Morga D, Van Den Abbeele J. The Dermis as a Delivery Site of Trypanosoma brucei for Tsetse Flies. PLoS Pathog. 2016;12: 1–22. doi:10.1371/journal.ppat.1005744

29. Canela A, Maman Y, Jung S, Wong N, Callen E, Day A, et al. Genome Organization Drives Chromosome Fragility. Cell. 2017; 507–521. doi:10.1016/j.cell.2017.06.034

30. Capewell P, Cren-Travaillï C, Marchesi F, Johnston P, Clucas C, Benson RA, et al. The skin is a significant but overlooked anatomical reservoir for vector-borne African trypanosomes. Elife. 2016;5: 1–17. doi:10.7554/eLife.17716

31. Carneiro DG, Clarke T, Davies CC, Bailey D. Identifying novel protein interactions: Proteomic methods, optimisation approaches and data analysis pipelines. Methods. 2016;95: 46–54. doi:10.1016/j.ymeth.2015.08.022

32. Carpenter AE, Jones TR, Lamprecht MR, Clarke C, Kang IH, Friman O, et al. CellProfiler: image analysis software for identifying and quantifying cell phenotypes. Genome Biol. 2006;7. doi:10.1186/gb-2006-7-10-r100

33. Carvalho T, Trindade S, Pimenta S, Santos AB, Rijo-Ferreira F, Figueiredo LM. Trypanosoma brucei triggers a marked immune response in male reproductive organs. PLoS Negl Trop Dis. 2018;12: e0006690. doi:10.1371/journal.pntd.0006690

34. Cayrou C, Coulombe P, Vigneron A, Stanojcic S, Ganier O, Peiffer I, et al. Genome-scale analysis of metazoan replication origins reveals their organization in specific but flexible sites defined by conserved features. Genome Res. 2011;21: 1438–1449. doi:10.1101/gr.121830.111

35. Chakalova L, Debrand E, Mitchell JA, Osborne CS, Fraser P. Replication and transcription: Shaping the landscape of the genome. Nat Rev Genet. 2005;6: 669–677. doi:10.1038/nrg1673

36. Champoux JJ. DNA TOPOISOMERASES : Structure,Function ,. Annu Rev Biochem. 2001;70: 369–413.

37. Chandler J, Vandoros A V., Mozeleski B, Klingbeil MM. Stem-loop silencing reveals that a third mitochondrial DNA polymerase, POLID, is required for kinetoplast DNA replication in trypanosomes. Eukaryot Cell. 2008;7: 2141–2146. doi:10.1128/EC.00199-08

38. Chang EJ, Begum R, Chait BT, Gaasterland T. Prediction of Cyclin-Dependent Kinase Phosphorylation Substrates. PLoS One. 2007;2: e656. doi:10.1371/journal.pone.0000656

39. Chaudhuri AR, Callen E, Ding X, Gogola E, Duarte AA, Lee JE, et al. Replication fork stability confers chemoresistance in BRCA-deficient cells. Nature. 2016;535: 382–387. doi:10.1038/nature18325

40. Chen R, Wold MS. Replication protein A: Single-stranded DNA's first responder: Dynamic DNA-interactions allow replication protein A to direct single-strand DNA intermediates into different pathways for synthesis or repair Prospects & Overviews R. Chen and M. S. Wold. BioEssays. 2014;36: 1156–1161. doi:10.1002/bies.201400107

41. Chiraniya A, Finkelstein J, Bloom LB. A Novel Function for the Conserved Glutamate Residue in the Walker B Motif of Replication Factor C. Genes. 2013; 134–151. doi:10.3390/genes4020134

42. Claes F, Vodnala SK, Van Reet N, Boucher N, Lunden-Miguel H, Baltz T, et al. Bioluminescent imaging of Trypanosoma brucei shows preferential testis dissemination which may hamper drug efficacy in sleeping sickness. PLoS Negl Trop Dis. 2009;3: 1–10. doi:10.1371/journal.pntd.0000486

43. Claverys JP, Martin B, Polard P. The genetic transformation machinery: Composition, localization, and mechanism. FEMS Microbiol Rev. 2009;33: 643–656. doi:10.1111/j.1574-6976.2009.00164.x

44. Coloma J, Johnson RE, Prakash L, Prakash S, Aggarwal AK. Human DNA polymerase α in binary complex with a DNA:DNA template-primer. Sci Rep. Nature Publishing Group; 2016;6: 1–10. doi:10.1038/srep23784

45. Concepción-Acevedo J, Luo J, Klingbeil MM. Dynamic localization of Trypanosoma brucei mitochondrial DNA polymerase ID. Eukaryot Cell. 2012;11: 844–55. doi:10.1128/EC.05291-11

46. Conti C, Sacca B, Herrick J, Lalou C, Pommier Y, Bensimon A. Replication Fork Velocities at Adjacent Replication Origins Are Coordinately Modified during DNA Replication in Human Cells. Int J Biol Sci. 2007;6: 569–583. doi:10.1091/mbc.E06

47. Cortez D. Proteomic Analyses of the Eukaryotic Replication Machinery. 1st ed. Methods in Enzymology. 2017. doi:10.1016/bs.mie.2017.03.002

48. Costa A, Hood I V., Berger JM. Mechanisms for Initiating Cellular DNA Replication. Annu Rev Biochem. 2013;82: 25–54. doi:10.1146/annurev-biochem-052610-094414

49. Cross GAM, Kim HS, Wickstead B. Capturing the variant surface glycoprotein repertoire (the VSGnome) of Trypanosoma brucei Lister 427. Mol Biochem Parasitol. Elsevier B.V.; 2014;195: 59–73. doi:10.1016/j.molbiopara.2014.06.004

50. da Silva MS, Pavani RS, Damasceno JD, Marques CA, McCulloch R, Tosi LRO, et al. Nuclear DNA Replication in Trypanosomatids: There Are No Easy Methods for Solving Difficult Problems. Trends Parasitol. Elsevier Ltd; 2017;33: 858–874. doi:10.1016/j.pt.2017.08.002

51. Daigaku Y, Keszthelyi A, Müller CA, Miyabe I, Brooks T, Retkute R, et al. A global profile of replicative polymerase usage. 2015;22. doi:10.1038/nsmb.2962

52. Dang HQ, Li Z. The Cdc45 Mcm2-7 GINS protein complex in trypanosomes regulates DNA replication and interacts with two Orc1-like proteins in the origin recognition complex. J Biol Chem. 2011;286: 32424–32435. doi:10.1074/jbc.M111.240143

53. Dang HQ, Zhou Q, Rowlett VW, Hu H, Lee KJ, Margolin W, et al. Proximity Interactions among Basal Body Components in Trypanosoma brucei Identify Novel Regulators of Basal Body Biogenesis and Inheritance. MBio. 2017;8: 1–15. doi:10.1128/mBio.02120-16

54. Daniels J-P, Gull K, Wickstead B. Cell Biology of the Trypanosome Genome. Microbiol Mol Biol Rev. 2010;74: 552–569. doi:10.1128/MMBR.00024-10

55. Davies AA, Masson J, Mcilwraith MJ, Stasiak AZ, Stasiak A, Venkitaraman AR, et al. Role of BRCA2 in Control of the RAD51 Recombination and DNA Repair Protein Adelina. Mol Cell. 2001;7: 273–282. doi:10.1016/S1097-2765(01)00175-7

56. De Melo Godoy PD, Nogueira-Junior LA, Paes LS, Cornejo A, Martins RM, Silber AM, et al. Trypanosome prereplication machinery contains a single functional Orc1/Cdc6 protein, which is typical of archaea. Eukaryot Cell. 2009;8: 1592–1603. doi:10.1128/EC.00161-09

57. Dean S, Sunter JD, Wheeler RJ. TrypTag.org: A Trypanosome Genome-wide Protein Localisation Resource. Trends Parasitol. 2017;33: 80–82. doi:10.1016/j.pt.2016.10.009

58. Dekker J, Belmont AS, Guttman M, Leshyk VO, Lis JT, Lomvardas S, et al. The 4D nucleome project. Nature. 2017;549: 219–226. doi:10.1038/nature23884

59. Dellino GI, Cittaro D, Piccioni R, Luzi L, Banfi S, Segalla S, et al. Genome-wide mapping of human DNA-replication origins: Levels of transcription at ORC1 sites regulate origin selection and replication timing. Genome Res. 2013;23: 1–11. doi:10.1101/gr.142331.112

60. Dembowski JA, DeLuca NA. Selective Recruitment of Nuclear Factors to Productively Replicating Herpes Simplex Virus Genomes. PLoS Pathog. 2015;11: 1–35. doi:10.1371/journal.ppat.1004939

61. DePamphillls M, Bell SD. Genome duplication. Concepts, mechanisms, evolution, and disease. New York: Garland Science; 2011.

62. Devbhandari S, Jiang J, Kumar C, Whitehouse I, Remus D. Chromatin Constrains the Initiation and Elongation of DNA Replication. Mol Cell. Elsevier Inc.; 2017;65: 131–141. doi:10.1016/j.molcel.2016.10.035

63. Devlin R, Marques CA, Paape D, Prorocic M, Zurita-Leal AC, Campbell SJ, et al. Mapping replication dynamics in Trypanosoma brucei reveals a link with telomere transcription and antigenic variation. Elife. 2016;5: 1–30. doi:10.7554/eLife.12765

64. Dewar JM, Walter JC. Mechanisms of DNA replication. Nat Rev Mol Cell Biol. Nature Publishing Group; 2013;18: 403–19. doi:10.5772/52656

65. Dey B, Thukral S, Krishnan S, Chakrobarty M, Gupta S, Manghani C, et al. DNA-protein interactions: Methods for detection and analysis. Mol Cell Biochem. 2012;365: 279–299. doi:10.1007/s11010-012-1269-z

66. Dinkel H, Roey K Van, Michael S, Kumar M, Uyar B, Altenberg B, et al. ELM 2016 –data update and new functionality of the eukaryotic linear motif resource. 2018;44: 294–300. doi:10.1093/nar/gkv1291

67. Downey N, Hines JC, Sinha KM, Ray DS. Mitochondrial DNA Ligases of Trypanosoma brucei. Eukaryot Cell. 2005;4: 765–774. doi:10.1128/EC.4.4.765-774.2005

68. Drazic A, Myklebust LM, Ree R, Arnesen T. The world of protein acetylation. Biochim Biophys Acta - Proteins Proteomics. 2016;1864: 1372–1401. doi:10.1016/j.bbapap.2016.06.007

69. DuBois KN, Alsford S, Holden JM, Buisson J, Swiderski M, Bart JM, et al. NUP-1 is a large coiled-coil nucleoskeletal protein in trypanosomes with lamin-like functions. PLoS Biol. 2012;10. doi:10.1371/journal.pbio.1001287

70. Duncker BP, Chesnokov IN, McConkey BJ. The origin recognition complex protein family. Genome Biol. 2009;10: 214. doi:10.1186/gb-2009-10-3-214

71. Dungrawala H, Rose KL, Bhat KP, Mohni KN, Glick GG, Couch FB, et al. The Replication Checkpoint Prevents Two Types of Fork Collapse without Regulating Replisome Stability. Mol Cell. 2015;59: 998–1010. doi:10.1016/j.molcel.2015.07.030

72. Durocher D, Jackson SP. The FHA domain. FEBS Lett. 2002;513: 58–66. doi:10.1016/S0014-5793(01)03294-X

73. Eliceiri K, Schneider CA, Rasband WS, Eliceiri KW. NIH Image to ImageJ : 25 years of image analysis HISTORICAL commentary NIH Image to ImageJ : 25 years of image analysis. Nat Methods. 2012;9: 671–675. doi:10.1038/nmeth.2089

74. Engel ML, Ray DS. A structure-specific DNA endonuclease is enriched in kinetoplasts purified from Crithidia fasciculata. Nucleic Acids Res. 1998;26: 4733–4738. doi:10.1093/nar/26.20.4733

75. Engel ML, Ray DS. The kinetoplast structure-specific endonuclease I is related to the 5' exo/endonuclease domain of bacterial DNA polymerase I and colocalizes with the kinetoplast topoisomerase II and DNA polymerase beta during replication. Proc Natl Acad Sci U S A. 1999;96: 8455–60. doi:10.1073/PNAS.96.15.8455

76. Englund PT. Free Minicircles of Kinetoplast DNA in Crithidia fasciculata. J Biol Chem. 1979;254..

77. Errico A, Deshmukh K, Tanaka Y, Pozniakovsky A, Hunt T. Identification of substrates for cyclin dependent kinases. Adv Enzyme Regul. 2010;50: 375–399. doi:10.1016/j.advenzreg.2009.12.001

78. Farr H, Gull K. Cytokinesis in trypanosomes. Cytoskeleton. 2012;69: 931–941. doi:10.1002/cm.21074

79. Felipe-Abrio I, Lafuente-Barquero J, García-Rubio ML, Aguilera A. RNA polymerase II contributes to preventing transcription-mediated replication fork stalls. EMBO J. 2015;34: 236–50. doi:10.15252/embj.201488544

80. Ferguson ML, Torri AF, Pérez-Morga D, Ward DC, Englund PT. Kinetoplast DNA replication: Mechanistic differences between Trypanosoma brucei and Crithidia fasciculata. J Cell Biol. 1994;126: 631–639. doi:10.1083/jcb.126.3.631

81. Fragkos M, Ganier O, Coulombe P, Méchali M. DNA replication origin activation in space and time. Nat Rev Mol Cell Biol. Nature Publishing Group; 2015;16: 360–374. doi:10.1038/nrm4002

82. Fuller RS, Funnell BE, Kornberg A. The dnaA protein complex with the E. coli chromosomal replication origin (oriC) and other DNA sites. Cell. 1984;38: 889–900. doi:10.1016/0092-8674(84)90284-8

83. Garbacz MA, Lujan SA, Burkholder AB, Cox PB, Wu Q, Zhou Z, et al. Evidence that DNA polymerase δ contributes to initiating leading strand DNA replication in Saccharomyces cerevisiae. Nat Commun. S: 1–11. doi:10.1038/s41467-018-03270-4

84. Garvey D, H BJ. Cdk phosphorylation of a Nucleoporin controls localization of active genes through the Cell Cylce. Mol Biol Cell. 2010;21: 3421–3432. doi:10.1091/mbc.E10

85. Gassen A, Brechtefeld D, Schandry N, Arteaga-Salas JM, Israel L, Imhof A, et al. DOT1A-dependent H3K76 methylation is required for replication regulation in Trypanosoma brucei. Nucleic Acids Res. 2012;40: 10302–10311. doi:10.1093/nar/gks801

86. Georgescu R, Langston L, O'Donnell M. A proposal: Evolution of PCNA's role as a marker of newly replicated DNA. DNA Repair (Amst). Elsevier B.V.; 2015;29: 4–15. doi:10.1016/j.dnarep.2015.01.015

87. Gillespie PJ, Gambus A, Blow JJ. Preparation and use of Xenopus egg extracts to study DNA replication and chromatin associated proteins. Methods. 2012;57: 203–213. doi:10.1016/j.ymeth.2012.03.029

88. Gillespie PJ, Khoudoli GA, Stewart G, Swedlow JR, Blow JJ. ELYS/MEL-28 Chromatin Association Coordinates Nuclear Pore Complex Assembly and Replication Licensing. Curr Biol. 2007;17: 1657–1662. doi:10.1016/j.cub.2007.08.041

89. Girdhar S, Girdhar A, Lather V, Pandita D. Novel Therapeutic Targets for Human African Trypanosomiasis. Curr Treat Options Infect Dis. 2017;9: 200–209. doi:10.1007/s40506-017-0120-1

90. Glover L, Hutchinson S, Alsford S, Mcculloch R, Field MC, Horn D. Antigenic variation in African trypanosomes: The importance of chromosomal and nuclear context in VSG expression control. Cell Microbiol. 2013;15: 1984–1993. doi:10.1111/cmi.12215

91. Gluenz E, Povelones ML, Englund PT, Gull K. The kinetoplast duplication cycle in Trypanosoma brucei is orchestrated by cytoskeleton-mediated cell morphogenesis. Mol Cell Biol. 2011;31: 1012–21. doi:10.1128/MCB.01176-10

92. Gluenz E, Sharma R, Carrington M, Gull K. Functional characterization of cohesin subunit SCC1 in Trypanosoma brucei and dissection of mutant phenotypes in two life cycle stages. Mol Microbiol. 2008;69: 666–680. doi:10.1111/j.1365-2958.2008.06320.x

93. Gómez-Escoda B, Jenny Wu PY. The organization of genome duplication is a critical determinant of the landscape of genome maintenance. Genome Res. 2018;28: 1179–1192. doi:10.1101/gr.224527.117

94. Gommers-ampt JH, Teixeira AJR, Van De Werken G, Van Dijk WJ, Borst P. The identification of hydroxymethyluracil in DNA of Trypanosoma brucei. Nucleic Acids Res. 1993;21: 2039–2043. doi:10.1093/nar/21.9.2039

95. Goos C, Dejung M, Janzen CJ, Butter F, Kramer S. The nuclear proteome of Trypanosoma brucei. PLoS One. 2017;12: e0181884. doi:10.1371/journal.pone.0181884

96. Gourguechon S, Savich JM, Wang CC. The Multiple Roles of cyclin E1 in Controlling Cell Cycle Progression and Cellular Morphology of Trypanosoma brucei. J Mol Biol. 2007;368: 939–950. doi:10.1016/j.jmb.2007.02.050

97. Gratzner HG. Monoclonal Antibody to 5-Bromo- and 5-Iododeoxyuridine : A New Reagent for Detection of DNA Replication Placental Mononuclear Phagocytes as a Source of Interleukin-1. Science. 1982;218: 474–475. doi:10.1126/science.7123245

98. Groth A, Corpet A, Cook AJL, Roche D, Bartek J, Lukas J, et al. Regulation of Replication Fork Supply and Demand. Science (80-). 2007;318: 1928–1932.

99. Günzl A, Bruderer T, Laufer G, Tu L, Chung H, Lee P, et al. RNA Polymerase I Transcribes Procyclin Genes and Variant Surface Glycoprotein Gene Expression Sites in Trypanosoma brucei RNA Polymerase I Transcribes Procyclin Genes and Variant Surface Glycoprotein Gene Expression Sites in Trypanosoma brucei. Eukaryot Cell. 2003;2: 542–551. doi:10.1128/EC.2.3.542

100. Hammarton TC, Clark J, Douglas F, Boshart M, Mottram JC. Stage-specific differences in cell cycle control in Trypanosoma brucei revealed by RNA interference of a mitotic cyclin. J Biol Chem. 2003;278: 22877–22886. doi:10.1074/jbc.M300813200

101. Hanna JS, Kroll ES, Lundblad V, Spencer F a. Saccharomyces cerevisiae CTF18 and CTF4 are required for sister chromatid cohesion. Mol Cell Biol. 2001;21: 3144–3158. doi:10.1128/MCB.21.9.3144-3158.2001

102. Hartley CL, McCulloch R. Trypanosoma brucei BRCA2 acts in antigenic variation and has undergone a recent expansion in BRC repeat number that is important during homologous recombination. Mol Microbiol. 2008;68: 1237–1251. doi:10.1111/j.1365-2958.2008.06230.x

103. Hoffmann A, Käser S, Jakob M, Amodeo S, Peitsch C, Týč J, et al. Molecular model of the mitochondrial genome segregation machinery in Trypanosoma brucei. Proc Natl Acad Sci. 2018; 201716582. doi:10.1073/pnas.1716582115

104. Horn D, McCulloch R. Molecular mechanisms underlying the control of antigenic variation in African trypanosomes. Curr Opin Microbiol. 2010;13: 700–705. doi:10.1016/j.mib.2010.08.009

105. Horn D. Antigenic variation in African trypanosomes. Mol Biochem Parasitol. Elsevier B.V.; 2014;195: 123–129. doi:10.1016/j.molbiopara.2014.05.001

106. Ibarra A, Hetzer MW. Nuclear pore proteins and the control of genome function. Genes Dev. 2015;29: 337–349. doi:10.1101/gad.256495.114.Cytoplasmic

107. Iborra FJ, Pombo A, Jackson D a, Cook PR. Active RNA polymerases are localized within discrete transcription "factories'' in human nuclei." J Cell Sci. 1996;109; Pt 6: 1427–1436.

108. Imboden MA, Laird PW, Affolter M, Seebeck T. Transcription of the intergenic regions of the tubulin gene cluster of Trypanosoma brucei: Evidence for a polyclstronic transcription unit in a eukaryote. Nucleic Acids Res. 1987;15: 7357–7368. doi:10.1093/nar/15.18.7357

109. Jackson DA, Hassan AB, Errington RJ, Cook PR. Visualization of focal sites of transcription within human nuclei. EMBO J. 1993;12: 1059–65.

110. Jackson DA, Pombo A. Replicon Clusters Are Stable Units of Chromosome Structure Evidence That Nuclear Organization Contributes to the Efficient Activation and Propagation of S Phase in Human Cells. 1998;140: 1285–1295.

111. Jacobs RT, Nare B, Wring SA, Orr MD, Chen D, Sligar JM, et al. Scyx-7158, an orally-active benzoxaborole for the treatment of stage 2 human african trypanosomiasis. PLoS Negl Trop Dis. 2011;5. doi:10.1371/journal.pntd.0001151

112. Janzen CJ, Hake SB, Lowell JE, Cross GAM. Selective Di- or Trimethylation of Histone H3 Lysine 76 by Two DOT1 Homologs Is Important for Cell Cycle Regulation in Trypanosoma brucei. Mol Cell. 2006;23: 497–507. doi:10.1016/j.molcel.2006.06.027

113. Jensen BC, Ramasamy G, Vasconcelos EJR, Ingolia NT, Myler PJ, Parsons M. Extensive stage-regulation of translation revealed by ribosome profiling of trypanosoma brucei. BMC Genomics. 2014;15: 1–21. doi:10.1186/1471-2164-15-911

114. Jensen RE, Englund PT. Network news: the replication of kinetoplast DNA. Annu Rev Microbiol. 2012;66: 473–91. doi:10.1146/annurev-micro-092611-150057

115. Johnson A, Yao NY, Bowman GD, Kuriyan J, Donnell MO. The Replication Factor C Clamp Loader Requires Arginine Finger Sensors to Drive

DNA Binding and Proliferating Cell Nuclear Antigen Loading. J Biol Chem. 2006;281: 35531–35543. doi:10.1074/jbc.M606090200

116. Johnson CE, Englund PT. Changes in organization of Crithidia fasciculata kinetoplast DNA replication proteins during the cell cycle. J Cell Biol. 1998;143: 911–9.

117. Johnson N, Shapiro GI. Cyclin-dependent kinases (cdks) and the DNA damage response: rationale for cdk inhibitor–chemotherapy combinations as an anticancer strategy for solid tumors. Expert Opin Ther Targets. 2010;14: 1199–1212. doi:10.1111/j.1743-6109.2008.01122.x.Endothelial

118. Johnson RE, Klassen R, Prakash L, Prakash S. A Major Role of DNA Polymerase delta in Replication of Both the Leading and Lagging DNA Strands. Mol Cell. Elsevier Inc.; 2015;59: 163–175. doi:10.1016/j.molcel.2015.05.038

119. Kaiser M, Bray MA, Cal M, Trunz BB, Torreele E, Brun R. Antitrypanosomal activity of fexinidazole, a new oral nitroimidazole drug candidate for treatment of sleeping sickness. Antimicrob Agents Chemother. 2011;55: 5602–5608. doi:10.1128/AAC.00246-11

120. Kanter DM, Bruck I, Kaplan DL. Mcm subunits can assemble into two different active unwinding complexes. J Biol Chem. 2008;283: 31172–31182. doi:10.1074/jbc.M804686200

121. Kaufer A, Ellis J, Stark D, Barratt J. The evolution of trypanosomatid taxonomy. Parasites and Vectors. Parasites & Vectors; 2017;10: 1–17. doi:10.1186/s13071-017-2204-7

122. Kaufmann D, Gassen A, Maiser A, Leonhardt H, Janzen CJ. Regulation and spatial organization of PCNA in Trypanosoma brucei. Biochem Biophys Res Commun. 2012;419: 698–702. doi:10.1016/j.bbrc.2012.02.082

123. Kaykov A, Taillefumier T, Bensimon A, Nurse P. Molecular Combing of Single DNA Molecules on the 10 Megabase Scale. Sci Rep. 2016;6: 80–84. doi:10.1038/srep19636

124. Kim H, Loparo JJ. Multistep assembly of DNA condensation clusters by SMC. Nat Commun. 2016;7: 1–12. doi:10.1038/ncomms10200

125. Kim J, MacNeill SA. Genome Stability: A New Member of the RFC family. Curr Biol. 2003;13: 873–875. doi:10.1016/j.cub.2003.10.048

126. Klingbeil MM, Motyka SA, Englund PT. Multiple Mitochondrial DNA Polymerases in Trypanosoma brucei. Mol Cell. 2002;10: 175–186.

127. Kolb HC, Finn MG, Sharpless KB. Click Chemistry: Diverse Chemical Function from a Few Good Reactions. Angew Chem Inte Ed. 2001;40: 2004–2021. doi:10.1002/1521-3773(20010601)40:11<2004::AID-ANIE2004>3.0.CO;2-5

128. Koltzscher M, Neumann C, Kö S, Gerke V. A High-Order Trans-Membrane Structural Linkage Is Responsible for Mitochondrial Genome Positioning and Segregation by Flagellar Basal Bodies in Trypanosomes. Mol Biol Cell. 2003;14: 2372–2384. doi:10.1091/mbc.E02

129. Kubota Y, Takase Y, Komori Y, Hashimoto Y, Arata T, Kamimura Y. A novel ring-like complex of Xenopus proteins essential for the initiation of DNA replication A novel ring-like complex of Xenopus proteins essential for the initiation of DNA replication. Genes Dev. 2003;17: 1141–1152. doi:10.1101/gad.1070003

130. Kunkel TA, Burgers PMJ. Arranging eukaryotic nuclear DNA polymerases for replication: Specific interactions with accessory proteins arrange Pols α, δ, and ϵ in the replisome for leading-strand and lagging-strand DNA replication. BioEssays. 2017;39: 1–6. doi:10.1002/bies.201700070

131. Kurat CF, Yeeles JTP, Patel H, Early A, Diffley JFX. Chromatin Controls DNA Replication Origin Selection, Lagging-Strand Synthesis, and Replication Fork Rates. Mol Cell. Elsevier Inc.; 2017;65: 117–130. doi:10.1016/j.molcel.2016.11.016

132. Lakadamyali M, Cosma MP. Advanced microscopy methods for visualizing chromatin structure. FEBS Lett. 2015;589: 3023–3030. doi:10.1016/j.febslet.2015.04.012

133. Lamb JR, Fu V, Wirtz E, Bangs JD. Functional Analysis of the Trypanosomal AAA Protein TbVCP with trans-Dominant ATP Hydrolysis Mutants. J Biol Chem. 2001;276: 21512–21520. doi:10.1074/jbc.M100235200

134. Langley AR, Gräff S, Smith JC, Krude T. Genome-wide identification and characterisation of human DNA replication origins by initiation site sequencing (ini-seq). Nucleic Acids Res. 2016;44: 10230–10247. doi:10.1093/nar/gkw760

135. Langston LD, Zhang D, Yurieva O, Georgescu RE, Finkelstein J, Yao NY, et al. CMG helicase and DNA polymerase form a functional 15-subunit holoenzyme for eukaryotic leading-strand DNA replication. Proc Natl Acad Sci. 2014;111: 15390–15395. doi:10.1073/pnas.1418334111

136. Lecona E, Rodriguez-Acebes S, Specks J, Lopez-Contreras AJ, Ruppen I, Murga M, et al. USP7 is a SUMO deubiquitinase essential for DNA replication. Nat Struct Mol Biol. 2016;23: 270–277. doi:10.1038/nsmb.3185

137. Leman AR, Noguchi E. The replication fork: Understanding the eukaryotic replication machinery and the challenges to genome duplication. Genes. 2013. doi:10.3390/genes4010001

138. Li B. DNA double-strand breaks and telomeres play important roles in Trypanosoma brucei antigenic variation. Eukaryot Cell. 2015;14: 196–205. doi:10.1128/EC.00207-14

139. Li C, Englund PT. A mitochondrial DNA primase from the trypanosomatid Crithidia fasciculata. J Biol Chem. 1997;272: 20787–20792. doi:10.1074/jbc.272.33.20787

140. Li JJ, Herskowitz I. Isolation of ORC6, a component of the yeast origin recognition complex by a one-hybrid system. Science.1993;262: 1870–1874. doi:10.1126/science.8266075

141. Li Z, Lee JH, Chu F, Burlingame AL, G??nzl A, Wang CC. Identification of a novel chromosomal passenger complex and its unique localization during cytokinesis in Trypanosoma brucei. PLoS One. 2008;3. doi:10.1371/journal.pone.0002354

142. Li Z, Wang CC. A PHO80-like cyclin and a B-type cyclin control the cell cycle of the procyclic form of Trypanosoma brucei. J Biol Chem. 2003;278: 20652–20658. doi:10.1074/jbc.M301635200

143. Li Z, Wang CC. Changing roles of aurora-B kinase in two life cycle stages of Trypanosoma brucei. Eukaryot Cell. 2006;5: 1026–1035. doi:10.1128/EC.00129-06

144. Li Z. Regulation of the cell division cycle in Trypanosoma brucei. Eukaryot Cell. 2012;11: 1180–1190. doi:10.1128/EC.00145-12

145. Li, Huilin; Stillman B. The Eukaryotic Replisome: a Guide to Protein Structure and Function. 2012;62: 37–58. doi:10.1007/978-94-007-4572-8

146. Liang X, Haritan A, Uliel S. trans and cis Splicing in Trypanosomatids : Mechanism , Factors , and Regulation MINIREVIEWS trans and cis Splicing in Trypanosomatids : Mechanism , Factors , and Regulation. Eukaryot Cell. 2003;2: 830–840. doi:10.1128/EC.2.5.830

147. Lindsay ME, Gluenz E, Gull K, Englund PT. A new function of Trypanosoma brucei mitochondrial topoisomerase II is to maintain kinetoplast DNA network topology. Mol Microbiol. 2008;70: 1465–1476. doi:10.1111/j.1365-2958.2008.06493.x

148. Liu B, Molina H, Kalume D, Pandey A, Griffith JD, Englund PT. Role of p38 in Replication of Trypanosoma brucei Kinetoplast DNA. Mol Cell Biol. 2006;26: 5382–5393. doi:10.1128/MCB.00369-06

149. Liu B, Wang J, Yaffe N, Lindsay ME, Zhao Z, Zick A, et al. Trypanosomes have six mitochondrial DNA helicases with one controlling kinetoplast maxicircle replication. Mol Cell. 2009;35: 490–501. doi:10.1016/j.molcel.2009.07.004

150. Liu B, Yildirir G, Wang J, Tolun G, Griffith JD, Englund PT. TbPIF1, a Trypanosoma brucei mitochondrial DNA helicase, is essential for kinetoplast minicircle replication. J Biol Chem. 2010;285: 7056–66. doi:10.1074/jbc.M109.084038

151. Liu S, Xu Z, Leng H, Zheng P, Yang J, Chen K, et al. RPA binds histone H3-H4 and functions in DNA replication-coupled nucleosome assembly. Science. 2017;355: 415–420. doi:10.1126/science.aah4712

152. Liu T, Huang J. Replication protein A and more: Single-stranded DNA-binding proteins in eukaryotic cells. Acta Biochim Biophys Sin (Shanghai). 2016;48: 665–670. doi:10.1093/abbs/gmw041

153. Lombraña R, Alvarez A, Fernandez-Justel JM, Almeida R, Poza-Carrion C, Gomes F, et al. Transcriptionally Driven DNA Replication Program of the Human Parasite Leishmania major. Cell Rep. 2016;16: 1774–1786. doi:10.1016/j.celrep.2016.07.007

154. Lõoke M, Maloney MF, Bell SP. Mcm10 regulates DNA replication elongation by stimulating the CMG replicative helicase. Genes Dev. 2017;31: 291–305. doi:10.1101/gad.291336.116

155. Lopez-Contreras AJ, Ruppen I, Nieto-Soler M, Murga M, Rodriguez-Acebes S, Remeseiro S, et al. A Proteomic Characterization of Factors Enriched at Nascent DNA Molecules. Cell Rep. 2013;3: 1105–1116. doi:10.1016/j.celrep.2013.03.009

156. Lossaint G, Larroque M, Ribeyre C, Bec N, Larroque C, Décaillet C, et al. FANCD2 Binds MCM Proteins and Controls Replisome Function upon Activation of S Phase Checkpoint Signaling. Mol Cell. 2013;51: 678–690. doi:10.1016/j.molcel.2013.07.023

157. Lubelsky Y, Prinz J a, Denapoli L, Li Y, Belsky J a, Macalpine DM. DNA replication and transcription programs respond to the same chromatin cues. Genome Research. 2014; 1102–1114. doi:10.1101/gr.160010.113

158. Lukeš J, Hashimi H, Zíková A. Unexplained complexity of the mitochondrial genome and transcriptome in kinetoplastid flagellates. Curr Genet. 2005;48: 277–299. doi:10.1007/s00294-005-0027-0

159. Ma L, Aslanian A, Sun H, Jin M, Shi Y, Yates JR, et al. Identification of Small Ubiquitin-like Modifier Substrates with Diverse Functions Using the

Xenopus Egg Extract System. Mol Cell Proteomics. 2014;13: 1659–1675. doi:10.1074/mcp.M113.035626

160. MacAlpine DM, Macalpine DM, Rodriguez HK, Bell SP, Bell SP. Coordination of replication and transcription along a. Genes Dev. 2004; 3094–3105. doi:10.1101/gad.1246404.ster

161. MacGregor P, Szöo'R B, Savill NJ, Matthews KR. Trypanosomal immune evasion, chronicity and transmission: An elegant balancing act. Nat Rev Microbiol. 2012;10: 431–438. doi:10.1038/nrmicro2779

162. Madamba EV, Berthet EB, Francis NJ. Inheritance of Histones H3 and H4 during DNA Replication In Vitro. Cell Rep. 2017;21: 1361–1374. doi:10.1016/j.celrep.2017.10.033

163. Marchal C, Sasaki T, Vera D, Wilson K, Sima J, Rivera-Mulia JC, et al. Genome-wide analysis of replication timing by next-generation sequencing with E/L Repli-seq. Nat Protoc. 2018;13: 819–839. doi:10.1038/nprot.2017.148

164. Marchetti MA, Tschudi C, Silva E, Ullu E. Physical and transcriptional analysis of the Trypanosoma brucei genome reveals a typical eukaryotic arrangement with close interspersion of RNA polymerase II- and III-transcribed genes. Nucleic Acids Res. 1998;26: 3591–3598. doi:10.1093/nar/26.15.3591

165. Marchler-Bauer A, Bo Y, Han L, He J, Lanczycki CJ, Lu S, et al. CDD/SPARCLE: Functional classification of proteins via subfamily domain architectures. Nucleic Acids Res. 2017;45: D200–D203. doi:10.1093/nar/gkw1129

166. Markaki Y, Gunkel M, Schermelleh L. Functional Nuclear Organization of Transcription and DNA Replication : A Topographical Marriage between Chromatin Domains and the Interchromatin Compartment Functional Nuclear Organization of Transcription and DNA Replication A Topographical Marriage betw. 2011;LXXV. doi:10.1101/sqb.2010.75.042

167. Marques CA, Dickens NJ, Paape D, Campbell SJ, McCulloch R. Genome-wide mapping reveals single-origin chromosome replication in Leishmania, a

eukaryotic microbe. Genome Biol. Genome Biology; 2015;16: 230. doi:10.1186/s13059-015-0788-9

168. Martinez MP, Wacker AL, Bruck I, Kaplan DL. Eukaryotic replicative helicase subunit interaction with DNA and its role in DNA replication. Genes (Basel). 2017;8. doi:10.3390/genes8040117

169. Masai H, Matsumoto S, You Z, Yoshizawa-Sugata N, Oda M. Eukaryotic Chromosome DNA Replication: Where, When, and How? Annu Rev Biochem. 2010;79: 89–130. doi:10.1146/annurev.biochem.052308.103205

170. Matthews KR, McCulloch R, Morrison LJ. The within-host dynamics of African trypanosome infections. Philos Trans R Soc B Biol Sci. 2015;370: 20140288. doi:10.1098/rstb.2014.0288

171. Mazin A V., Mazina OM, Bugreev D V., Rossi MJ. Rad54, the motor of homologous recombination. DNA Repair. 2010;9: 286–302. doi:10.1016/j.dnarep.2009.12.006

172. McCulloch R, Barry JD. A role for RAD51 and homologous recombination in Trypanosoma brucei antigenic variation. Genes Dev. 1999;13: 2875–2888. doi:10.1101/gad.13.21.2875

173. McKean PG. Coordination of cell cycle and cytokinesis in Trypanosoma brucei. Curr Opin Microbiol. 2003;6: 600–607. doi:10.1016/j.mib.2003.10.010

174. Mead TJ, Lefebvre V. Proliferation Assays (BrdU and EdU) on Skeletal tissue sections. In: Hilton M, editor. Skeletal Development and Repair Methods in Molecular Biology. 2014. pp. 233–243. doi:10.1007/978-1-62703-989-5

175. Mead TJ, Lefebvre V. Skeletal Development and Repair. 2014;1130: 1–10. doi:10.1007/978-1-62703-989-5

176. Mi H, Muruganujan A, Casagrande JT, Thomas PD. Large-scale gene function analysis with the panther classification system. Nat Protoc. 2013;8: 1551–1566. doi:10.1038/nprot.2013.092

177. Milhausen M, Nelson RG, Sather S, Selkirk M, Agabian N. Identification of a small RNA containing the trypanosome spliced leader: A donor of shared 5´sequences of trypanosomatid mRNAs? Cell. 1984;38: 721–729. doi:10.1016/0092-8674(84)90267-8

178. Milman N, Motyka SA, Englund PT, Robinson D, Shlomai J. Mitochondrial origin-binding protein UMSBP mediates DNA replication and segregation in trypanosomes. Proc Natl Acad Sci U S A. 2007;104: 19250–19255. doi:10.1073/pnas.0706858104

179. Misteli T. Concepts in nuclear architecture. BioEssays. 2005;27: 477–487. doi:10.1002/bies.20226

180. Mitra AK, Mawson AR. Neglected Tropical Diseases: Epidemiology and Global Burden. Trop Med Infect Dis. 2017;2: 36. doi:10.3390/tropicalmed2030036

181. Mogk S, Boßelmann CM, Mudogo CN, Stein J, Wolburg H, Duszenko M. African trypanosomes and brain infection – the unsolved question. 2017;1679: 1675–1687. doi:10.1111/brv.12301

182. Mortier-barrie I, Velten M, Dupaigne P, Mirouze N, Pie O, Mcgovern S, et al. A Key Presynaptic Role in Transformation for a Widespread Bacterial Protein : DprA Conveys Incoming ssDNA to RecA. Cell. 2007; 824–836. doi:10.1016/j.cell.2007.07.038

183. Muhich ML, Boothroyd JC. Polycistronic transcripts in trypanosomes and their accumulation during heat shock: evidence for a precursor role in mRNA synthesis. Mol Cell Biol. 1988;8: 3837–46. doi:10.1128/MCB.8.9.3837.

184. Naftelberg S, Schor IE, Ast G, Kornblihtt AR. Regulation of Alternative Splicing Through Coupling with Transcription and Chromatin Structure. Annu Rev Biochem. 2015;84: 165–198. doi:10.1146/annurev-biochem-060614-034242

185. Navarro M, Gull K. A poll transcriptional body associated with VSG mono-allelic expression in Trypanosoma brucei. Nature. 2001;414: 759–763. doi:10.1038/414759a

186. Nesvizhskii AI, Keller A. A statistical model for identifying proteins by tandem mass spectrometry. Anal Chem. 2003;75: 4646–4658. doi:10.1021/ac0341261

187. Neuwald AF. Evolutionary clues to eukaryotic DNA clamp-loading mechanisms : analysis of the functional constraints imposed on replication factor C AAA + ATPases. Nucleic Acids Res. 2005;33: 3614–3628. doi:10.1093/nar/gki6744

188. Nguyen VQ, Co C, Irie K, Li JJ. Clb/Cdc28 kinases promote nuclear export of the replication initiator proteins Mcm2-7. Curr Biol. 2000;10: 195–205. doi:10.1016/S0960-9822(00)00337-7

189. Nilsson D, Gunasekera K, Mani J, Osteras M, Farinelli L, Baerlocher L, et al. Spliced leader trapping reveals widespread alternative splicing patterns in the highly dynamic transcriptome of Trypanosoma brucei. PLoS Pathog. 2010;6: 21–22. doi:10.1371/journal.ppat.1001037

190. Obado SO, Brillantes M, Uryu K, Zhang W, Ketaren NE, Chait BT, et al. Interactome Mapping Reveals the Evolutionary History of the Nuclear Pore Complex. PLoS Biol. 2016;14: 1–30. doi:10.1371/journal.pbio.1002365

191. Ong S-E, Blagoev B, Kratchmarova I, Kristensen DB, Steen H, Pandey A, et al. Stable Isotope Labeling by Amino Acids in Cell Culture, SILAC, as a Simple and Accurate Approach to Expression Proteomics. Mol Cell Proteomics. 2002;1: 376–386. doi:10.1074/mcp.M200025-MCP200

192. Ooi C-P, Bastin P. More than meets the eye: understanding Trypanosoma brucei morphology in the tsetse. Front Cell Infect Microbiol. 2013;3: 1–12. doi:10.3389/fcimb.2013.00071

193. Pasternack DA, Sharma AI, Olson CL, Epting CL, Engman DM. Sphingosine kinase regulates microtubule dynamics and organelle positioning necessary for proper G1/s cell cycle transition in trypanosoma brucei. MBio. 2015;6: 1–11. doi:10.1128/mBio.01291-15

194. Pellegrini L, Costa A. New Insights into the Mechanism of DNA Duplication by the Eukaryotic Replisome. Trends Biochem Sci. Elsevier Ltd; 2016;41: 859–871. doi:10.1016/j.tibs.2016.07.011

195. Perera RL, Torella R, Klinge S, Kilkenny ML, Maman JD, Pellegrini L. Mechanism for priming DNA synthesis by yeast DNA Polymerase α. Elife. 2013;2013: 1–22. doi:10.7554/eLife.00482

196. Pollok S, Grosse F. Cdc45 degradation during differentiation and apoptosis. Biochem Biophys Res Commun. 2007;362: 910–915. doi:10.1016/j.bbrc.2007.08.069

197. Ponte-sucre A. An Overview of Trypanosoma brucei Infections : An Intense Host – Parasite Interaction. 2016;7: 1–12. doi:10.3389/fmicb.2016.02126

198. Povelones ML. Beyond replication: division and segregation of mitochondrial DNA in kinetoplastids. Mol Biochem Parasitol. 2014;196: 53–60. doi:10.1016/j.molbiopara.2014.03.008

199. Powers M, Evans EK, Yang J, Kornbluth S. Preparation and use of interphase Xenopus egg extracts. Curr Protoc Cell Biol. 2001;Chapter 11: Unit 11.10. doi:10.1002/0471143030.cb1110s09

200. Prado F, Maya D. Regulation of replication fork advance and stability by nucleosome assembly. Genes. 2017;8. doi:10.3390/genes8020049

201. Quinet A, Carvajal-Maldonado D, Lemacon D, Vindigni A. DNA Fiber Analysis: Mind the Gap! 1st ed. Methods in Enzymology. 2017. doi:10.1016/bs.mie.2017.03.019

202. Quinet A, Lemaçon D, Vindigni A. Replication Fork Reversal: Players and Guardians. Mol Cell. 2017;68: 830–833. doi:10.1016/j.molcel.2017.11.022

203. Ragoczy T, Bender MA, Telling A, Byron R, Groudine M. The locus control region is required for association of the murine B-globin locus with engaged transcription factories during erythroid maturation. Genes Dev. 2006;20: 1447–1457. doi:10.1101/gad.1419506

204. Ranjbarian F, Vodnala M, Vodnala SM, Rofougaran R, Thelander L, Hofer A. Trypanosoma brucei thymidine kinase is tandem protein consisting of two homologous parts, which together enable efficient substrate binding. J Biol Chem. 2012;287: 17628–17636. doi:10.1074/jbc.M112.340059

205. Reinhart M, Cardoso MC. A journey through the microscopic ages of DNA replication. Protoplasma. 2017;254: 1151–1162. doi:10.1007/s00709-016-1058-8

206. Reverón-Gómez N, González-Aguilera C, Stewart-Morgan KR, Petryk N, Flury V, Graziano S, et al. Accurate Recycling of Parental Histones Reproduces the Histone Modification Landscape during DNA Replication. Mol Cell. 2018; 1–11. doi:10.1016/j.molcel.2018.08.010

207. Riera A, Barbon M, Noguchi Y, Reuter LM, Schneider S, Speck C. From structure to mechanism—understanding initiation of DNA replication. Genes Dev. 2017;31: 1073–1088. doi:10.1101/gad.298232.117

208. Robinson NP, Dionne I, Lundgren M, Marsh VL, Bernander R, Bell SD. Identification of Two Origins of Replication in the Single Chromosome of the Archaeon Sulfolobus solfataricus. Cell. 2004;116: 25–38. doi:10.1016/S0092-8674(03)01034-1

209. Robinson, D.R & Gull K. Basal Body movement as a mechanism for mitochondrial genome segregation in the trypanosome cell cycle. Nature. 1991;352: 731–733.

210. Rocha-Granados MC, Klingbeil MM. Leishmania DNA Replication Timing: A Stochastic Event? Trends Parasitol. 2016;32: 755–757. doi:10.1016/j.pt.2016.05.011

211. Ross PL, Huang YN, Marchese JN, Williamson B, Parker K, Hattan S, et al. Multiplexed Protein Quantitation in Saccharomyces cerevisiae Using Amine-reactive Isobaric Tagging Reagents. Mol Cell Proteomics. 2004;3: 1154–1169. doi:10.1074/mcp.M400129-MCP200

212. Roy S, Luzwick JW, Schlacher K. SIRF : Quantitative in situ analysis of protein interactions at DNA replication forks. J Cell Biol. 2018;JCB: 1–16. doi:10.1083/jcb.201709121

213. Sakyiama J, Zimmer SL, Ciganda M, Williams N, Read LK. Ribosome biogenesis requires a highly diverged XRN family 5'->3' exoribonuclease for rRNA processing in Trypanosoma brucei. Rna. 2013;19: 1419–1431. doi:10.1261/rna.038547.113

214. Salic A, Mitchison TJ. A chemical method for fast and sensitive detection of DNA synthesis in vivo. Proc Natl Acad Sci U S A. 2008;105: 2415–2420. doi:10.1073/pnas.0712168105

215. Saredi G, Huang H, Hammond CM, Alabert C, Bekker-Jensen S, Forne I, et al. H4K20me0 marks post-replicative chromatin and recruits the TONSL–MMS22L DNA repair complex. Nature. 2016;534: 714–718. doi:10.1038/nature18312

216. Savage AF, Kolev NG, Franklin JB, Vigneron A, Aksoy S, Tschudi C. Transcriptome profiling of Trypanosoma brucei development in the tsetse fly vector Glossina morsitans. PLoS One. 2016;11: 1–20. doi:10.1371/journal.pone.0168877

217. Saxowsky TT, Choudhary G, Klingbeil MM, Englund PT. Trypanosoma brucei has two distinct mitochondrial DNA polymerase beta enzymes. J Biol Chem. 2003;278: 49095–49101. doi:10.1074/jbc.M308565200

218. Schimanski B, Nguyen TN, Gu A. Highly Efficient Tandem Affinity Purification of Trypanosome Protein Complexes Based on a Novel Epitope Combination. Eukaryot Cell. 2005;4: 1942–1950. doi:10.1128/EC.4.11.1942

219. Schimanski B, Nguyen TN, Gunzl A. Characterization of a Multisubunit Transcription Factor Complex Essential for Spliced-Leader RNA Gene Transcription in Trypanosoma brucei. Mol Cell Biol. 2005;25: 7303–7313. doi:10.1128/MCB.25.16.7303

220. Schneider R, Grosschedl R. Dynamics and interplay of nuclear architecture , genome organization , and gene expression. 2007; 3027–3043. doi:10.1101/gad.1604607.

221. Schübeler D, Scalzo D, Kooperberg C, van Steensel B, Delrow J, Groudine M. Genome-wide DNA replication profile for Drosophila melanogaster: a link between transcription and replication timing. Nat Genet. 2002;32: 438–442. doi:10.1038/ng1005

222. Schwanhüusser B, Busse D, Li N, Dittmar G, Schuchhardt J, Wolf J, et al. Global quantification of mammalian gene expression control. Nature. 2011;473: 337–342. doi:10.1038/nature10098

223. Scocca JR, Shapiro TA. A mitochondrial topoisomerase IA essential for late theta structure resolution in African trypanosomes. Mol Microbiol. 2008;67: 820–829. doi:10.1111/j.1365-2958.2007.06087.x

224. Senkevich TG, Katsafanas GC, Weisberg A, Olano LR, Moss B. Identification of vaccinia virus replisome and transcriptome proteins by isolation of proteins on nascent DNA coupled with mass spectrometry. J Virol. 2017;91: 1–20. doi:10.1128/JVI.01015-17

225. Sequeira-Mendes J, Díaz-Uriarte R, Apedaile A, Huntley D, Brockdorff N, Gómez M. Transcription initiation activity sets replication origin efficiency in mammalian cells. PLoS Genet. 2009;5. doi:10.1371/journal.pgen.1000446

226. Sherwin T, Gull K. Visualization of detyrosination along single microtubules reveals novel mechanisms of assembly during cytoskeletal duplication in trypanosomes. Cell. 1989;57: 211–221. doi:10.1016/0092-8674(89)90959-8

227. Shintomi, Keishi; Inoue, Fukashi; Watanabe, Hiroshi; Ohsumi, Keita; Ohsugi, Miho; Hirano T. Mitotic chromosome assembly despite nucleosome depeltion in Xenopous egg extracts. Science. 2017;356: 1284–1287.

228. Shiomi Y, Hayashi A, Ishii T, Shinmyozu K, Nakayama J -i., Sugasawa K, et al. Two Different Replication Factor C Proteins, Ctf18 and RFC1, Separately Control PCNA-CRL4Cdt2-Mediated Cdt1 Proteolysis during S Phase

and following UV Irradiation. Mol Cell Biol. 2012;32: 2279–2288. doi:10.1128/MCB.06506-11

229. Shiomi Y, Nishitani H. Control of genome integrity by RFC complexes; conductors of PCNA loading onto and unloading from chromatin during DNA replication. Genes. 2017;8. doi:10.3390/genes8020052

230. Siegel TN, Gunasekera K, Cross GAM, Ochsenreiter T. Gene expression in Trypanosoma brucei: Lessons from high-throughput RNA sequencing. Trends Parasitol. Elsevier Ltd; 2011;27: 434–441. doi:10.1016/j.pt.2011.05.006

231. Siegel TN, Hekstra DR, Cross GAM. Analysis of the Trypanosoma brucei cell cycle by quantitative DAPI imaging. Mol Biochem Parasitol. 2008;160: 171–174. doi:10.1016/j.molbiopara.2008.04.004

232. Siegel TN, Hekstra DR, Kemp LE, Figueiredo LM, Lowell JE, Fenyo D, et al. Four histone variants mark the boundaries of polycistronic transcription units in Trypanosoma brucei. Genes Dev. 2009;23: 1063–1076.doi:10.1101/gad.1790409.7

233. Siegel TN, Hekstra DR, Wang X, Dewell S, Cross GAM. Genome-wide analysis of mRNA abundance in two life-cycle stages of Trypanosoma brucei and identification of splicing and polyadenylation sites. Nucleic Acids Res. 2010;38: 4946–4957. doi:10.1093/nar/gkq237

234. Siegel TN, Kawahara T, DeGrasse JA, Janzen CJ, Horn D, Cross GAM. Acetylation of histone H4K4 is cell cycle regulated and mediated by HAT3 in Trypanosoma brucei. Mol Microbiol. 2008;67: 762–771. doi:10.1111/j.1365-2958.2007.06079.x

235. Sievers F, Wilm A, Dineen D, Gibson TJ, Karplus K, Li W, et al. Fast, scalable generation of high-quality protein multiple sequence alignments using Clustal Omega. Mol Syst Biol. 2011;7. doi:10.1038/msb.2011.75

236. Silvester E, McWilliam K, Matthews K. The Cytological Events and Molecular Control of Life Cycle Development of Trypanosoma brucei in the Mammalian Bloodstream. Pathogens. 2017;6: 29. doi:10.3390/pathogens6030029

237. Simon M, Giot L, Faye G. The 3 ’ to 5 ’ exonuclease activity located in the DNA polymerase 6 subunit of Saccharomyces cerevisiae is required for accurate replication. EMBO J. 1991;10: 2165–2170. doi:10.1002/j.1460-2075.1991.tb07751.x

238. Singh BN, Achary VMM, Panditi V, Sopory SK, Reddy MK. Dynamics of tobacco DNA topoisomerases II in cell cycle regulation: to manage topological constrains during replication, transcription and mitotic chromosome condensation and segregation. Plant Mol Biol. 2017;94: 595–607. doi:10.1007/s11103-017-0626-4

239. Sirbu BM, Couch FB, Cortez D. Monitoring the spatiotemporal dynamics of proteins at replication forks and in assembled chromatin using isolation of proteins on nascent DNA. Nat Protoc. 2012;7: 594–605. doi:10.1038/nprot.2012.010

240. Sirbu BM, Couch FB, Feigerle JT, Bhaskara S, Hiebert SW, Cortez D. Analysis of protein dynamics at active , stalled , and collapsed replication forks. Genes Dev. 2011;25: 1320–1327. doi:10.1101/gad.2053211.

241. Sirbu BM, McDonald WH, Dungrawala H, Badu-Nkansah A, Kavanaugh GM, Chen Y, et al. Identification of proteins at active, stalled, and collapsed replication forks using isolation of proteins on nascent DNA (iPOND) coupled with mass spectrometry. J Biol Chem. 2013;288: 31458–31467. doi:10.1074/jbc.M113.511337

242. Smith TK, Bringaud F, Nolan DP, Figueiredo LM. Metabolic reprogramming during the Trypanosoma brucei life cycle. F1000Research. 2017;6: 683. doi:10.12688/f1000research.10342.1

243. Smoot ME, Ono K, Ruscheinski J, Wang PL, Ideker T. Cytoscape 2.8: New features for data integration and network visualization. Bioinformatics. 2011;27: 431–432. doi:10.1093/bioinformatics/btq675

244. Sogo, J.M; Stahl, H;Koller, Th;Knippers R. Structure of Replicating Simian Virus 40 Minichromosomes The Replication Fork, Core Histone Segregation and Terminal Structures. J mo. 1986; 189–204.

245. Srivastava A, Badjatia N, Lee JH, Hao B, Günzl A. An RNA polymerase II-associated TFIIF-like complex is indispensable for SL RNA gene transcription in Trypanosoma brucei. Nucleic Acids Res. 2017;46: 1695–1709. doi:10.1093/nar/gkx1198

246. Stanojcic S, Sollelis L, Kuk N, Crobu L, Balard Y, Schwob E, et al. Single-molecule analysis of DNA replication reveals novel features in the divergent eukaryotes Leishmania and Trypanosoma brucei versus mammalian cells. Sci Rep. 2016;6: 23142. doi:10.1038/srep23142

247. Stijlemans B, Caljon G, Van Den Abbeele J, Van Ginderachter JA, Magez S, De Trez C. Immune evasion strategies of Trypanosoma brucei within the mammalian host: Progression to pathogenicity. Front Immunol. 2016;7. doi:10.3389/fimmu.2016.00233

248. Stillman B. Reconsidering DNA Polymerases at the Replication Fork in Eukaryotes. Mol Cell. Elsevier Inc.; 2015;59: 139–141. doi:10.1016/j.molcel.2015.07.004

249. Stinchcomb DT, Struhl K, Davis RW. Isolation and characterisation of a yeast chromosomal replicator. Nature. 1979;282: 39–43. doi:10.1038/282039a0

250. Stodola JL, Burgers PM. Mechanism of DNA replication in eukaryotes. In: Masai H, Foiani M, editors. DNA Replication Advances in Experimental Medicine and Biology. Springer, Singapore; 2017. pp. 117–133.

251. Stratmann SA, van Oijen AM. DNA replication at the single-molecule level. Chem Soc Rev. 2014;43: 1201. doi:10.1039/c3cs60391a

252. Sutherland CS, Stone CM, Steinmann P, Tanner M, Tediosi F. Seeing beyond 2020: an economic evaluation of contemporary and emerging strategies for elimination of Trypanosoma brucei gambiense. Lancet Glob Heal. The Author(s). Published by Elsevier Ltd. This is an Open Access article under the CC BY license; 2017;5: e69–e79. doi:10.1016/S2214-109X(16)30237-6

253. Szklarczyk D, Franceschini A, Wyder S, Forslund K, Heller D, Huerta-Cepas J, et al. STRING v10: Protein-protein interaction networks, integrated over

the tree of life. Nucleic Acids Res. 2015;43: D447–D452. doi:10.1093/nar/gku1003

254. Tang Z, Luo OJ, Li X, Zheng M, Zhu JJ, Szalaj P, et al. CTCF-Mediated Human 3D Genome Architecture Reveals Chromatin Topology for Transcription. Cell. 2015;163: 1611–1627. doi:10.1016/j.cell.2015.11.024

255. Taylor JA, Ouimet MC, Wargachuk R, Marczynski GT. The Caulobacter crescentus chromosome replication origin evolved two classes of weak DnaA binding sites. Mol Microbiol. 2011;82: 312–326. doi:10.1111/j.1365-2958.2011.07785.x

256. Técher H, Koundrioukoff S, Azar D, Wilhelm T, Carignon S, Brison O, et al. Replication dynamics: Biases and robustness of DNA fiber analysis. J Mol Biol. 2013;425: 4845–4855. doi:10.1016/j.jmb.2013.03.040

257. Thangavel S, Berti M, Levikova M, Pinto C, Gomathinayagam S, Vujanovic M, et al. DNA2 drives processing and restart of reversed replication forks in human cells. J. Cell. Biol. 2015;208:545-562. doi:10.1083/jcb.201406100

258. Tiengwe C, Marcello L, Farr H, Dickens N, Kelly S, Swiderski M, et al. Genome-wide analysis reveals extensive functional interaction between DNA replication initiation and transcription in the genome of trypanosoma brucei. Cell Rep. Elsevier; 2012;2: 185–197. doi:10.1016/j.celrep.2012.06.007

259. Tiengwe C, Marcello L, Farr H, Gadelha C, Burchmore R, Barry JD, et al. Identification of ORC1/CDC6-interacting factors in trypanosoma brucei reveals critical features of origin recognition complex architecture. PLoS One. 2012;7: 22–24. doi:10.1371/journal.pone.0032674

260. Tiengwe C, Marques CA, McCulloch R. Nuclear DNA replication initiation in kinetoplastid parasites: New insights into an ancient process. Trends Parasitol. Elsevier Ltd; 2014;30: 27–36. doi:10.1016/j.pt.2013.10.009

261. Trindade S, Rijo-Ferreira F, Carvalho T, Pinto-Neves D, Guegan F, Aresta-Branco F, et al. Trypanosoma brucei Parasites Occupy and Functionally Adapt to the Adipose Tissue in Mice. Cell Host Microbe. 2016;19: 837–848. doi:10.1016/j.chom.2016.05.002

262. Tu X, Kumar P, Li Z, Wang CC. An aurora kinase homologue is involved in regulating both mitosis and cytokinesis in Trypanosoma brucei. J Biol Chem. 2006;281: 9677–9687. doi:10.1074/jbc.M511504200

263. Tu X, Wang CC. Pairwise knockdowns of cdc2-related kinases (CRKs) in Trypanosoma brucei identified the CRKs for G1/S and G2/M transitions and demonstrated distinctive cytokinetic regulations between two developmental stages of the organism. Eukaryot Cell. 2005;4: 755–764. doi:10.1128/EC.4.4.755-764.2005

264. Ulrich HD. New insights into replication clamp unloading. J Mol Biol. Elsevier Ltd; 2013;425: 4727–4732. doi:10.1016/j.jmb.2013.05.003

265. Umeyama T, Wang CC. Polo-like kinase is expressed in S/G2/M phase and associated with the flagellum attachment zone in both procyclic and bloodstream forms of Trypanosoma brucei. Eukaryot Cell. 2008;7: 1582–1590. doi:10.1128/EC.00150-08

266. Urbaniak MD, Martin DMA, Ferguson MAJ. Global quantitative SILAC phosphoproteomics reveals differential phosphorylation is widespread between the procyclic and bloodstream form lifecycle stages of Trypanosoma brucei. J Proteome Res. 2013;12: 2233–2244. doi:10.1021/pr400086y

267. Valenciano AL, Knudsen GM, Mackey ZB. Extracellular-signal regulated kinase 8 of Trypanosoma brucei uniquely phosphorylates its proliferating cell nuclear antigen homolog and reveals exploitable properties. Cell Cycle. Taylor & Francis; 2016;15: 2827–2841. doi:10.1080/15384101.2016.1222340

268. Valenciano AL, Ramsey AC, Mackey ZB. Deviating the level of proliferating cell nuclear antigen in trypanosoma brucei elicits distinct mechanisms for inhibiting proliferation and cell cycle progression. Cell Cycle. 2015;14: 674–688. doi:10.4161/15384101.2014.987611

269. Van Luenen HGAM, Farris C, Jan S, Genest PA, Tripathi P, Velds A, et al. Glucosylated hydroxymethyluracil, DNA base J, prevents transcriptional readthrough in Leishmania. Cell. 2012;150: 909–921. doi:10.1016/j.cell.2012.07.030

270. Veitch N, Johnson PCD, Trivedi U, Terry S, Wildridge D, MacLeod A. Digital gene expression analysis of two life cycle stages of the human-infective parasite , Trypanosoma clusters of co-regulated genes . 2010; 1–14. doi:10.1186/1471-2164-11-124

271. Venclovas E, Colvin ME, Thelen MP. Molecular modeling-based analysis of interactions in the RFC-dependent clamp-loading process. Protein Science. 2002; 11: 2403–2416. doi:10.1110/ps.0214302.Protein

272. Venter JC, Adams MD, Myers EW, Li PW, Mural RJ, Sutton GG, et al. The sequence of the human genome. Science. 2009;291: 1304–1351. doi:10.1126/science.1058040

273. Vindigni A, Lopes M. Combining electron microscopy with single molecule DNA fiber approaches to study DNA replication dynamics. Biophys Chem. 2017;225: 3–9. doi:10.1016/j.bpc.2016.11.014

274. Vos SM, Tretter EM, Schmidt BH, Berger JM. All tangled up: how cells direct, manage and exploit topoisomerase function. Nat Rev Mol Cell Biol. 2011;12: 827–41. doi:10.1038/nrm3228

275. Votýpka J, d'Avila-Levy CM, Grellier P, Maslov DA, Lukeš J, Yurchenko V. New Approaches to Systematics of Trypanosomatidae: Criteria for Taxonomic (Re)description. Trends Parasitol. 2015;31: 460–469. doi:10.1016/j.pt.2015.06.015

276. Waga S, Stillman B. Anatomy of a DNA replication fork revealed by reconstitution of SV40 DNA replication in vitro. Nature. 1994;369.

277. Wang S-C, Nakajima Y, Yu Y-L, Xia W, Chen C-T, Yang C-C, et al. Tyrosine phosphorylation controls PCNA function through protein stability. Nat Cell Biol. 2006;8: 1359–1368. doi:10.1038/ncb1501

278. Wang Z, Morris JC, Drew ME, Englund PT. Inhibition of Trypanosoma brucei gene expression by RNA interference using an integratable vector with opposing T7 promoters. J Biol Chem. 2000;275: 40174–40179. doi:10.1074/jbc.M008405200

279. Wedel C, Förstner KU, Derr R, Siegel TN. GT-rich promoters can drive RNA pol II transcription and deposition of H2A.Z in African trypanosomes. EMBO J. 2017;36: e201695323. doi:10.15252/embj.201695323

280. Wheeler RJ, Scheumann N, Wickstead B, Gull K, Vaughan S. Cytokinesis in trypanosoma brucei differs between bloodstream and tsetse trypomastigote forms: Implications for microtubule-based morphogenesis and mutant analysis. Mol Microbiol. 2013;90: 1339–1355. doi:10.1111/mmi.12436

281. WHO. Report of the first WHO stakeholders meeting on rhodesiense human African trypanosomiasis elimination. 2015; 1–106.

282. Wiese S, Reidegeld KA, Meyer HE, Warscheid B. Protein labeling by iTRAQ: A new tool for quantitative mass spectrometry in proteome research. Proteomics. 2007;7: 340–350. doi:10.1002/pmic.200600422

283. Wiest NE, Tomkinson AE. Optimization of Native and Formaldehyde iPOND Techniques for Use in Suspension Cells [Internet]. 1st ed. Methods in Enzymology. 2017. doi:10.1016/bs.mie.2017.03.001

284. Woodward R, Gull K. Timing of nuclear and kinetoplast DNA replication and early morphological events in the cell cycle of Trypanosoma brucei. J Cell Sci. 1990;95: 49–57.

285. Yadav T, Carrasco B, Myers AR, George NP, Keck JL, Alonso JC. Genetic recombination in Bacillus subtilis: A division of labor between two single-strand DNA-binding proteins. Nucleic Acids Res. 2012;40: 5546–5559. doi:10.1093/nar/gks173

286. Yadav T, Whitehouse I. Replication-Coupled Nucleosome Assembly and Positioning by ATP-Dependent Chromatin-Remodeling Enzymes. Cell Rep. 2016;15: 715–723. doi:10.1016/j.celrep.2016.03.059

287. Yadav T, Whitehouse I. Replication-Coupled Nucleosome Assembly and Positioning by ATP-Dependent Chromatin-Remodeling Enzymes. Cell Rep. 2016;15: 715–723. doi:10.1016/j.celrep.2016.03.059

288. Yao N, O'Donnell M. Bacterial and Eukaryotic Replisome Machines. JSM Biochem Mol Biol. 2016;3: 1–15. doi:10.1038/nbt.3121.ChIP-nexus

289. Yao NY, Donnell MO. The RFC Clamp Loader: Structure and Function. Subcell Biochem. 2012; 62: 259–279. doi:10.1007/978-94-007-4572-8

290. Yardimci H, Walter JC. Prereplication-complex formation: A molecular double take? Nat Struct Mol Biol. Nature Publishing Group; 2014;21: 20–25. doi:10.1038/nsmb.2738

291. Yu C, Gan H, Han J, Zhou ZX, Jia S, Chabes A, et al. Strand-Specific Analysis Shows Protein Binding at Replication Forks and PCNA Unloading from Lagging Strands when Forks Stall. Mol Cell. 2014;56: 551–563. doi:10.1016/j.molcel.2014.09.017

292. Yu S, Yang F, Shen WH. Genome maintenance in the context of 4D chromatin condensation. Cell Mol Life Sci. Springer International Publishing; 2016;73: 3137–3150. doi:10.1007/s00018-016-2221-2

293. Zhu W, Ukomadu C, Jha S, Senga T, Dhar SK, Wohlschlegel J a, et al. Mcm10 and And-1 / CTF4 recruit DNA polymerase α to chromatin for initiation of DNA replication. Genes Dev. 2007; 2288–2299. doi:10.1101/gad.1585607.

294. Zou L, Cortez D, Elledge SJ. Regulation of ATR substrate selection by Rad17-dependent loading of Rad9 complexes onto chromatin. Genes Dev. 2002;16: 198–208. doi:10.1101/gad.950302